Three-dimensional Biomechanical Analysis of Fast Bowling in Cricket

A thesis submitted to the

University of Waikato

for the degree

of

Doctor of Philosophy in Physics

By

René Ferdinands

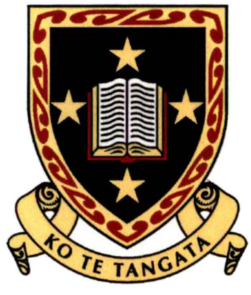

The University of Waikato

Te Whare Wānanga o Waikato

University of Waikato

2003

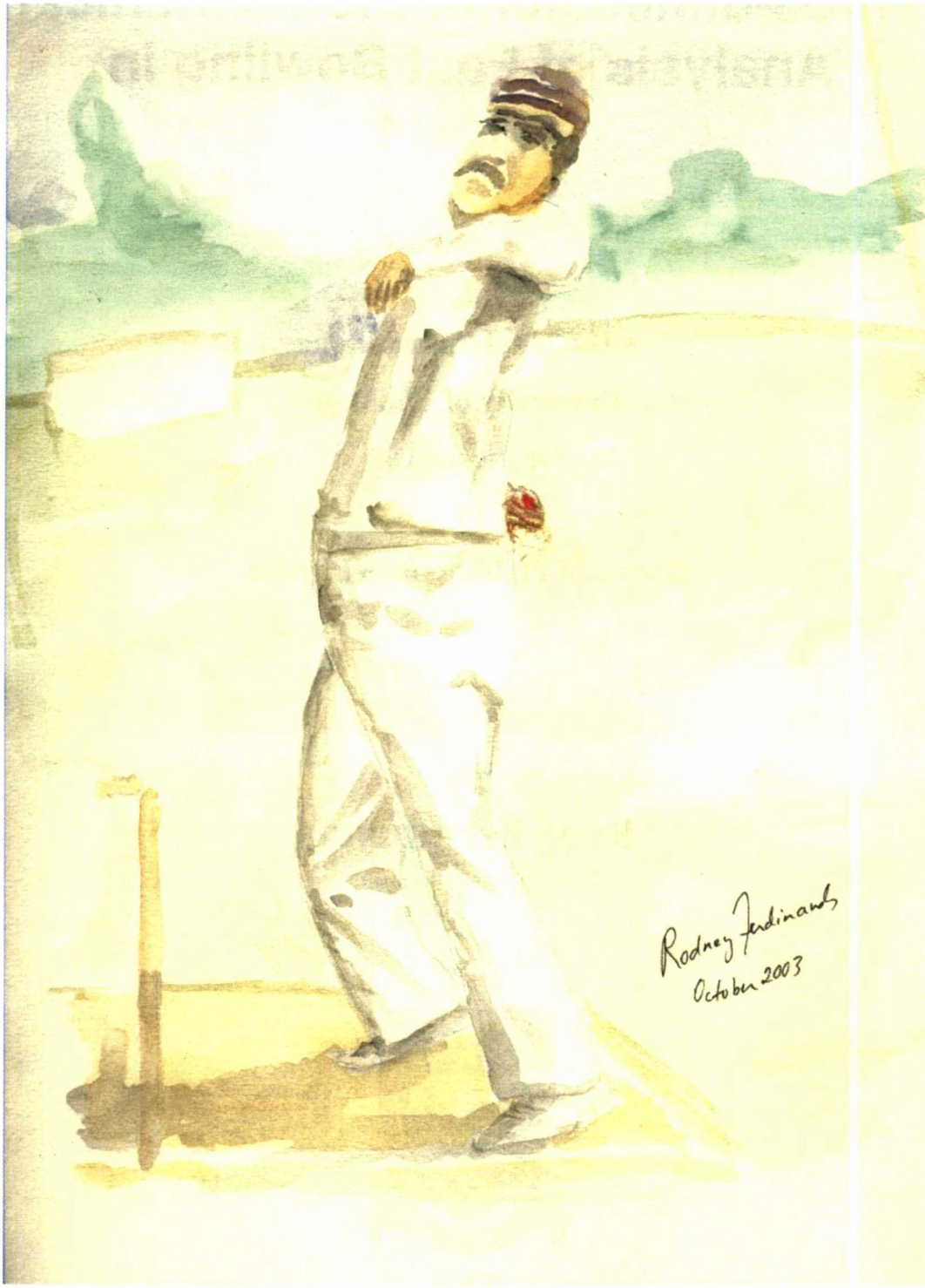

Frontispiece: The great Fred Spofforth from Australia was arguably the first great fast bowler, who possessed a wide array of weapons. He used a slinging-type action, and once bowled a ball through W.G. Grace's beard. [Picture courtesy of Dr. Rodney Ferdinands]

Dedication

In memory of the late Denis 'Papa' VanderGert.

'Now inhabiting the heavenly spheres of existence where truth is the final reality'

Abstract

A three-dimensional (3-D) dynamics model of the human body has been developed to provide a mechanical basis for evaluating fast bowling technique. Thirty-four fast bowlers were selected for study and divided into four groups according to ball release speed. A five camera 240 Hz motion analysis system (Motion Analysis Corp.) was used to track markers on the bowler delivering a series of balls at a target in line with the wickets, and a Bertec force plate was used to measure ground reaction forces. The marker arrangement allowed for the 3-D motion tracking of all major body segments. The resulting kinematic and force plate data of a typical ball were fed into a computer model using Mathematica's Mechanical Systems Pack. This is a set of packages designed for the analysis of spatial rigid body mechanisms by implementing a dynamics formulation with Lagrangian multipliers. The computer model gives a 3-D representation of the human body as a system of fifteen rigid body segments with mass and inertia properties. The model can output the kinematics, inverse solution dynamics, kinetics and powers for each body segment of a bowler delivering a ball.

Bowling in cricket is a unique method of propelling a ball at high speed so that it reaches a batter 20 m away after having bounced once off the pitch. Fast bowlers reduce the time available for the batsman to execute the correct stroke, and therefore increase the chance of error. There are a number of coaching texts available that propose various hypotheses on the correct technique of fast bowling, which have been mostly based on the experiences of successful fast bowlers. However, dynamics has not played any meaningful role in the development of fast bowling technique.

In this thesis, the synthesis of a 3-D rigid body model of bowling was used to calculate the inverse solution dynamics, kinematics, kinetics and segment power flows to test certain established hypotheses on the mechanics of bowling technique. The analysis also probed for mechanical differences in technique between bowling speed groups. It was found that lower trunk, upper trunk,

bowling arm, front arm, front leg, and rear leg interacted in such a way that each segmental motion was subject to a kinematic sequencing pattern and a dynamics actuation pattern determined by the calculation of muscle powers. Also, it was possible to differentiate between the consequential motion of a segment, and the actuation of a segment motion. This information provides a perspective of how the body needs to move in order to achieve correct technical form. The results show that that certain established concepts of bowling technique, such as front arm 'sweeping' and 'pull down', lower trunk flexion, and rear leg action have only been partially specified. Also, in certain technical and sequencing aspects there are differences between the bowling speed groups.

Preface

In this modern age, the scientific method is used as the tool of investigation. Every facet of our material existence has been changed by science. Whether it is transport, communication, electronics, or medicine, science has made immense strides in these areas in a relatively short period of time. Just think back to the cars on the road in the 1950s, or the computers in use just 20 years ago. It is time more science is applied to the art of bowling in cricket.

In recent years there has been some excellent biomechanical research in fast bowling, particularly with respect to the identification of the mixed bowling technique, which produces a higher incidence of lower lumbar injury. Yet, much of the information on what constitutes correct bowling technique is based largely on the subjective experiences of past and present fast bowlers. Some of it is of definite value, and can be used to improve the performance of bowlers. However, in some cases, the proposed technical theories have little scientific basis. In other cases, prescribed techniques are only applicable to a particular type of bowler. This is the danger of the current situation. It is assumed that what works well for a particular elite bowler is applicable to others. The issue of individuality may not be given its due place. For instance, every human on this planet has a different anthropometry from the next, with some deviating from the norm more than others. This is one reason why each person has a unique gait – no two people are likely to walk in exactly the same manner. Also, no two people are likely to generate exactly the same set of motor patterns to perform the same task, or movement sequence. There is plenty of evidence of this in bowling. Compare the bowling actions of *Joel Garner* with *Malcolm Marshall*, or *Dennis Lillee* with *Bob Willis*, and there is evidence that people can perform the same task successfully in different ways.

There is a danger that in the proliferation of bowling technical coaching today, bowlers are forced to conform to certain qualitative biomechanical models, which have not undergone formal scientific scrutiny, and are also singularly prescriptive in their schemes for optimality. Coaching manuals of bowling technique

generally embody such an approach, but strangely contain little more information than the coaching texts of at least 50 years ago. Is it possible that the paradigm of bowling technique established in the early days still strongly influences the development of qualitative bowling biomechanics today?

Unfortunately, the mechanics of bowling has had relatively little biomechanics attention. Many of the idealised configurations in the coaching manuals have not been tested scientifically. As a result, the wonderful range of techniques used by bowlers to confound batsmen throughout the world may be reducing with time, and for no apparent reason. On a personal note, as an ex-first class cricketer and experienced cricket coach, I have seen naturally talented bowlers lose their effectiveness in a matter of minutes due to perhaps a well-intentioned, but misinformed coach. Perhaps this situation is more prevalent in countries where there is a lot of coaching. And, on a philosophical note, perhaps a lack of knowledge brings out the innate desire in humans to make people conform as some sort of psychological defense mechanism? We need to know. Uncertainty is undesirable!

In this thesis, a study of the fast bowling action is carried out. This thesis is not written with the objective of solving the mechanics of fast bowling. Bowling is a complex activity, involving the interaction of many segments in a synchronous manner to propel the ball. Instead, I hope this work will prove to be a small step in the right direction by showing that the science of biomechanics can reveal much about the mysteries of bowling. It is only when a deeper knowledge of the intricacies involved in bowling is gained, that the value of one's subjective experiences can be shared with others in the right context. Then there is an improved chance that the coach can make a genuine contribution to improving the performance of fast bowling in cricket, particularly by increasing the overall efficiency of the action, which would generally lead to a higher level of accuracy and faster ball release speed.

The thesis consists of five chapters, and is structured as below:

Chapter 1 introduces the thesis, giving a brief background, stating the thesis objective, and presenting the overall structure of the thesis.

Chapter 2 reviews the current literature on the biomechanics of bowling, and also provides the necessary background for the research. This chapter is designed so that it explains the basic technical characteristics of bowling in light of (i) the findings of other researchers in the field, and (ii) the experiences of past players. It also shows that past researchers have recognised the importance of understanding the role and relative contribution of the technical components of the bowling action.

Chapter 3 presents the methodology of the thesis, proceeding from data collection and 3-D motion analysis procedures to the development of a 3-D rigid body dynamic model of the bowler.

Chapter 4 analyses the results of the study. It presents and discusses the kinematics, dynamics, kinetics and power calculations in relation to bowling mechanics to verify or refute current hypotheses on bowling technique, and determine mechanical differences between bowling speed groups.

Chapter 5 is the conclusion of the thesis, and discusses the results of the thesis, their importance and applicability. It also shows a direction for future research into the biomechanics of bowling.

Also, any supplementary material is placed in the appendices.

During the term of this thesis, the following papers and presentations were published:

Marshall, R.N. and Ferdinands, R.E.D., 2003. The effect of a flexed elbow on bowling speed in cricket. *Sports Biomechanics*, 2 (1), 65 – 72.

Ferdinands, R.E.D., Marshall, R.N., Round, H. and Broughan, K.A., 2003. Ball speed generation by fast bowlers in cricket. In *Proceedings of the XVIII Congress*

of the International Society of Biomechanics, edited by Milburn,P., Wilson, B. and Yanai, T. (Dunedin: University of Otago), p. 103.

Ferdinands, R.E.D., Marshall, R.N., Round, H. and Broughan, K.A., 2003. An inverse/forward solution model of bowling in cricket. In *Proceedings of the IX International Symposium on Computer Simulation in Biomechanics*, edited by Smith, R., Casolo F., Hubbard, M., Sinclair P., Glitsch, U. (Sydney: University of Sydney), p. 33.

Ferdinands, R.E.D., Broughan, K.A. and Round, H., 2002. A time-variant forward solution model of the bowling arm in cricket. In *International Research in Sports Biomechanics*, edited by Hong, Y. (London: Routledge), pp. 56-65.

Ferdinands, R., Marshall, R.N., Round, H., & Broughan, K.A. 2002. Bowling arm and trunk mechanics of fast bowlers in cricket. In *Proceedings of the Fourth Australasian Biomechanics Conference*, edited by T.M. Bach, D. Orr, R.Baker, W.A. Sparrow (Melbourne: La Trobe University), pp. 176-177.

Ferdinands, R.E.D., Broughan, K.A., Round, H. and Marshall, R.N., 2001. A fifteen-segment 3-D rigid body model of bowling in cricket. In *Computer Simulation in Biomechanics*, edited by Casolo, F., Lorenzi, V. and Zappa, B. (Milan: Libreria CLUP), pp. 99-104.

Ferdinands, R.E.D., Broughan, K.A., Round, H. and Marshall, R.N., 2001. A fifteen-segment 3-D rigid body model of bowling in cricket. In *XVIII Congress of the International Society of Biomechanics*, edited by Muller, R., Gerber, H., and Stacoff, A. (Zurich: ETH), p. 236.

Ferdinands, R.E.D., Broughan, K.A. and Round, H., 2000. Cricket bowling: a two-segment Lagrangian model. In *Proceedings of the XVIII International Symposium on Biomechanics in Sports*, edited by Hong, Y. and Johns, D. (Hong Kong: CUHK Press), pp. 517-520.

Ferdinands, R.E.D., Broughan, K.A. and Round, H., 2000. Cricket bowling: a two-segment Lagrangian model. In *Proceedings of the Fifth Australian Conference on Mathematics and Computers in Sport*, edited by Cohen, G. and Langtry, T. (Sydney: UTS Printing Services), p. 197.

Also, award nominations were received for abstract and presentation at the following conferences:

Highly Commendable Young Investigator Award at Fourth Australasian Biomechanics Conference 2002 (Melbourne).

Finalist for ISB 2003 Young Investigator Award for Podium Presentation at XVIII Congress of the International Society of Biomechanics (Dunedin).

Acknowledgements

First and foremost, I would like to thank my supervisor Dr. Howell Round, for not only dedicating substantial time in planning and reviewing this work, but for giving me the unique opportunity to perform research in the field of biomechanics in the Department of Physics and Electronic Engineering. I am very grateful to him for his sound advice and invaluable experience, which have proved so important throughout the duration of this work, especially when things were tough. I will try to keep in touch with Howell in the years to come.

I thank Prof. Kevin Broughan for spending the time to construct a special topic in mathematics to suit my research requirements. The tools he gave me have served as the foundation of my cricket research. Also, his experience and knowledge have been of tremendous benefit to me. It has been a real pleasure working with Kevin, and perhaps we may conduct further research together at some date in the future. Special thanks also to Dr. Nick Ling for supporting this project, and having a good deal to do with its success. He was one of the first to support my research project despite its inauspicious beginnings.

Special thanks to Prof. Bob Marshall, who first supported the idea of a collaborative research venture between University of Waikato and the University of Auckland, and has helped me throughout all phases of my PhD research. His knowledge and experience in the field of biomechanics is second to none, and it was a great privilege to have him as one of my supervisors. I look forward to doing further research with him in the future.

Without Heidi Eschmann this thesis may not yet be completed. Her secretarial skills and practical ideas have consistently bailed me out of trouble spots over the last four years. The department is most fortunate to have her services. Thanks also to the men behind the scenes, Bruce Rhodes, Stewart Finlay, Scott Forbes and Dave Bugden. They have consistently proved that nothing is possible without quality technicians. Other notable staff that have helped me many times out of

difficult spots have been Dr. Alistair Steyn-Ross and Dr. Michael Cree. I also thank Dr. Murray Jorgensen for giving some much needed help with the statistics.

Thanks to the GaitLab at the University of Auckland and their knowledgeable staff for supervising the use of the laboratory and equipment. A special thanks to Joe Hunter who collaborated with me during the exhausting testing sessions. I wish him the best for his PhD on athletic sprinting.

Special thanks to Warren Frost of New Zealand Cricket, and Kaushik Patel of the Auckland Cricket Association, who both supported this study by dedicating the time and effort to provide me with quality subjects, sometimes at short notice.

Huge thanks to Mum and Dad for their unconditional love, support, encouragement, and advice throughout my academic life. I will always remain indebted to them. Thanks also to Dr. Edred Ferdinands, Dr. Rodney Ferdinands and the late 'Babs" Pierre Ferdinands for their unique blend of practical and intellectual wisdom on a limitless range of topics. These greatest of great men lifted my level of thinking to greater heights. I look forward to continuing this process of mind building in the near future.

A special thanks to Dr. Rodney Ferdinands for supplying me with one of his many artistic paintings of cricketers to use as the frontispiece in this thesis. Also, thanks to Darren Ferdinands for readily discussing his highly intellectual views on all aspects of cricket, and stimulating my mind in times of need.

I thank Ranjit and Jyotsna (Daddy & Mummy) from the bottom of my heart for their loving support and tolerance during my stay with them. My ability to finish my thesis would not have been possible without them.

A great thanks to Hema, who helped register my businesses in biomechanics, and is always ready to talk about all subjects and matters. A special thanks to Neetu, who is always ready to help in need, and makes things easier for us at home. These two people in their very different ways are very special people to me.

Finally, most importantly, thanks to my wonderful wife, Mira, for being perfect in an infinite multitude of ways. Her love is the motivating force of my life, and therefore this thesis is also dedicated to her.

TABLE OF CONTENTS

LIST OF TABLES

LIST OF FIGURES

LIST OF ABBREVIATIONS

ASIS	anterior superior iliac spines
BFC	back foot contact
BW	body weight
CoM	centre of mass
DOF	degrees of freedom
FFC	front foot contact
G	gravity vector
GRF	ground reaction force
LRS	local reference system
PC	phase cycle
PC_{KEmax}	phase point of maximum kinetic energy
PSIS	posterior superior iliac spines
REL	ball release
STP	sequence transition point
TCDF	torque contribution difference factor
VM2	virtual marker based on two known markers
$VM2_{dist}$	virtual marker defined as distance between two markers
$VM2_{\%}$	virtual marker defined as percentage distance between two markers
VM3	virtual marker based on three known markers
$VM3_{dist}$	virtual marker based on distance in the local coordinate system
$VM3_{\%}$	virtual marker based on percentage distance from origin and local Y-axis in local coordinate system
VR	variance ratio
2-D	two dimensional
3-D	three dimensional

Chapter 1 INTRODUCTION

1.1 BACKGROUND

Cricket derives its name from the Old English word "cryce", which means stick. The termination "et" refers to small in size. The game therefore is named after its main weapon of attack, a little stick or staff, referred to as the bat. Originally the game was played by country lads who bowled a ball at a tree stump, or at the hurdle gate that led into their sheep pens. This consisted of two vertical bars separated by a small distance, and a crossbar resting on their slotted tops. Later these evolved into what is called the "wicket" and "bail".

During these early stages of the game, bowling was no more than the strict meaning of the word, i.e. rolling the ball along the ground (Wilkins, 1991). Such bowling was termed "under-arm", where the trajectory of the bowling arm had to be kept below the level of the shoulder. Later, under-arm bowlers began delivering the ball through the air, and pitching it at a length from the batsman. This process made run scoring easier, so the "under-armers" introduced spin, and swerve to their deliveries. In his venture to continually make things more difficult for the batsman, a bowler named Tom Walker around the year of 1790 eventually stretched his arm out horizontally. Such bowling was called "round-arm". The extra speed and bounce generated by this technique required a drastic change in batting technique to counter it. Though there was an attempt to ban this mode of delivery from the game, the Code of Laws in 1835 officially legalized it, and the game began its evolution towards the modern form. The process was completed when bowlers began raising the arm higher and higher in defiance of the law. Again there was much controversy during this period of development, but eventually good sense prevailed, and the modern "over-arm" bowling action was born.

Since these primitive beginnings, the art of serious bowling has gradually evolved into a professional activity. In fact, many international bowlers are now in a position to earn a livelihood from the game. Sponsorships, advertising contracts

and the like make the game even more lucrative for the elite. The demand on these players is high, not only as a result of their own desire to succeed, but through the external pressures imposed on them by corporate bodies, cricket boards, and not least of all, the public. This professional drive leads to a demand for higher performance levels. It is not surprising that interest in the biomechanics of bowling increased as the game became more professional.

Much of the early interest in the 1980s was focused on the study of injuries sustained by fast bowlers. The incidence of lower back injuries to fast bowlers, particularly to young ones, seemed to be increasing. Sometimes these injuries were crippling in nature, forcing bowlers out of the game prematurely. This became a concern for cricket administrators, as fast bowlers are often responsible for winning matches. Also, fast bowling was in danger of being labeled a high-risk activity. Prominent researchers delved deeply into the biomechanics of lower lumbar injury, citing improper bowling technique, inadequate physical preparation, and overloading as thepossible causes.

Other researchers analysed the kinematic characteristics of bowling by using cinematographic techniques, or more recently, video motion analysis systems. Typical research schemes centred on selecting a sample of bowlers, and then dividing them into two groups based on speed. The bowling characteristics of the faster group were then compared to those of the slower group in an attempt to correlate certain kinematic parameters with ball speed. Much useful research was conducted in this way giving coaches a deeper understanding of the technical factors involved in the art of bowling. However, much more research is needed. Bartlett et al. (1996) completely reviewed the biomechanical research on bowling, stated that cricket, in general, had not been well served by biomechanical research. They went further and stated "*there is clear agreement on the importance of ball release speed in fast bowling, but no consensus in the scientific literature on the elements of the bowling technique which contribute most to this*". The aim of this thesis is to make a further contribution to biomechanics research on bowling technique by examining some of the outstanding issues.

1.2 STATEMENT OF THE PROBLEM

Success in fast bowling is determined by a combination of many factors. Assuming a reasonable degree of bowling accuracy, then the one extremely important variable is the speed at which the ball is released. In fact, a reasonable conception of an efficient bowling technique would be one that allows the bowler to bowl fast with a relatively low level of injury risk (Bartlett et al., 1996).

Biomechanics uses the various branches of mechanics to study human movement. In this thesis, kinematics, kinetics, and dynamics were used to find the mechanical factors that underlie the execution of the fast bowling action (Figure 1-1). Primarily the focus was on relating these factors to the production of fast ball release speed, as this is one of the main purposes of fast bowling. An added ball release speed would multiply the effect of the other more refined skills, such as accuracy, swing, and cut. However, some consideration was also given to the safety of the action as the high injury rates in fast bowling are of great concern in cricketing countries. Also, biomechanics should always look at performance enhancement within the safe range of anatomical constraints.

The purpose of this study was to use a three-dimensional (3-D) rigid body dynamics model of the human body to resolve current hypotheses about the mechanics of fast bowling technique. There were three main aspects of this investigation:

1. The use of a sufficiently sophisticated 3-D motion analysis system and force platform to experimentally collect the kinematic and ground reaction force (GRF) data of fast bowlers, respectively. This included the development of a full body kinematic model of the human body in the motion analysis software to convert captured data points into link segments.
2. The construction of an appropriate 3-D rigid body dynamics model of the human body to mathematically calculate the segmental forces and joint torques on fast bowlers during delivery.

3. Comparison of the analytically determined solutions for different performance measures. This included the analysis of kinematics, dynamics, kinetics and segment power data.

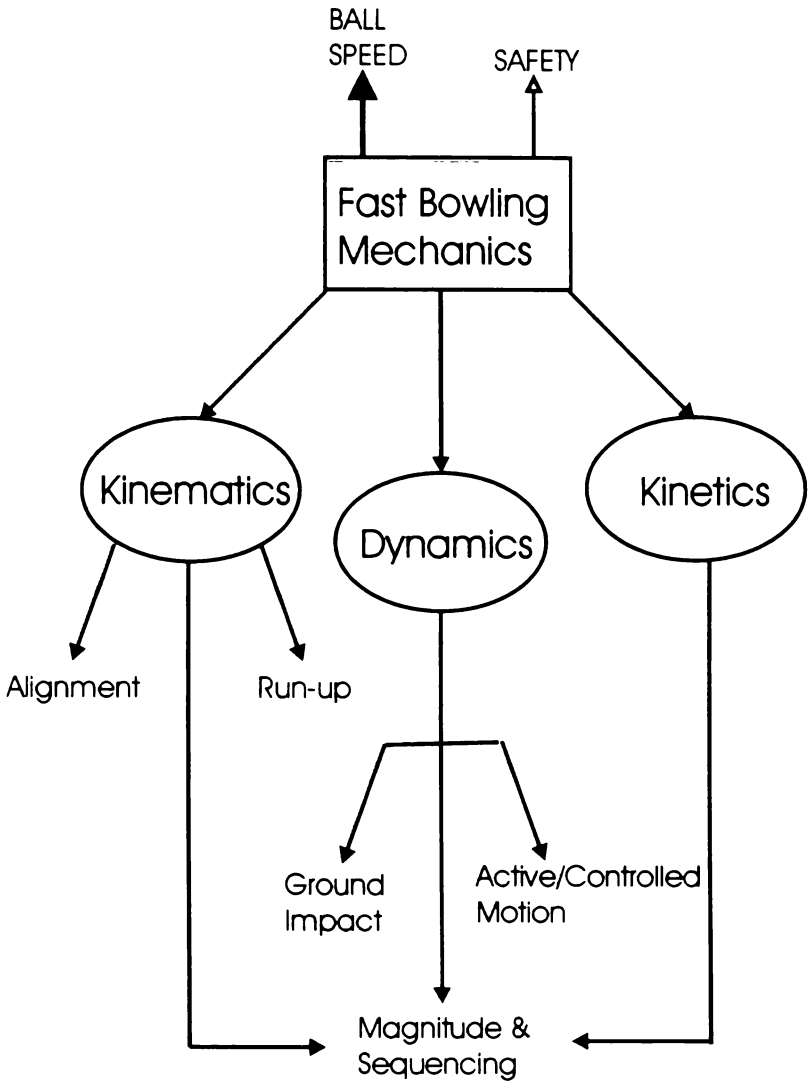

Figure 1-1: Flow chart showing the interrelationship between the branches of mechanics in the analysis of fast bowling with respect to the output factors - ball release speed and safety.

Fast bowling technique involves the complex interaction of all the major body segments, which move at high velocities, and rotate in different planes of motion depending on the phase of bowling. Therefore, a sophisticated 3-D motion analysis system was used to accurately track the motion of the limbs of a subject during the process of bowling a ball. A high-speed red light motion analysis system, capable of processing a frame rate of 240 Hz, and capturing accurate

kinematic data, was determined to be an appropriate system, despite being limited to the confines of the laboratory.

The red-light motion analysis system is marker-based, so a human body link-segment model was developed to translate the positions of the markers on each segment to represent segment joint centres, which were linked to form a rigid body skeleton. The movement trajectory of the bowler's limbs during delivery could then be represented as the motion of this skeleton. In the laboratory, a force platform was employed so that back and front foot contact GRFs could be measured during delivery stride. The kinematic and ground reaction force data could then be fed into an appropriate dynamics model to calculate the segmental forces and joint torques during delivery.

To develop a dynamics model, the human body is represented as a system of rigid body segments with mass and inertial characteristics chosen to approximate those of the body. The equations could be derived by hand using a variety of dynamics formulations, such as the Newton-Euler method, Kane's method, and the Lagrangian method. However, the number and complexity of the equations that need to be derived and then solved for this model would be very large, and therefore the solution process slow and prone to error. A more practical approach was to implement a dynamics software package to assist in this task.

With the 3-D motion analysis system and force platform ready to collect data, and the rigid body dynamics model of the human body completed, the final step was to select a suitable sample of subjects for testing. The ideal sample had to be large, and contain bowlers of various standards, so that correlations could be made within the sample. This was achieved by recruiting fast bowlers from different competition levels, including international and provincial representatives.

Once the subjects were selected, a trial-based protocol was established to ensure that testing procedures were the same for each subject, and carried out safely and within the designated period of time. Ideally, the researcher wants to obtain a comprehensive data set. However, there needs to be a compromise between the size of the data set, and the available testing time. A sample of over thirty fast

bowlers was large when compared to samples that had been previously tested in cricket.

When data collection was completed, the motion analysis software was used to automatically track the trajectory of the markers on the body. This process was not perfect, and was supplemented with manual tracking. The result was a set of kinematic data, which could be smoothed, and then used as input for the dynamics model along with the force platform data, yielding the forces and torques on each of the major body segments of the bowler during delivery.

The final stage was the integrated analysis of kinematics, dynamics, kinetics, and power output data to investigate the mechanics of fast bowling technique. The process involved the examination of the underlying characteristics common to fast bowlers, so that certain fundamental mechanics of bowling technique could be established. Also, the mechanical features that differentiated between bowling groups of different ball release speed were determined. The ultimate purpose of this analysis was to test the validity of existing hypotheses on what constitutes proper bowling technique.

1.3 THESIS HYPOTHESES

Based on the review of scientific and coaching literature the following hypotheses were formulated:

- Ball release speed varies with the pattern of active versus controlled movement.
- The overall segmental sequencing of the bowling action is from the lower body upwards, and for the upper body proximal to distal.
- Ball release speed varies with the kinematics of the bowler's centre of mass.
- New Zealand bowlers predominantly use mixed action techniques.

Cricket coaching programmes are now commonplace throughout most of the recognised cricket countries, and specifically target populations of young prospective bowlers with the intention of developing their abilities to play at the higher levels. This task is a difficult one beset with a range of problems. This is mainly because there have been no kinetics and dynamics studies of the bowling action, leading to a lack of knowledge on which segment movements are performed actively (i.e. when the joint torque and angular velocity act in the same sense), and which ones are controlled or resisted (i.e. when the joint torque and angular velocity act in the opposite sense). As a famous coach once said: "Do not confuse what happens with what needs to be done!" When a torque is used to accelerate a segment that instead should be decelerated, a reaction is induced that is transmitted throughout the kinetic link chain, and may adversely effect the segmental sequencing. Current coaching methods are based chiefly on kinematic studies, or from the mere observation of video footage of proficient bowlers, or even through the pure subjective method: the opinions of past successful bowlers based on the interpretation of their kinesthetic awareness while delivering a ball. Kinematics has an important role to play in biomechanics, but it cannot effectively determine how the segments are moved. A problem with the subjective method is that there is a time lag between the actual execution of a movement and the perception of a movement due to the fast but finite speed of the nerve impulses. A consistently accurate interpretation of fast movement sequences is therefore unlikely. It is also almost impossible to accurately differentiate between active and controlled motion. Therefore, certain theories on aspects of fast bowling technique may need revision under the scrutiny of a formal biomechanical analysis.

In this thesis, therefore, not only is segmental sequencing analysed from a kinematic perspective, but also with respect to the patterns of active and controlled motion. Generally in biomechanics it is considered that segmental sequencing is important in producing efficient movements involving multiple segments, particularly if such movement sequences produce a fast end-effector speed, such as in throwing, golf, and tennis. Cricket bowling is such a movement sequence, so it is plausible that faster bowlers are able to produce more optimal segmental sequencing schemes than slower bowlers. In biomechanics, it has been

traditionally asserted (with some notable exceptions) that efficient sequencing schemes are proximal to distal. However, to what extent this is true in bowling has not been sufficiently determined. Analysing the sequencing patterns of bowlers, and determining whether there are differences between fast bowlers of different speeds should produce important findings on what constitutes good bowling technique.

Previous research has mainly focused on the role of the run-up in terms of its velocity contribution to ball release speed (Bartlett et al., 1996). However, there is more to the run-up than achieving maximum pre-delivery velocity. The run-up must also enable the fast bowler to go through the delivery stride in a balanced manner. To study how a fast bowler is able to do this, the kinematics of the bowler's centre of mass could be calculated during delivery stride. Also, the faster bowlers may exhibit different kinematic properties from the slower bowlers.

Also, the important issue of bowling safety is addressed. There is scientifically valid evidence that the mixed action technique increases the susceptibility to lower lumbar injury (Elliott, 2002). As the sample of fast bowlers tested is large and representative of different competition levels in New Zealand, the determination of the percentage of mixed action bowlers in this sample may indicate the prevalence of this type of action throughout the country in general. The number of cases that are reported through the media, and through the local cricket associations of fast bowlers sustaining lower back injury suggest that the mixed action technique is more common than previously thought. Therefore, these results would be important to the governing cricket authorities in New Zealand.

1.4 DELIMITATIONS OF THE STUDY

Subjects for the present study were 34 male fast bowlers from four competition levels in New Zealand: international (9), national (10), provincial (8), and regional (7). Generally, the subjects were chosen so that the sample would contain bowlers with a good spread of abilities and ball release speeds.

Each subject performed two trial types, each requiring the bowler to deliver six balls at the wickets within an acceptable range on a standard 20 m pitch length. Each ball was delivered at maximum speed. Subjects were allowed to have a few minutes rest between balls, if required, to minimize any effect of fatigue. The only difference between the trial types was that in the first one the subject had to make front foot contact with the force platform, whereas in the second one, he had to make back foot contact. The order of the subjects was randomly assigned.

1.5 LIMITATIONS OF THE STUDY

The nature of biomechanical research means that a compromise needs to be made between sample size and the number of trials. The selection of sample size is not only dependent on the available number of qualified subjects, but also dependent on the experimental and data processing time per subject. The statistical concepts of effect-size and power can be used to test that for the sample number chosen statistical significance can be established for differences between the variables measured. Previous bowling studies have shown such statistical significance with similar or lower sample numbers than used in this study, so the sample number was determined to be appropriate. As this time was of the order of weeks per subject, and ball release speed was a major factor in this study, only the maximum ball release speed trial was chosen for analysis from each data set. Though this does ignore intra-subject performance variability, this may not be so important if there are found to be common mechanical features in subjects having similar ball release speeds. Also, a common basis was established on which to choose the trial for analysis (i.e. maximum ball release speed).

As there was only one force platform in the laboratory that could be used in the study, there was no method of measuring the ground reaction forces simultaneously during delivery stride. Therefore, front foot and back foot contact trials were conducted separately. All kinematic data were collected for the front foot contact trials, so the front foot ground reaction forces corresponded directly with the kinematic data. The back foot ground reaction forces for this kinematic data set were then found by taking the average of the back foot ground reaction forces measured from the back foot contact trials. The back foot ground reaction

forces may therefore not exactly reflect what is happening during back foot contact. However, the ground reaction forces on the front foot are on average 2-3 times higher than for the back foot, and also the forces on the back foot are not believed to play an important role in the power generation phases of the bowling action, which is the most important period of analysis.

The kinematic data of bowlers was collected via a marker-based motion analysis system. The determination of joint centres based on different marker arrangements may have an effect on the measured kinematics, which would subsequently have a larger effect on the dynamics. This is not such a limitation for the lower limbs as there have been several marker sets developed and validated for clinical gait trials. However, the development of a standardised marker set for the upper body is at an early stage due to the variety, complexity and range of upper extremity movements (Rau et al., 2000). This can also be considered part of the overall problem of marker based measurement. For instance, there is always a difference between the trajectories of the external markers and those of the skeleton, which will also influence the accuracy of the results (Cheze, 2000). In addition, the placement of markers will vary slightly on each subject. The best the researcher can do at the moment is minimise such errors to produce a reasonably consistent kinematic dataset.

Considering the data collection was inside a biomechanics laboratory, where a run-up was performed on a synthetic athletics track, and front foot and back foot contact made on a vinyl-covered force platform, the bowling action analysed may not fully reflect that performed in a match situation. The synthetic surface also required the subjects to wear bowling rubbers instead of spikes as they would normally do in a match. In some cases, subjects required longer run-ups than the 18 m allowed for by the facility, and so this may have effected their rhythm and timing. However, none of the subjects reported that ball release speed was significantly lowered due to this restriction.

1.6 ASSUMPTIONS OF THE STUDY

It was assumed that the subjects accurately reported that they were free from any injury or physical dysfunction that would effect their performance. Considering the relatively small number of trials compared with the number of balls that a fast bowler is required to bowl in a spell, it was assumed that the effect of fatigue in bowling performance was negligible. However, to reduce this likelihood further, verbal confirmation from the bowlers as to their physical status was regularly received. Finally, it was assumed that the characteristics of bowling performance in the lab were similar to those exhibited in a match situation.

1.7 SUMMARY

Resolving the four listed hypotheses would therefore be of considerable interest and importance to the cricket community, both at a local and international level. To an appreciable extent, these hypotheses were resolved in this thesis by examining and interpreting the kinematics, dynamics, and kinetics data of fast bowlers. Such information could provide the basis for assessing and improving bowling technique. It gives coaches the diagnostic tools to evaluate bowling technique from a more scientific viewpoint, and therefore more accurately prescribe technical changes to increase the efficiency of a bowler's action. The impact of this would be two-fold: a more efficient action is more likely to enhance performance in terms of speed and accuracy, and may also place less strain on critical anatomical structures, which could then lead to an overall decrease in susceptibility to injury.

Chapter 2 REVIEW OF LITERATURE

2.1 INTRODUCTION

The purpose of this chapter is to briefly cover the fundamentals of the basic bowling action within a review of the current literature on the biomechanics of bowling. The reviewed literature shows that much of the past research in bowling biomechanics has concerned itself with trying to establish the role and importance of the various technical components in the generation of ball speed. This was usually performed by obtaining various kinematic data of bowlers using cinematographic techniques or a video motion analysis system, and then investigating this data for correlations between the data and ball speed. Sometimes a force plate, (a floor mounted device to measure ground reaction forces from the athlete's feet contacting the ground), and electromyography were used to supplement this data.

The basic steps involved in the bowling action are described in terms of the side-on technique. This does not imply that this technique is the only or best means of delivering a ball. It happens to be that the basic bowling action specified in most texts is almost always described in terms of the side-on technique. The reason is partly because it has been traditionally established as the optimal technique, and that most of the successful bowlers in the past have been known to use it (N.S.W.C.A., 1966; Marylebone Cricket Club, 1976). Also, most coaches believe that the basic mechanics of the side-on bowling technique serve as the best introduction to those who are first learning the game. It is easier to understand the front-on action in terms of the side-on action, rather than the other way around. However, the literature review reports research on both the side-on and front-on actions, and the findings made in thesis should be considered important to both types of bowling actions.

Note that the convention of using italics to name bowlers is adopted here in order to distinguish them from the names of researchers. Also, this thesis adopts the convention of referring to a right-hand bowler.

2.2 THE FAST BOWLING TECHNIQUE

2.2.1 Basic Action

The purpose of the bowling action is to deliver a ball at the desired speed and trajectory on a good length from a comfortable, well-balanced position, whereby the maximum efficiency is obtained from the co-ordination of fingers, wrist, shoulders and body (Bradman, 1958). To do this consistently, a bowling technique must be established. Much of the advice in this area has been handed down by former elite players from their personal experiences and careful observations over the years.

The two accepted bowling actions in cricket are the side-on and front-on (or open) bowling actions, which differ in the orientation of the shoulders and hips during the delivery stride. In the former technique, lines running through the shoulders and hips approximately point in the direction of the stumps, and the torso is hidden from the view of the batter. In the latter case, the torso is more or less directly facing the batsman. In both actions, the angle between the shoulders and hips at back foot ground contact is minimised to promote the best chances of obtaining a good length at a high speed with minimal risk of injury (Bartlett et al., 1996). For the reasons discussed before, the fundamentals of bowling will be described in terms of the side-on action.

The basic sequence that constitutes the side-on action is as follows:

1) A comfortable, smooth, rhythmic run-up that gradually builds up in momentum as the bowler approaches the crease. All bowling actions are commenced with a run-up, and this varies in length depending on the type of bowler. Generally fast bowlers use longer run-ups than slower ones.

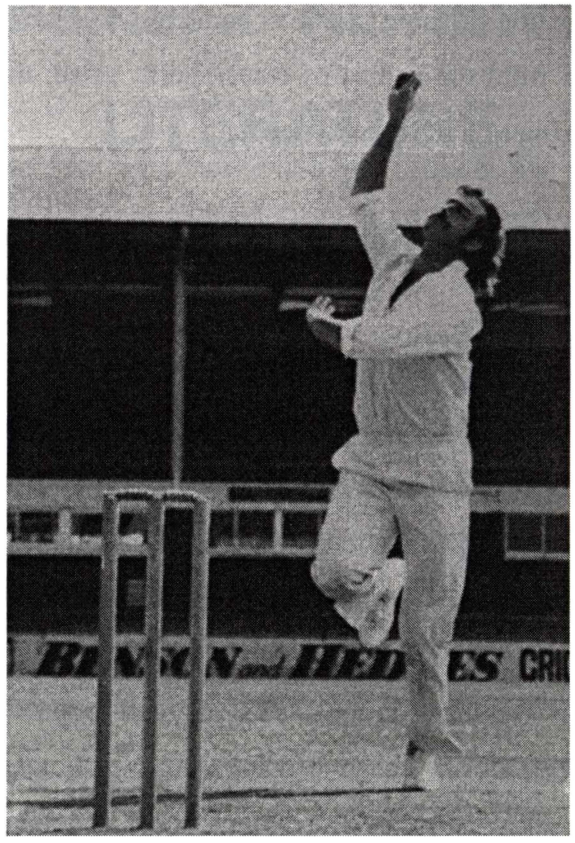

Figure 2-1: The predelivery jump off the left foot demonstrated by Dennis Lillee, arguably the greatest fast bowler in the history of the game [Photo from Lillee, D. 1977. *The Art of Bowling*, Collins, Sydney]

2) On the last stride of the run-up, a jump off the left foot propels the body into the air (Figure 2-1). This is a difficult stage to master, and it requires good co-ordination. Sometimes young bowlers jump off the right foot during this stage. Such bowlers compromise the fluency of their transition from run-up to pre-delivery stride, performing a hopping-type motion as they land on the same foot to make back foot contact.

3) Once in the air, the legs cross over, and the hips and shoulders rotate a half-turn to the right. The non-bowling arm is bent and in front of the body. This is commonly referred to as the "cradle" position. Note that the period before which the bowling arm is straightened or "locked" is referred to as the "pre-locked phase of bowling" (Ferdinands, 2000a & b; Ferdinands et al., 2002a). The arm gradually straightens as the non-bowling arm sweeps upward, and the bowler approaches the stage of making back foot contact with the ground.

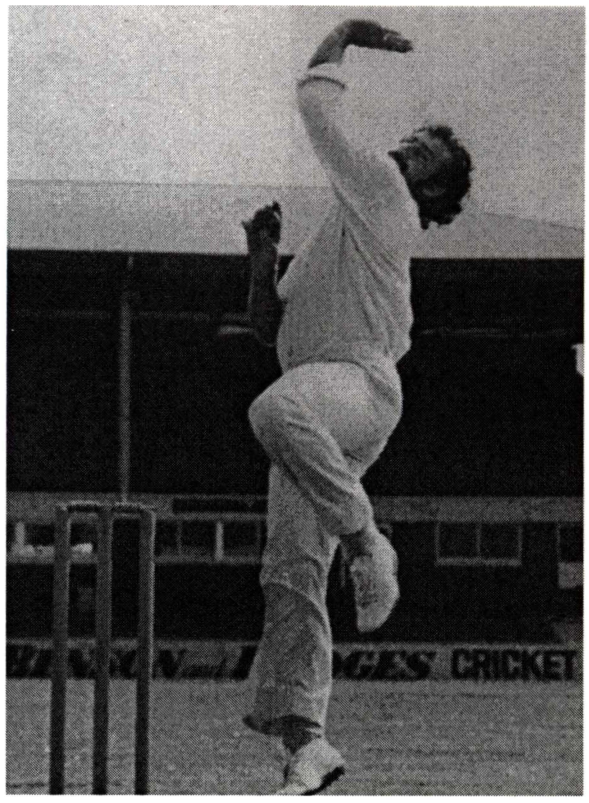

Figure 2-2: Dennis Lillee making back foot contact. [Photo from Lillee, D. 1977. *The Art of Bowling*, Collins, Sydney]

4) From the cradle position, the non-delivery foot (right foot) begins rotating so that it will land parallel to the bowling crease (Figure 2-2). As the right foot makes contact with the ground, the non-bowling arm performs a sweeping upwards motion, so that at back foot contact it is vertically in front of the head. The eyes are sighting the target from behind, or just a little to either side of the non-bowling arm.

5) During back foot contact, the weight is transferring to the back foot, the left leg raises, and the bowling hand moves near the right hip (Figure 2-3). Note that at this stage the arm is "locked", i.e. the bowling arm is now straight. This marks the beginning of the "post-locked stage" of the bowling arm action (Ferdinands et al., 2002a). Back foot contact marks the beginning of the delivery stride.

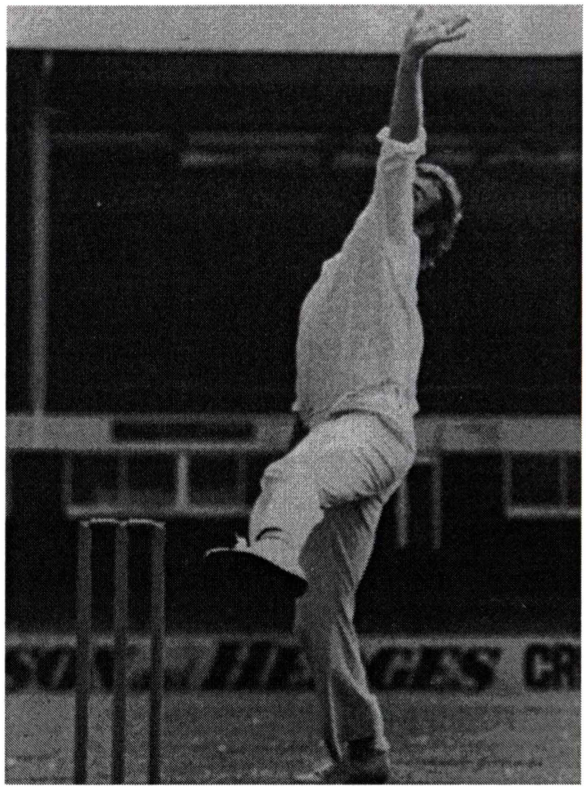

Figure 2-3: During back foot contact the arm is locked, and the front arm high. The delivery stride is initiated. [Photo from Lillee, D. 1977. *The Art of Bowling*, Collins, Sydney]

6) The forward swing progresses during the delivery stride as the ground reaction forces on the back foot are reducing. The motion of the non-bowling arm flexing vertically downwards is synchronised with the lowering of the left leg, the raising of the bowling arm, and the initiation of hip rotation to the left (Figure 2-4). During this stage, much of the power in the action is generated. Also, some bowlers take long delivery strides, while others prefer to take shorter ones.

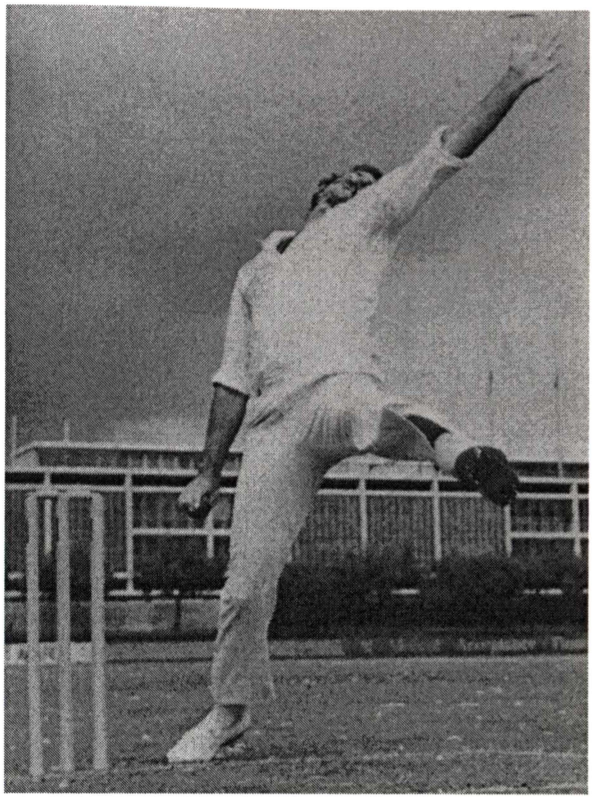

Figure 2-4: Forward swing during delivery stride. Back foot ground reaction forces reduce during the forward swing. [Photo from Lillee, D. 1977. *The Art of Bowling*, Collins, Sydney]

7) Towards the end of the forward swing, the front foot is approaching contact with the ground. During this time the non-bowling arm is adducting vertically, the hips make a quarter turn to the left, and the bowling arm is extending to a horizontal position behind the body.

8) At front foot contact, the front foot is pointing in the direction towards fine leg (i.e. behind and slightly to the left of a right hand batter) (Appendix L). The bowling arm is continually rotated vertically upwards causing the back foot to lift from the ground, and a further rotation of the hips to the left. The non-bowling arm continues its downward path past the left side of the body (Figure 2-5).

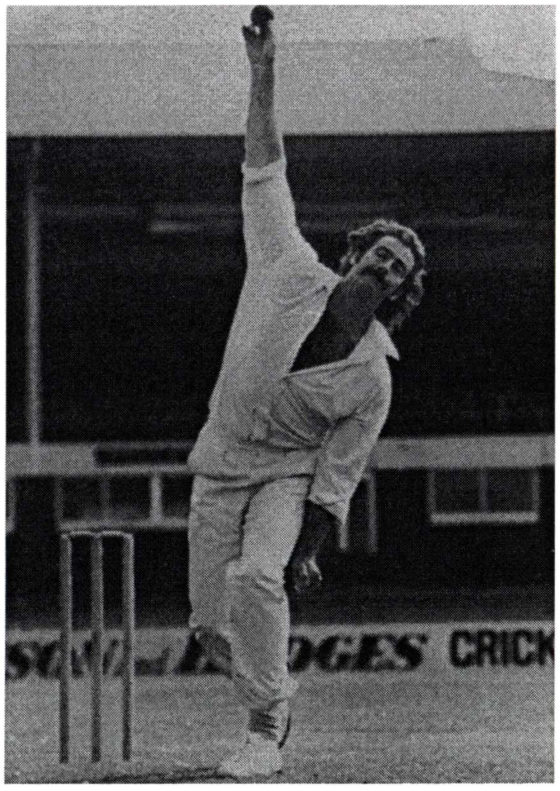

Figure 2-5: Ball release is executed during front foot contact. [Photo from Lillee, D. 1977. *The Art of Bowling*, Collins, Sydney]

9) At ball release, the bowling arm is just in front of the vertical, and a full pivot of the hips and shoulders is completed, so that the full weight is over the left leg (Figure 2-5).

10) The follow-through: the bowling arm has finished its revolution, and the right shoulder is pointing down the wicket. The non-bowling arm has been carried past the hips, and ends up behind the body on the left hand side. The right leg has past the left leg, initiating the final strides of the bowler towards the left side of the wicket. The objective of the follow-through is to take the bowler off the wicket, and absorb the forces of the bowling action (Figure 2-6).

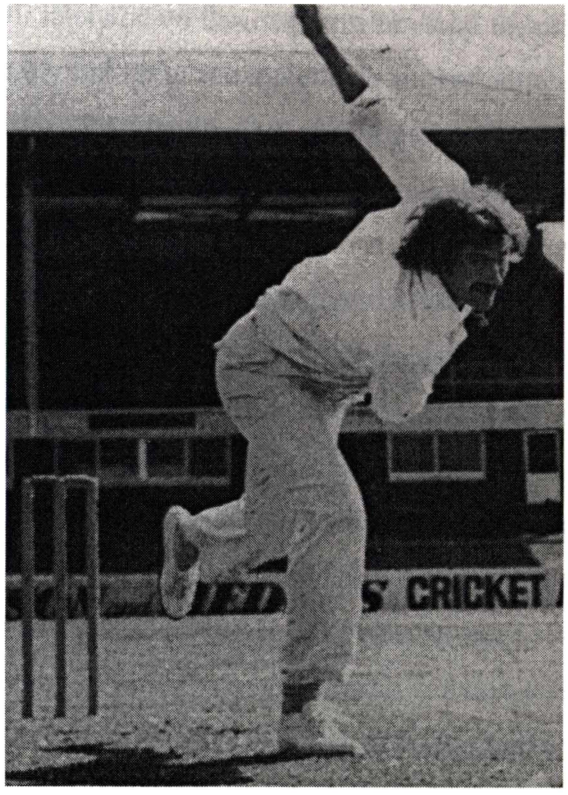

Figure 2-6: The powerful follow-through of Dennis Lillee. **[Photo from Lillee, D. 1977. *The Art of Bowling*, Collins, Sydney]**

In the following sections the key biomechanical aspects of the bowling action will be reviewed in more detail, largely based upon the findings of previous research.

2.2.2 Run-Up

The first stage of any successful bowling action is the run-up. A good run-up must be smooth, rhythmic, balanced, and sufficiently long to ensure that maximum impetus of forward movement is added to the momentum of the body behind the ball in the delivery stride (Tyson, 1976). The run-up is usually straight, but some front-on bowlers have also used curved run-up approaches to help them establish a more closed shoulder line at back foot contact. Philpott (1973) and Tyson (1976) both believe that a diagonal or curved approach enables the body to more easily achieve a side-on position at delivery, because the shoulders are already partially 'closed' during the run-up.

There are many different types of run-ups used by bowlers. It seems that run-ups vary to accommodate the unique characteristics of an individual's bowling action. For instance, *Malcolm Marshall* (West Indies), only 1.72 m tall used quick short strides in his approach to the wicket, whereas his counterpart, *Joel Garner*, a 2.06 m 'giant', used huge bounding strides to lope up to the wicket (Sobers & Smith, 1985). However, regardless of bowling style, the run-up of a fast bowler is an explosive activity with each foot strike during run-up generating forces of approximately three times the weight of the bowler (Elliott et al., 1989b).

Some authors believe that the run-up should start off slowly, gradually accelerating so that maximum speed is attained during the penultimate delivery stride (Gover, 1980; Bradman, 1958). However, biomechanical studies tend to indicate that elite fast bowlers do not commonly employ this strategy. Based on cinematographic studies of fast bowlers, Foster et al. (1984) reported that maximum speed is obtained three to four strides before delivery after which a slight deceleration occurs as the bowler "gathers" for the delivery stride. Mason et al. (1989) sampled several elite fast bowlers from the Australian Institute of Sport (A.I.S.), and found that they reached a mean maximum running velocity of 6.14 m s^{-1} in the run-up, 12 to 8 m from the popping crease, which was reduced to 5.6 m s^{-1} in the 4 m interval before release. Foster & Elliott (1985) observed that Dennis Lillee's run-up speed reduced from a maximum of 8.9 m s^{-1} to 5.4 m s^{-1} during the penultimate delivery stride. Lillee (1977) stated that it is very difficult to twist the body to a side-on position when running in at maximum speed.

The situation is conceivably different for the front-on bowlers. Side-on bowlers lose more run-up speed than front-on bowlers due to the braking action that must occur immediately prior to back foot impact so that a side-on foot and shoulder positioning can be achieved (Elliott & Foster, 1989a). Fast bowlers who use the front-on technique may be able to utilise faster run-ups without any appreciable slowing-down or 'gather' phase. Foster & Elliott (1985) reported that the two most side-on bowlers in their study, (*Alderman* and *Thomson*), had the slowest approach velocities (4.0 m s^{-1} and 3.8 m s^{-1} respectively). The more 'open' bowlers, (*Lawson and Lillee*), had higher velocities (4.6 m s^{-1} and 5.4 m s^{-1} respectively).

Davis and Blanksby (1976a) said that fast bowlers tend to move 15% faster than medium pace bowlers just prior to ball release, and that the perfect run-up contributes 19% to the speed of the ball. Elliott et al. (1986) reported a similar figure for the run-up contribution, 15%. Both studies obtained their figures by subtracting the bowler's centre of mass speed and expressing it as percentage of final ball speed. This method of determination is flawed because it assumes that the techniques adopted by each bowler were the same (Bartlett et al., 1996). Bowling techniques generally vary considerably between individuals, so the percentage contribution of the run-up to ball release speed will vary between bowlers (Bartlett et al., 1996). Brees (1989) reported that there was a correlation between run-up speed and ball speed from tests on a sample of seven bowlers, who were requested to consciously alter their run-up speeds (fast, medium and slow), while trying to bowl as fast and accurately as possible. However, the problem with this approach is that a change in run-up speed also alters a bowler's rhythm and technique, which can both have an effect on ball release speed. Though from a mechanical point of view, run-up speed must have an effect on ball release speed, current research does not conclusively indicated the nature of this correlation under match conditions (Bartlett et al., 1996).

2.2.3 Delivery Jump

The run-up culminates in a delivery jump of the left foot followed by a cross-over step in mid-air, enabling the trunk to make a rapid twist to the left so that the body can assume a side-on position while in flight (Elliott & Foster, 1989a). The height and duration of the delivery jump may be dependent on the bowling technique used by the bowler. For instance, *Wasim Akram*, a side-on express fast bowler from Pakistan, concentrates almost solely on maintaining the initial horizontal momentum of the run-up by minimising the vertical height of the delivery jump. Also, bowlers who have a diagonal or curved run-up or use the front-on technique do not need to make significant twists of the torso prior to delivery, so these bowlers may not require delivery jumps that are as high or far as their traditional side-on counterparts. A survey indicated that 57% of coaches believed that it was either of little or no importance to jump into the last stride (Davis & Blanksby, 1976a).

2.2.4 Angle Conventions

In the following sections, various angles are used to describe the alignment characteristics of the bowling action. The angles used to define the position of the back foot, hip and shoulders are measured anticlockwise relative to the positive *X*-axis, directed in the plane of the wicket running from the bowler's to batsmen's end (Figure 2-7(a)). When back foot, hip and shoulder alignment angles are quoted, they refer to the direction in which the following lines point: from the heel to the tip of the second toe (midline of the foot); from the left to right hip (hip alignment); and from the left to right shoulder (shoulder alignment) (Bartlett et al., 1996). For instance, Figure 2-7(b) shows the typical shoulder alignment of a front-on bowler. The line drawn from the left to right shoulder is represented as running from point *A* to point *B*, where *A* represents the left shoulder, and *B* the right shoulder. Then the shoulder alignment angle is specified by measuring the angle (anticlockwise) from the *X*-axis to the line *AB*. In this way, back foot and hip alignment angles are also specified.

2.2.5 Back-Foot Angle and Action Classification

The delivery stride begins when the bowler lands on the back foot after completing the delivery jump. Generally, the angle of the back foot upon contact on the ground indicates how far the body has turned towards the side-on position (Bartlett et al., 1996). Therefore, it has been suggested that upon back foot contact, either one or both of (i) the angle of a line joining the two hip joints (hip alignment) and (ii) the angle of a line joining the acromion processes of both scapulae (shoulder alignment) could be used to classify fast bowling technique (Burnett et al., 1995; Stockhill & Bartlett, 1992). The adopted convention by Burnett et al. (1995) is that if an alignment of the shoulders at the back foot impact is less than 200°, then the bowler is considered side-on; if this alignment is greater than 200°, the bowler is front-on (Figure 2-7(b)). Foster et al. (1989) had previously proposed a classification system, which defined a front-on bowler as having a shoulder alignment of greater than 200° at either back foot or front foot strikes, and a side-on bowler as having a shoulder alignment of less than 190° between back foot and front foot strike (Bartlett et al., 1996). Neither of these

classification systems took into account foot position. A new system proposed by Elliot et al. (1992) did this by defining a side-on bowler as having a shoulder alignment of 190° or less with the angle of the back foot at contact 280° or less, whereas a bowler was front-on when the shoulder alignment of greater than 190° and a back foot angle of less than 280° was observed (Elliott et al., 1993).

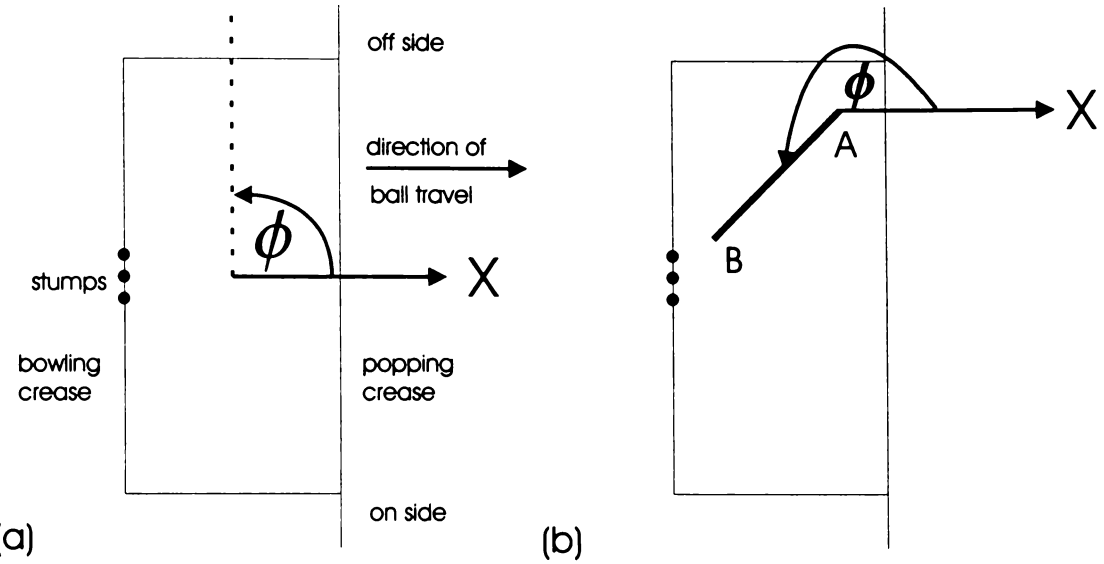

Figure 2-7 (a) The basic action classification system. (b) Shows the typical shoulder alignment of a right-hand front-on bowler ($\phi \approx 240°$). The line drawn from the left to right shoulder is represented as running from point *A* to point *B*.

A proportion of front-on bowlers are further classified as using the 'mixed' technique, if during delivery stride, the lower body is front-on but the shoulder alignment is typically side-on (Elliott & Foster, 1989a). This mixed action generally develops when coaches emphasise a side-on shoulder position without much consideration of correct foot placement and alignment. When a bowler has a front-on foot placement and hip alignment, but attempts to attain a side-on upper body position, there occurs a counter-rotation of the shoulders between back foot and front foot strike (Elliott et al., 1990). Elliott et al. (1993) defined the mixed action as one that had a shoulder alignment of greater than 190° with any foot placement, and a counter-rotation of the shoulders during the delivery stride of greater than 10°. Burnett et al. (1995) made the distinction between front-on and mixed bowlers by examining the pelvis/shoulder separation angle at back foot

impact and the subsequent counter-rotation of the shoulders in the transverse plane. If either of these variables is less than 20°, the bowler is considered front-on; otherwise, the bowler has a mixed action.

Studies have shown that the mixed action technique tends to increase the susceptibility of a fast bowler to lower lumbar injury (Elliott, 2000; Portus et al., 2000). Though it is recognised that the causes of back injury are multifactorial, such as poor hamstring or lower back flexibility, and bowling loads (Bartlett et al., 1996; Burnett et al., 1995), Elliott et al. (1992) provided the most conclusive evidence that the mixed technique predisposes a bowler to abnormal radiological features in the lower spine. This is because it places the spine in an unnecessarily awkward and potentially injurious position when front foot ground reaction forces are at their highest. Other studies such as Foster et al. (1989) and Burnett et al. (1995) have also shown a correlation of the presence of disc abnormalities with the mixed action technique. Although, previous research has reported counter-rotations of 40° (Foster et al., 1989; Portus et al., 2000) and 30° (Elliott et al., 1992) sufficient to predispose individuals to back injuries, it is unlikely that a single figure is applicable for all bowlers. Counter-rotations of 12 - 40° during a delivery stride have predicted an increased incidence of lumbar spondylolysis, disc abnormality and muscle injury in fast bowlers (Elliott, 2000).

2.2.6 Front Foot Contact

Front foot contact follows back foot contact - the weight transferred from the back to front foot with the front foot on landing pointing straight down the wicket or slightly towards fine leg (Tyson, 1976). Tyson (1976) advocated that front foot should be 'stamped' down in order to generate ball release speed. However, a survey by Davis & Blanksby (1976a) indicated that this is an area of contention among coaches with 38% suggesting that is important for the front foot to rapidly hit the ground, while another 31% believed it is not. The point to bear in mind is that maximum vertical ground reaction forces of almost five times body weight have been recorded when the front foot was planted on the force platform, and this was independent of the type of action used (Elliott & Foster, 1984). Mason et al. (1989) reported higher values with the mean peak vertical ground reaction forces

for all subjects being nine times body weight and occurring approximately 0.01 seconds after delivery foot contact. The body must eventually absorb the these ground reaction forces. As well as doing this, the body is also flexing, extending laterally and rotating to achieve maximum power in delivery (Elliott & Foster, 1984). Therefore, an exaggerated stamping of the foot may generate even higher magnitudes of ground reaction forces, which may lead to an increased susceptibility to injury, and for no evident purpose. For instance, Saunders & Coleman (1991) found no significant correlations between peak ground reaction force values and any kinematic parameter they studied (Bartlett et al., 1996).

2.2.7 Stride Length and Alignment

The three major components of the delivery stride are back foot contact, front foot contact and ball release. Stride length is defined as the distance between front and back foot during delivery when both feet are still in contact with the ground. Stride length is dependent on approach velocity, and it seems that those who approach the bowling crease at too high a velocity use shorter delivery strides, which may inhibit their ability to adequately summate forces during the side-on delivery (Elliott & Foster, 1989a). As a good rule thumb, delivery stride length should be approximately 75-85% of a bowler's standing height (Elliott & Foster, 1989a).

Observations have shown that fast bowlers decelerate in the penultimate delivery stride. Davis & Blanksby (1976a) reported that the fastest bowlers tend to have a last stride immediately prior to delivery, which decelerates the horizontal motion of the bowler. Accompanying this deceleration was a reduction in this penultimate stride length of about 12% for the faster group of bowlers, and 6% for the slower group. This is probably associated with the need to slow down before the final thrust. If the bowler is to continue to accelerate, then there could be insufficient time available to adopt a side-on shoulder position during delivery resulting in an inefficient summation of forces (Davis & Blanksby, 1976a). However, front-on bowlers may be able to avoid this deceleration, because there is no need to twist the shoulders into line prior to delivery.

Stride alignment is a critical feature of bowling technique. It is defined relative to a line running through the leading edge of the front and back feet during the delivery stride, and can determine the type of action employed by the bowler. Tyson (1976) suggested that the front foot on landing should point straight down the wicket or slightly towards fine leg and in a straight line with the rear foot to retain a side-on position. Four of the five actions sampled by Elliott & Foster (1984) adhered to this alignment principle. Also, 67% of all subjects sampled by Davis & Blanksby (1976a) directed the front foot directly at the target. Elliott et al. (1986) reported that this principle is broken by front-on bowlers, who tend to place their front foot more towards the off-side (Appendix L). However, Elliott et al. (1992) reported that a group of elite fast bowlers using a predominantly front-on action had a front foot alignment slightly to the on-side of the wicket compared to the back foot, which is also typical of a side-on stride alignment. This was a significant result, as it is generally believed that such a stride alignment for front-on bowlers is unsuitable because it would induce a rotated and hyperextended position of the lumbar spine (Elliott et al., 1992; Bartlett et al., 1996). However, there have been no formal studies correlating front foot angle with action type and lower lumbar injury susceptibility. It could well be that front-on bowlers can safely tolerate a front foot orientation slightly towards fine leg.

2.2.8 Front Knee Angle

The front leg is given special attention during the delivery stride because it supports the action during the critical part of the delivery (Sobers & Smith, 1985). Traditionally it has been accepted that the front knee angle should be kept as straight as possible during delivery, so that it can act as a rigid lever over which the body can pivot (Gover, 1980; N.S.W.C.A, 1966). This is known as 'bracing' the front leg, or bowling with a 'braced' knee (i.e. knee angle is 180°). Some authors consider that flexing the knee at any stage during delivery produces a mechanically inefficient action. Others believe that it is acceptable for the bowler to flex at front foot contact as long as it is braced when the weight passes over it just prior to or at ball release (Lillee, 1994; Tyson, 1976).

In the biomechanics literature, many movements of the front knee have been reported. Mason et al. (1989) sampled fifteen elite bowlers. Eight of the bowlers contacted the ground intially with a fully extended delivery knee, while the remaining bowlers partially flexed the knee on impact. During peak vertical ground reaction force, seven bowlers maintained a full extension of the delivery leg, while another seven bowlers partially flexed at the knee. The remaining bowler 'collapsed' the front knee, i.e. demonstrated a larger degree of flexion in comparison to the norm. In contrast, at ball release the delivery leg of seven of the bowlers experienced some flexion, but three of these bowlers appeared to collapse at the knee joint. These three bowlers had longer final delivery strides. Of the seven other bowlers who extended the delivery leg, five of these hyperextended at the knee. However, the study did not point out whether these seven bowlers initially had the knee in a flexed or extended position at front foot contact. Penrose et al. (1976) observed that *Thomson* (Australia) and *Holding* (West Indies) pivoted on a straight (*braced*) front leg, whereas *Lillee* and *Roberts* (West Indies) tended to collapse the front leg upon delivery. The sample tested by Elliott et al. (1986), (including such bowlers as *Lillee*, *Alderman* (Australia) and *Marshall*), flexed the front knee slightly from angles of approximately 168° at front foot contact to 159° at ball release (Elliott & Foster, 1989a). Elliott and Foster (1984) also showed that the knee could move from a slightly flexed position to an extended position during this transition. *Thomson* and *Lawson* (Australia) had a slightly flexed knee joint (approximately 173°), which became fully extended at ball release. Yet other bowlers, such as *Callen* (Australia) and *Alderman*, displayed more knee flexion at front foot contact (150°), which was virtually retained up to ball release (146°) (Elliott & Foster, 1984).

It is evident that the action of the front knee is complex, and varies significantly with the bowling style of the individual. To draw general conclusions from the research to date is therefore difficult. However, the majority of bowlers sampled thus far have tended to flex the knee at front foot contact, so it is likely that the front knee should be slightly flexed to assist in the absorption of the forces experienced when the foot impacts the ground (Elliott et al., 1990). Elliot & Foster (1984) reported that the front foot impact forces of *Thomson* and *Lawson*

were reduced from about 4.5 times body weight at contact to about 1.3 times body weight at ball release. Neither *Thomson* nor *Lawson* flexed the knee significantly upon front foot impact, but it is possible that bowlers who use of this "knee flexing" technique can attenuate the ground reaction forces in this way. It is also reasonable to suggest that the front knee should not flex too much, less than 30° (Elliott et al., 1986). Davis and Blanksby (1976a) suggested that an overly flexed leg at the knee would significantly shorten the lever acting on the front foot about which the body pivots, and this in turn could tend to decrease the velocity of the ball. They supported this contention by reporting that the mean angle between thigh and leg at release was 25° closer to full extension for the faster bowlers of their sampled group - a difference of 15%.

2.2.9 Trunk Flexion

During delivery stride from back foot contact to front foot contact, the bowler has to transfer body weight from the back foot to the front foot. This process is initiated during back foot contact, when by means of a rock or pivot at the hips, the body is made to lean back in the sagittal plane (Benaud, 1976). This allows the trunk to incline slightly backwards to allow the front leg and arm to be in a position to drive vigorously downwards, particularly for the side-on action. Mason et al. (1989) reported that all bowlers in their group demonstrated a degree of backward lean of approximately 10° from the vertical. A more vertical trunk at this point is common with those employing the front-on action (Elliott & Foster, 1989a; Lillee, 1994).

During the period from initial back foot contact to front foot contact, the trunk flexes, laterally bends, and rotates possibly releasing any elastic energy that may be stored in the musculoskeletal structures. Mason et al. (1989) reported that at peak vertical ground reaction force of the front foot, all but two bowlers were flexed forward at the hips. Seven bowlers flexed the trunk to a position that was less than 90° to the thigh of the delivery leg, while six bowlers flexed at the hips to an angle greater than 90°. Trunk flexion is a fundamental characteristic of bowling. However, Davis & Blanksby (1976a) recorded almost identical results for the trunk angle at ball release for both the fastest and slowest group of sampled

bowlers. They hypothesised that range of trunk movement may not be a contributing factor to speed development, but suggested that "no measure of muscular force was included in the study for this could have been an important factor" (Davis & Blanksby, 1976a). Contradicting these results, Burden & Bartlett (1990b) found that although the trunk angles of a group of elite bowlers (county and international level) and group of college bowlers displayed similar trunk angles at back foot and front foot contact, there was considerable difference in the trunk angle at ball release. The trunk was in a more flexed position for the elite bowlers (49 ± 4°) than the college bowlers (60 ± 6°). However, perhaps a more definitive relationship exists between ball release speed and the angular velocity or angular acceleration of the trunk rather than its angular displacement. This was somewhat confirmed by Burden & Bartlett (1990b), who reported that an elite group of bowlers displayed higher trunk angular velocities (529 ± 80° s^{-1}) than a group of college bowlers (355 ± 80° s^{-1}).

There is also some lateral trunk bending in the bowling action. Mason et al. (1989) reported that five bowlers from their sampled group of sixteen displayed a lateral bend of approximately 10° to the left with respect to the vertical during ball release, and in the direction away from the delivery arm. How this contributes to ball release speed has not been determined.

2.2.10 Rotation of Hips and Shoulders

Hip and shoulder rotation occurs while the trunk laterally bends and flexes (and extends) during the delivery stride. It has been hypothesised that the shoulders could store energy in the penultimate delivery stride much like the coiling of a spring. Consequently, some coaches believe it is necessary to keep the left shoulder and hip pointing at the batsman for as long as possible to remain side-on during the delivery stride (Elliott & Foster, 1984; Tyson, 1976). In the study by Elliott & Foster (1984), the side-on group of fast bowlers delayed the shoulder rotation considerably longer than the front-on group. For instance, the shoulder position of *Thomson*, a side-on bowler, at front foot impact was 187°. *Lawson*, who bowled with a more open action, had a shoulder position of 210° at the corresponding time. This is significant because *Thomson* is one of the fastest

bowlers in recorded history, considerably faster than *Lawson*. In fact, *Thomson* had a unique 'slinging-type' action. When more traditional fast bowlers plant their front foot during delivery, their bowling arm has begun its delivery arc and is at shoulder level behind the body; whereas for *Thomson*, at the corresponding time, the bowling arm would be just leaving his right side (Penrose et al., 1976). However, more evidence is needed to establish whether the correlation of a delayed shoulder rotation with ball release speed in these studies was due to an increase in the stored energy between the trunk and bowling arm. It could well be the result of another biomechanical principle – for instance, the overall sequencing pattern could have been altered to a more optimal one.

Apart from delaying the onset of shoulder rotation, it was found that side-on bowlers had a much greater arc of shoulder swing from back foot contact to ball release than front-on bowlers (Foster & Elliott, 1985). For instance, in this time period *Thomson's* shoulder moved through an arc of 120°, whereas *Lawson's* shoulder moved through an arc of only 95° (Elliott & Foster, 1984). Elliott & Foster (1984) stated that side-on bowlers are able to use this added angular movement to summate body forces more effectively than front-on bowlers, a factor which may reduce the stress placed on body segments and joints. Such conclusions reinforced the position that a front-on action is inefficient, because it reduces the range of shoulder rotation and therefore the contribution of body rotation to final ball velocity. However, Elliott & Foster (1989a) countered this by suggesting that front-on bowlers can compensate for this by maintaining a higher proportion of the run-up speed at delivery than side-on bowlers.

Finally, it is worth mentioning that shoulder rotation is generally initiated in the period between initial delivery foot contact and peak vertical ground reaction force, while the bowling arm is extended behind the body at approximately the horizontal position (Mason et al., 1989). At ball release, all bowlers (front-on and side-on) tend to assume a completely open position with the shoulders aligned with the hips (Mason et al., 1989). Elliott et al. (1986) believes that this is caused by the forceful action of rotation and thrust of the upper body through an arc facilitated by the continued motion of the non-bowling arm to a position behind the body.

2.2.11 Bowling Arm

Ultimately, the bowling arm is the most important limb in bowling. Release speed is dependent on both the angular velocity of the bowling arm, and the linear velocity of the shoulder joint at ball release (Stockhill & Bartlett, 1994). Accuracy is dependent on the release speed and projection angle of the bowling arm. Also, by manipulating the motion of the bowling arm with the aid of the wrist, much variation could be added to the delivery: change of pace, height of delivery, swerve (the curve of the ball in flight due to spin), swing (the curve of the ball in flight due to the airflow over the seam of the ball) and spin (the deviation of the ball after ground contact due to spin on the ball). An understanding of the mechanics of the bowling arm trajectory is therefore critical to the development of a successful bowling action.

The motion of the bowling arm generally begins with the bowling hand at about face level so that at ball release, when the bowling arm is near the vertical, almost a full revolution of the bowling arm about the glenohumeral joint would have been completed (Benaud, 1981). Sobers & Smith (1985) and Lillee (1994) suggested that at back foot contact the bowling arm should commence its downward swing from a position in front of the chest. Wilkins (1991) believed a long, loose, circular swing such as that used by *Barnes* (England) will provide the bowler with the means to optimise ball release speed, while preventing an excessive bending of the back, which can reduce the strain placed on the lower lumbar region. The logic behind these arguments seems to be that the longer the arc traversed by the bowling arm, the more distance is available to generate speed. Elite bowlers, such as *Lillee*, *Hadlee*, *Holding* and *Garner*, appeared to use this strategy effectively. A notable exception was *Thomson*, who started his action at around the hips. However, *Thomson's* 'slinging-type' action stands almost alone in its uniqueness.

2.2.12 Non-Bowling Arm

The action of the non-bowling arm is believed to play a part in achieving directional accuracy and fast ball release speed. During back foot contact, the

non-bowling (front) arm should be almost vertical and placed such that the bowler can (i) look over the side of the front arm at the target prior to front foot impact for a side-on technique, or (ii) look inside the front arm for a front-on technique (Elliott & Foster, 1989a). At this stage, the non-bowling arm is used primarily as a targeting mechanism (Elliott et al., 1990), particularly for the side-on bowler. It may also help the trunk lean backwards, so that much of the weight is on the back foot in preparation for the downswing (Davis & Blanksby, 1976a). Another possible function of lifting the non-bowling arm could be to bring the right shoulder below the left shoulder, thus increasing the range of motion through which the right (bowling) shoulder must move from this point onwards to the time of ball release.

At front foot impact, the non-bowling arm should be tucked into the ribs in a downward motion as the arc of the bowling arm begins to assist in the forceful flexion of the trunk (Philpott, 1973; Elliott & Foster, 1989a). This aspect of forcibly tucking in the non-bowling arm is emphasised by many coaches, and can be substantiated with some kinematic evidence. Davis & Blanksby (1976a) found that faster bowlers tend to have higher a non-bowling arm velocity than slower bowlers. Bowling technique also seems to effect the velocity of the non-bowling arm. Side-on bowlers record higher velocities of the non-bowling elbow (Elliott & Foster, 1989a). Elliott & Foster (1984) found that a side-on group of bowlers were better able to accelerate the elbow of the front arm into the side of the trunk than the group of front-on bowlers: mean elbow velocity 3.2 m s^{-1} for side-on group, as opposed to 2.4 m s^{-1} for the front-on group. A group of front-on bowlers tested by Elliott et al. (1986) had a front elbow velocity of 2.8 m s^{-1}, which endorsed these previous findings. However, no study of dynamics has been made to assess whether the torques on the non-bowling arm actually do act to force it into the side during delivery. Also, the exact sequencing of this motion in relation to that of the trunk, hip and bowling arm has not been assessed.

2.2.13 Ball Release

At the end of the delivery stride, the bowler must release the ball. Mason et al. (1989) found that the bowling arm of bowlers at release is close to fully extended

and slightly forward of the vertical alignment (Mason et al., 1989). Elliott and Foster (1989a) agreed with this, and also suggested that the bowling arm lags the trunk by about 20°. This latter observation is supported by a majority of findings with only Davis & Blanksby (1976a) in disagreement, possibly from an inaccurate identification of ball release owing to their use of a relatively slow frame rate of 64 Hz (Bartlett et al., 1996).

Many coaches believe that at ball release the full weight of the body should be over the front leg (Lillee, 1994). This view may have arisen from the assumption that during the release period of the delivery, the front leg must remain straight and strong to bear the weight of delivery as the bowler brings the bowling arm up and over (Sobers & Smith, 1985; Tyson, 1976). However, Mason et al. (1989) reported that during the period from back foot contact to ball release, the front foot vertical ground reaction force is at its lowest level at ball release.

2.2.14 Follow-Through

The follow-through is the final stage of bowling and occurs after ball release. Unfortunately, limited data are available on this aspect of bowling as most analyses stop shortly after ball release (Bartlett et al., 1996). The general idea behind the follow-through is to allow a gradual reduction in body momentum by the gradual slowing down of body segments to lessen the stress placed on the joints (Elliott & Foster, 1989a). Tyson (1976) suggested that after the general explosiveness of the bowling action, the follow-through needs to become relaxed so as to allow for maximal absorption of the trauma and shock of the bowling action. The bowling arm itself should follow-through down to the outside of the left leg so that it almost brushes the ground, while the bowler moves off the pitch and recovers balance (Elliott & Foster, 1989a). At the completion of the follow-through, the right shoulder should point at the batsman (Benaud, 1976), and the left hand side of the body rather than the back of the bowler should be visible from behind the bowler (Elliott & Foster, 1989a).

2.2.15 Segment Velocity Contribution

There is much debate among coaches on the relative velocity contribution of the various body segments involved in fast bowling. Davis & Blanksby (1976b) investigated segmental velocity contribution by attempting to isolate the various body parts with the systematic use of restraints, so that their relative importance could be measured. The major contributions to bowling speed in this study were provided from the bowling arm (41%), the rotation of the hips and leg drive (23%), trunk (11%), and the run-up (19%). The data also indicated that the faster bowlers tend to rely more heavily on run-up and arm action to generate speed, whereas the slower bowlers depend more heavily (about 12% more) on trunk plus shoulder rotation than the faster bowlers. Interestingly, Peterson (1973) also used the process of applying systematic restraints to analyse the corresponding segmental contributions of a baseball pitch. It was found that major contributions to pitching speed are the legs and hip rotation (36.6%), trunk and shoulder rotation (15.2%), arm (24.4%), and hand (23.6%). Unfortunately, there is no run-up associated with the baseball pitch, so the applicability of these results to bowling is limited. A significant problem with the studies completed by Davis & Blanksby (1976b) and Peterson (1973) is that the procedure of isolating body parts assumes that the actions of body segments are unaffected by the action of more proximal and distal segments (Bartlett et al., 1996). This implies that the movement of each segment relies on muscular activity alone, which is not the case (Burden, 1990; Bartlett et al., 1996). On these grounds, analysis by means of cinematography or video seems a more accurate means of understanding the segmental contributions in fast bowling.

Elliott et al. (1986), using cinematographical techniques, reported the following percentage segment contributions: bowling arm (50%), trunk (13%), run-up (15%). Significant differences exist in determining the percentage velocity contribution of the wrist. Elliott et al. (1986) reported a 24% ball velocity contribution attributable to wrist flexion. However, with the wrist only having a range of motion of approximately 7° in this phase of the motion, this contribution seems higher than what should be expected (Elliott et al., 1986). Davis & Blanksby (1976a) divided a sample of bowlers into two groups of six each. The

first group consisted of the six fastest bowlers, while the second one comprised the slowest six. Using cinematographic techniques, a measurement of the mean velocities of both these groups revealed that at front foot plant a difference in ball velocity of 1.3 m s^{-1} existed between the groups. At 0.045 sec before the release, only 0.3 m s^{-1} difference existed. However, in the remaining time before ball release, this difference was increased to 4.41 m s^{-1}, which indicated that a crucial period for velocity development occurred in the last fraction of a second before the ball release. The period of most rapid hand flexion coincided precisely with the sudden change in the velocity differences between groups exhibited in this phase. The results of this study were in agreement with Lindwall (1957), who suggested that rapid flexion of the hand from a position of hyperextension was important just prior to release of the ball. However, this was not supported by Elliott & Foster (1989a), who suggested that the wrist is the last segment to add velocity to the ball, and plays a minimal role in speed generation. They found that the wrist at front foot contact only changes minimally until the hand and the arm are aligned at ball release. With the wide range of data reported, it is evident that issue of wrist contribution is still not satisfactorily resolved. On the whole, more research is needed into the segmental contributions to ball release speed, including energy transfers between segments and aspects of segment kinetics (Bartlett et al., 1996).

2.3 BOWLING INJURIES

No review of the biomechanics of bowling would be complete without a brief account of the nature and causes of injury sustained by bowlers. Causes of injury are various, and can be due to one or a number of the following factors: inappropriate warming-up and stretching, poor footwear, excessively long run-up, faulty action, bowling under fatigue, bowling too many balls at maximum speed (i.e. repeated maximum loading of musculoskeletal structures), unsuitable playing surface, temperature, congenital defects of lower spine, and not limiting the amount of bowling by adolescents (Fitch, 1989). Only the possible mechanical causes of injury will be considered here.

Much of the biomechanics research to date has tried to identify techniques that would enable the bowler to release the cricket ball at high speeds without being subjected to an excessively high risk of injury, particularly to the lower lumbar region. Significant progress was made in this area with the identification of the mixed technique (Section 2.2.4), which is essentially a bowling action that combines a front-on foot position with a side-on shoulder orientation (Elliott et al., 1989). Thus, the mixed-technique bowler changes shoulder alignment from a front-on position at back foot contact to a more closed (or side-on) position at front foot contact (Elliott & Foster, 1989a). This action twists the lower lumbar region of the back during hyperextension and places stress on the lower lumbar vertebrae, which has the potential to cause injury (Elliott & Khangure, 2002; Elliott, 2000; Elliott et al., 1990; Elliott & Foster, 1989 a & b; Fitch, 1989). Bowlers using the mixed technique are more susceptible to major developmental defects of the lower lumbar spine, such as spondyloylsis (breaks in one or both sides of the neural arch), and spondylolisthesis (breaks on both sides of the neural arch with a forward slip of the vertebra just above the breaks) (Elliott, 2000; Fitch, 1989). A bowler who has been diagnosed with either of these conditions is unlikely to bowl fast again (Fitch, 1989). Other spinal conditions such as bulging or prolapsed discs, facet joint strains, and injury to the muscles of the back are also more likely to plague mixed action bowlers (Fitch, 1989).

The magnitude of the ground reaction forces experienced by the bowler during delivery stride is also believed to increase the likelihood of back injury. Elliott et al. (1986) suggested that back injuries occur as a consequence of muscular activity associated with lateral and rotational activity of the spinal column together with the compression forces transmitted to the spine as a result of foot impact. Elliott & Foster (1984) reported that side-on bowlers minimise risk of back injury because they delay the initiation of hip and shoulder rotation until after the time of peak vertical ground reaction force on the front foot. However, for the front-on bowlers it was suggested that the lumbar axis is effectively isolated as the primary axis of body rotation, and that the upper body rotates around the lumbar spine region at the time of peak vertical ground reaction force. However, this theory was discounted when it was realised that in the 1980s the West Indies were producing the world's fastest bowlers, who mainly used front-on actions, and sustained

comparatively little back injury. Mason et al. (1989) found that during the initiation of hip rotation, a sample of bowlers with a history of back injury tended to lift the fully extended front leg to a position near or above the horizontal, and recorded the highest peak vertical ground reaction force at delivery foot contact. These back-injured bowlers also showed a high degree of lateral flexion, hyperextension and rotation at the time of peak vertical ground reaction force. Therefore, it appears that the back-injured bowlers in this study used a mixed technique. In summary, the modern consensus is that the side-on and front-on actions are both biomechanically safe techniques, but that the mixed action provides an unsafe movement pattern, which may be compounded by the problem of vertical ground forces.

Though fast bowlers are significantly more susceptible to back injury than any other ailment, there are nevertheless many other types of injury that can afflict such bowlers. Of these, injuries to the shoulder, groin, knee and ankle are most common (Fitch, 1989). Therefore, any scientific attempt to understand fast bowling technique must consider the full range of anatomical and technical constraints that enable a bowling action to be performed safely. For instance, if it was found that the fastest bowlers in a sample made front foot ground contact while the front knee was fully extended, then the knee joint does not play an effective role in the attenuation of impact forces (Bartlett et al, 1996). Despite the possibility of producing a faster ball release speed, the potential of sustaining injury due to the higher loading on the musculoskeletal structures would need to be assessed before any such 'straight-knee' landing technique could be recommended.

2.4 RIGID BODY DYNAMICS

When Sir Isaac Newton published his *Philosophiae Naturalis Principia Mathematica* in 1687, he officially gave birth to the field of classical dynamics. In the study of dynamics, motions can be predicted from a given set of forces, or the resultant forces calculated from the motions. When the sum of all interactions causes an acceleration of a body, then according to Newton's second law a net force has acted upon that body. The *Newton-Euler* method became the traditional

method to analyse rigid body systems with force diagrams made for each free body, and the equations calculated iteratively for each segment in the defined sequence of the segment link chain. However, with the analysis of complex systems this method could be difficult to implement, and time consuming, particularly with respect to the calculation of constraint forces. Also, with the advent of digital computers, dynamicists began looking for alternative methods that lent themselves more easily to a general dynamic simulation program (Winter, 1990). This stirred a renewed interest in analytic dynamics methods (Moon, 1998).

Analytic mechanics is an outstanding theoretical invention of the 18^{th} and 19^{th} centuries. It was largely a product of the minds of Euler, Lagrange, Hamilton, and Jacobi. The term "analytical" means that it is an application of the infinitesimal calculus invented by Newton and Leibniz at the end of the 17^{th} century. It extended the Newtonian ideas of momentum and force by using concepts of energy and work. Therefore, analytic mechanics is essentially a mathematical, not a physical development, though it is completely equivalent to Newton's theory of motion (Lanczos, 1970). In contrast to Newtonian mechanics, which relates the forces acting on a system to the motion of the system, analytical mechanics seeks to describe the motion of a particle in terms of a variational principle, so that the path taken by the system in configuration space minimises some function, referred to as the action. The system evolves along a path that corresponds to a minimum of the action. Such approaches involve kinetic and potential energy functions, and are called *variational methods* or *energy methods*. These analytic methods are generally based on the minimisation of energy, and depend heavily on the differential calculus of several variables (Moon, 1998). Therefore, analytic mechanics generated a new range of dynamics concepts, such as generalised coordinates, holonomic and non-holonomic constraints, virtual displacements, virtual work principle, and Lagrange multipliers.

There are a large variety of analytic dynamics formulations: Hamilton (Ginsberg, 1998), Lagrange (Greenwood, 1988), Gibbs-Appel (Baruh, 1999), and Kane (Kane & Levinson, 1985). The details of the differences in these methods are of little importance. The main choice revolves upon modelling constraints by either

reducing the number of coordinates needed to describe the system's state, or introducing additional forces into the system to maintain the constraints (Baraff, 1996). The *Lagrange Multiplier Method* adopts the latter technique, i.e. enforcing constraints by introducing constraint forces into the system. A general, non-iterative linear-time simulation method based on Lagrange multipliers has the following advantages:

> Lagrange multiplier approaches are extremely important for interactive computer graphics applications, because they allow an arbitrary set of constraints to be combined. This is difficult (often impossible) to achieve with a reduced-coordinate formulation. Additionally, Lagrange multiplier formulations allow (and frankly encourage) a highly modular knowledge/software design, in which bodies, constraints, and geometry regard each other as black-box entities. Lagrange multipliers also allow us to handle constraints, such as velocity-dependent constraints; reduced-coordinate approaches inherently lack this capability (Baraff 1996, p. 137).

Dynamics simulation software generally embody an analytic dynamics formulation. For instance, two common packages used in biomechanics are Autolev (OnLine Dynamics, Inc.) and SD/Fast (Symbolic Dynamics, Inc.). The Mechanical Systems Pack (Wolfram Research, Inc.), which is used for the dynamics analysis of rigid body mechanisms, and therefore has applications in biomechanical systems, uses the Lagrangian multiplier iteration method.

Chapter 3

METHODS AND PROCEDURES

3.1 3-D KINEMATIC ANALYSIS OF BOWLING

3.1.1 Sample

The subjects for the study were 34 male fast bowlers chosen from five different competition levels. In order of increasing performance level, 12 were classified as *local* (i.e. local club cricketers), 5 as *provincial* (i.e. regional representative cricketers), 8 as *national B* (i.e. reserve first-class cricketers), 4 as *national A* (i.e. first class cricketers), and 5 as *international* (i.e. test cricketers). The nature of cricket selection meant that there were overlaps of ability between the groups. The sample was also classified according to ranges of ball release speed: *fast* (> 33. 3 m s^{-1}), *med-fast* (31.9 m s^{-1} to 33.3 m s^{-1}), *medium* (30.6 m s^{-1} to 31.9 m s^{-1}), and *slow* (27.8 m s^{-1} to 30.6 m s^{-1}). The terms and speed ranges are adapted from the classification of bowlers by ball release speed used by Bartlett et al. (1996) and Abernethy (1981), though it must be noted that no formal convention for such a classification has been agreed upon. Also, the bowling speed ranges defining these categories were scaled down to compensate for the possible underestimation of ball speed measurement, and for any speed reduction due to performance in the laboratory environment.

All the subjects were free from any injury or physical dysfunction, which may have effected bowling performance at the time of data collection sessions. The ethics committees of the University of Waikato, and the University of Auckland granted approval for the study.

The sample size and the number of trials were determined on the availability of suitable subjects, and the practical time allowance for data processing and analysis. However, despite the scale of the research, the sample size was still one of the largest that has been studied in bowling.

3.1.2 Apparatus

Eight Motion Analysis High Resolution cameras with frame rates of 240 Hz were placed around the subject so that the field of view was sufficient to capture the performance area of the trials (Figure 3-1). The cameras had ring lights, which, placed around the camera lens, produced a bright red strobed light. This light illuminated the retro-reflective markers placed on the subject to produce clear video images of each marker during the bowling of a ball. Motion Analysis Corporation recommended that (i) there should be a sufficient number of cameras to ensure that during the entire motion all markers remain visible in a minimum of two, or preferably three cameras, and (ii) the use of a minimum of eight cameras for larger capture volumes to decrease the probability of markers being occluded from view. Both of these recommendations were followed, as well as that of placing the cameras about 3 m above the floor.

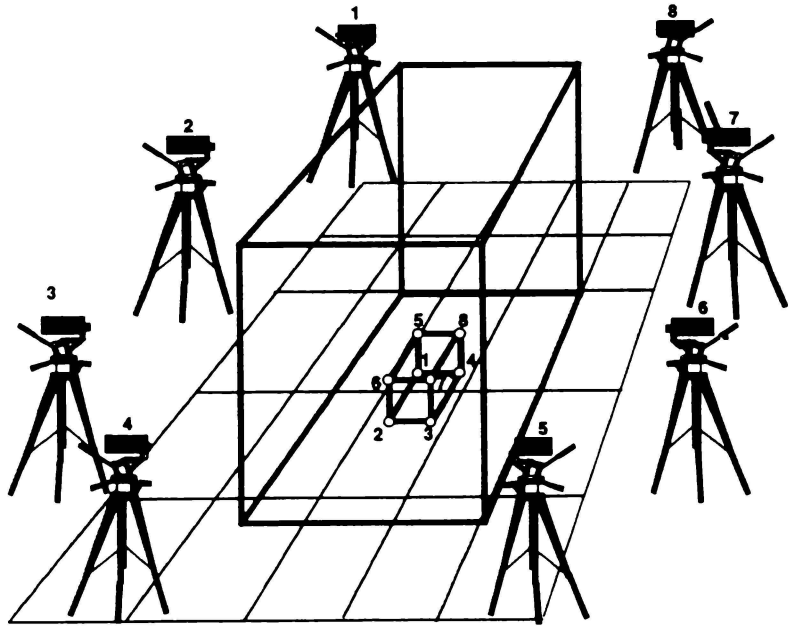

Figure 3-1: Schematic representation of eight-camera system surrounding performance area depicted by the large cube. The small numbered cube is the calibration cube placed over the force platform.

The performance area was centred on a running track under which was embedded a Bertec force plate, Type 6090-15, operating at 960 Hz (Appendix B, Figure B-1). It had four transducers, which measured the three orthogonal components of the resultant force, and the three components of the generated moment acting on the platform in the same orthogonal co-ordinate system. The point of application

of the force and the couple acting on the platform were calculated from the measured force and moment components (Appendix B). The platform also included a pre-amplifier mounted inside the force plate that improved the signal-to-noise ratio and permitted the use of long connector cables. The main amplifier (Bertec AM3-6) was set on a gain of 2, and had an automatic bridge zeroing capability to zero offset loads of up to the full range of force plate.

The camera and force plate were integrated into the Eva 6.0 motion analysis system (*Motion Analysis Corporation*), which is a completely integrated hardware-software system for video and analog data acquisition and processing (Fig. 3-2). The video processor computer (MIDAS) accepted video input from the motion capture cameras and analog input from the force plate. The MIDAS computer was a 350 MHz Pentium III with 256 MB RAM, using a Windows NT 4.0 operating system with a 6.4 GB IDE hard drive, and had a 3Com Fast 10/100 Ethernet interface. The host computer (HR Tracking Computer) was used to configure the system, collect data, and produce final results. It accepted video image data from the MIDAS computer via an Ethernet connection. The HR Tacking Computer was a 350 MHz Pentium III running on Windows NT 4.0, had 8 MB video RAM, a 8.2 GB IDE hard drive, and a 3Com Fast 10/100 Ethernet interface. It also used an associated SVGA monitor with a minimum of 1280x1024 pixel resolution. A video monitor switch box was used to view input when necessary. Also, a Multisync video monitor was used to view the outputs of the video capture cameras.

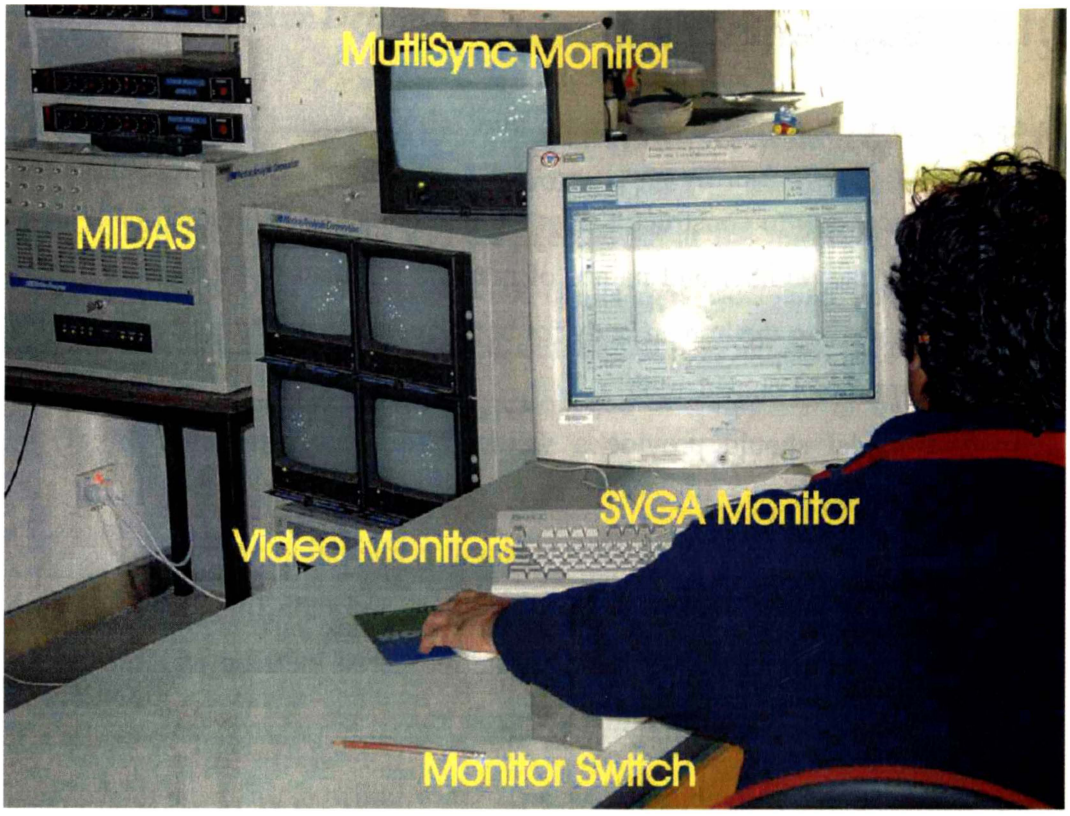

Figure 3-2: EVa 6.0 system standard configuration in laboratory.

The laboratory global reference system was a conventional three orthogonal axes system. The *X*-axis pointed in the direction of the wickets, and therefore in the general direction of ball release. The *Z*-axis was the vertical axis. The cross product of the *Z*-axis direction and the *X*-axis direction, defined the direction of the *Y*-axis, which, if a person was standing in the anatomical position so that the posterior-anterior axis was the *X*-axis, then the *Y*-axis would be parallel to a horizontal axis in the frontal plane. Therefore, the *X*-*Z* plane represented the plane of progression of the motion (sagittal plane), the *Y*-*Z* plane the frontal plane, and the *X*-*Y* plane the transverse plane. The force platform coordinate system was oriented differently to the global reference system of the laboratory, so ground reaction forces and centre of pressure data were transformed into the laboratory coordinate system.

3.1.3 Segment Link Model

3.1.3.1 Segment Definitions

It was first necessary to construct a segment link model of the human body prior to determining the number and names of markers that had to be defined in Eva 6.0. When modelling the human body for both kinematic and kinetic analysis the following points were considered:

1. The model should provide a valid approximate representation of the human body.
2. The model is more accurate if it is based on internal joint centres.
3. The mean relative centre of mass position, and radii of gyration of each segment could be calculated from the measured location of joint centres according to a scientific study.

The number and names of markers were chosen so that a 3-D 15-segment model based almost entirely on internal ('virtual') joint centres could model all the major upper and lower body segments (Table 3-1). The exceptions were the head-neck, foot and hand segments where a suitable end point other than a joint centre was chosen.

Table 3-1: Definition of segments based on joint centres (de Leva, 1996).

Segment	Origin	End Point
Head-Neck	Cervicale (C7)	Vertex Of Head
Upper-Trunk	Xiphoid Process	Cervicale
Lower-Trunk	Mid-Hips	Mid-Back (end of sternum projected on trunk longitudinal axis)
Upper Arm	Shoulder	Elbow
Forearm	Elbow	Wrist
Hand	Wrist	3rd Knuckle
Thigh	Hip	Knee
Shank	Knee	Ankle
Foot	Heel	2nd Toe Tip (Acropodion)

3.1.3.2 *Marker Definitions*

A simple method of calculating the joint centre was to put a marker on either side of the joint so that a line joining the centroids of the two markers defined the joint axis. Then the joint centre was assumed to lie at the midpoint of these two markers. For example, the knee joint centre was calculated as the midpoint between markers placed on the lateral and medial epicondyles. For other joints, such as the hip, the joint centre was calculated as a function of the position of three markers.

A major problem with placing markers on the body was that, depending on the type of movement trial, some markers would either impede normal performance or be removed in the process. For example, the markers on the medial epicondyle of each knee joint would cause a subject to walk bow-legged, and would be knocked off in a fast bowling trial. The way around this problem was to first collect a *static trial* in which the subject stood stationary wearing all the markers required for EVa 6.0 to calculate the joint centres, and then, as a second step, to remove those 'problem' markers (*temporary markers*) before the *moving trials* were performed (i.e. bowling trials). The markers that remained during the moving trials were known as *permanent markers*. Both the permanent and temporary markers were *real markers* in the sense that they were physically attached to the body.

From the static trial, the position of the joint centres relative to the permanent markers were known. Also, *virtual markers* were calculated to represent the markers that were removed, i.e. the temporary markers. This allowed joint centres to be calculated from the combination of permanent and virtual markers used for the moving trials. The critical aspect of this process was to determine where to place the markers and which ones to remove before performing the moving trials. Later, the full permanent and virtual marker system designed for the segment link model will be described. However, before this, it is first necessary to describe the different types of virtual markers.

Once identified, real markers were entered directly into the Eva 6.0. A virtual marker was created by defining its position relative to other known markers, which was a real marker or another virtual marker calculated previously. There were two types of virtual markers:

- Virtual marker based on two other known markers (VM2).
- Virtual marker based on three other known markers (VM3).

Also, both of these types of virtual markers had two different ways of measuring the offsets (i.e. the distances of the virtual marker from the known (permanent or temporary) markers).

For a VM2, two known markers were used: one as the origin; and the other as the *Y*-axis marker. It was a relatively simple process to derive a point somewhere along the *Y*-axis defined by these two markers (Figure 3-3). The offset (or distance) along the *Y*-axis from the origin could be defined as a percentage of the distance between the two real markers ($VM2_{\%}$), or alternatively, as a real-life distance (e.g. in millimetres) from the origin ($VM2_{dist}$).

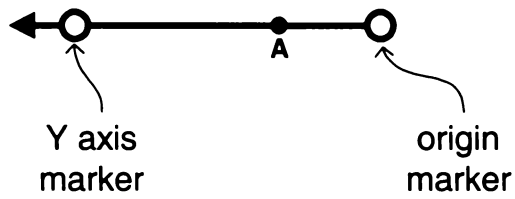

Figure 3-3: Virtual marker (A) was 'created' on the *Y*-axis from the position of two real markers. The local axis (as defined by the two real markers) could move to any position within the global (laboratory) coordinate system and, subsequently, its virtual marker(s) would move with it.

A VM3 used its own local *XYZ* coordinate system (*not* the local segment coordinate system). To specify any body-fixed local coordinate system in EVa 6.0 relative to the global laboratory coordinate system, three markers for each segment were required: an origin marker, an *Y*-axis marker, and an *XY*-plane maker (Figure 3-4). EVa 6.0 then calculated the *Z*-axis direction by taking the cross product of (i) the unit vector describing the orientation of the *XY*-plane maker with respect to the origin, and (ii) the unit vector describing the orientation of the *Y*-axis with respect to the origin. Finally, the *X*-axis was found by taking

the cross product of the unit vectors describing the *Y*- and *Z*-axis. Once the local coordinate system was defined, VM3 could be expressed either as a percentage of the distance between the origin and *Y*-axis marker ($VM3_{\%}$), or alternatively, as a real-life distance ($VM3_{dist}$) in the local *XYZ* coordinate system.

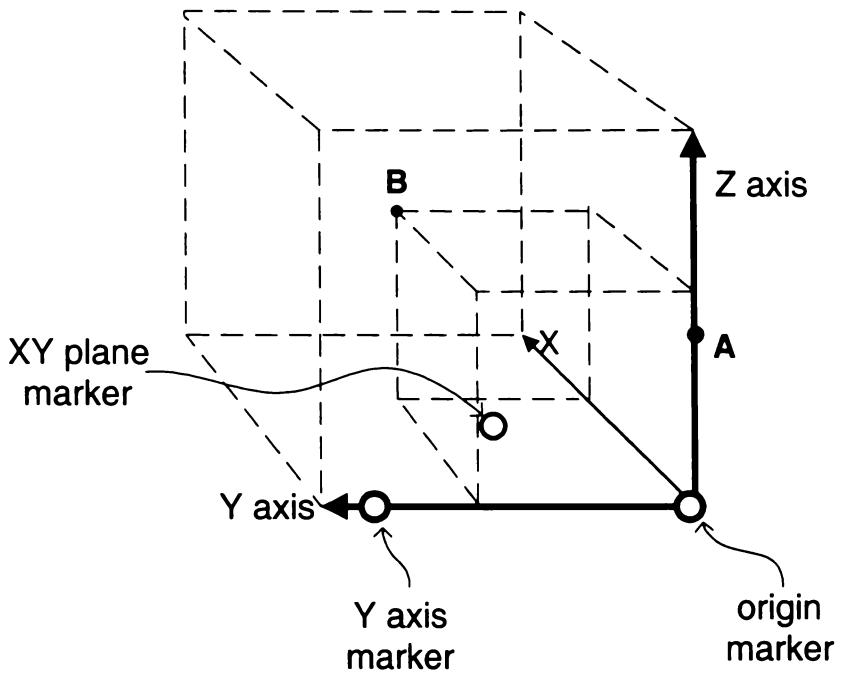

Figure 3-4: Two examples (A and B) of virtual markers based on a local coordinate system defined by three known markers. Both of these virtual markers are specified with *XYZ* coordinates of the local *XYZ* coordinate system (defined by the three known markers). A local coordinate system could move to any position within the global (laboratory) coordinate system and, subsequently, its virtual marker(s) would move with it. Virtual markers A and B are only two examples of an infinite number of possibilities.

When assigning markers to define a local coordinate system, the following protocol was established:

1. The three markers assigned to a segment were attached as rigidly as possible to the segment. However, at a hinge joint connecting two segments, the marker attached to the second segment could also be used as the *XY*-plane marker for the first segment.
2. The three markers assigned to the segment should never fall in a straight line. In fact, there should be as large an angle as possible between the *XY*-plane marker vector and the corresponding *Y*-axis.

3.1.3.3 *Static Trial Marker Set*

Forty-five real markers were worn for the static trial (Figure 3-5). Fourteen markers were removed (indicated with an asterix in the following list) before the moving trials were performed. All markers were worn on the left and right sides of the body except for the mid-PSIS (half-way between the posterior superior iliac spines), 7th cervical vertebrae, supra-sternal notch, and the head. Most of the marker positions were based on those listed in Zatsiorsky (1998). Exceptions were the position of the shoulder, mid-trunk, hip markers, and cricket ball. The positions of the ASIS (anterior superior iliac spine), mid-PSIS, and greater trochanter markers were based on those listed in Bell et. al. (1990). The anatomical placement of these markers is described below:

- *Forefoot:* directly over the 2nd metatarsal, approximately one or two centimetres posterior from its head so as to allow for the metatarso-phalangeal joints to flex without the marker being disturbed.
- **Toe-shoe:* on the tip of the second toe, or on the front tip of the shoe.
- *Heel:* on the posterior surface of the calcaneus with the marker hovering just above floor level with the foot flat against the ground.
- *Lateral ankle:* tip of the lateral malleolus of the fibula.
- **Medial ankle:* 5mm distal to the tibial malleolus.
- *Mid-shank:* approximately half way up the anterior surface of the shank.
- *Lateral knee:* on the posterior convexity of the lateral femoral epicondyle.
- **Medial knee:* on the posterior convexity of the medial femoral epicondyle.
- *ASIS:* directly on the anterior superior iliac spine.
- *Mid-PSIS:* on the lower back, mid-way between the posterior superior iliac spines.
- **Greater trochanter:* on the lateral hip placed over the greater trochanter.
- *7th cervical vertebrae:* on the superior palpable point of the spinous process of the seventh cervical vertebrae.
- *Supra-sternal notch:* a few centimetres above the supra-sternal notch.
- *Xiphoid process:* on the xiphoid process.

- *Mid-back*: placed on approximately the middle of the back directly opposite the xiphoid process marker.
- **Acromion:* placed on top of the acromion process.
- *High-tricep*: on the posterior surface of the upper arm, approximately 10-12 cm down from the glenohumeral joint (depending on length of arm).
- *Lat-bicep*: placed approximately in the middle of the lateral side of the upper–arm when the arm is held in the anatomical position.
- **Anterior deltoid*: visually positioned such that the half-way point from the posterior deltoid marker placement with arm vertically abducted 90° approximated the position of glenohumeral joint.
- **Posterior deltoid*: visually positioned such that the half-way point from the anterior deltoid marker placement with arm vertically abducted 90° approximated the position of glenohumeral joint.
- *Crown:* on the most cranial point of the head.
- *Forehead*: middle of forehead (frontal bone) in line with nasal bone.
- **Medial elbow:* placed on the medial epicondyle of the humerus.
- *Lateral elbow:* placed on the lateral epicondyle of the humerus.
- *Medial wrist:* placed on the medial side of the wrist joint, near styloid process of ulna.
- *Lateral wrist:* placed on the lateral side of the wrist joint, near styloid process of radius.
- *Hand:* just before the distal end of the 3rd metarcapal bone.
- *Cricket ball:* held in fingers of hand.

The selection of these markers determined an appropriate set of joint centres that effectively linked the segments together, and enabled the creation of virtual markers to replace those that would inhibit motion or be consistently knocked off during the bowling action. The key was to select joint centres that delimited segment lengths in accordance with the calculation of segment inertia parameters, so that kinematic data could be substituted into a comparable dynamics model.

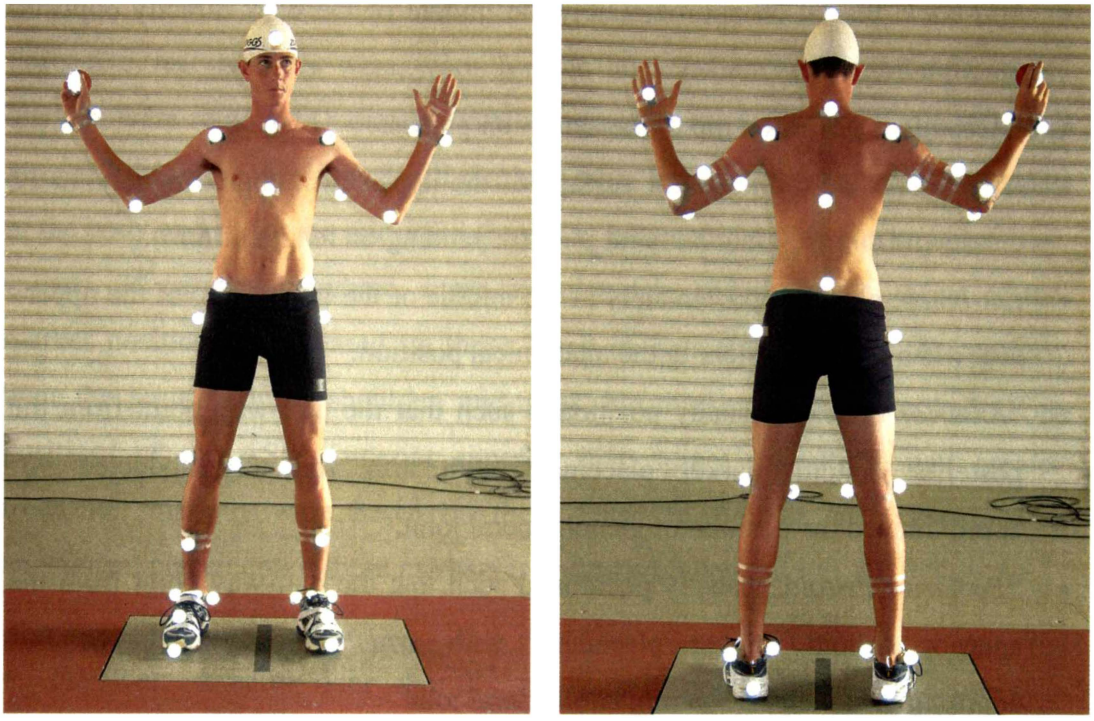

Figure 3-5: Anterior and posterior views of full static trial marker set.

3.1.3.4 Joint Centre Calculations

Joint centres were thought of as linkage points from which the origins of the segment coordinate systems could be defined (Table 3-1). The term 'linkage points' was preferred because some of the calculated linkage points were not actually 'true' joint centres. Therefore, from now on the terms 'joint centres' and 'linkage points' will be used interchangeably.

In the process of calculating joint centres *some local XYZ coordinate systems that were <u>not</u> based on joint centres were used to create virtual markers.* These local coordinate systems were intermediate steps to calculating joint centres and were referred to as *intermediate coordinate systems.* Likewise, some virtual markers were created only for the purpose of subsequent calculations to produce another joint centre virtual marker. These were called *intermediate virtual markers.*

<u>Example: Glenohumeral Linkage Point (i.e. Shoulder Joint Centre)</u>

The glenohumeral joint centre was derived by placing markers on the anterior and posterior deltoid, while the upper arm was horizontally abducted 90° from the

anatomical position, and calculating the midpoint between them. The position of the glenohumeral joint was calculated during the static trial and then the position of this joint centre measured relative to an intermediate coordinate system fixed to the upper arm. The following steps were used to calculate the position of the glenohumeral joint centre during moving trials for any position of the upper arm:

Step 1 – from the static trial, create an intermediate virtual marker of the glenohumeral joint centre:

- $VM2_{\%}$ with an offset of 50%
- Origin marker: posterior deltoid (temporary marker)
- *Y*-axis marker: anterior deltoid (temporary marker)

Step 2 – Set up an appropriate intermediate coordinate system: For the left glenohumeral joint centre, the intermediate coordinate system was set up as follows (Figure 3-6):

- Origin marker: lateral elbow (permanent marker)
- *Y*-axis marker: lateral biceps (permanent marker)
- *XY*-plane marker: high triceps (permanent marker)

Step 3 – from the static trial, measure the relative position of the intermediate glenohumeral joint centre (calculated in step 1) relative to the intermediate coordinate system: All *X*, *Y* and *Z* coordinates were required.

Step 4 – during the moving trials, create a virtual marker of the glenohumeral joint centre: The position of the glenohumeral joint centre was calculated because its position relative to the intermediate coordinate system was known (Figure 3-6). That is, $VM3_{dist}$ was used to create a virtual marker of the glenohumeral joint centre.

The sets of calculations needed to determine the other joint centres making up the link segment model are shown in Appendix C.

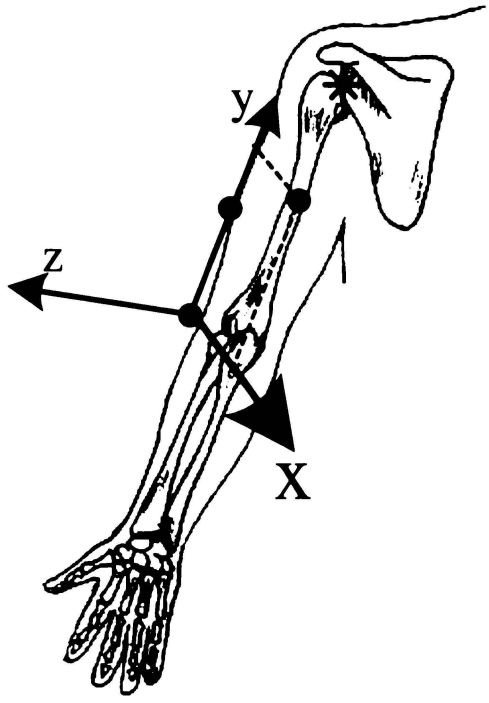

Figure 3-6: Intermediate co-ordinate system used in the calculation of the left glenohumeral joint centre. The diagram shows a rear view of the left arm and shoulder. The black spots represent the lateral elbow, lateral biceps, and high triceps markers. The asterix indicates the glenohumeral joint centre that was calculated in step 1.

The current state of technology for marker-based motion analysis systems determines that the process of creating joint centres by offsetting the positions of real and virtual markers in a suitable local coordinate system is the only way to calculate a set of internal joint centres and significantly reduce the number of markers placed on the body, allowing the subject to perform relatively free as in a normal practice situation (Figure 3-7). This produced more accurate 3-D kinematic data, than if only the position of skin based markers were used to represent joint motion. This is important, because inaccuracies in the kinematic data could cause significant errors in the calculation of an inverse solution.

3.1.3.5 Segment Coordinate System

After the virtual markers were defined, an internal virtual skeleton was created by linking all the joint centres, and effectively giving a rigid body representation of the human body (Figure 3-7). The purpose of all the work thus far was to

produce a complete set of joint centres and markers (real and virtual) that could be used to derive the local segment coordinate systems of a fifteen-segment rigid body model. *XYZ*, Euler or quaternion formulations could then be used to describe the motion of these coordinate systems, and therefore the rigid body model, in 3-D space. However, the first step was to derive the segment coordinates systems from the *XYZ* coordinates of the markers (real and virtual) on each body segment.

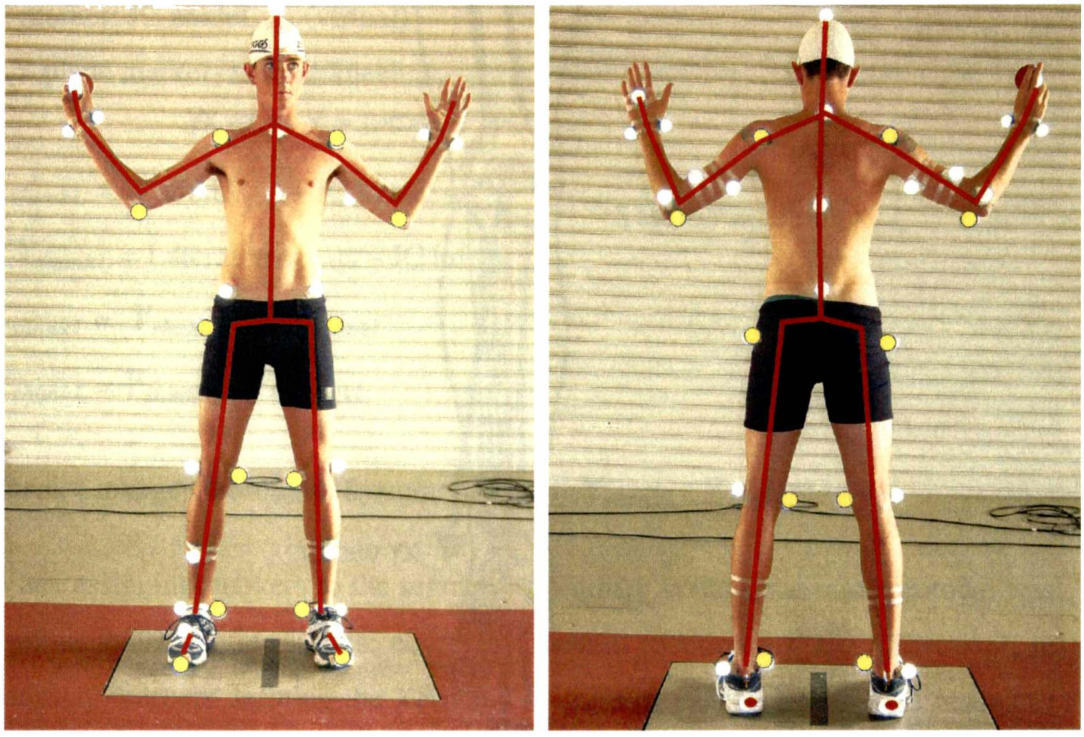

Figure 3-7: Front and back views of the EVa 6.0 fifteen-segment link model ('internal virtual skeleton') created by linking the virtual joint centre markers. The fourteen temporary markers that were removed for the moving trials are shown in yellow. Note that the foot link runs from the heel to the top of the shoe.

The *Y*-axis vector was generally defined to run along the long axis of the segment from proximal to distal end. It was calculated by subtracting the *XYZ* coordinates of the proximal marker from the *XYZ* coordinates of the origin marker. Then the cross product of the *XY*-plane vector (or *XY*-vector) and the *Y*-axis vector was calculated to generate the *Z*-axis vector. Note that the *XY*-vector was found by subtracting the *XYZ* coordinates of the *XY*-plane marker from the *XYZ* coordinates of the origin marker. The *Z*-axis vector had to be always orthogonal to the

anterior surface of the segment in the anatomical position, so either the *XY*-vector prior to the cross product or the *Z*-vector was rotated to meet this convention. Then the cross product of the *Y*-axis and *Z*-axis vector was calculated to find the *X*-axis. In this way, the *X*-, *Y*- and *Z*-axes were calculated for each segment (Figure 3-8).

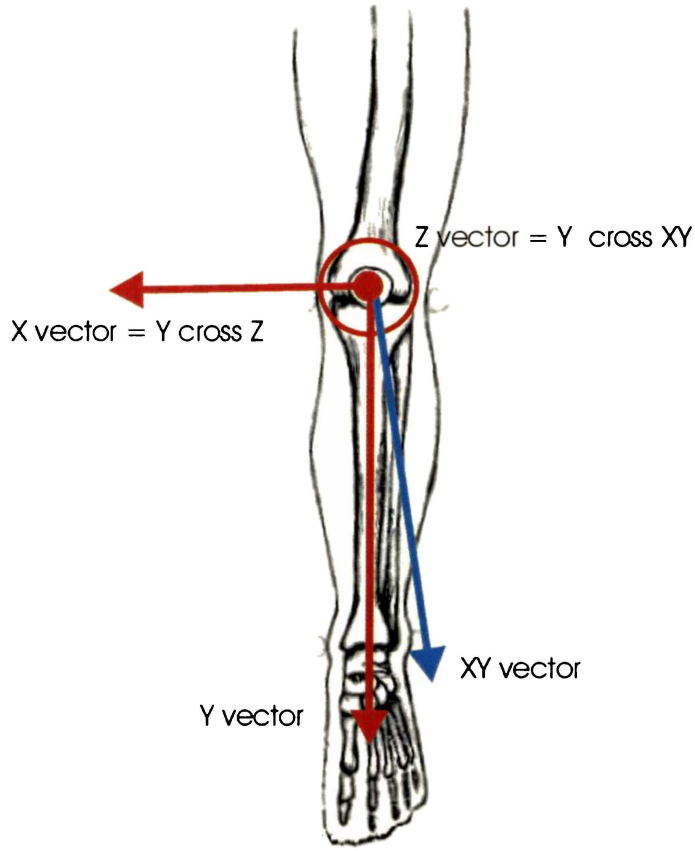

Figure 3-8: Method for determining link segment coordinate system for the left shank segment. First calculate vectors *Y* and *XY*, and then take their cross product to determine *Z* (red circle with dot indicating that *Z* points out of the page). Finally to calculate *X*, take the cross product of *Y* and *Z*.

Example: Left shank segment (Figure 3-8)

Step 1: Determine origin point → Joint Centre (JC) knee left (virtual marker coordinates)

Step 2: Determine *Y* vector (red) → JC ankle left coordinates *minus* origin point coordinates

Step 3: Determine *XY* vector (blue) → lateral ankle marker coordinates *minus* origin point coordinates

Step 4: Calculate cross product of Y and XY so that Z points out from superior surface of segment in anatomical position → Y vector CROSS XY vector

Step 5: Calculate orthogonal X vector → Y vector CROSS Z vector

Final link segment coordinate set (**X vector, Y vector, Z vector**)

Therefore, in terms of notational short hand, for the left shank:

Origin marker: JC kneeL $_{xyz}$ (virtual)

Y marker: JC ankleL $_{xyz}$ (virtual)

XY plane marker: Lateral kneeL $_{xyz}$

$\boldsymbol{Y}_{shankL}$ = JC ankleL $_{xyz}$– JC kneeL $_{xyz}$

$\boldsymbol{XY}_{shankL}$ = Lateral kneeL$_{xyz}$ – JC kneeL $_{xyz}$

$\boldsymbol{Z}_{shankL} = \boldsymbol{Y}_{shankL} \times \boldsymbol{XY}_{shankL}$

$\boldsymbol{X}_{shankL} = \boldsymbol{Y}_{shankL} \times \boldsymbol{Z}_{shankL}$

Shank Linkage Coordinate System: ($\boldsymbol{X}_{shankL}$,$\boldsymbol{Y}_{shankL}$, $\boldsymbol{Z}_{shankL}$)

When assigning markers to the segment coordinate system, the same protocol was used as that to define a local coordinate system (Section 3.1.3.1). However, in addition, markers defining the XY-plane markers of each segment were placed as far as possible away from each other to ensure that the positions of these markers were not incorrectly identified with that of the adjacent segment for any appreciable time.

The calculation of the segment coordinate systems for each of the segments is shown in Appendix D.

In summary, the relative location and orientation of the local segment coordinate systems were specified with respect to the laboratory (global) coordinate system. Offset angles for the X-axis and Z-axis were chosen so that the Z-axis was set orthogonal to the anterior surface of the segment, when the subject was standing in the anatomical position, i.e. pointed outwards or forwards from all segments

(Figure 3-9). The whole purpose of carrying out this extensive process of developing a marker-based arrangement to define 3-D local segment cordinate systems on the human body was to represent the motion of the bowler as the motion of the link segment model. Then the bowling action could be described in terms of 3-D kinematics.

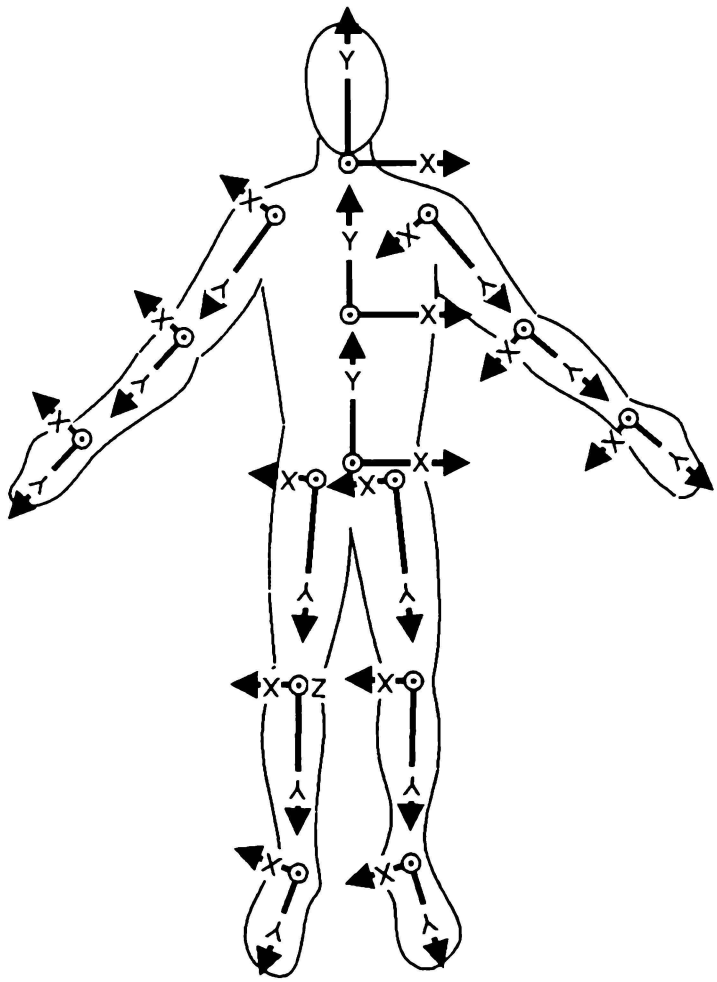

Figure 3-9: Segment coordinate systems for 15-segment link model. If the lower trunk is considered the root segment, then for each segment coordinate system the origin is the proximal joint centre, the *Y*-axis is the longitudinal axis of the segment, and *Z*-axis ⊙ points forward, or more accurately, orthogonal to the anterior surface of the segment in the anatomical position.

3.1.4 Segment Hierarchy Definitions

After defining the segment coordinate systems, EVa 6.0 required 'child-parent' relationships between the segments to be defined. The root segment was the lower trunk segment, which was defined with respect to the global coordinate system. All other segments were defined in a proximal to distal sequence from the lower trunk, so that the translations and rotations of each segment could be calculated relative to each preceding local coordinate system.

3.1.5 Segment Linkage Definitions

After the marker names were defined, linkages were made between the markers. The function of this was two-fold: (i) to display the link segment model as a stick figure, and (ii) to enable EVa 6.0 to optimise tracking of markers at a later stage. Some care had to be taken when creating the linkage order, because this could effect the tracking process. In general, *Motion Analysis Corporation* recommended that

- Markers are ordered such that each successive marker builds the segment linkage mode from top to bottom without any back tracking.
- The first markers are linked into a triangle to optimise marker identification. For this reason the pelvis was linked first, linking the right ASIS, left ASIS and mid-PSIS in a linkage order of 1-2, 1-3, and 2-3.

3.1.6 Pre-testing

3.1.6.1 Capture Volume

The combined views of the fast motion analysis cameras map out a 3-D capture volume in which the bowling trials were to be performed. This had to be carefully defined. The portion of the bowling action for analysis was from back foot contact to ball release. Observing pilot trials of bowlers delivering balls at maximum speed identified the approximate volume of the required experimental area. Adding a tolerance of one metre, which would allow for variations in performance and height differences in subjects, the horizontal range of the capture

volume was marked off with reflective tape. To mark the capture volume height, poles covered with markers were secured at each end lengthwise of the tracking area, and at the edge of the force platform (Figure 3-10). The height was nearly uniform throughout the length of the capture volume, but additional height was specified at the start of the capture volume, when back foot contact occurs, to capture markers on the raised non-bowling arm, and near the force platform where the bowling arm reaches the vertical position. The width was a little more than the width of the athletics track on which the subjects were to bowl, but to accommodate the height and horizontal length of the capture volume, the width was always larger than this, and in some camera views more than others.

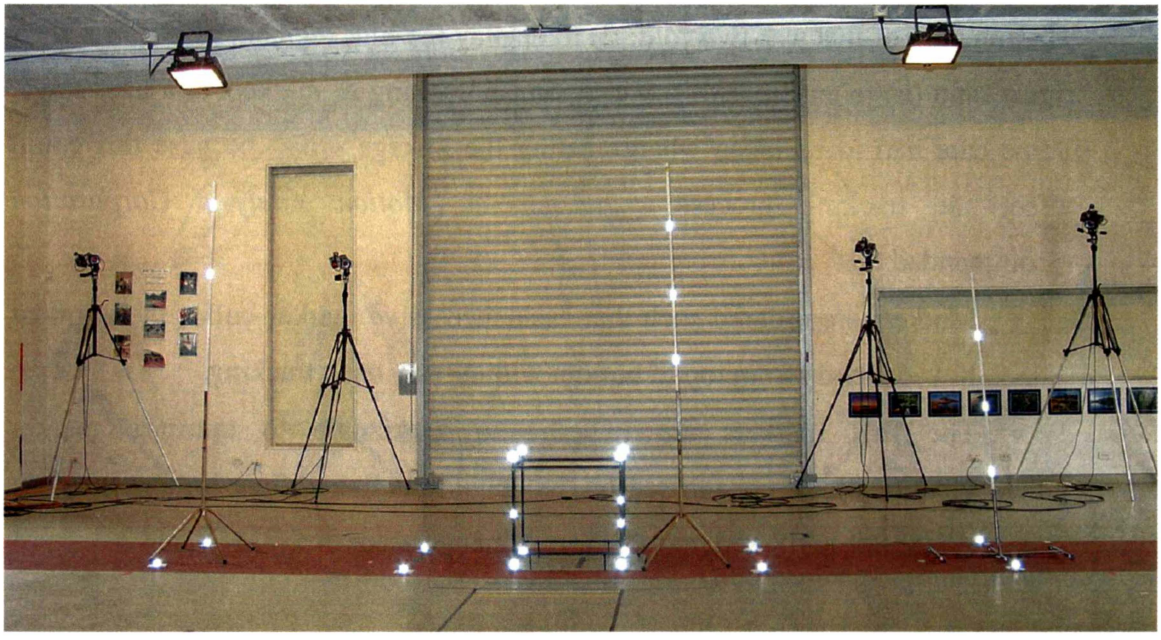

Figure 3-10: The lateral view of the capture volume delimited by reflective markers. Poles secured in stands were placed with markers to specify the height of the capture volume. Note how a high pole was placed on the edge of the force platform to accommodate the height of the vertical bowling arm during delivery. The calibration cube was placed on the force platform.

The cameras were placed around the capture volume in such positions that they would yield the highest possible resolution without excluding any part of the capture volume. Cameras were therefore placed as evenly as possible around the performance area. The restriction of laboratory space in certain directions meant that some cameras could only view a portion of the capture volume. However, as long as all the markers were visible in at least two or preferably three cameras, they could be mapped in 3-D coordinates. Also, to optimise the camera views to

capture at the highest resolution, while excluding as much of the area outside the capture area as possible, it was necessary to tilt some cameras away from the horizontal.

3.1.6.2 Calibration

To translate the marker images in all the cameras into 3-D coordinate values, the system needed to be calibrated. For Eva 6.0, and motion analysis systems in general, this must be done whenever the cameras are moved, the coordinate system orientation changed, or different units of measure used.

The initial system calibration was performed with a cube having eight precisely located markers. These calibration markers are known as control points, and a minimum of six non-coplanar control points were required to calibrate each camera view. The control points are the three-dimensional equivalent of the simple scaled rod used for two-dimensional studies. Before performing any calibration, the location of the origin and orientation of the cube was fixed carefully, because this determined the orientation of the laboratory coordinate system. The cube was placed so that the *Z*–axis pointed vertically upwards, the *X*-axis was in the direction of the forward motion, and the *Y*-axis was to the left as viewed in the forward direction (Figure 3-11). Also, great care was taken to make sure that the centre point of the reflective sphere corresponding to control point 1 was placed exactly over the back right corner of the force platform. This very precisely located the origin of the laboratory coordinate system, and therefore acted as a constant reference system for all the trials. Also, its constant placement meant that measurements in the force platform coordinate system, which had its origin at the centre of the platform, the *X*- and Y-axes swapped (with respect to the laboratory coordinate system), and the *Z*-axis pointing downwards, could be transformed into the laboratory coordinate system.

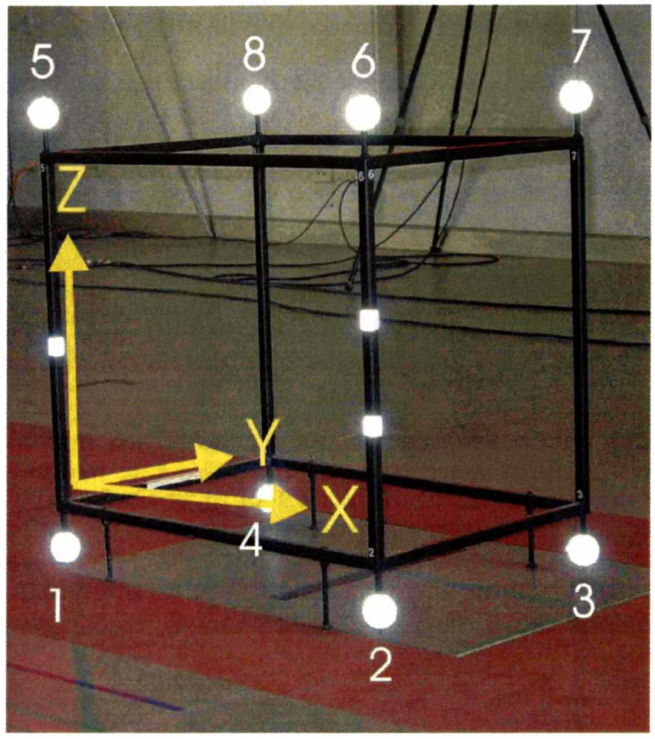

Figure 3-11: The calibration cube with eight control points. The placement and orientation of the cube determined the laboratory coordinate system.

The actual calibration calculation was highly automated and easy to perform. Once the cube was filmed, a mouse click on a toggle box next to the control box name digitised the control points. Occluded or partially occluded control points were not used. As long as a minimum of six control points per camera view were correctly digitised, the system could perform the calibration. The cube calibration files were then saved into the corresponding project file.

Next, a precisely measured wand (1.0 m) was carried through the entire capture volume. This second step was required because the cube calibration directly calibrated only the space near the cube. Measurements made some distance away from the cube had reduced accuracy since they were only extrapolations based on the directly calibrated space near the cube. Therefore, such a wand calibration was performed so that the entire capture volume was calibrated. Using wand calibration data, EVa 6.0 established the location of each camera and accounted for any geometric distortion that the camera lenses may have had.

The method of moving the wand was to capture images of the wand parallel to each of the three axes throughout the capture volume. Though there are various

techniques of doing this, the one which worked better was to first walk back and forth along the length of capture volume with the wand parallel to the *Y*-axis, traversing the wand in a vertical serpentine path on each turn. When the full vertical volume was covered, the wand was turned parallel to the *X*-axis, and made to traverse the width of the capture volume in a vertical serpentine path while proceeding from one end to another. The final walk had the wand held vertically, progresively sweeping out a higher level of vertical space on each turn. This wand calibration data collection process was set to run for two minutes. The raw wand data was then viewed and if sufficient capture volume was covered by the wand, and the number of usable frames per camera was greater than 30, then the wand calibration was considered successful, and loaded into the corresponding project file.

3.1.6.3 Force Plate Initialisation

Before every testing session, the force plate was initialised to zero by pressing the auto-zero button, which balanced the Wheatstone bridge circuits. Also, a subject stood on the platform to confirm that the vertical ground reaction force matched his weight. Finally, the subject would perform a series of jumps on the force plate to confirm that ground reaction forces were being measured in all three coordinates.

3.1.6.4 Camera and Force Plate Synchronisation

To test the synchronicity of the cameras and the force platform, a spherical marker covered with reflective tape, was rolled slowly off a table 1.76 m above the ground. The table was placed so that the marker would fall approximately in the middle of the force platform. Twenty trials were performed, and two linear regressions done for ten points on either side of the bounce to estimate the bounce of the marker (Figure 3-12). Five measurements by the camera system of a marker placed on the force platform gave an average centroid height of 18.3 ± 0.3 mm. Therefore, it was estimated that when marker first reached this height above the ground, initial ground contact was made. Synchronisation error was

determined by comparing this estimated ground contact time with that measured by the force platform.

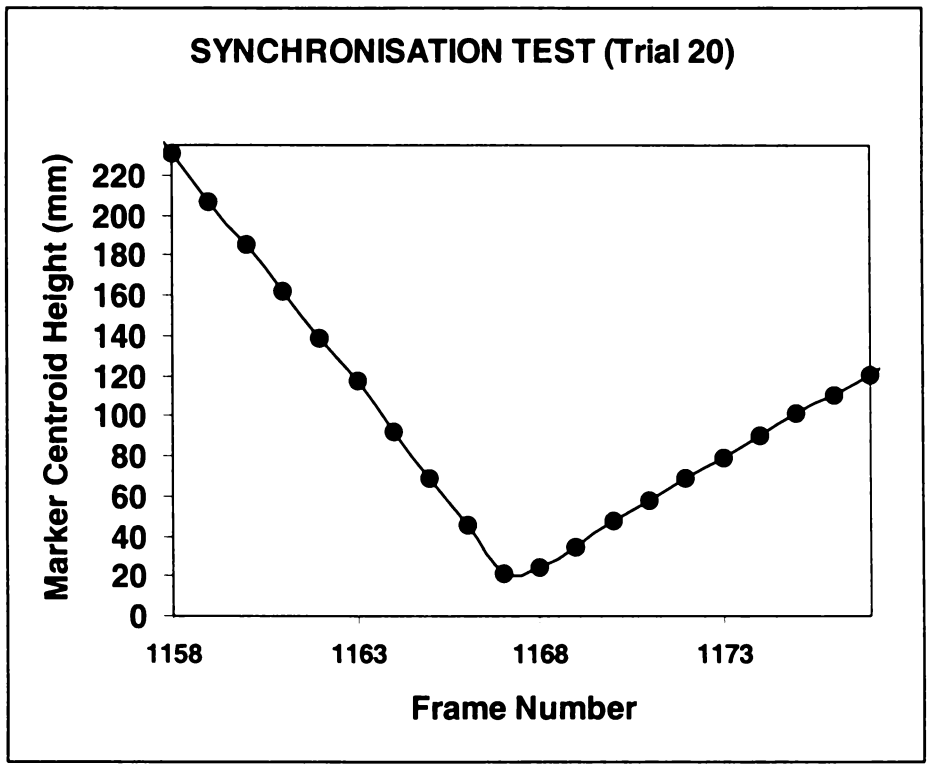

Figure 3-12: Synchronisation test for the last trial. The regression equation y = -23.23 x + 27.13 was used to find when the marker height was equal to 18.3 mm, where *y* is marker centroid height and *x* is frame number.

Expressing the synchronisation error as a ratio of the camera frame rate showed that the video data lagged the force plate data by 0.19 ± 0.07 frames. This is less than a quarter of a frame, and no compensation in the camera time scale was made, as it could not be determined how much of this time lag was due to errors in the measurement process itself. However, it was confirmed from this simple test that the EVa 6.0 motion analysis system achieved synchronisation between the camera and force plate.

3.1.7 Experimental Protocol

Prior to data collection, each subject signed a Subject Consent Form (Appendix A, Figure A.1) after reading the Subject Information Sheet (Appendix A, Figure A.2). Also, a Subject Data Sheet was filled out during data collection (Appendix A, Figure A.3). Subjects were also given a fifteen-minute explanation of the

experimental protocol, including the basic operational function of the camera-based motion analysis system and force platform.

To ensure that all the designated markers could be placed on the body, subjects were required to wear shorts (preferably bicycle shorts), socks, and low-cut running shoes. After the subject completed his standard warm-up, the static trial marker set of forty-five markers was placed on the body. The markers were table-tennis balls covered with retro-reflective tape. Markers were secured to small rectangular strips of Velcro™, and then attached to the body by means of Scotch™ double-sided tape. The diameter of the markers was 39 mm, which, for the capture volume used, was within the range to attain optimal accuracy according to specifications in the *Eva 6.0 Reference Manual.*

For the static trial, the subject was oriented so that the posterior-anterior axis was parallel to the laboratory *X*-axis, and the medio-lateral axis parallel to the laboratory *Y*-axis, as determined by the placement of the calibration cube (Figure 3-14). The subject stood upright with the knees slightly flexed, approximately shoulder-width apart, and the arms vertically abducted ninety-degees, slightly flexed at the elbows, with the palms facing the front. Ten seconds of data on the static trial were collected, and a preliminary check was made to see whether all the markers were tracked.

Following successful completion of the static trial, fourteen markers were removed for the moving trials. The moving trials were of two types. In *trial type I*, the subject had to make front foot contact with the force platform, while delivering six balls to land on the athletics track, which were (i) within a 12 m to 20 m range, and (ii) approximately in line with a set of wickets. Distances were measured from the front foot landing crease represented by a white line on the middle of the force platform. The distance of the wickets from the front foot crease was a proper pitch length, and the acceptable range of delivery was roughly in accordance with that delivered in a match. In the second trial type (*trial type II*), the subject had to perform the same as trial type I, but instead make back foot contact with the force platform. The front foot landing crease was now moved 1 m forward of the force platform to accommodate back foot contact, and the

wickets shifted back accordingly. It was ascertained whether proper contact was made by the correct foot on the force platform for both trial types. If there was any doubt that even a portion of the foot landed outside the force platform, then another trial was recorded.

Fast bowlers requires a sufficient run-up to produce fast ball release speeds. Such an activity could not be solely contained within the confines of the laboratory, and needed both entry and exit doors open: the former to allow for an 18 m run-up, and the latter to propel the ball through. To ensure that the trials were executed safely, a person was stationed outside to watch for people crossing the path of the ball, and warning signs were placed on the surroundings of the experimental area.

After each ball, the markers were tracked to determine whether all the markers were captured for a sufficient number of frames. It was not realistic to expect every marker to be tracked at all times due to the large number of markers moving at high speed, some of which were in relatively close proximity to each other, and others in positions which were temporarily occluded during phases of the motion. Also, with the laboratory doors open to accommodate the run-up and ball release, there was a higher level of ambient light than is typically used for such motion analysis systems, making it more difficult to track markers. To minimise this problem, early morning and evening trial times were avoided when the sun was closer to the horizon, reducing the amount of light shining through the laboratory doors.

3.1.8 Digitisation and Tracking

Once a trial was captured, the data consisted of a collection of video files containing images of markers. Each camera had its own video file. Turning the 2-D video image data into 3-D data required the calibration data. The video data was converted into tracked marker paths, and the display showed each marker's position in 3-D space. In many cases, only a little further editing of the tracks was required. If there were obscured markers for short periods, then it was possible to interpolate their positions. There were also times when markers were specified as unidentified for portions of the time line, and manual identification of the tracks

was performed. However, for most of the markers, the actual identity of each marker was only determined manually for a single frame of data. Once this was completed for a good frame of data, the marker identities were rectified for the entire range of frames.

3.1.9 Static Trial Calculations

One output file format contained the hierarchical translations and rotations for each body segment. After tracking the static trial, these were saved and exported into *Micrsoft Excel* to read the rotational *X*-, *Y*-, and *Z*-axis offsets for the segment coordinate systems to locate the virtual markers with respect to the temporary markers. These offset values were then entered into Eva 6.0, and the positions of the virtual joint centres were calculated. Therefore, all internal joint centres were calculated, and the link segment model defined. The project was then saved, so that the same virtual marker offset values could be used to calculate the joint centres in subsequent moving trials for the same subject. For each subject, this process had to be repeated.

3.1.10 Moving Trial Calculations

After tracking the moving trial, the tracks of all virtual markers and permanent markers were calculated, and saved in *XYZ* coordinates as an ASCII Type 4 (.trc) file. From this data, each local segment coordinate system was reconstructed as a set of orthogonal vectors in cartesian 3-D space. Then mathematical formulae were derived to calculate the orientation of the local coordinate systems into Euler *ZYX* sequences relative to the global reference system, determined by the orientation of the calibration cube (Appendix E). The kinematic data set could now be used as input to a 3-D inverse solution dynamics model.

3.2 ANALYTIC MECHANICS OF MULTI-BODY SYSTEMS

3.2.1 Introduction

The Mechanical Systems Pack is a dynamics software implementing the Lagrange Multiplier Method to analyse rigid body mechanisms. This pack is written entirely in the Mathematica programming language and is completely portable and platform independent. Mathematica (V 3.0, Wolfram Research Ltd.) integrates a numeric and symbolic computational engine, graphics system, and programming language to perform various mathematical computations. Using the library of 3-D geometric constraints in the Mechanical Systems Pack, complex mechanical relationships and algebraic constraints were used to model the human body as a system of rigid body segments. Object-oriented, model-building commands assemble constraints to connect rigid bodies into a complete mechanism that were solved for dynamic forces when segment inertia properties were defined. Also, any number and size of external loads could be applied to the model. Both inverse and forward solution dynamics could be calculated.

This section on the methodology of the modelling process will include an overview of the mathematics and mechanics of the Lagrange multiplier method utilised by the software. An introduction to the basic concepts of kinematics applicable to rigid body systems is also included to provide a foundation for the subsequent section on dynamics. Therefore, the concepts of algebraic constraint equations, coordinate systems, and degrees of freedom are introduced here. Then a concise treatment of dynamics establishes the Newton-Euler equations as the fundamental tool in the dynamic analysis of rigid body systems that are connected by kinematically constrained joints. This is followed by the development of the Lagrange multiplier formulation for constrained systems, which calculates the joint reaction forces in terms of Lagrange multipliers.

Finally, an outline of the Mechanical Systems Pack programme is given. This follows naturally as the software programme is basically a systemised collection of black box entities, each performing a specified mathematical functional task.

3.2.2 Vectors and Matrices

Vector analysis is a traditional tool for describing the kinematics and dynamics of mechanical systems. However, in its geometric form, vector algebra is not well suited to computer implementation. Therefore, an *algebraic matrix vector representation* was used by the Mechanical Systems Pack, which makes it easier to manipulate formulae in the programming environment.

In general, a matrix with m rows and n columns of dimension m x n is denoted by a boldface capital letter and is written as

$$\mathbf{A} \equiv [a_{ij}] \equiv \begin{bmatrix} a_{11} & a_{12} & \cdots & a_{1n} \\ a_{21} & a_{22} & \cdots & a_{2n} \\ \vdots & \vdots & & \vdots \\ a_{m1} & a_{m2} & \cdots & a_{mn} \end{bmatrix}$$

where a typical element, a_{ij}, is located at the intersection of the ith row and jth column. A matrix with only one column is called a *column matrix* and is denoted by a boldface lower-case letter, e.g. **a**. Using this convention, a *row matrix*, which has only one row, would be represented as $\mathbf{a}^T$ (i.e. the transpose of a column matrix), where the superscript T designates the transpose of a matrix.

A vector $\vec{\mathbf{a}}$ in its traditional geometric form can be resolved into its cartesian components a_x, a_y, and a_z along the x, y, and z axes of a cartesian coordinate system. If the unit vectors $\vec{u}_x, \vec{u}_y$, and $\vec{u}_z$ are directed along their respective coordinate axes, then the vector could be expressed as the sum of its components

$$\vec{\mathbf{a}} = a_x \vec{\mathbf{u}}_x + a_y \vec{\mathbf{u}}_y + a_z \vec{\mathbf{u}}_z$$

Alternatively, the vector $\vec{\mathbf{a}}$ can be expressed in matrix notation as

$$\mathbf{a} = \begin{bmatrix} a_x \\ a_y \\ a_z \end{bmatrix} \equiv [a_x, a_y, a_z]^T$$

This is the *algebraic* (or *component*) *representation of a vector*, which is a powerful tool for vector algebra. An important concept of this approach is the definition of the *skew-symmetric matrix*, which for vector **a** would yield

$$\tilde{\mathbf{a}} = \begin{bmatrix} 0 & -a_z & a_y \\ a_z & 0 & -a_x \\ -a_y & a_x & 0 \end{bmatrix}$$

where the *tilde* over the vector indicates that the components of the vector are used to generate the skew-symmetric matrix. Now the vector or cross product $\vec{a} \times \vec{b}$ can be calculated directly in terms of its components

$$\mathbf{c} = \tilde{\mathbf{a}}\,\mathbf{b} = \begin{bmatrix} a_y b_z - a_z b_y \\ a_z b_x - a_x b_z \\ a_x b_y - a_y b_x \end{bmatrix}$$

where $\mathbf{b} = [b_x \;\; b_y \;\; b_z]^{\mathrm{T}}$.

This allows the calculation of various vector algebraic operations by the use of simple matrix multiplication

$$\vec{\mathbf{a}} \cdot \left(\vec{\mathbf{b}} \times \vec{\mathbf{c}}\right) = \mathbf{a}^{\mathrm{T}}\,\tilde{\mathbf{b}}\,\mathbf{c}$$
$$\vec{\mathbf{a}} \times \left(\vec{\mathbf{b}} \times \vec{\mathbf{c}}\right) = \tilde{\mathbf{a}}\,\tilde{\mathbf{b}}\,\mathbf{c}$$
$$(\vec{\mathbf{a}} \times \vec{\mathbf{b}}) \times \vec{\mathbf{c}} = \tilde{\tilde{\mathbf{a}}}\,\mathbf{b}\,\mathbf{c}$$

As the Mechanical Systems Pack implements the matrix vector algebraic formulation, the dynamic equations of motion, which will be treated later, were derived with respect to this notation.

Time derivatives of vectors can easily be expressed using matrix vector algebra to analyse kinematics. The time derivative of a vector $\mathbf{a} \equiv \mathbf{a}(t) = [a_1(t), a_2(t), a_3(t)]^{\mathrm{T}}$ is denoted by

$$\frac{d}{dt}\mathbf{a}(t) = \left[\frac{d}{dt}a_1(t), \frac{d}{dt}a_2(t), \frac{d}{dt}a_3(t)\right]^{\mathrm{T}} \equiv \dot{\mathbf{a}}$$

Similarly, as in the differentiation of a vector function, the derivative of a matrix $\mathbf{A}(t) = [a_{ij}(t)]$ whose components are functions of time t is expressed as

$$\frac{d}{dt}\mathbf{A}(t) = \left[\frac{d}{dt}a_{ij}(t)\right] \equiv \dot{\mathbf{A}}$$

For partial derivatives, which are used in various non-linear differential and algebraic equations of several variables, a special matrix calculus notation is needed. If Φ is a scalar differentiable function of $\mathbf{q}$, which is a vector of k real variables, then for $\boldsymbol{\Phi}(\mathbf{q}) = [\Phi_1(\mathbf{q}), \Phi_2(\mathbf{q}), \ldots, \Phi_m(\mathbf{q})]^T$, a vector of m differentiable functions of $\mathbf{q}$, the following notation is defined

$$\boldsymbol{\Phi}_{\mathbf{q}} \equiv \frac{\partial \boldsymbol{\Phi}}{\partial \mathbf{q}} \equiv \left[\frac{\partial \Phi_i}{\partial q_j}\right]_{(m \times k)}$$

where i is the row index, and j is the column index.

3.2.3 Multiple Rigid Bodies in 3-D Space

A *rigid body* is defined as a system of particles where the distance between particles remains constant. Therefore, if any position vector is fixed on a particle of a rigid body, this vector would never change it is position relative to the body, even when the body is in motion. Though in reality all solid bodies deform to some extent with the application of a force, all dynamic analysis in this thesis is based upon this approximation of rigidity.

A *mechanism* is a collection of rigid bodies connected by *links* or *linkages* that allow rigid bodies to articulate about each other. An assemblage of interconnected links is called a *kinematic chain.* A *closed-loop* mechanism is formed from a closed chain, wherein each link is connected to precisely two other links of the mechanism. However, an *open-loop* mechanism is formed from a collection of links or bodies that are kinematically connected to each other but for which it is impossible to move to successive links across kinematic joints and return to the starting link.

Any set of parameters that uniquely specifies the position or configuration of all bodies in a mechanism is called a set of *generalised coordinates.* Vectors of coordinates are commonly specified as column vectors $\mathbf{q} \equiv [q_1, q_2, q_3, \ldots, q_n]^T$, where n is the total number of coordinates used in describing the system. The minimum number of generalised coordinates to fully describe the configuration of a mechanism is called the number of *degrees of freedom* (DOF) of the system. A

rigid body in 3-D space has six DOF: three for location, and three for orientation. Any set of coordinates that are equal in number to the degrees of freedom of the system is called a set of *independent coordinates*. If the number of coordinates exceeds that of the DOF then there are *dependent coordinates*, which may be determined from some function of a subset of the independent coordinates. A *cartesian coordinate system formulation* is one that defines the position of each body in space relative to a fixed global system.

A rigid body representation of the human body is essentially a multi-linked open-loop mechanism, and the common method of describing the configuration of such a system in 3-D space is to

1. Specify three linear independent coordinates, usually cartesian, to locate the centre of mass (CoM) of each rigid body relative to the origin of some global cartesian coordinate system (*G*).
2. Specify three independent ordered angular coordinates, commonly Euler angle sequences, to orient each body-fixed local coordinate system relative to the global system *G*.
3. Determine the degrees of freedom (DoF) of the linkage system to indicate the number of independent generalised coordinates to specify the location and orientation of the whole linkage system.

Using Euler angles, the complete description of the rotation of a rigid body in 3-D space requires the specification of three independent direction angles to orient a local frame (*xyz*), defined by an orthogonal set of body-fixed axes with respect to the global corrdinate system or fixed global reference frame (*XYZ*). Euler angles treat this matter as a specific sequence of three rotations. By using body-fixed rotations and selecting nonparallel axes about which the rotations are carried out, there are twelve possible ways to describe the rotation of a coordinate system in 3-D. For instance, if we start with a body oriented exactly with the *XYZ* global frame, and rotate it about any one of the global axes, then there are three possible choices – either *X, Y or Z* - and the resulting frame would be $X'Y'Z'$. For the next rotation there are two possible choices – either about the X', Y', *or* Z' axes, excluding the one that is equivalent to the previous rotation. This yields the x', y',

or z' set of axes. For the final rotation there are a further two choices, again ignoring the rotation about the axis that coincides with the previous rotation, and this produces the final *x, y, z* local body-fixed coordinate system with respect to the global coordinate system *G*. As a result, there are 3 x 2 x 2 = 12 possible Euler angle sequences:

1-2-1, 1-2-3, 1-3-1, 1-3-2, 2-1-2, 2-1-3, 2-3-1, 2-3-2, 3-1-2, 3-1-3, 3-2-1, 3-2-3

The numbers refer to the order of rotation and the axis of rotation. For instance, in a 3-2-1 sequence, the number '3' indicates that the first rotation ψ is about the global *Z*-axis, the number '2' that the second rotation θ is about the Y' axis, and the number '1' that the third rotation ϕ is about the x' axis (Figure 3-13).

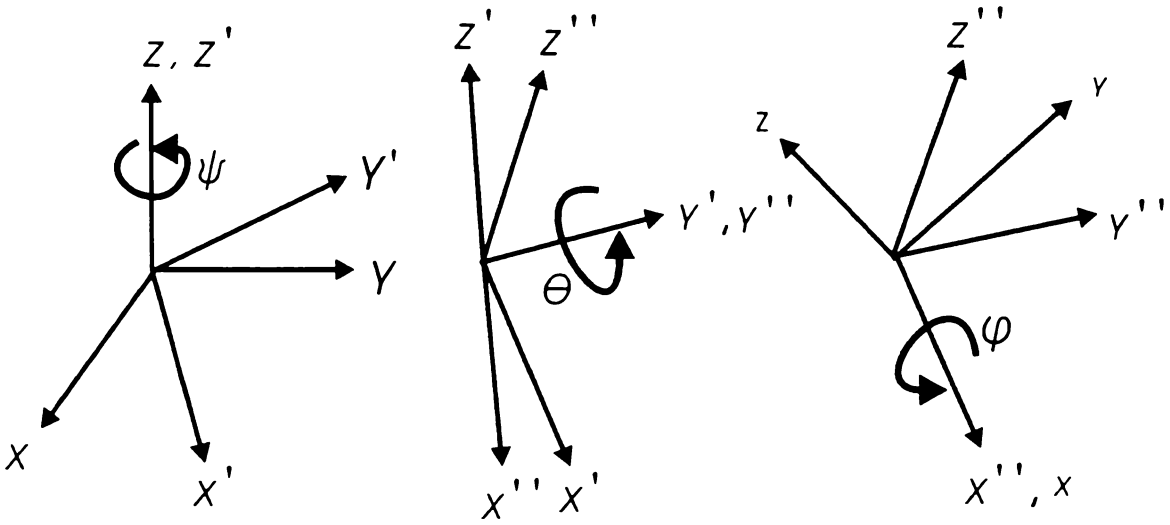

Figure 3-13: The Euler 321 or ZYX sequence.

Depending on the modelling problem, an independent set of angles can be selected to suit. A common Euler angle sequence is the 3-1-3 sequence, which has been traditionally used to describe rigid bodies. However, recently the 3-2-1 sequence has become popular for rigid body systems (Baruh, 1999), and is often used in biomechanical applications. For 3-2-1 transformations, the rotation angles are known as ψ heading, θ attitude, and ϕ bank. To obtain the combined transformation from the global *XYZ* coordinate system to the local *xyz* coordinate system, the matrix rotations are successively applied for each transformation:

$$\begin{bmatrix} X_1 \\ Y_1 \\ Z_1 \end{bmatrix} = \begin{bmatrix} \cos\psi & \sin\psi & 0 \\ -\sin\psi & \cos\psi & 0 \\ 0 & 0 & 1 \end{bmatrix} \begin{bmatrix} X \\ Y \\ Z \end{bmatrix}$$

$$\begin{bmatrix} X_2 \\ Y_2 \\ Z_2 \end{bmatrix} = \begin{bmatrix} \cos\theta & 0 & -\sin\theta \\ 0 & 1 & 0 \\ \sin\theta & 0 & \cos\theta \end{bmatrix} \begin{bmatrix} X_1 \\ Y_1 \\ Z_1 \end{bmatrix}$$

$$\begin{bmatrix} x \\ y \\ z \end{bmatrix} = \begin{bmatrix} \cos\phi & \sin\phi & 0 \\ -\sin\phi & \cos\phi & 0 \\ 0 & 0 & 1 \end{bmatrix} \begin{bmatrix} X_2 \\ Y_2 \\ Z_2 \end{bmatrix} \tag{3.0}$$

Combining the three transformations gives

$$\begin{bmatrix} x \\ y \\ z \end{bmatrix} = [R_{321}] \begin{bmatrix} X \\ Y \\ Z \end{bmatrix} \tag{3.1}$$

where

$R_{321}=$

$$\begin{bmatrix} \cos\theta\cos\psi & \cos\theta\sin\psi & -\sin\theta \\ (\sin\phi\sin\theta\cos\psi - \cos\phi\sin\psi) & (\sin\phi\sin\theta\sin\psi - \cos\phi\cos\psi) & \sin\phi\cos\theta \\ (\cos\phi\sin\theta\cos\psi + \sin\phi\cos\psi) & (\cos\phi\sin\theta\sin\psi - \sin\phi\cos\psi) & \cos\phi\cos\theta \end{bmatrix} \tag{3.2}$$

Once the location of the root segment (generally defined as 'segment 1') and the rotation matrices are known, then the global *XYZ* coordinates of each segment's centre of mass (CoM_i) of a *n*-link segment chain is found by using the following summation (Figure 3-14):

$$CoM_i = W_0 + \sum_{i=1}^{n} (l_{cd(i-1)} + l_{pc(i-1)} R_{(i-1)}) \tag{3.3}$$

where l_{cd} is the segment length from the cente of mass (*CoM*) to distal end, l_{pc} is the segment length from proximal end to the CoM, *R* is the rotation matrix, and W_0 is the distance from the origin of the global coordinate system to the CoM of the root segment of the kinematic chain. By using multiple linkage chain

structures to represent the human body, the cartesian coordinate system formulation was used for each segment, i.e. to find the location and orientation of each body-fixed coordinate system with respect to the global coordinate system.

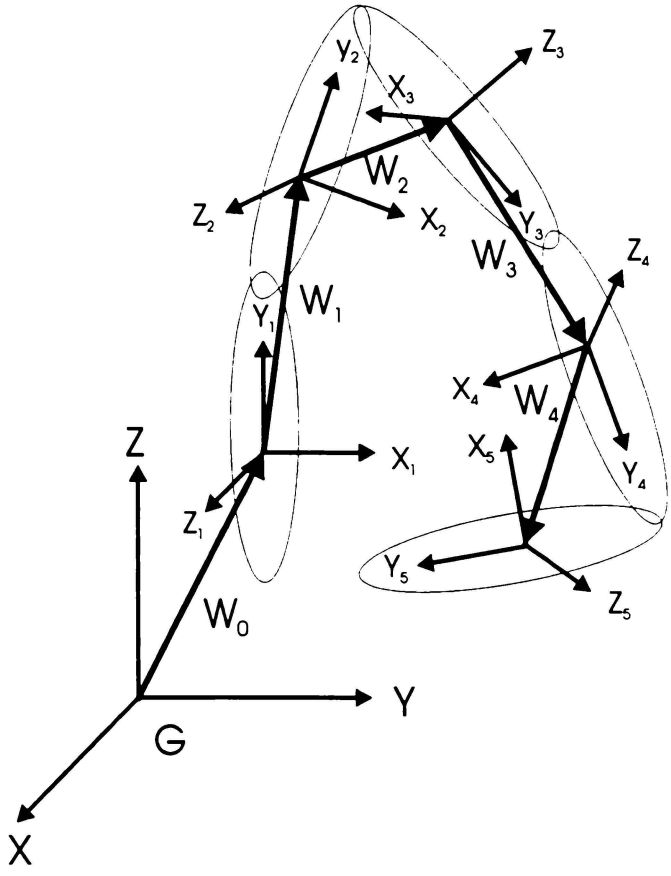

Figure 3-14: A 3-D five segment linkage system showing body fixed local coordinate systems with respect to the global coordinate system *G*. The local coordinate systems are fixed at the centre of mass, and the vector W_i used to calculate the global *XYZ* coordinates of each segmental centre of mass using the local coordinate systems.

Alternatively, Euler parameters could be used to specify the orientation of the body-fixed axes with respect to the global reference system. Euler parameters describe orientations as a set of four parameters, and so increase the number of variables from three to four, which introduces a redundancy. The expression of the Euler parameters for a particular coordinate system in 3-D space results from Euler's theorem in that a rotation of a rigid body about a fixed point of the body is equivalent to a rotation about a line that passes through this same point. This line is referred to as the *instantaneous axis of rotation*, and the point as the *centre of*

rotation. The four Euler parameters can be specified in terms of the rotation of the rigid body about the instantaneous axis of rotation *and* the direction cosines of the instantaneous axis of rotation (Figure 3-15). If $\theta_1, \theta_2,$ and θ_3 are the angles the instantaneous axis of rotation makes with a fixed reference coordinate axis system, then

$$c_1 = cos\theta_1 \qquad c_2 = cos\theta_2 \qquad c_3 = cos\theta_3 \tag{3.4}$$

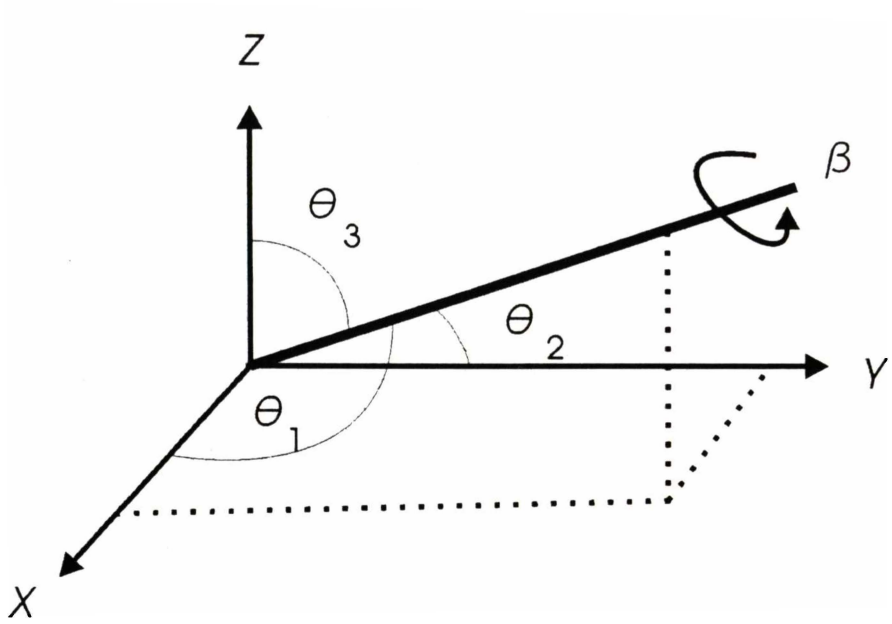

Figure 3-15: Euler's theorem states that a rotation of a rigid body can be described as a rotation (β) about its instantaneous axis of rotation.

Then the Euler parameters are defined as e_0, e_1, e_2, and e_3

$$e_0 = cos\left(\frac{\beta}{2}\right) \quad e_1 = c_1\ sin\left(\frac{\beta}{2}\right) \quad e_2 = c_2\ sin\left(\frac{\beta}{2}\right) \quad e_3 = c_3\ sin\left(\frac{\beta}{2}\right) \tag{3.5}$$

where β is the rotation angle about the instantaneous axis of rotation.

Also, the Euler parameters are related to each other so that

$$e_0^2 + e_1^2 + e_2^2 + e_3^2 = 1 \tag{3.6}$$

Therefore, in matrix algebraic form the four Euler parameters are put in a 4-vector as follows

$$\mathbf{p} = [e_0, e_1, e_2, e_3]^T \tag{3.7}$$

Then an important relation that is used in the Mechanical Systems Pack during the calculation of kinematics is

$$\mathbf{p}^T \mathbf{p} - 1 = 0 \tag{3.8}$$

The *Mechanical System Pack* uses the Euler parameters as a constant of the kinematic equations of motion, by calculating equation (3.8) at each step of the numerical integration to check for accuracy and numerical stability.

A disadvantage is that the Euler parameters do not lend themselves to a simple physical interpretation as do Euler angles. However, the Euler angles can always be calculated from the Euler parameters at each instant of motion whenever a physical interpretation or visualization is required. For instance, the R_{321} can be expressed in terms of Euler parameters

$$R_{321} = \begin{bmatrix} (e^2{}_0 + e^2{}_1 - e^2{}_2 - e^2{}_3) & 2(e_1 e_2 + e_0 q_3) & 2(e_1 e_3 - e_0 e_2) \\ 2(e_1 e_2 - e_0 e_3) & (e^2{}_0 - e^2{}_1 + e^2{}_2 - e^2{}_3) & 2(e_2 e_3 + e_0 e_1) \\ 2(e_1 e_3 + e_0 e_2) & 2(e_2 e_3 - e_0 e_1) & (e^2{}_0 - e^2{}_1 - e^2{}_2 + e^2{}_3) \end{bmatrix} \tag{3.9}$$

Then from the preceding rotation matrix, the following relationships between R_{321} elements and individual Euler angles hold

$$\begin{aligned} \phi &= \arctan\left(R_{321}(2,3) / R_{321}(3,3) \right) \\ &= \arctan\left(2(e_2 e_3 + e_0 e_1) / (e_0^2 - e_1^2 - e_2^2 + e_3^2) \right) \\ \theta &= \arcsin\left(-R_{321}(1,3) \right) \\ &= \arcsin\left(-2(e_1 e_3 - e_0 e_2) \right) \\ \psi &= \arctan\left(R_{321}(1,2) / R_{321}(1,1) \right) \\ &= \arctan(2(e_1 e_2 + e_0 e_3), (e_0^2 + e_1^2 - e_2^2 - e_3^2)) \end{aligned} \tag{3.10}$$

One major advantage is that Euler parameters are not subject to singularities, which is a property of Euler angles. Also, despite Euler parameters having to use four parameters and four differential equations of motion instead of three as for Euler angles, the linearity of the resulting equations and lack of singularities far outweigh the complexities introduced by the additional differential equation

(Baruh, 1999). For instance, when Euler angles relate the angular velocities to the rotation angles and their rates, the resulting equations are highly non-linear and have singularities, making them difficult to integrate, and perform any analytical or numerical work with them. Another advantage of the Euler parameter formulation is that it allows kinematic relationships for different pairs to be written in compact matrix form, so that compact and efficient computational algorithms can be developed (Nikravesh, 1988).

3.2.4 Constraint Equations

A *constraint* is any condition that reduces the number of degrees of freedom in a system. It is only through the specification of constraints that rigid bodies can be linked together to perform as a single mechanism. A geometric constraint that can be expressed analytically as an equation relating generalised coordinates and time is called *holonomic*. Therefore, a holonomic constraint equation describing a constraint condition on the vector of coordinates of a system can be expressed as

$$\Phi \equiv \Phi(\mathbf{q}, t) = 0 \tag{3.11}$$

Any geometric constraint that cannot be expressed analytically in the above form is known as *nonholonomic*. If the system is totally defined by a set of independent generalised coordinates, then the number of DOF equals the number of generalised coordinates minus the number of holonomic constraints. In this thesis, the term "constraint" refers only to holonomic constraints

3.2.5 Joint Constraints

Each rigid body in 3-D space has six DOF. To adequately model the human body, it was decided to design a mechanism of fifteen rigid body segments. Fifteen segments moving independently in 3-D space gives 90 DOF (i.e. 6 DOF x 15 segments). However, to incorporate these rigid bodies in a dynamic model of bowling, these rigid bodies need to form a mechanism that resembles the human body in which the segments are articulated at joint centres. To link adjacent rigid body segments, *spherical joints* were used. These joints constrain three DOF, and are equivalent to the human *ball-and-socket joint*, which allows flexion-extension, adduction-abduction, and internal-external rotation. This is the most general

constraint that accounts for the complete range of anatomical movements. In the model there are 15 joints, and all of these were modelled with spherical joints, reducing the number of DOF to 45. However, to account for the translation of the whole body, a *relative distance driving constraint* was applied to the virtual joint centre at the mid-hips. Note that for the shoulder joints, relative distance constraints were used in addition to the spherical joint constraint because the shoulder joint is movable against the upper trunk segment. The addition of the driving constraints at the mid-hips and shoulder joints increased the number of DOF to 54.

In the constraint equation formulation, it is necessary to express the components of all vectors in the same coordinate system, the most natural being the global coordinate system. The global components of a vector that are fixed in a body may be obtained from the global coordinates of its endpoints. To illustrate this, the *relative distance constraint* (**d**) between points B_i and B_j of two separated bodies is calculated as

$$\begin{aligned}\mathbf{d} &= (\mathbf{r}_j + \mathbf{s}_j^B) - (\mathbf{r}_i + \mathbf{s}_i^B) \\ &= \mathbf{r}_j + \mathbf{R}_j \mathbf{s}_j'^B - \mathbf{r}_i - \mathbf{R}_i \mathbf{s}_i'^B\end{aligned} \tag{3.12}$$

where $\mathbf{s}_i^B = \left[\xi^B, \eta^B, \zeta^B\right]_i^T$ and $\mathbf{s}_j^B = \left[\xi^B, \eta^B, \zeta^B\right]_j^T$ are known constant vector quantities, and $\mathbf{R}_i$ is the rotation matrix (Figure 3-16). Note that the global components of a vector that connect points on two bodies only depend on the global position of the bodies, i.e. on vectors $\mathbf{r}_i$ and $\mathbf{r}_j$ (i.e. using the Cartesian generalised coordinate formulation).

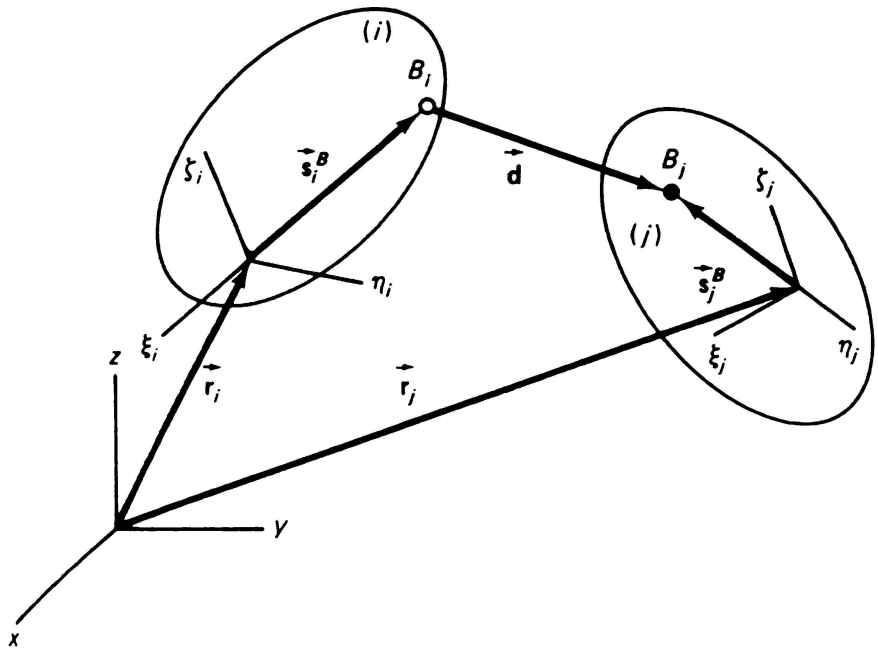

Figure 3-16: Representation of a variable distance constraint $\vec{d}$ between two bodies. The reference body-axis system can be made coincident with the global reference system to obtain a relative distance constraint of one body with respect to the global coordinate system [From Nikravesh, 1998].

A constraint between two vectors having constant magnitudes is referred to as a *Type 1* constraint. However, if there is a constraint between two vectors, where one has a fixed magnitude and the other variable, then this is known as a *Type 2* constraint. Constraint equations are often characterized by assigning two indices. The first index denotes the type of constraint, and the second one the number of independent equations in the expression. For instance, a relative distance constraint applied to the mid-hips to describe the linear motion of the human body with respect to the global coordinate system can be expressed as

$$\mathbf{\Phi}^{(d2,3)} = \mathbf{r}_j \tag{3.13}$$

where $\mathbf{r}_j$ is the variable vector from the mid-hips to the origin of the global coordinate system, $\mathbf{r}_i$ is equal to zero, $d2$ refers to a Type 2 distance constraint, and the second index refers to the number of DOF constrained.

The spherical constraint was used to link adjacent rigid bodies throughout the segment link chain (Figure 3-17). Consider the general case for two adjacent

bodies i and j, where the point P has constant coordinates with respect to the $\xi_i\eta_i\zeta_i$ and the $\xi_j\eta_j\zeta_j$ coordinate systems. There are three algebraic equations for this joint, which can be expressed generally as

$$\mathbf{\Phi}^{(s,3)} = \mathbf{r}_i + \mathbf{R}_j\mathbf{s}_j'^P - \mathbf{R}_i\mathbf{s}_i'^P - \mathbf{r}_j \tag{3.14}$$

where the first index s refers to spherical constraint, and the second index to the three DOF that are constrained.

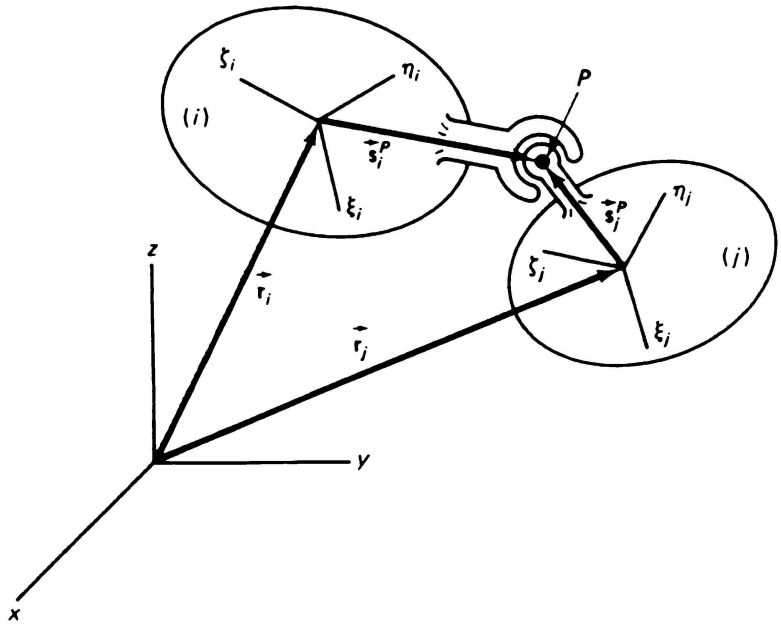

Figure 3-17: A schematic representation of a spherical joint constraint linking two bodies [From Nikravesh, P.E. 1988. *Computer-Aided Analysis of Mechanical Systems*, Prentice Hall, New Jersey].

The other constraint that could be used to represent hinge joints such as the knee is the *revolute joint constraint.* For a revolute joint between two bodies i and j, any point on the revolute-joint axis has constant coordinates in both local coordinate systems (Figure 3-18). Equation 3.14 is imposed on the arbitrary point P on the joint axis. Two other points, Q_i on body i and Q_j on body j, are also chosen arbitrarily on the joint axis. To specify the revolute joint, vectors $\mathbf{s}_i$ and $\mathbf{s}_j$ must be parallel. Therefore, there are five constraint equations for a revolute joint

$$\begin{aligned} \mathbf{\Phi}^{(s,3)} &= 0 \\ \mathbf{\Phi}^{(p1,2)} &= \mathbf{s}_i \times \mathbf{s}_j = \tilde{\mathbf{s}}_i\mathbf{s}_j = 0 \end{aligned} \tag{3.15}$$

By adding the second indices together, it is evident that there is only one relative degree of freedom between two bodies connected by a revolute joint.

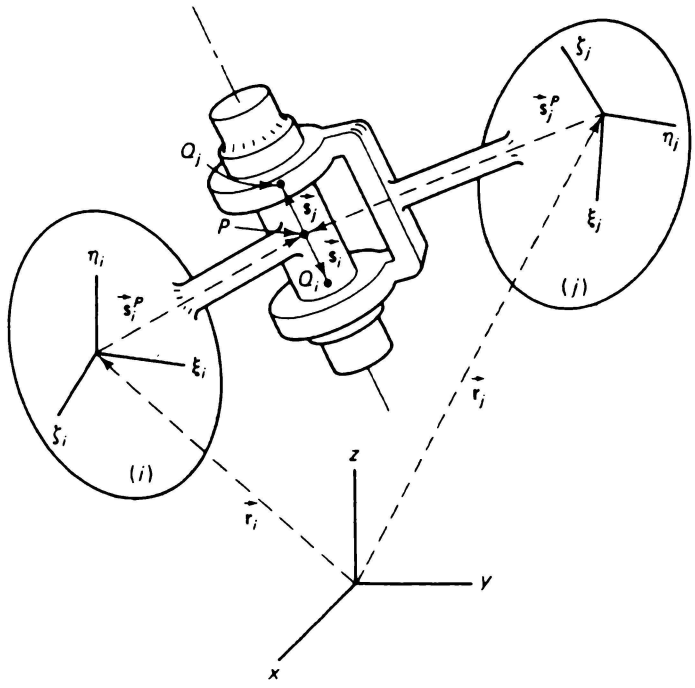

Figure 3-18: A revolute joint linking two bodies [From Nikravesh, P.E. 1988. *Computer-Aided Analysis of Mechanical Systems*, Prentice Hall, New Jersey].

3.2.6 Solving Kinematic Equations of Motion

Frequently it is required in scientific work to find the roots of one or a set of non-linear algebraic equations of the form

$$\mathbf{\Phi(q)=0} \tag{3.16}$$

i.e., zeros of the functions $\mathbf{\Phi(q)}$. The kinematic constraint equations are all of this form, and are usually solved using a numerical solution technique. The most common and frequently used numerical method is the *Newton-Raphson method.*

Consider n nonlinear algebraic equations in n unknowns

$$\begin{aligned}
&\Phi_1(\mathbf{q}) \equiv \Phi_1(q_1, q_2, \ldots, q_n) = 0 \\
&\Phi_2(\mathbf{q}) \equiv \Phi_2(q_1, q_2, \ldots, q_n) = 0 \\
&\vdots \\
&\Phi_n(\mathbf{q}) \equiv \Phi_n(q_1, q_2, \ldots, q_n) = 0
\end{aligned} \tag{3.17}$$

where a solution vector $\mathbf{q}$ is to be found. The Newton-Raphson algorithm for n equations is stated as

$$\mathbf{q}^{j+1} = \mathbf{q}^{j} - \mathbf{\Phi}_{\mathbf{q}}^{-1}(\mathbf{q}^{j})\mathbf{\Phi}(\mathbf{q}^{j}) \tag{3.18}$$

where

$$\mathbf{\Phi}_{\mathbf{q}}^{-1}(\mathbf{q}^{j}) \equiv \left[\frac{\partial \mathbf{\Phi}}{\partial \mathbf{q}}\right]^{-1} \tag{3.19}$$

is the *inverse* of the Jacobian matrix evaluated at $\mathbf{q} = \mathbf{q}^{j}$. The Jacobian matrix $\mathbf{\Phi}_{\mathbf{q}} \equiv [\partial \mathbf{\Phi} / \partial \mathbf{q}]$ contains partial derivatives of the constraint equations with respect to the coordinates. The term $\mathbf{\Phi}(\mathbf{q}^{j})$ on the right-hand side of Equation 3.18 is known as the vector of residuals, which corresponds to the violation in the equations. Equation 3.19 can be restated as a two-step operation

$$\mathbf{\Phi}_{\mathbf{q}}(\mathbf{q}^{j})\Delta \mathbf{q}^{j} = -\mathbf{\Phi}(\mathbf{q}^{j}) \tag{3.20}$$

$$\mathbf{q}^{j+1} = \mathbf{q}^{j} + \Delta \mathbf{q}^{j} \tag{3.21}$$

where Equation 3.20, a set of n linear equations, is solved for $\Delta \mathbf{q}^{j}$. Then, $\mathbf{q}^{j+1}$ is evaluated from Equation 3.21. Gaussian elimination or L-U factorization methods (a compact form of the Gaussian eliminination method, where the original matrix is factored into the product of a lower triangular (L) and upper triangular (U) matrix) can be employed to solve Equation 3.20. The term $\Delta \mathbf{q}^{j} = \mathbf{q}^{j+1} - \mathbf{q}^{j}$, known as the *Newton difference*, shows the amount of correction to the approximated solution in the j^{th} iteration.

The basic computational algorithm is as follows:

1. Set the iteration counter $j = 0$.
2. An initial estimate $\mathbf{q}^{0}$ is made of the solution.
3. The functions $\mathbf{\Phi}(\mathbf{q}^{j})$ are evaluated. If the magnitudes of all the residuals $\mathbf{\Phi}_{i}(\mathbf{q}^{j})$, i = 1, ... , n, are less than a specified tolerance ε, i.e., if $|\mathbf{\Phi}_{i}| < \varepsilon$, i = 1, ... , n, then $\mathbf{q}^{j}$ is the desired solution, and the algorithm terminates. Otherwise, go to 4.

4. Evaluate the Jacobian matrix $\Phi_{\mathbf{q}}(\mathbf{q}^j)$ and solve Equations 3.20 and 3.21 for $\mathbf{q}^{j+1}$.
5. Increment j by setting j to $j + 1$. If j is greater than the number of specified allowed number of iterations, then stop. Otherwise go to 3.

This is the algorithm for the Newton-Raphson method in its simplest form. There are numerous techniques that could be included in the algorithm to improve its convergence as used in the Mechanical Systems Pack. These techniques are found in many textbooks on numerical analysis (Atkinson, 1978).

Kinematics is not only concerned with positional analysis, but also with the velocity and acceleration of mechanisms. Actuators may be employed to specify the time history of the position or orientation of one body relative to another or relative to the global reference in a mechanical system. Such time-dependent constraints are called *driving constraints*. Therefore, to solve the first and second derivatives of the constraint equations to yield the kinematic and acceleration equations, the *method of appended driving constraints* was used. This method incorporates *driving constraints*, equal in number to the DOF, by appending them to the original kinematic constraint equations [Haug, 1989]. In general, if there are m kinematic constraints (Equation 3.22a), then the k driving constraints (Equation 3.22b) are appended to the kinematic constraints to obtain $n = m + k$ equations of the form

$$\Phi \equiv \Phi(\mathbf{q}) = \mathbf{0} \tag{3.22a}$$

$$\Phi^d \equiv \Phi(\mathbf{q},t) = \mathbf{0} \tag{3.22b}$$

where superscript d denotes the driving constraints. The system of n equations represents n unknowns of $\mathbf{q}$ that can be solved at any time t.

The velocity equations are obtained by taking the time derivatives of Equations 3.22a and 3.22b yielding

$$\Phi_{\mathbf{q}}\,\dot{\mathbf{q}} = \mathbf{0} \tag{3.23a}$$

$$\Phi^d_{\mathbf{q}}\,\dot{\mathbf{q}} + \Phi^d_t = 0 \tag{3.23b}$$

or equivalently

$$\begin{bmatrix} \boldsymbol{\Phi}_{\mathbf{q}} \\ \boldsymbol{\Phi}_{\mathbf{q}}^{d} \end{bmatrix} \dot{\mathbf{q}} = \begin{bmatrix} 0 \\ -\boldsymbol{\Phi}_{t}^{d} \end{bmatrix} \tag{3.24}$$

which represents n algebraic equations, linear in terms of $\dot{\mathbf{q}}$.

Similarly, the time derivatives of Equation 3.23a and 3.23b yield the acceleration equations

$$\boldsymbol{\Phi}_{\mathbf{q}} \ddot{\mathbf{q}} + (\boldsymbol{\Phi}_{\mathbf{q}} \dot{\mathbf{q}})_{\mathbf{q}} \dot{\mathbf{q}} = 0 \tag{3.25a}$$

$$\boldsymbol{\Phi}_{\mathbf{q}}^{d} \ddot{\mathbf{q}} + \left(\boldsymbol{\Phi}_{\mathbf{q}}^{d} \dot{\mathbf{q}}\right)_{\mathbf{q}} \dot{\mathbf{q}} + 2\boldsymbol{\Phi}_{\mathbf{q}t}^{d} \dot{\mathbf{q}} + \boldsymbol{\Phi}_{tt}^{d} = 0 \tag{3.25b}$$

which is equivalent to

$$\begin{bmatrix} \boldsymbol{\Phi}_{\mathbf{q}} \\ \boldsymbol{\Phi}_{\mathbf{q}}^{d} \end{bmatrix} \ddot{\mathbf{q}} = \begin{bmatrix} -\left(\boldsymbol{\Phi}_{\mathbf{q}}^{d} \dot{\mathbf{q}}\right)_{\mathbf{q}} \dot{\mathbf{q}} \\ -\left(\boldsymbol{\Phi}_{\mathbf{q}} \dot{\mathbf{q}}\right)_{\mathbf{q}} \dot{\mathbf{q}} - 2\boldsymbol{\Phi}_{\mathbf{q}t}^{d} \dot{\mathbf{q}} - \boldsymbol{\Phi}_{tt}^{d} \end{bmatrix} \tag{3.26}$$

which represents n algebraic equations linear in terms of $\ddot{\mathbf{q}}$.

Therefore, the general algorithmic procedure for kinematic analysis is summarized below:

1. Set a time step counter i to $i = 0$ and initialise $t^i = t^o$ (initial time).
2. Append k driving equations to the constraint equations.
3. Solve Equations 3.22a and 3.22b iteratively using the Newton-Raphson method to obtain $\mathbf{q}^i$.
4. Solve Equation 3.24 to obtain $\dot{\mathbf{q}}^i$.
5. Solve Equation 3.26 to obtain $\ddot{\mathbf{q}}^i$.
6. If final time is reached, then terminate; otherwise increment $t^i \rightarrow t^{i+1}$, let $i \rightarrow i+1$, and go to 3.

3.2.7 Dynamics Equations of Motion

The mathematical basis of spatial system dynamics (i.e. 3-D dynamics) is largely taken from Haug (1989), which is the key source reference for the computer implementation of mechanics in the Mechanical System Pack. As the full derivation of the equations is extensive, a concise formulation that only covers the key elements of the derivation is presented in the main body of this thesis.

The equations of motion for spatial dynamics require more algebraic complexity to represent the orientation of the bodies, and the equations have a more non-linear character than in the planar (i.e. 2-D) case. The derivation of these equations considers a rigid body, which is located in space by a vector **r** and a set of generalised coordinates that defines the orientation of the $x'y'z'$ body-fixed frame relative to an inertial xyz global reference frame (Figure 3-19). A differential mass $dm(P)$ at a typical point P is located on the body vector $\mathbf{s}^P$. Forces that act on a differential element of mass at point P include the external force $\mathbf{F}(P)$ per unit mass at point P and the internal force $\mathbf{f}(P, R)$ per unit of masses at points P and R. Internal forces are modelled as the gravitational interaction and distance constraints.

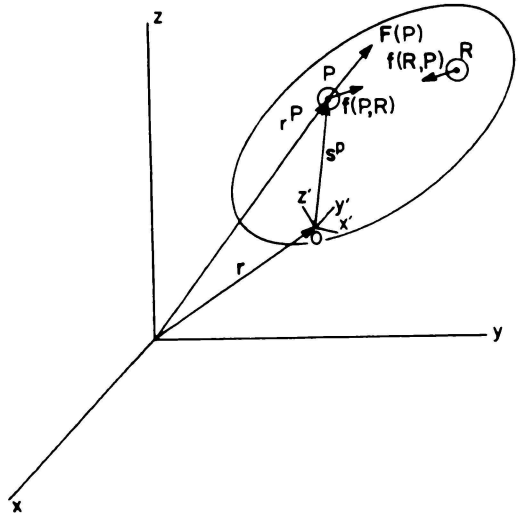

Figure 3-19: Forces acting on a rigid body in space.

Newton's equation of motion for differential mass $dm(P)$ is

$$\ddot{\mathbf{r}}dm(P) - \mathbf{F}(P)dm(P) - \int_m f(P,R)dm(R)dm(P) = 0 \qquad (3.27)$$

where integration of the internal force $\mathbf{f}(P, R)$ is taken over the whole body. Using Equation 3.27, the *Newton-Euler variational equations of motion* can be derived for a rigid body with a body-fixed reference frame at the centre of mass

$$\partial \mathbf{r}^{\mathrm{T}}[m\ddot{\mathbf{r}} - \mathbf{F}] + \partial \boldsymbol{\pi}'^{\mathrm{T}}[\mathbf{J}'\dot{\mathbf{w}}' + \tilde{\mathbf{w}}'\mathbf{J}'\mathbf{w}' - \mathbf{n}'] = \mathbf{0} \tag{3.28}$$

where $\mathbf{r}$ is the position vector of origin of body-fixed coordinate system (i.e. $x'y'z'$ frame), $\partial \mathbf{r}$ is the virtual displacement of the body, $\partial \boldsymbol{\pi}'$ the virtual rotation of the body with respect to local $x'y'z'$ frame or *local reference system* (*LRS*), $\mathbf{J}'$ the inertia matrix with respect to the LRS, $\mathbf{w}'$ the angular velocity with respect to the LRS, $\mathbf{F}$ the total external force on the body, and $\mathbf{n}'$ the moment (or joint torque) of the external forces with respect to the LRS. The full derivation of the Newton-Euler equations for spatial dynamics is given in Appendix F.

To implement the variational Newton-Euler equations for a system of bodies, Equation 3.28 is evaluated for each body in the system, and the resulting equations added to obtain the Newton-Euler variational equations of motion for the system. The notation for Equation 3.28 now becomes

$$\begin{aligned}
\partial \mathbf{r} &= \left[\partial \mathbf{r}_1^{\mathrm{T}}, \partial \mathbf{r}_2^{\mathrm{T}}, \ldots, \partial \mathbf{r}_n^{\mathrm{T}}\right]^{\mathrm{T}} \\
\mathbf{M} &\equiv [m_1, m_2, \ldots, m_3] \\
\partial \boldsymbol{\pi}' &\equiv \left[\partial \boldsymbol{\pi}_1'^{\mathrm{T}}, \partial \boldsymbol{\pi}_2'^{\mathrm{T}}, \ldots, \partial \boldsymbol{\pi}_n'^{\mathrm{T}}\right]^{\mathrm{T}} \\
\mathbf{F} &\equiv \left[\mathbf{F}_1^{\mathrm{T}}, \mathbf{F}_2^{\mathrm{T}}, \ldots, \mathbf{F}_n^{\mathrm{T}},\right]^{\mathrm{T}} \\
\mathbf{J}' &\equiv diag\left(\mathbf{J}_1', \mathbf{J}_2', \ldots, \mathbf{J}_3'\right) \\
\mathbf{w}' &\equiv \left[\mathbf{w}_1'^{\mathrm{T}}, \mathbf{w}_2'^{\mathrm{T}}, \ldots, \mathbf{w}_n'^{\mathrm{T}},\right]^{\mathrm{T}} \\
\mathbf{n}' &\equiv \left[\mathbf{n}_1'^{\mathrm{T}}, \mathbf{n}_2'^{\mathrm{T}}, \ldots, \mathbf{n}_n'^{\mathrm{T}},\right]^{\mathrm{T}} \\
\tilde{\mathbf{w}}' &\equiv diag\left(\tilde{\mathbf{w}}_1', \tilde{\mathbf{w}}_2', \ldots, \tilde{\mathbf{w}}_n'\right)
\end{aligned} \tag{3.29}$$

The forces and torques that now act on the system are partitioned into *applied forces* $\mathbf{F}^A$, *applied torques* $\mathbf{n}'^A$, *constraint forces* $\mathbf{F}^C$ and *constraint torques* $\mathbf{n}'^C$. Note that virtual displacements or rotations, such as $\partial \mathbf{r}$ and $\partial \boldsymbol{\pi}'$ respectively, have the following properties:

- They are infinitesimal displacements or rotations.
- They are consistent with the system constraints, but are arbitrary otherwise.

- The variation of displacements or rotations is obtained by holding time fixed. Therefore, they can be considered as occurring instantaneously, and time is not involved in their applications.

This gives rise to the variational approach to dynamics, which makes the dynamics formulation concise, while having a meaningful physical interpretation (Baruh, 1999). The means by which this is achieved is though the *virtual work principle* denoted by ∂W, which states the following:

> The work performed by a holonomic constraint force in any virtual displacement or virtual rotation (which can be expressed as a virtual displacement) is zero for any holonomic constraint.

For example, $\partial W = \mathbf{F}^A \cdot \partial \mathbf{r} = 0$ for a holonomic constraint, because the constraint forces are always orthogonal to the applied force. Therefore, for all holonomic constraints, the forces of constraint do no work as long as the virtual displacements and rotations are consistent with the constraints, which means that

$$\partial \mathbf{r}^T \mathbf{F}^C + \partial \boldsymbol{\pi}'^T \mathbf{n}'^C = 0 \tag{3.30}$$

Thus, with $\mathbf{F} = \mathbf{F}^A + \mathbf{F}^C$, $\mathbf{n}' = \mathbf{n}'^A + \mathbf{n}'^C$, and Equation 3.30, the *variational equation of motion for a constrained system* becomes

$$\partial \mathbf{r}^{\mathrm{T}} [m\ddot{\mathbf{r}} - \mathbf{F}^{\mathrm{A}}] + \partial \boldsymbol{\pi}'^{\mathrm{T}} [\mathbf{J}'\dot{\mathbf{w}}' + \tilde{\mathbf{w}}'\mathbf{J}'\mathbf{w}' - \mathbf{n}'^{\mathrm{A}}] = \mathbf{0} \tag{3.31}$$

which must hold for all kinematically admissible virtual displacements and rotations.

A classical method in mechanics is to introduce Lagrange multipliers to reduce the variational equation of Equation 3.31 to a mixed system of differential-algebraic equations. This can be done using a theorem of optimisation theory, which states that for **b** a vector of *n* constants, **x** an *n* vector of variables, and **A** an *m* x *n* constant matrix, if

$$\mathbf{b}^{\mathrm{T}} \mathbf{x} = 0 \tag{3.32}$$

holds for all **x** that satisfy

$$\mathbf{A}\mathbf{x} = 0 \tag{3.33}$$

then there exists an *m* vector $\boldsymbol{\lambda}$ of *Lagrange multipliers* such that

$$\mathbf{b}^{\mathrm{T}}\mathbf{x} + \boldsymbol{\lambda}^{\mathrm{T}}\mathbf{A}\mathbf{x} = 0 \tag{3.34}$$

for arbitrary $\mathbf{x}$.

Since the kinematic and driving constraints that act on the system are of the form

$$\boldsymbol{\Phi}(\mathbf{r},\mathbf{p},t) = 0 \tag{3.35}$$

which must also satisfy the Euler parameter normalisation constraints

$$\boldsymbol{\Phi}_P \equiv \begin{bmatrix} \mathbf{p}_1^{\mathrm{T}}\mathbf{p}_1 - 1 \\ \vdots \\ \mathbf{p}_n^{\mathrm{T}}\mathbf{p}_n - 1 \end{bmatrix} = 0 \tag{3.36}$$

where $\mathbf{p} = (e_0, e_1, e_2, e_3)^{\mathrm{T}}$. Then the virtual displacements $\partial\mathbf{r}$ and virtual rotations $\partial\boldsymbol{\pi}'$ are kinematically admissible for the constraints if

$$\boldsymbol{\Phi}_{\mathbf{r}}\partial\mathbf{r} + \boldsymbol{\Phi}_{\boldsymbol{\pi}'}\partial\boldsymbol{\pi}' = 0 \tag{3.37}$$

Since Equation 3.31 must hold for all $\partial\mathbf{r}$ and $\partial\boldsymbol{\pi}'$ that satisfy Equation 3.37, then from Equation 3.34 there exists a Lagrange multiplier vector $\boldsymbol{\lambda}$ such that

$$\partial\mathbf{r}^{\mathrm{T}}[m\ddot{\mathbf{r}} - \mathbf{F}^{\mathbf{A}} + \boldsymbol{\Phi}_{\mathbf{r}}^{\mathrm{T}}\boldsymbol{\lambda}] + \partial\boldsymbol{\pi}'^{\mathrm{T}}[\mathbf{J}'\dot{\mathbf{w}}' + \tilde{\mathbf{w}}'\mathbf{J}'\mathbf{w}' - \mathbf{n}'^{\mathbf{A}} + \boldsymbol{\Phi}_{\boldsymbol{\pi}'}^{\mathrm{T}}\boldsymbol{\lambda}] = \mathbf{0} \tag{3.38}$$

for arbitrary $\partial\mathbf{r}$ and $\partial\boldsymbol{\pi}'$. The coefficients of these arbitrary variations must be zero, yielding the *constrained Newton-Euler equations* or *Newton-Lagrange equations* of motion

$$\begin{aligned} \mathbf{M}\ddot{\mathbf{r}} + \boldsymbol{\Phi}_{\mathbf{r}}^{\mathrm{T}} &= \mathbf{F}^{A} \\ \mathbf{J}'\dot{\mathbf{w}}' + \boldsymbol{\Phi}_{\boldsymbol{\pi}'}^{\mathrm{T}} &= \mathbf{n}'^{A} - \tilde{\mathbf{w}}'\mathbf{J}'\mathbf{w}' \end{aligned} \tag{3.39}$$

To complete the equations of motion, acceleration equations associated with the kinematic constraints must be obtained. The *velocity equation* is obtained by taking the time derivative of Equation 3.35

$$\boldsymbol{\Phi}_{\mathbf{r}}\dot{\mathbf{r}} + \boldsymbol{\Phi}_{\boldsymbol{\pi}'}\mathbf{w}' = -\boldsymbol{\Phi}_t \equiv \mathbf{v} \tag{3.40}$$

The time derivative of this equation yields the *acceleration equation*

$$\boldsymbol{\Phi}_{\mathbf{r}}\ddot{\mathbf{r}} + \boldsymbol{\Phi}_{\boldsymbol{\pi}'}\dot{\mathbf{w}}' = \boldsymbol{\lambda} \tag{3.41}$$

where vector $\boldsymbol{\lambda}$ is found by double differentiating the constraint equation, and therefore depends on the type of constraint. For example, for a spherical constraint, $\boldsymbol{\lambda} = \boldsymbol{\lambda}^S$ equals

$$\boldsymbol{\lambda}^S = \mathbf{R}_i\tilde{\mathbf{w}}_i'\tilde{\mathbf{w}}_i'\mathbf{s}_i'^P + \mathbf{R}_j\tilde{\mathbf{w}}_j'\tilde{\mathbf{w}}_j'\mathbf{s}_j'^P \tag{3.42}$$

Combining Equations 3.39 and 3.41, the *system acceleration equations* are

$$\begin{bmatrix} \mathbf{M} & 0 & \boldsymbol{\Phi}_r^{\mathrm{T}} \\ 0 & \mathbf{J}' & \boldsymbol{\Phi}_{\pi'}^{\mathrm{T}} \\ \boldsymbol{\Phi}_{\mathbf{r}} & \boldsymbol{\Phi}_{\pi'} & 0 \end{bmatrix} \begin{bmatrix} \ddot{\mathbf{r}} \\ \dot{\mathbf{w}}' \\ \boldsymbol{\lambda} \end{bmatrix} = \begin{bmatrix} \mathbf{F}^A \\ \mathbf{n}'^A - \tilde{\mathbf{w}}'\mathbf{J}'\mathbf{w}' \\ \boldsymbol{\lambda} \end{bmatrix} \tag{3.43}$$

These equations of motion, taken with the kinematic constraint equations of Equation 3.35 and the velocity equations of Equation 3.40, yield a mixed system of *differential-algebraic equations of motion* for the system. Technically, this is a system of mixed first-order differential algebraic equations for velocity variables $\dot{\mathbf{r}}$ and $\mathbf{w}'$ and the algebraic variables $\boldsymbol{\lambda}$. It is not a second-order differential-algebraic system, since the angular velocity $\mathbf{w}'$ is not integrable.

Initial conditions on the position, orientation and velocity must be provided to define the dynamics of a system. Since the orientation of a body is specified by Euler parameters, initial conditions on the position and orientation are specified in the form

$$\boldsymbol{\Phi}(\mathbf{r},\mathbf{p},t_0) = 0 \tag{3.44}$$

where $\mathbf{r}$ and $\mathbf{p}$ must satisfy Equation 3.35 at t_0 and the Euler parameter normalisation constraints. Therefore, the inverse dynamics of driven spatial multi-body systems is first solved iteratively for position, velocity and acceleration. Then the equations of motion are solved algebraically for Lagrange multipliers associated with the constraints.

Finally, the reaction forces and torques associated with both the kinematic and driving constraints are calculated. For a typical joint k in body i, with a joint definition point P in the local coordinate system, constraint equations $\boldsymbol{\Phi}^k = 0$, and associated Lagrange multipliers $\boldsymbol{\lambda}^k$, the desired expressions for joint reaction forces and torques on body i at joint k are given as

$$\begin{aligned} \mathbf{F}_i^k &= -\mathbf{C}_i^{\mathrm{T}}\mathbf{R}_i^{\mathrm{T}}\boldsymbol{\Phi}_{\mathbf{r}_i}^{k\mathrm{T}}\boldsymbol{\lambda}^k \\ \mathbf{T}_i^k &= -\mathbf{C}_i^T(\boldsymbol{\Phi}_{\boldsymbol{\pi}_i}^{k\mathrm{T}} - \tilde{\mathbf{s}}_i'^P\mathbf{R}_i^{\mathrm{T}}\boldsymbol{\Phi}_{\mathbf{r}_i}^{k\mathrm{T}})\boldsymbol{\lambda}^k \end{aligned} \tag{3.45}$$

where $\mathbf{C}_i$ is the direct cosine matrix.

3.2.8 Solving Differential-Algebraic Equations of Motion

The dynamic equations of motion for constrained multibody systems are solved numerically. There are at least three distinct methods for the solution of mixed differential-algebraic equations, and some hybrid versions that take advantage of the favourable properties of each method. The basic process involves the numerical reduction of the mixed differential-algebraic equations to a system of first-order differential equations than are integrated using the standard numerical algorithms. For example, though the exact method used by the Mechanical Systems Pack is not documented, one alternative is to define an intermediate variable $\mathbf{s} \equiv \dot{\mathbf{r}}$, forming a first-order system of differential-algebraic equations using Equation 3.43, and the following relationship between the Euler parameters and the angular velocity

$$\dot{\mathbf{p}} = \frac{1}{2}\mathbf{G}^{\mathrm{T}}(\mathbf{p})\mathbf{w}' \tag{3.46}$$

where for $\mathbf{e} \equiv [e_1, e_2, e_3]$ matrix $\mathbf{G}$ is defined as

$$\mathbf{G} \equiv \left[-\mathbf{e}, \tilde{\mathbf{e}} + e_0\mathbf{I}\right] = \begin{bmatrix} -e_1 & e_0 & e_3 & -e_2 \\ -e_2 & -e_3 & e_0 & e_1 \\ -e_3 & e_2 & -e_1 & e_0 \end{bmatrix} \tag{3.47}$$

Then the first order system of differential-algebraic equations of the system are

$$\begin{bmatrix} \mathbf{M} & 0 & \boldsymbol{\Phi}_{\mathbf{r}}^{\mathrm{T}} \\ 0 & \mathbf{J}' & \boldsymbol{\Phi}_{\boldsymbol{\pi}'}^{\mathrm{T}} \\ \boldsymbol{\Phi}_{\mathbf{r}} & \boldsymbol{\Phi}_{\boldsymbol{\pi}'} & 0 \end{bmatrix} \begin{bmatrix} \ddot{\mathbf{r}} \\ \dot{\mathbf{w}}' \\ \boldsymbol{\lambda} \end{bmatrix} = \begin{bmatrix} \mathbf{F} \\ \mathbf{n}' - \tilde{\mathbf{w}}'\mathbf{J}'\mathbf{w}' \\ \boldsymbol{\lambda} \end{bmatrix}$$

$$\dot{\mathbf{r}} = \mathbf{s} \tag{3.48}$$

$$\dot{\mathbf{p}} = \frac{1}{2}\mathbf{G}^{\mathrm{T}}(\mathbf{p})\mathbf{w}'$$

Once the equations are in the form of a system of first order differential equations, then various standard numerical integration algorithms can be applied. The Mechanical Systems Pack uses an Adams-Bashforth-type numerical integration algorithm to numerically integrate the equations of motion to obtain the motion history for a specified time domain. It is a variable order, variable step size and adaptive algorithm that changes the order and step size as necessary during the

integration to achieve convergence. Therefore, new Mathematica functions are created and used as the algorithm proceeds: it is essentially a self-modifying code.

3.2.9 Mechanical Systems Computational Architecture

It is apparent that there is much complexity in the formulation and solution of the spatial dynamic equations of motion for a system of rigid bodies. However, from the viewpoint of the user of the Mechanical Systems Pack, essentially all the algebraic and numerical complexity is hidden in the computer intensive calculations. Though it is always advantageous for the scientist to understand the basic dynamic formulation in order to construct physically meaningful models, and perhaps quickly identify any gross solution errors, the physical models themselves are structured at a higher information level. This makes it relatively easy and time-efficient to construct complex mechanical models by using the higher-level Mechanical Systems Pack programming functions within the symbolic manipulation language environment of Mathematica.

The Mechanical Systems Pack performs five major tasks:

1. Reads input data directly from the Mathematica front end.
2. Checks the model definitions of the rigid body system.
3. Checks whether the model satisfies the constraint definitions.
4. Solves for kinematic, inverse dynamics or forward dynamics depending on the solution option.
5. Runs the output functions.

The input data were the kinematic data of the markers obtained from the Eva 6.0 motion analysis system *.*trc* files. These were processed in Mathematica to calculate the local body segment axes in cartesian *xyz* coordinates. Then the data were converted to Euler angles or Euler parameters. An Euler 3-2-1 sequence was chosen, and the conversion formulae are presented in Section 3.2.11.

Before the equations of motion are solved, a model assembly and constraint analysis phase is carried out. At each iteration of the minimisation process,

modules generate the constraint equations and Jacobian information. Following successful assembly, an analysis subroutine carries out a computational check on the rank of the constraint Jacobian to identify any redundant constraints that may exist. If a feasible model has been specified, the analysis proceeds. Otherwise, the calculations are terminated, and a constraint solution error generated.

The solution module is designed with options for kinematics, inverse dynamics or forward dynamics solution. For a full kinematic analysis, the position analysis is carried out first using the iterative Newton-Raphson method (Equations 3.20 and 3.21). During each iteration, modules provide information on constraint equation violations and Jacobians. Upon completion of position iteration at a given time step, velocity analysis is initiated, and the modules evaluate constraint Jacobian entries and the right side of the velocity equation (Equation 3.22). Following completion of the velocity analysis at the given time step, acceleration analysis is carried out. Modules provide only the right side of the acceleration equations, since the constraint Jacobian is identical to that constructed during velocity analysis (Equation 3.26). Upon completion of the acceleration analysis, if the final specified time has been reached, the programme terminates.

For an inverse dynamics solution, the system is assembled and checked for feasibility just as in the kinematic analysis. Then the analysis is carried out by solving the kinematic equations for a kinematically determined system, assembling the equations of motion, and solving for Lagrangian multipliers (Equation 3.45). The reaction forces, driving forces and torques that correspond to the movement of the system are subsequently calculated. Finally, if a forward solution is called upon, the system feasibility is checked as before, and the mass-, constraint-, and force-related matrices are assembled. The analysis is carried out by numerically integrating the mixed differential-algebraic equations of motion (Equation 3.47). Table 3-2 relates the computational flow generated during the dynamics model assembly phase with the use of high-level Mechanical System functions.

Table 3-2: Mechanical Systems Pack dynamics analysis flow and high-level functions for the model-builidng phase.

MECHANICAL SYSTEMS FUNCTION	DYNAMICS FUNCTION
Input Data and Model Assembly	
Body[], SetBodies []	• Each body assigned a unique number, *bnum*. • Sets the inertia properties for each body: mass, location of centroid. and moments of inertia. • Points on bodies are defined. • Initial location estimate for body specified.
Constraint[]	• Bodies are linked through the specification of constraints. • Assign each constraint a unique constraint number, *cnum*. • Builds constraint equations.
Model Feasibility	
SetConstraints[]	• Check that each constraint has a unique constraint number. • Check that the number of DOFs. constrained is equal to number of dependent variables. • Check that all of the local points that are specified by point number have been defined in *SetBodies*.
External Loads	
SetLoads[]	• Applies load vector to any point on defined body.

Essentially the high level operations assign each rigid body in the system a number by using a *Body*[ ] function, and then combines them using the

SetBodies[ ] function. Then each body is linked to one or two adjacent bodies by specifying an appropriate set of constraints using the *Constraint*[ ] function. The total system of constraints is then generated and tested using *SetConstraints*[ ], and a link segment model is formed. Therefore, merely adding or changing modules composed of *Body*[ ] and *Constraint*[ ] functions can generate a wide variety of complex rigid body models. The external loads imposed upon the system by gravity and ground contact (in the form of ground reaction forces) could be implemented by using the *SetLoads* function.

Table 3-3 relates the computational flow and information generated during the solution phase with the use of high-level Mechanical System functions. A variety

Table 3-3: Mechanical Systems Pack dynamics analysis flow and high-level functions for the solution phase.

MECHANICAL SYSTEMS FUNCTION	DYNAMICS FUNCTION
Kinematic Solution	
SolveMech[*rules, Solution* → *Acceleration*]	• Solves kinematic equations of motion with Newton-Raphson method.
Inverse Dynamics Solution	
SolveMech[*rules, Solution* → *Dynamic*]	• Solves kinematic equations of motion. • Evaluates Lagrange multipliers to calculate forces and torques. • Equations solved iteratively using Newton-Raphson method.
Forward Dynamics Solution	
SolveFree[*rules, endtime, options*]	• Solves acceleration equations. • Integrates for position and velocity. • Evaluates constraint Jacobians and Lagrange multipliers. • Equations solved iteratively using Adams-Bashforth method.

of solution options can be chosen. This thesis largely used the dynamic solution option, because this solves for both kinematics and inverse dynamics of the system. The main point is that the high level function *SolveMech* solves the complex kinematic and dynamics equations of motion with the specification of just a few parameters.

3.2.10 Segment Model Definitions

To create a system of multiple linked rigid bodies in the Mechanical Systems Pack, a series of *Body* and *Constraint* functions were used. The process was logical: specify the names of the bodies, number them appropriately, and choose the most economical system of constraints. Each body in 3-D space was assigned a body-fixed local coordinate system located at its centre of mass. Also, each independent body was specified with a unique positive integer body number. The choice of each number was arbitrary except for the ground body, which had to always be numbered as *body 1*, so that its coordinate axes could be defined as the global coordinate system. These body numbers were used throughout the model to reference each body. The numbering scheme was chosen to design a fifteen rigid body segment model of the human body that corresponded to the Eva 6.0 link segment model. The rigid bodies were numbered from 2 to 16: upperarmRIGHT=2; forearmRIGHT=3; handRIGHT=4; uppertrunk=5; lowertrunk=6; upperarmLEFT=7; forearmLEFT=8; handLEFT=9; headneck=10; thighRIGHT=11; calfRIGHT=12; footRIGHT=13; thighLEFT=14; calfLEFT=15; footLEFT=16. These body numbers were placed as the first argument of the *Body* function. Points on a segment that delimited the segment endpoints were specified as point objects in the local coordinate system of the segment, but any number of other points could also be defined. These filled the second argument of *Body* function. Other properties of the body segment such as initial location estimate, mass, centre of mass location, and moments of inertia were also defined. For example, the *Body* function module used to define the properties of the right thigh segment was

bd[thighRIGHT] = Body[thighRIGHT, PointList →

(*P1*) {0, -thighCoM, 0},

(*P2*) {0, thighlength - thighCoM, 0}},

InitialGuess → {xyz_{thr}, eul_{thr}},

Mass → thighmass,

Centroid → thighcentroid,

Inertia → {I_{xx} thigh, I_{yy} thigh, I_{zz} thigh, 0, 0, 0}];

Points *P1* and *P2* defined the segment end points, and therefore the segment length. By default the origin of the body-fixed axes was placed at {0, 0, 0}, which, from the way the points were defined, corresponded to the location of the centre of mass. The *Initial Guess* was specified by the location of the centre of mass, and global orientation of the body in terms of Euler parameters. The definitions of the mass, centroid, and moments of inertia (or collectively *segment inertial parameters*) were accordingly defined in their respective positions in the module. In general, it was relatively simple to define points on a body segment. However, the points in the *Body* function were always in local coordinates. Therefore, some points such as the shoulder joint centre, needed to be converted from global coordinates to local coordinates before they could be incorporated in the *Body* function object (Appendix G).

To set the orientation of the body-fixed axes in accordance with those of the Eva 6.0 link segment model, the segment endpoints *P1* and *P2* were defined along the local *y*-axis. The *y*-axis therefore represented the longitudinal axis of the segment as it did for the input kinematic data. Also, for both Eva 6.0 and the Mechanical Systems Pack, once the longitudinal axis was defined, the orientation of a segment's body-fixed axes were initially aligned to match with the global coordinate system. The Euler angle sequences related the orientation of the body-fixed axes to the global coordinate system. Also, the global and local coordinate systems were defined to correspond exactly with that of the link segment model in Eva 6.0 (i.e. the kinematic model) (Figure 3-12).

The values of the segment inertia parameters were obtained from de Leva (1996), who adjusted Zatsiorsky-Seluyanov's segment inertia parameters (Zatsiorsky et al., 1990) so that the mean relative centre of mass positions and radii of gyration were referenced to joint centres (or other commonly used landmarks). The original study provides a comprehensive set of inertial parameters for young adult Caucasians, but used bony landmarks, many of which are markedly distant from the joint centres commonly used by biomechanists as reference points. Also, for the rigid body model the segments were represented as articulating at joint centres, and the dynamics equations calculated forces and torques at or about these joints, respectively. It therefore made sense to use the modified inertial parameter set.

The *Initial Guess* option for the *Body* function needed an estimate of the body's location coordinates. This was required because the Mechanical Systems Pack iteratively solves the kinematic equations, which are usually non-linear, using the Newton-Raphson method. As with many numeric procedures, an initial estimate was used from which repeated iterations would cause a solution to converge within a set tolerance. Initial guesses of a body's location and orientation are referred to as the permanent initial guesses, because each subsequent solution attempt uses the previous solution as its initial guess. The *Initial Guess* option required each segment's CoM and orientation to be specified in terms of global *xyz* coordinates and Euler parameters, respectively. The global coordinates of each segment's CoM were calculated using Equation (3.3).

After the local points on each segment body have been defined, construction of the model was then a matter of tying the points together with the use of mechanical constraints. There are a variety of choices from a library of mechanical constraint objects that impose physical constraints on the model as a system of mathematical equations. The number of DoF for a 3-D rigid body system equals six times the number of segments minus the number of constraints. There were fifteen segments in the model, so if the system was not constrained, there would be 90 DoF. The primary constraint object chosen was the *Spherical3* constraint, a spherical constraint causing two points in 3-D space to be coincident with each other, creating joint or articulating centres by constraining 3 DOF. This

object was used to link the ends of adjacent segments together. The other constraint used was the *RelativeDist* constraint, which constrained a point to be a specified x, y, or z distance units from the global reference frame.

With the lower trunk as the root segment, all the body segments were linked together by starting with the most proximal segment, linking its distal end to the proximal end of the adjacent segment, and continuing onwards throughout the kinematic chains. The *Spherical3* constraint was used to create joints or articulating centres at the knees, hips, midtrunk, neck, shoulders, elbows, and wrists. For example, the code below shows how the proximal end of the lower trunk (*Point*[*lowertrunk,2*]) was constrained to the distal end of the upper trunk (*Point*[*uppertrunk,1*]):

```
cs[5]=Spherical3[5,Point[uppertrunk,1],Point[lowertrunk,2]];
```

The *RelativeDist* constraint was used to specify the shank-foot connection (Appendix G).

In total, 36 DOF of the system were effectively constrained. Therefore, driving constraints had to be defined to satisfy the remaining 54 DOF of the system. Three DoF were used to specify the linear translation of the whole system with *RelativeX1*, *RelativeY1*, and *RelativeZ1* driving constraints, which constrained the proximal end of the root segment to be a distance of x, y, and z units away from the origin of the global coordinate system, respectively. The code below shows how these constraints were specified:

```
cs[1] = RelativeX1[1, Point[lowertrunk, 1], Point[ground, 1], x_trl];
cs[2] = RelativeY1[2, Point[lowertrunk, 1], Point[ground, 1], y_trl];
cs[3] = RelativeZ1[3, Point[lowertrunk, 1], Point[ground, 1], z_trl];
```

Point[*lowertrunk,1*] represents the proximal end of the lower trunk, which, by the application of each constraint consecutively, is $\{x_{trl}, y_{trl}, z_{trl}\}$ units from

Point[ground,1], the origin of the global reference system.

Another 6 DoF were used to specify the linear motion of the glenohumeal joint using relative distance driving constraints. The remaining 45 DoF were constrained with the *RotationLock3* driving constraint, which locked the angular orientation of each segment with respect to the global coordinate system as an Euler (*z-y-x* or 3-2-1) angle sequence. For example, the right forearm was constrained to be a rotational sequence of φ about the *z*-axis, θ about the *y*-axis, and Ψ about the *x*-axis:

cs[10] = RotationLock3[10, forearmRIGHT, ground, {φ, z}, {θ, y}, {Ψ, x}];

In this way, all 90 DOF of the link segment model of the bowler were accounted for, and the model could be solved for kinematics. However, to solve for dynamics the external loads had to first be added.

3.2.11 Adding External Loads

Various external loads were added to the model to simulate the loads experienced by the bowler. The most fundamental load experienced by the body is that of gravity *G*, which was defined to act vertically downwards for each segment with a magnitude of 9.81 ms^{-2}. This was modelled using the *Gravity[vector,G]* object that applied a force of magnitude *mass*G* in the direction of the specified *vector* to the centroid of each body:

Grav = Gravity[Vector[ground,{0,0,-1}], 9.81, {upperarmRIGHT, forearmRIGHT, handRIGHT, uppertrunk, lowertrunk, upperarmLEFT, forearmLEFT, handLEFT, headneck, thighRIGHT, calfRIGHT, footRIGHT, thighLEFT, calfLEFT, footLEFT}];

The more difficult external loads to define were the ground reaction forces, which acted in the vertical, medio-lateral, and anterior-posterior directions. The main reason was that these loads were only active for a short period of time during the

bowling phase, and so a series of switching constraints had to be specified. Therefore, the *TimeSwitch*[*load0,time1*, ... , *timen*, *loadn*] load constraint function was used, where the first and last *loadi* were applied from *time1* to *timen*. For example, for the vertical ground reaction force through the left foot, *GroundReactLEFTZ*, the programme module was of the form

```
GroundReactLEFTZ = TimeSwitch[time1,
Force[footLEFT,
Axis[ground, {CoPx[T], CoPy[T], CoPz[T]}, {0, 0, 1}], GRFLEFTz[T]], time2];
```

where the vertical ground reaction force time function *GRFLEFTz*[*T*] was applied between times *time1* and *time2*, and acted through the left foot (i.e *footLEFT*) through the *x*, *y*, and *z* coordinates of the centre of pressure *{CoPx[T], CoPy[T], CoPz[T]}* in the global vertical direction (i.e. *ground*) specified by vector *{0, 0, 1}*. Note that the centre of pressure was calculated from the force platform readings (Appendix B).

Similarly, the time switching load constraint was used to define the external load imposed by the cricket ball on the system

```
BallLoadRIGHT= TimeSwitch[time1,
Force[handRIGHT, Axis[Point[handRIGHT,2], Vector[ground,{0,0,-1}]],
ballmass*9.8], BallReleaseTime];
```

where the gravitational load of the ball *ballmass*9.8* was applied to the bowling hand from *time1*, the initial time of the bowling action, to *BallReleaseTime*, the time at which the ball was released.

Finally, all the loads were applied to the model using *SetLoads*[*loads*], which generated the Lagrange Multiplier equations of motion:

```
SetLoads[Grav, GroundReactRIGHTX, GroundReactRIGHTY,
GroundReactRIGHTZ, GroundReactLEFTX, GroundReactLEFTY,
GroundReactLEFTZ, BallLoadRIGHT]
```

3.2.12 Solving the Dynamics Equations of Motion

To calculate the inverse dynamics solution the *SolveMech*[*rules*, *Solution*, *options*] algorithmic function was used

SolveMech[{T_init, T_fin}, iter_num, Solution → Dynamic,
Interpolation → True,
MakeRules → {Location, Velocity, Acceleration, Generalised}]

where *T_init* and *T_fin* were the initial and final times of the solution. The equations were solved for *iter_num* time intervals between the solution times, the solution data was interpolated, and both kinematics and dynamics data were outputted. Note that *Dynamic* is a setting for the *Solution* option for the *SolveMech* functions. Setting *Solution → Dynamic* caused such functions to seek a solution for the location, velocity, acceleration, and dynamic loading of the current mechanism.

To run a forward solution the *SolveFree*[*freesys*, *options*] algorithmic function could be used to integrate the equations of motion for the model for a specified time domain. An Adams-Bashforth method was used (Haug,1989).

3.2.13 Data Output

Once *SolveMech* had been run, then it was possible to graphically simulate the model to provide a visual check of the solution was correct. The Mechanical Systems Pack has its own graphics directives, which was implemented in a programme to simulate the output data. For the solution to be correct, the output kinematic data had to at least match the original input kinematic data. The simulation was in 3-D, and the rigid segments were modelled as a combination of conic, cylindrical and spherical objects (Figure 3-20). The bowling action could therefore be simulated over the full solution, and any set of data could be visually correlated with key points in the action.

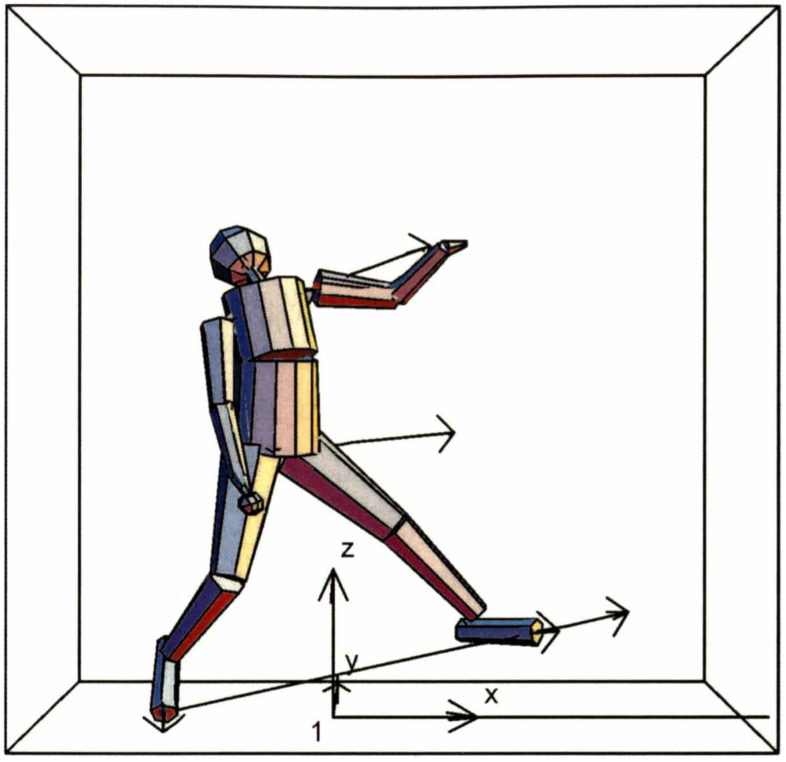

Figure 3-20: The simulation of a fast bowler captured during mid-stride. The arrows represent shoulder, hip, stride, and foot alignments which are the important kinematic aspects of the bowling action.

The Mechanical Systems Pack has many output functions. To calculate segment powers, alignments and dynamics the following functions were used:

Omega[*bnum*] returns the angular velocity of body *bnum*.

ProjectedAngle[*vector1, vector2, vector3*] returns the counterclockwise angle measured from the direction of *vector2* to the direction of *vector1*, as projected on a plane that is orthogonal to *vector3*.

Reaction[*cnum, bnum, point*] returns the reaction loads applied by constraint *cnum* to body *bnum*, calculated about the specified *point*. Loads are returned in the format: {*force, moment*}. **Reaction** accepts the option **Coordinates→Local** to return the load vectors in local coordinates, relative to body *bnum*. **Reaction** is also a setting for the **Type** option for **Loads**.

To calculate the centre of mass of the whole body, the *CompositeIntertia* function was used:

CompositeInertia[{*centroid1, mass1, inertia1*}, ...,{*centroidn, massn, inertian*}] returns the list {*centroid, mass, inertia*} of the inertia properties of a composite body *B* made up of the *n* specified subcomponents. In the Mechanical Systems Pack, arguments to **CompositeInertia** can have the form {*centroidn, massn, inertian, rotationn*} to specify subcomponents that are rotated relative to the composite body *B*.

All kinematic data, such as displacements, velocity, and acceleration could be obtained directly from the *SolveMech* output. A more complete list of common Mechanical Systems Pack output functions is presented in Appendix H.

To verify that the Mechanical Systems Pack does correctly calculate the dynamics of rigid body systems, code was written to represent the motion of a double pendulum. Inverse solutions of the motion were then calculated for various sets of kinematic inputs. These solutions were compared with inverse solutions using Lagrangian dynamic equations of motion to represent the same double pendulum. The forces and torques generated by the two methods were the same.

3.3 STATISTICAL ANALYSIS

3.3.1 Smoothing

A recursive Butterworth fourth-order low-pass filter was used to smooth the kinematic data from Eva 6.0 before runing in the inverse dynamics solution. The format of the recursive digital filter, which processed the raw data in the time domain, is shown below (Winter, 1990):

$$\begin{aligned} X^{1}(nT) = a_o X(nT) + a_1 X(nT-T) + a_2 X(nT-2T) \\ + b_1 X^{1}(nT-T) + b_2 X^{1}(nT-2T) \end{aligned} \tag{3.49}$$

where X^1 are the filtered output coordinates, X are the unfiltered coordinate data, nT the n^{th} sample, $(nT-T)$ the $(n-1)^{th}$ sample, and $(nT-2T)$ the $(n-2)^{th}$ sample. The filter coefficients of coordinate data were calculated from

$$\begin{aligned} a_0 &= \frac{K_2}{(1+K_1+K_2)} \\ a_1 &= 2a_0 \\ a_2 &= a_0 \end{aligned} \tag{3.50}$$

where

$$\begin{aligned} K_2 &= \omega_c^2 \\ K_1 &= \sqrt{2\omega_c} \end{aligned} \tag{3.51}$$

and ω_c is a normalised cut-off frequency parameter given by

$$tan\left(\frac{\pi f_c}{f_s}\right) \tag{3.52}$$

where f_c is the cut-off frequency, and f_s is the signal frequency, which is equal to 240 Hz.

The filter coefficients of the filtered output coordinates were calculated from

$$\begin{aligned} b_1 &= -2a_0 + K_3 \\ b_2 &= 1 - 2a_0 - K_3 \end{aligned} \tag{3.53}$$

where

$$K_3 = \frac{2a_0}{K_2} \tag{3.54}$$

The use of this second-order recursive filter in Equation 3.49, results in a 90° phase lag at the cut-off frequency. To cancel out this phase distortion, the once-filtered data was filtered again, but this time in the reverse direction of time (Winter et al., 1974). This introduced an equal and opposite phase lead so that the net phase shift was zero, and in effect created a fourth-order zero-phase-shift filter (Winter, 1990). However, the cut-off frequency was now 0.802 of the original cut-off frequency of the original second-order filter, so this adjustment had to be made in Equation 3.52 in order to end up with the desired cut-off frequency for the fourth-order filter.

An algorithm was written in Mathematica to perform the recursive Butterworth filtering operation for all the kinematic data. The choice of cut-off frequency was determined manually by specifying a cut-off frequency and then observing its effect on the acceleration data. If the curve was sufficiently smooth without losing significant signal content, then the cut-off frequency was deemed adequate. This process was repeated many times for each data set, and for each subject. The process was lengthy, and therefore much experience was gained as to the appropriate choice of cut-off frequency. Though a complex automatic filtering method could have been used, it was found that after much testing, a set of cut-off frequencies was obtained that gave smooth acceleration curves, and was rather uniform across the sample. However, as the testing was performed over several months, and subjects were unlikely to share exactly the same kinematic characteristics, there were almost always minor adjustments made to the original cut-off frequency set to make the data suitably smooth for use in the inverse solution. The range of cut-off frequencies varied for each segment. The range of cut-off frequencies for the hands and feet was 8-12 Hz. The range of cut-off frequencies for the arms was 7-10 Hz. The larger and more proximal segments, such as the thigh and trunk segments, had the lowest range of cut-off frequencies from 6-8 Hz.

3.3.2 Variance Ratio

To have some objective index or number to assess the variability between time-varying or phase-varying kinematic and dynamics data, the *variance ratio* (*VR*) was calculated as proposed by Hershler and Milner (1978) and given by

$$VR = \frac{\sum_{i=1}^{m}\sum_{j=1}^{n}\left(E_{ij} - \overline{E}_i\right)^2 / m(n-1)}{\sum_{i=1}^{m}\sum_{j=1}^{n}\left(E_{ij} - \overline{E}\right)^2 / (mn-1)} \tag{3.55}$$

where m is the number of temporal points, n is the number of cycles over which VR is evaluated, E_{ij} is the value of the j^{th} data point at time epoch i, $\overline{E}_i$ is the average of the data values at time epoch i, $\overline{E}_{ij}$ is the average of the data values at time epoch i averaged over j cycles, and $\overline{E}$ is the grand mean average of the data.

The VR is a measure of repeatability of waveforms with low values indicating high levels of repeatability (Kadaba et al., 1985). Therefore, it can also be used to quantify variability or similarity between curves. The coefficient of variation (CV) could also be used to perform this same task (Winter, 1984). However, one advantage of the VR is that everything is expressed as a fraction of 1.

3.3.3 Significance Testing

A one-way analysis of variance (ANOVA) was used to test for significant differences among observed group mean data. A *Boneferroni simultaneous confidence intervals output* was used to determine which pairs of population means differed significantly at $\alpha = 0.05$, while reducing the likelihood of type 1 errors (i.e. false rejection of null hypotheses) by guaranteeing that any false rejection among all comparisons made was no greater than 5% (Moore & McCabe, 1998). Note that population means are expressed in the form of $\mu \pm \sqrt{\sigma/n}$, where μ is the mean, σ the standard deviation, and n the sample number. All significance testing was performed using the statistical software package *Minitab Version 13.0 for Windows*.

3.3.4 Simple Linear Regression

Linear regression analysis of selected kinematic data was performed using the statistical software package *Minitab Version 13.0 for Windows*.

3.4 POWER CALCULATIONS

Power is defined as the rate of work or the rate of energy flow. Two power measures can be obtained from the joint kinetics. The *joint force power* is defined as the scalar product of the net joint force and the joint velocity

$$P_{ji} = \mathbf{F}_{ji} \cdot \mathbf{V}j \tag{3.57}$$

where P_{ji} is the power into segment i from segment j, $\mathbf{F}_{ji}$ the net joint force of joint j on joint i, and $\mathbf{v}_j$ the velocity of the joint j. In a n joint system there will be n power flows, but the algebraic sum of all these power flows will be zero (for a

system with no external forces), because these flows are passive and therefore do not change the total body energy (Winter, 1990).

The *muscle power* is defined as the scalar product of the joint torque and the segment's angular velocity

$$P_m = \mathbf{T}_j \cdot \boldsymbol{\omega}_j \tag{3.58}$$

where P_m is the muscle power, $\mathbf{T}_j$ the joint torque, and $\boldsymbol{\omega}_j$ the segment angular velocity.

Joint muscle powers were used to define the terms *active* and *controlled* segment motion with respect to the muscles crossing the proximal joint. An active motion occurs when the joint torque and angular velocity of a segment act in the same direction. A controlled motion occurs when the joint torque and angular velocity of a segment act in opposite directions. For instance, for the motion of the thigh and shank segment about the medio-lateral axis of the knee joint shown in Figure 3-21, the knee extensors act on the shank to produce a positive power $T\omega_2$ at the knee joint, which produces an active extension of the shank segment. In contrast, the value of the power $T\omega_1$ is negative, because $\mathbf{T}$ acts in the opposite direction to $\boldsymbol{\omega}_1$, and shows that energy is leaving the shank and being absorbed by the knee extensor muscles of the thigh. However, in this thesis, these distal end powers were not calculated. One of the problems with dealing with the net joint power $T(\omega_1 - \omega_2)$ is that if the joint angle is fixed, then the net joint power is zero, which can give a misleading impression of the muscle power produced. For instance, if $\boldsymbol{\omega}_1$ equaled $\boldsymbol{\omega}_2$ in Figure 3-22, so that the knee joint angle was fixed, and a 50 kg weight attached to the foot was lifted by the action of hip flexors, then the net joint power would give 0 W. However, this may not always yield a useful result, because, depending on the speed at which the foot was lifted, the knee extensors could have exerted considerable power on the shank to resist the inertial forces of the shank, foot and weight in order to maintain the constant knee flexion angle. In this thesis, the focus was on identifying and quantifying such muscle powers as they have important implications for the execution of bowling technique.

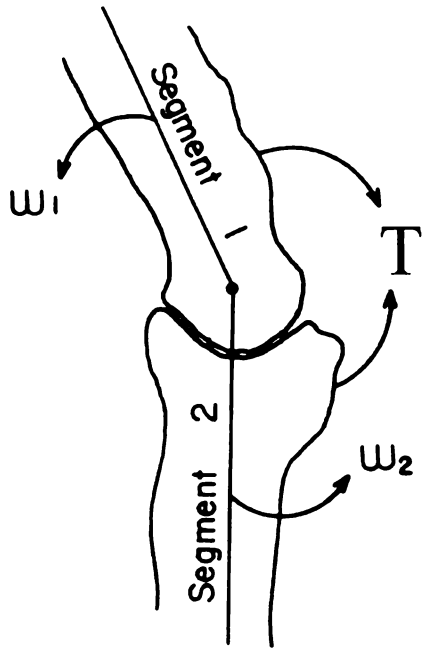

Figure 3-21: Power calculations for thigh (Segment 1), and shank (Segment 2), where T is the joint torque, and ω_1 and ω_2 are the respective segment angular velocities about the knee flexion-extension axis.

For the 3-D case, the definition of active and controlled power is the same. In Figure 3-22, for the more proximal segment, the power $T_{Y1}\omega_{Y1}$ represents the controlled power about the local Y-axis at joint D_1. The power is controlled because $\mathbf{T}_{Y1}$ is positive and $\boldsymbol{\omega}_{Y1}$ is negative as defined according to the right hand screw rule with respect to the direction of the local Y_1-axis. The local Y_i -axis generally represented the long-axis of the body segment. Therefore, if a positive long-axis rotation represents internal rotation, the body is undergoing a controlled external rotation. For the more distal segment, the power $T_{X2}\omega_{X2}$ represents the active power about the local X_2-axis at joint D_2. The local X_i -axis generally represents the flexion-extension axis in the rigid body model. Therefore, if a positive rotation about this axis is flexion, then the segment is undergoing an active flexion. It is also important to point out that in these power calculations, the calculated muscle power does not take into account the power expended by or needed to overcome cocontraction. For instance, the simple act of lifting the foot by extending the leg at the knee could be performed easily with minimum muscle power exerted by the quadriceps, or the task could be made difficult and therefore inefficient by a powerful cocontraction of the quadriceps and hamstring muscles.

Also, in even the simplest anatomical movements there is a certain level of muscle cocontraction to provide joint stability (Luttgens et al., 1992). The power calculations would only give the minimum active or passive muscle power to perform a task. This should generally be significantly greater than the level of power consumed by cocontraction when movements are performed with speed and precision, such as in fast bowling. To calculate the total muscle power including muscle power expended due to cocontraction would require electromyography (EMG), which is beyond the scope of this thesis.

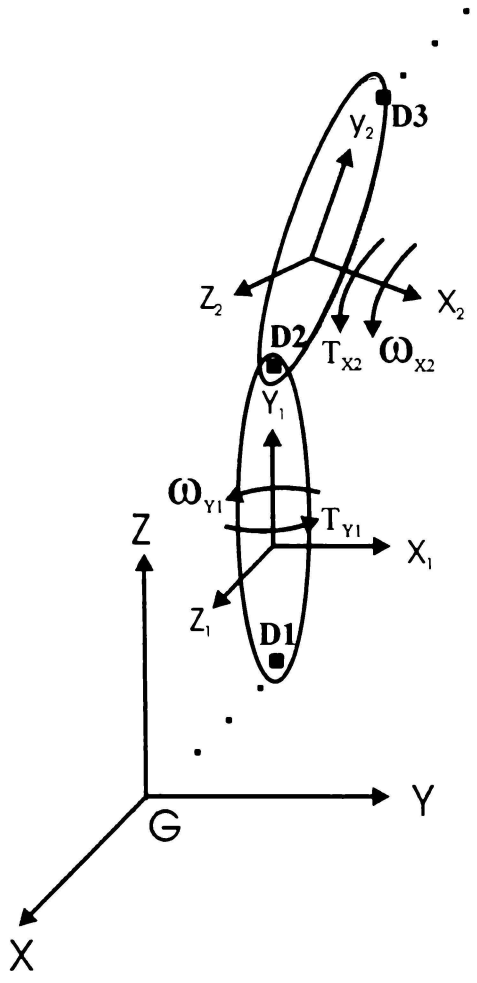

Figure 3-22: General link segment system with body fixed axes defined with respect to global reference system *G*. Torque and angular velocity vectors were defined with respect to local reference system, and about the proximal end, i.e. about D_1 or D_2. Vector direction was defined according to the right hand screw rule with respect to their corresponding body fixed axis.

In general, for a segment *i* having a local body-fixed axis system X_i, Y_i, Z_i where the local *X*-axis is the flexion-extension axis, the *Y*-axis the internal-external long axis rotation, and the *Z*-axis the adduction-abduction axis, there are a variety of

active and controlled anatomical movements resulting from the definition of power-type based on the direction of torque $\mathbf{T}_i$ and angular velocity ω_i vectors about the proximal joint D_i (Table 3-4).

Table 3-4: The conventions for defining power and movement type according to the directions of the torque and angular velocity vectors with respect to their respective body fixed axes. Note that positive rotations about the local body fixed *X*, *Y*, and *Z* axes are defined for flexion, internal rotation, and adduction, respectively.

$\mathbf{T}_i$	ω_i	Power Type	Movement
Positive (X-axis)	Positive (X-axis)	Active	Active Flexion
Positive (X-axis)	Negative (X-axis)	Controlled	Controlled Extension
Negative (X-axis)	Positive (X-axis)	Controlled	Controlled Flexion
Negative (X-axis)	Negative (X-axis)	Active	Active Extension
Positive (Y-axis)	Positive (Y-axis)	Active	Active Internal Rotation
Positive (Y-axis)	Negative (Y-axis)	Controlled	Controlled External Rotation
Negative (Y-axis)	Positive (Y-axis)	Controlled	Controlled internal Rotation
Negative (Y-axis)	Negative (Y-axis)	Active	Active External Rotation
Positive (Z-axis)	Positive (Z-axis)	Active	Active Adduction
Positive (Z-axis)	Negative (Z-axis)	Controlled	Controlled Abduction
Negative (Z-axis)	Positive (Z-axis)	Controlled	Controlled Adduction
Negative (Z-axis)	Negative (Z-axis)	Active	Active Abduction

3.5 SUMMARY

The methodology for this thesis generally involved the experimental collection of 3-D kinematic and ground reaction force data of a large sample of fast bowlers, and the development and use of a 3-D fifteen-segment rigid body inverse solution model of bowling. The smoothed kinematic data were fed into the inverse

solution model to generate dynamics and kinetics data. The outputs available for analysis as a result of this process were

- Linear and angular kinematic data for segment sequencing
- Joint torques
- Joint forces
- Muscle and joint powers
- Segment kinetic energies

Chapter 4

RESULTS AND DISCUSSION

4.1 BALL RELEASE SPEED

The 34 subjects from the test sample were ranked according to maximum ball release speed (Table 4-1). These subjects were also classified according to their highest competition level. Therefore, in order of increasing competition level, 12 were classified as *local* (i.e. local club cricketers), 5 as *provincial* (i.e. regional representative cricketers), 8 as *national B* (i.e. reserve first-class cricketers), 4 as *national A* (i.e. first class cricketers), and 5 as *international* (i.e. test cricketers).

Table 4-1: Percentage distribution of bowling group with ball release speed classification.

COMPETITION	Fast	Med-fast	Medium	Slow
International	60.0 %	20.0 %	20.0 %	0.0 %
National A	50.0 %	0.0 %	50.0 %	0.0 %
National B	50.0 %	37.5 %	12.5 %	0.0 %
Provincial	0.0 %	60.0 %	20.0 %	20.0 %
Local	0.0 %	25.0 %	25.0 %	50.0 %

The bowling speeds ranged from 27.9 m s^{-1} (100 kmh^{-1}) to 36.5 m s^{-1} (131 kmh^{-1}). To define an appropriate speed classification system, previous ball speed radar measurements of fast international bowlers were used as a guide. Today the two fastest bowlers in the world, *Shoaib Akhtar* (Pakistan) and *Brett Lee* (Australia) have delivered balls in excess of 43.1 m s^{-1} (155 kmh^{-1}). *Shoaib Akhtar* recently broke the world ball speed record of *Jeff Thomson's* 44.6 m s^{-1} (160.6 kmh^{-1} - 1975) by registering 44.7 m s^{-1} (160.9 kmh^{-1} - April 2002). There are now about ten bowlers in the world that can deliver balls in excess of 41.8 m s^{-1} (150 kmh^{-1}). These bowlers are sometimes classified as *express fast* bowlers (Smith, 2002). The *fast* group classification is commonly assigned to bowlers who register ball speeds in excess of 38.89 m s^{-1} (140 kmh^{-1}). Then in decrements of 1.39 m s^{-1} to 2.78 m s^{-1} (5 kmh^{-1} to 10 kmh^{-1}) the bowling groups

are often classified in order of decreasing speed as *medium-fast*, *medium*, and *slow*.

In the test sample, of the two fastest bowlers who had their ball speeds recorded in cricket matches, one bowled in excess of 40.3 m s^{-1} (145 kmh^{-1}), and the other bowled a ball at 42.2 m s^{-1} (152 kmh^{-1}). However, in the lab, these bowlers registered speeds just above 36.1 m s^{-1} (130 kmh^{-1}), though the faster bowler had only recently recovered from injury, and was probably not bowling at maximum speed. However, there was still a significant difference between ball speeds measured in field and laboratory. Either the subjects' performances were impaired in the laboratory or the ball speed measurement by high-speed cameras differs from that of speed radar guns. Therefore, the fast group for this study was defined for speeds in excess of 33.3 m s^{-1} (120 kmh^{-1}) assuming that there was a 2.78 m s^{-1} to 4.17 m s^{-1} (10-15 kmh^{-1}) difference in measurement between the lab and field. The extension of this scaling-down process for the other speed groups resulted in the following division of bowlers: slow, 27.8 m s^{-1} to 30.6 m s^{-1} (100-110 kmh^{-1}); medium, 30.6 m s^{-1} to 31.9 m s^{-1} (110-115 kmh^{-1}); medium-fast, 31.9 m s^{-1} to 33.3 m s^{-1} (115-120 kmh^{-1}); fast, greater than 33.3 m s^{-1} (>120 kmh^{-1}). This classification system gave 9 fast bowlers, 10 medium-fast bowlers, 8 medium bowlers, and 7 slow bowlers. The ball release speeds of all the test subjects sorted in order of bowling speed group and competition level are shown in Appendix I (Tables I-1 & I-2). Note that there is no universally recognised speed classification system. However, the classification system developed here was adapted from that of Bartlett et al., (1996) and Abernethy (1981).

There was a relationship between a bowler's highest playing level and ball release speed. Generally, the average maximum ball release speed increased with competition level (Figure. 4-1). For instance, 60% of the international cricketers, who represent the highest playing level, were classified as fast bowlers and none as slow-medium bowlers (Table 4-1). Conversely, 50% of club cricketers, representing the lowest playing level, were classified as slow-medium bowlers and none were placed in the fast bowling group. The National A and National B groups recorded intermediate ball release speeds. However, against the trend the National B group recorded a faster average maximum ball release speed than the

National A group. However, the National A group had only four subjects, and two of these were primarily 'limited-over' bowlers, who specialised on maintaining accuracy of length, and perhaps did not develop the technique to produce a fast ball release speed. Also, the National B group was unusual in that it produced the fastest and fourth fastest bowlers overall.

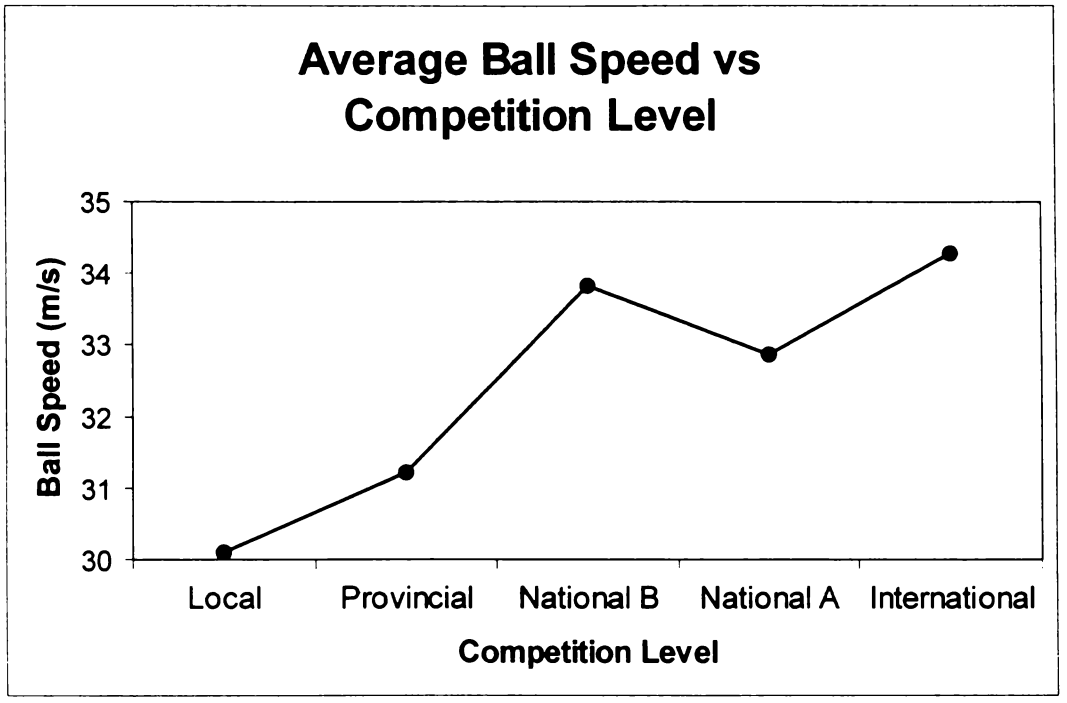

Figure 4-1: Average maximum ball release speed per group tended to increase competition level.

Speed is not the only factor that determines the success of an elite bowler. Certainly, successful bowling is a far more subtle and intricate art than merely releasing the ball as fast as possible in the vague direction towards the batter. However, apart from certain spin bowlers, a fast ball release speed should certainly aid in a bowler's effectiveness, because a faster ball speed reduces the reaction time for a batter to hit the ball, increasing the likelihood of an error in stroke production. Even from the relatively small sample of bowlers tested, it is evident that the more elite bowlers on the whole release the ball at higher velocities than the less elite ones. It is likely that this relationship would be more conclusively determined for a larger sample group.

4.2 RUN-UP

4.2.1 Centre of Mass Velocity

The run-up speed was defined as the horizontal component of centre of mass (CoM) velocity during the pre-delivery leap when both feet were in the air prior to back foot contact. For each of the speed classification groups, the average run-up speed was calculated (fast, 5.4 ± 0.10 m s^{-1}; med-fast, 5.52 ± 0.01 m s^{-1}; medium, 5.11 ± 0.22 m s^{-1}; slow, 4.58 ± 0.25 m s^{-1}). In general, the faster bowlers utilised higher run-up speeds than the slower bowlers. Also, a linear squares regression of ball release speed versus run-up speed for each subject had a positive slope with a correlation coefficient of 0.57 ($p < 0.0005$) (Figure 4-2). Davis and Blanksby (1976a) reported a similar finding that fast bowlers use a run-up approximately 15% faster than the medium-pace bowlers. However, despite this relationship, only 33% of the variation in ball speed is explained by the linear regression of ball speed on run-up speed.

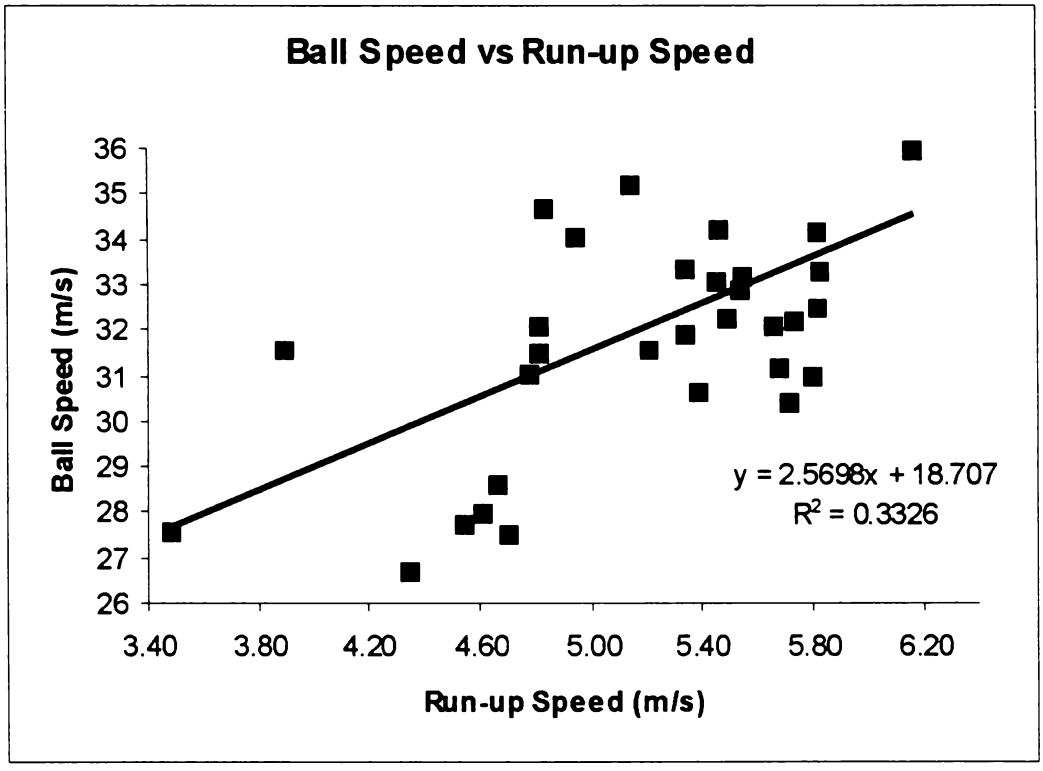

Figure 4-2: A linear regression of ball release speed versus run-up speed with linear correlation coefficient R equal to 0.57 ($p<0.0005$).

To show the distribution of run-up speeds, the measured run-up speeds were normalised with respect to the minimum and maximum values, and the frequency distribution of each bowling speed group was calculated in 10% incremental increases of normalised run-up speed (Fig. 4-3). Below 50% of the normalised run-up speed, 85.7% of the slow group, 37.5% of the medium group, 10% of the medium-fast group, and 0% of the fast group were represented. This suggests that faster bowlers are more likely to use faster run-up speeds, though it is worth noting that there was significant overlap between the faster bowling groups in the higher ranges of run-up speed.

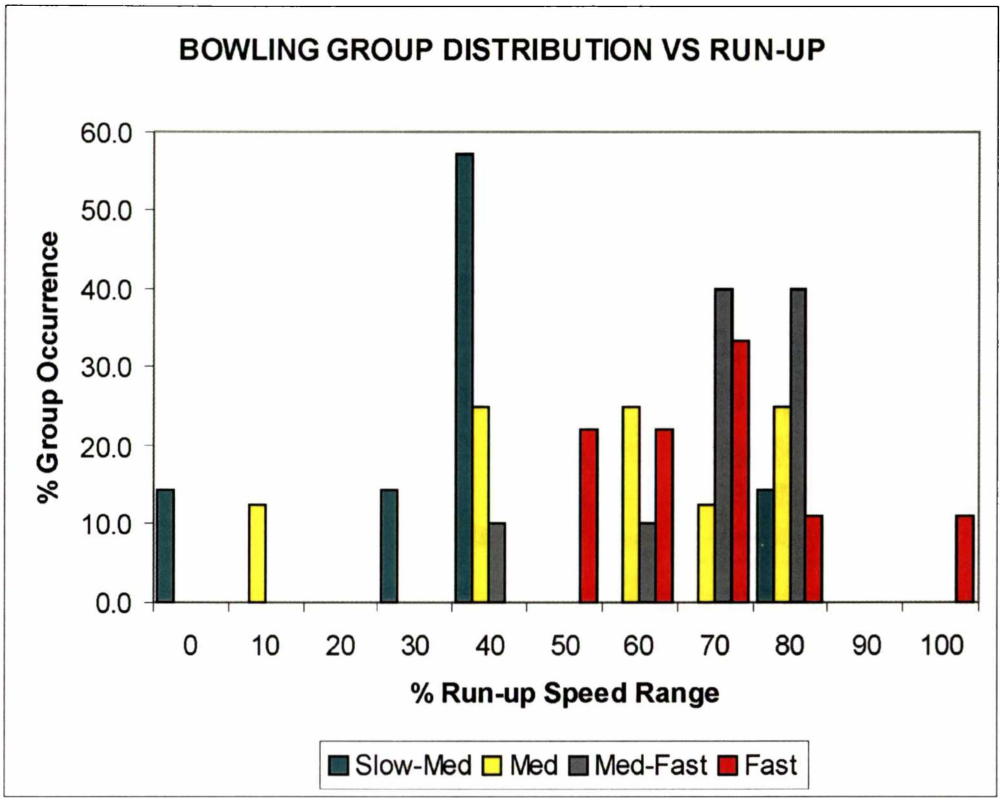

Figure 4-3: Ball speed distribution against normalised run-up speed.

4.2.2 Centre of Mass Acceleration (Back Foot Contact to Front Foot Contact)

Having ascertained that there is a relationship between run-up velocity and ball speed, the changes in this velocity that occur during the delivery stride were investigated. The average centre of mass acceleration (horizontal forward component) was calculated for each of the subjects from back foot contact (BFC)

to front foot contact (FFC) (Figure 4-4). The ball release speed was found to increase with the negative acceleration of the CoM (R = 0.62). To further support this finding, the average CoM acceleration from BFC to FFC was averaged over each bowling group. It was found that the negative accelerations were highest for the fast bowling group (-225 m s^{-2}), lower for the medium-fast and medium groups (-162 m s^{-2} and -159 m s^{-2}), and lowest for the slow group (-126 m s^{-2}). It was concluded that differences between the kinematics of the faster bowlers' actions and the slower bowlers was responsible these differences in CoM acceleration.

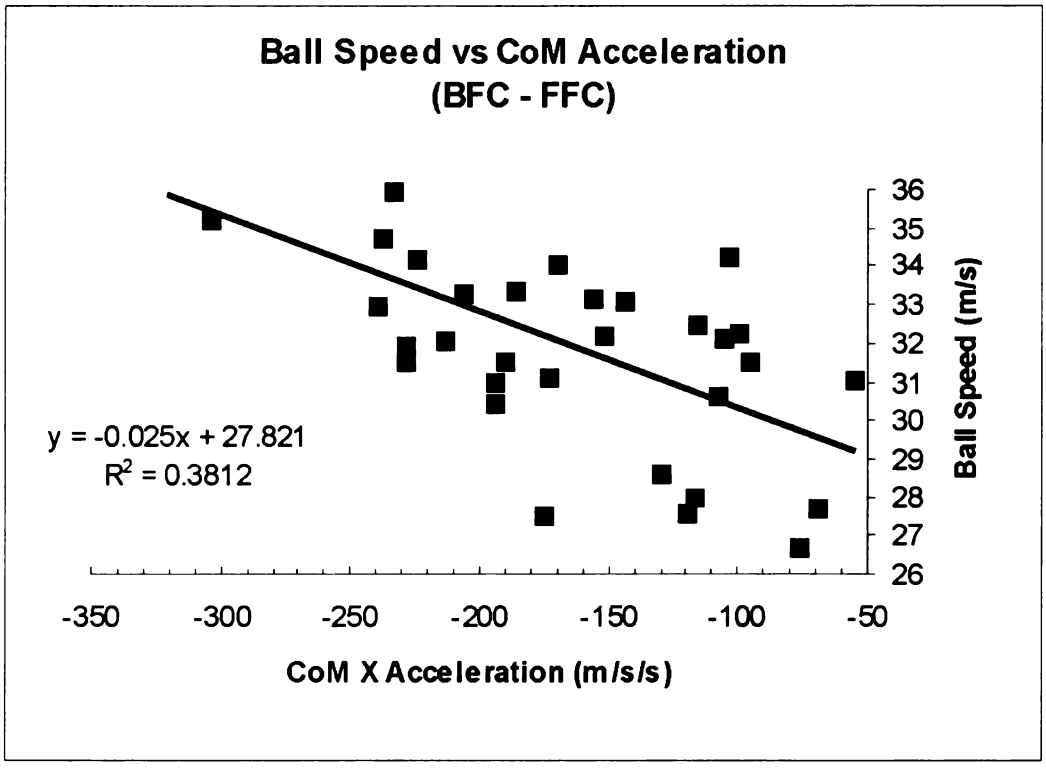

Figure 4-4: Centre of mass deceleration increases with ball speed (R = 0.62).

To examine the variation of CoM acceleration over the delivery stride, ensemble averages for each bowling group were calculated over the period from BFC (0%) to FFC (100%), which was defined as the *phase cycle* (PC) (Figure 4-5). The CoM negatively accelerated during early BFC, as the slight flexing of the rear leg absorbed energy in response to the vertical back foot ground reaction forces. From 0-20% PC, the average negative CoM acceleration was highest for the three fastest groups and lowest for the slow group: (fast, -1290 m s^{-2}; med-fast,

-1030 m s^{-2}; medium, -1310 m s^{-2}; slow, -896 m s^{-2}). It was initially hypothesised that this average negative acceleration would decrease with bowling speed group, because elite fast bowlers try to minimise the linear momentum loss at BFC (Bartlett et al., 1996). However, the results show no such relationship. Perhaps a certain magnitude of initial CoM negative acceleration is indicative of some technique for speed generation, and this may be why the slow group registered the lowest negative values. For instance, during early BFC, the trunk was still coiling, promoted by the raising of the front arm above the level of head. However, the low negative CoM acceleration of the slow group may also be a function of its relatively low run-up velocity.

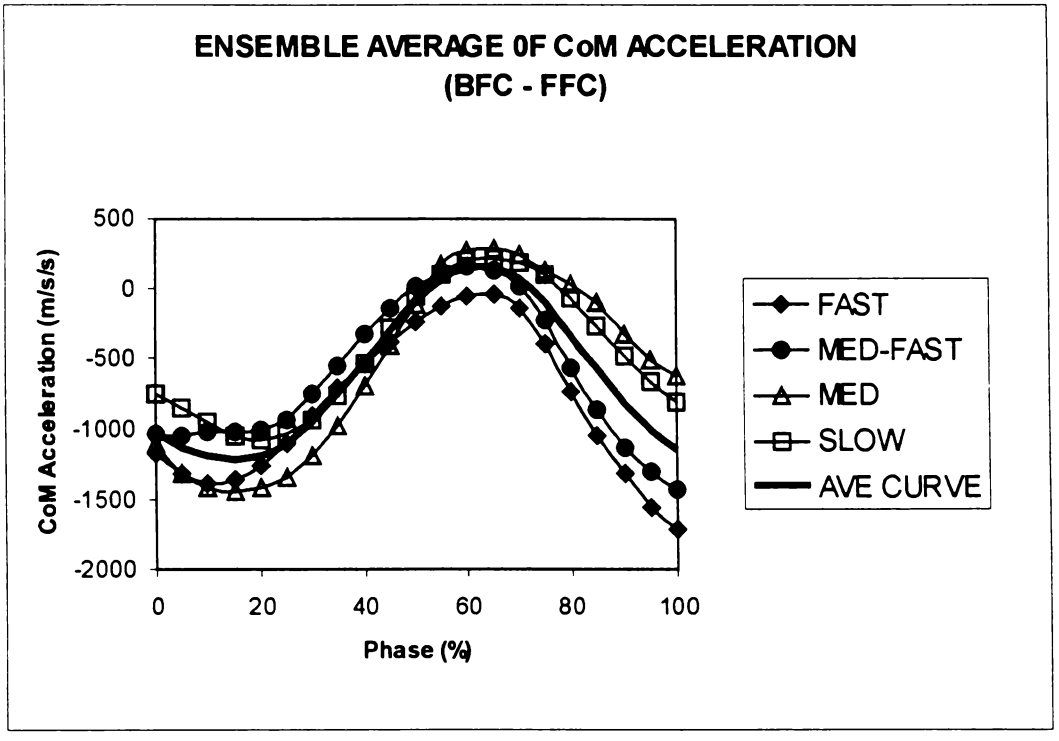

Figure 4-5: Ensemble averages of the CoM horizontal acceleration. Forward acceleration is defined as positive. The CoM shows a significant period of negative acceleration from BFC to FFC. Note that the AVERAGE curve (simple black) is the average of the ensemble average curves. Variance ratios (VR): fast, 0.41; med-fast, 0.37; medium, 0.31; slow, 0.34.

During the next period from 20-60% PC, the negative CoM acceleration was becoming more positive. At 60% PC, the value was only slightly negative for the fast group, and positive for the other groups (fast, -51 m s^{-2}; med-fast, 152 m s^{-2}; medium, 200 m s^{-2}; slow, 143 m s^{-2}). During this period the front arm was straightening and dropping to the level of the front shoulder, while the trunk was

flexing and laterally bending away from the direction of forward motion, and the front leg was extending forwards lengthening the delivery stride. The back leg supported this motion by withstanding the ground reaction forces through the back foot. Also, the front foot was extending horizontally and the trunk was leaning back in counterbalance. The initial negative CoM acceleration of the fast group may be evidence that these bowlers were able to better use this counterbalancing mechanism to stretch the trunk and shoulders during this phase. This may have been facilitated by their higher run-up speeds. For instance, a faster run-up could mean that the CoM must undergo a higher negative acceleration to achieve the counterbalanced position, and consequently place the trunk and shoulders under more dynamic stretch.

Large differences between the groups were apparent during the final period (60-100% PC) when the CoM acceleration was increasing negatively. The two fastest groups had much larger average negative accelerations than the two slower ones: (fast, -778 m s^{-2}; med-fast, -581 m s^{-2}; medium, -64 m s^{-2}; slow, -176 m s^{-2}). It was during this time that the body was preparing for FFC, when the front leg would act as a strong lever over which the upper body could propel itself, while withstanding large ground reaction forces of up to 5-8 times body weight (BW). The large differences in CoM acceleration between the two faster and two slower groups indicate that the anticipatory motion of the front leg prior to FFC could be a determining factor in the eventual ball release speed. It therefore makes good sense to examine the mechanics of the rear leg during the delivery stride, as it is through the back foot ground reaction forces acting through this segment that the horizontal CoM acceleration can be influenced.

4.2.3 Centre of Mass Acceleration (FFC to Ball Release)

During the period from FFC to ball release (REL), the front leg acts as a lever over which the upper body is propelled. This is the *power phase period* of bowling, because it is during this time that the trunk and bowling arm undergo their greatest acceleration (Elliott et al., 1990). Interestingly, the average negative acceleration of the CoM during the power phase was significantly higher than that

during the preceding phase (i.e. from BFC to FFC). The average negative acceleration over the entire FFC to REL phase for the total sample was –1,480 m s^{-2}, whereas for the preceding phase it was only –602 m s^{-2}. Also, the slope of the linear regression curve indicates a -36.6 m s^{-2} increase in negative CoM acceleration for every 5 kmh^{-1} of ball release speed (Fig. 4-6). This is an unusual concept in fast bowling. Coaches often talk about maintaining the linear momentum gained during the run-up throughout the delivery stride. The fact that the body's CoM is undergoing a high negative acceleration was not known. It is possible that fast bowling techniques could be developed that promote a high negative acceleration of the CoM, and as a result increase ball release speed.

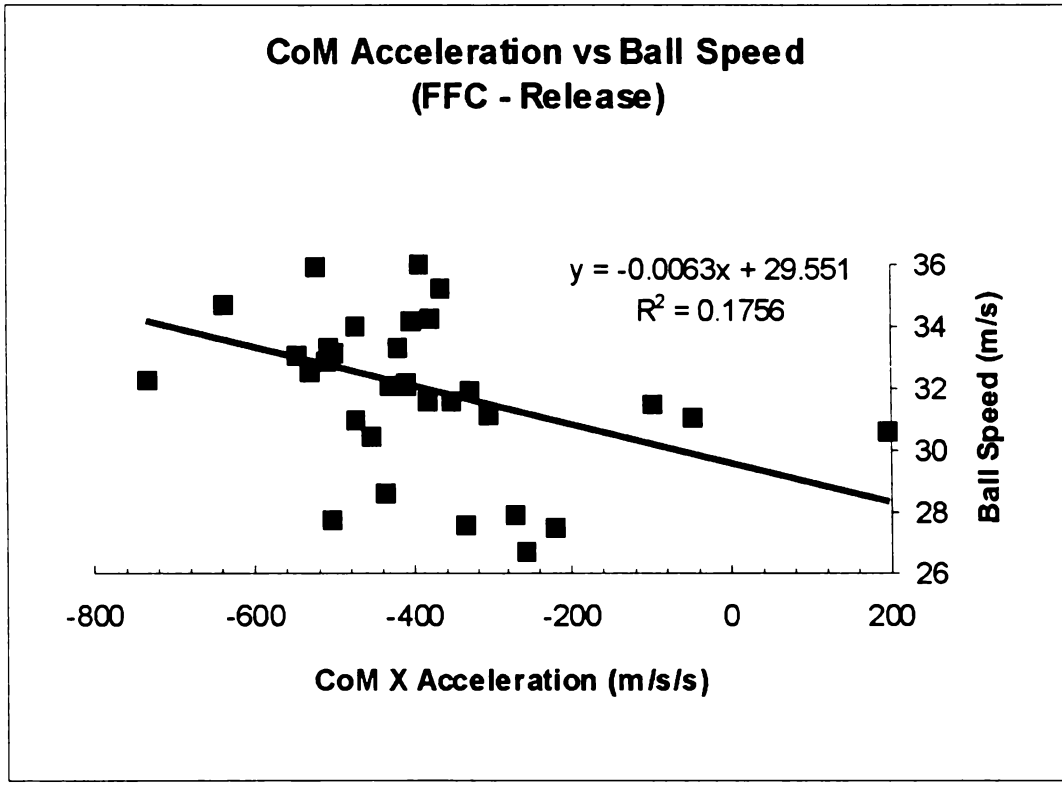

Figure 4-6: Centre of mass negative acceleration increased markedly with ball release speed (R = 0.42).

The mean of the CoM acceleration for the total sample is the black solid curve in Figure 4-7. It acts as a reference curve to compare the ensemble average CoM curves of each group. These curves show that the fast and medium-fast groups were largely below the reference curve, whereas the medium and slow groups were mostly above it. The faster two groups also had a substantially higher mean

negative acceleration of the CoM than the two slower groups: (fast, -1660 m s^{-2}; med-fast, -1830 m s^{-2}; medium, -1150 m s^{-2}; slow, -1270 m s^{-2}). Therefore, the data suggests that front leg action was used to negatively accelerate the CoM of the body. It could be that ball release speed is a function of how well this is done. Additionally, the fast group exhibited a unique difference the CoM curve. From 50-70% PC, the fast bowling group had a significant decrease in negative acceleration after which there was a rapid increase in negative acceleration lasting until the moment of ball release. In contrast, the other groups had a gradual negative increase in CoM acceleration over the phase. During this period, when the bowling arm had passed the horizontal position behind the body, there could have been an extra pull or thrust of the upper body over the front leg about the hip joint that was not apparent in the slower bowling groups. All this emphasises the importance of the front leg during delivery stride, which is the only limb subject to external forces (via the ground reaction forces through the foot). It must act to rapidly brake the motion of the body, and withstand the large ground reaction forces that result from this action.

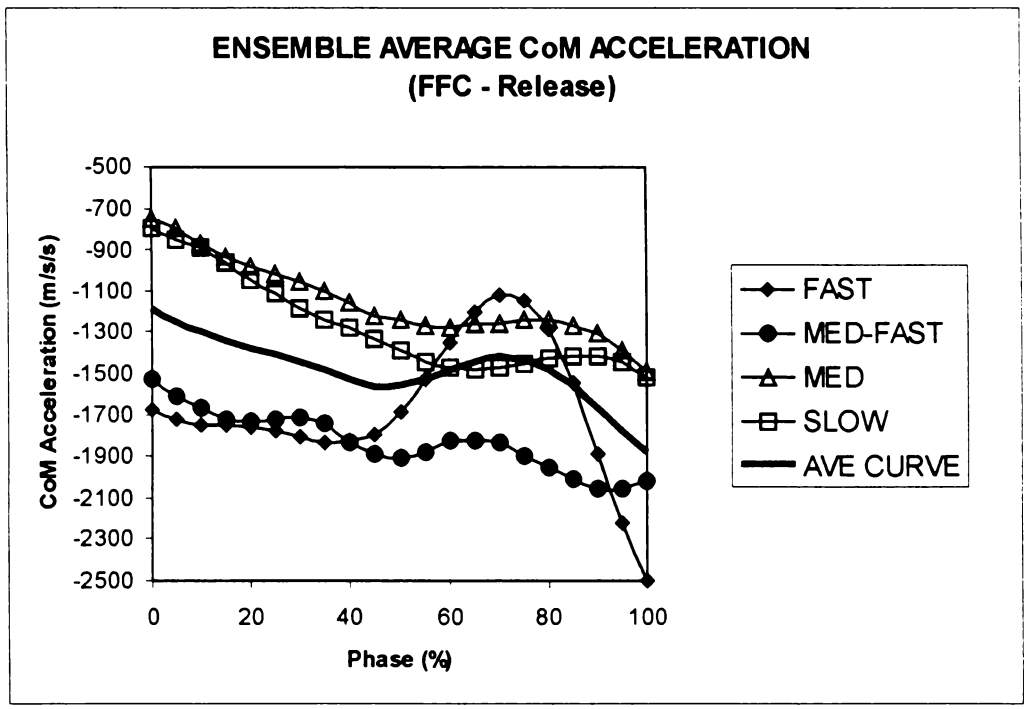

Figure 4-7: Ensemble averages of centre of mass acceleration for each bowling group from FFC to REL. (VR: fast, 0.51; med-fast, 0.36; medium, 0.28; slow, 0.33).

4.3 ACTION CLASSIFICATION

There have been several systems used to used to classify the action of a bowler as side-on, front-on or mixed. Essentially, these classification systems defined action type based on (i) *shoulder angle* and *back foot angle* at BFC, (ii) *shoulder separation angle* at BFC, which is the angle between the shoulders and hips projected in the transverse plane, and (iii) *shoulder counter-rotation*, which is the difference between the shoulder angle at BFC and the minimum shoulder angle projected in the transverse plane.

The shoulder separation angles at BFC and counter-rotation angles were measured for the sample of bowlers. Using the system by Portus et al. (2000), which was a modification of the classification criteria from Foster et al. (1989) and Burnett et al. (1996), a large proportion of the bowlers (64.7%) qualified as front-on bowlers (Table 4-2). This high percentage of front-on actions was attributed to the lenient criterion of 'safe' shoulder counter-rotation angle defined as less than 40°, so that many actions that would have normally qualified as mixed were now classified as front-on. Portus et al. (2000) defined the side-on action as having a shoulder angle of less than 190°, and a back foot angle of less than 280°. However, there was no account of the case where the shoulder angle satisfied the side-on criterion, but the back foot angle was greater than 280°, (and counter-rotation angles were less than 40°). Therefore, 14.7% of the sample remained unclassified.

Table 4-2: Percentage of bowling action types according to classification method.

ACTION TYPE	(Portus et al., 2000)	(Burnett et al., 1995)	Modified
Front-on	64.7	5.9	23.5
Side-on	2.9	8.8	11.8
Mixed	17.6	85.3	61.8
Closed Mixed	-	-	2.9
Side-on Mixed	-	-	0.0
Front-on Mixed	-	-	58.8
Unclassified	14.7	0.0	0.0

Using the action classification system of Burnett et al. (1995), which specifies a mixed action as one having a shoulder counter-rotation of greater than 20°, 85.3% of bowlers were mixed. The criterion of 20° acceptable shoulder counter-rotation seemed too stringent to meaningfully distinguish between the types of bowling action for this sample

From this preliminary analysis, the significant percentage of unclassified bowlers, the lenient criterion defined for safe counter-rotation angles, and the lack of differentiation between bowlers within the mixed action type, suggested the need for modifications to the existing classification systems. Hence, one is proposed that addresses these problems. It also uses a more intuitive alignment angle convention by defining the alignment as the angle between a segment running from the rear joint (A) to the leading joint (B) where the *X*-axis points directly in the line of the wicket (Figure 4-8). The *Y*-axis for the right-hand bowler points to the off-side (for right-hand batter), and therefore the *Z*-axis points directly

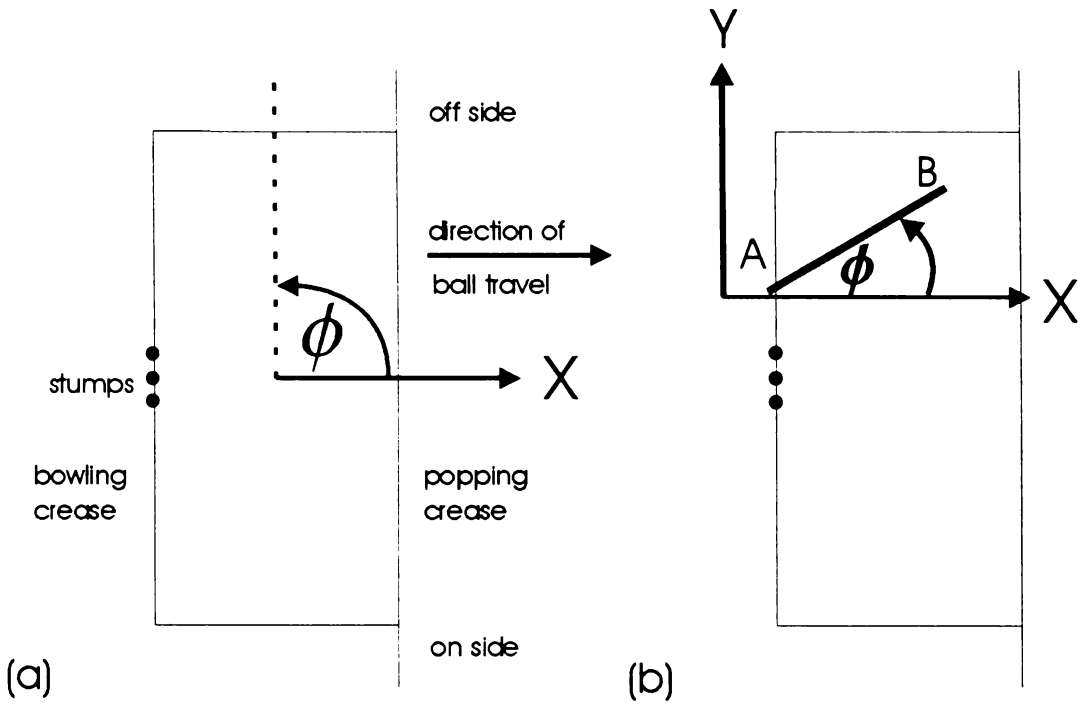

Figure 4-8: (a) The reference classification system. (b) Shows the typical shoulder alignment of a right hand front-on bowler (φ ≈ 35°). The line drawn from the right to left shoulder is represented as running from point A to point B.

upwards out of the page. For the left-hand bowler, the *Y*-axis points to the leg-side (for right hand batter) with the *Z*-axis pointing downwards into the page. Angle sign conventions are based on the right-hand screw rule. Based on this system, a perfectly side-on bowler would have a shoulder and hip alignment of 0°. A perfectly front-on bowler would have the leading shoulder pointing in the direction of the *Y*-axis, giving a shoulder alignment of 90°. The back foot of a right hand bowler pointing parallel to the bowling crease would have an alignment angle of –90°.

The following modified classification system was used to identify bowling action type:

Side-on: Shoulder alignment < 25° AND (shoulder separation angle at BFC < 30° AND shoulder counter-rotation < 30°)
Front-on: Shoulder alignment > 25° AND (shoulder separation angle at BFC < 30° AND shoulder counter-rotation < 30°)

Open Mixed: shoulder separation angle at BFC > 30°

- **Front-on Mixed:** shoulder alignment > 25° AND (shoulder separation angle at BFC > 30° OR shoulder counter-rotation > 30°)

Closed Mixed: shoulder separation angle at BFC < -20°

- **Side-on Mixed:** shoulder alignment < 25° AND (shoulder separation angle at BFC < -20° OR hip counter rotation > 10°)

This classification system is similar to Burden et al. (1995) in that it considers both the shoulder separation and shoulder counter-rotation angles in classifying mixed action. Also, the 40° counter-rotation criterion for mixed action type as specified by Portus et al. (2000) was reduced to 30°. This was considered appropriate, because previous research such as Elliott et al. (1992) reported 30° of counter-rotation sufficient to predispose individuals to back injuries (Elliott, 2000). In addition, the mixed action was differentiated as either open or closed mixed. These actions were further classified as front-on mixed and side-on mixed, which make up the majority of mixed action type bowlers. Only

occasionally would, for example, an open mixed action fail to also satisfy the conditions of a front-on mixed bowler. Similarly, it would be rare that a closed mixed action bowler not also be side-on mixed. However, in the preliminary trials of sub-elite bowlers, such exceptions were recorded, and they indicated actions of extreme risk, (because the lower back is placed under extreme stress to achieve such actions), further confirming the need to broaden the original classification systems.

In distinguishing the differences between these actions, the sign of the shoulder separation angle is important. The shoulder-hip separation angle was defined as the shoulder alignment angle minus the hip alignment angle at BFC. A negative shoulder-hip separation angle therefore indicates that the shoulders are more closed than the hips, whereas a positive separation angle indicates the opposite. Also, in a side-on mixed bowler, the hips may counter-rotate during delivery stride. The safe limit for hip counter-rotation was set at 10° because any hip counter-rotation values would be relatively small. Also, it may be that the side-on mixed action is more dangerous than its front-on counterpart, as it appears to require more hyperextension of the lower lumbar region, so the shoulder separation tolerance was defined 10° less than for the front-on mixed case. A notable example of a side-on mixed bowler is *Brett Lee* (Australia), who suffered lower lumbar injury, and subsequently took remediation measures to make his action safer (Figure 4-9).

Unlike the classification systems used by Portus et al. (2000), Elliott et al. (1993) and others, there was no treatment of back foot angle. The reason is that the effect of the back foot angle should manifest itself in the value of hip alignment angle, and therefore be a function of the shoulder-hip separation angle. A linear regression on hip alignment versus back foot angle confirmed this relationship, showing that the back foot angle became more positive (i.e. back foot tends to point more towards the batter) as the hips opened up ($R = 0.73$, $p<0.0005$) (Figure 4-10). It is possible that, for instance, a side-on bowler with a small shoulder-hip separation angle and counter-rotation angle, but with the back foot pointing straight down the wicket, would put more strain on the knees and lower lumbar region by the torsion created through the rear leg as a result of this straight

foot orientation. This, however, is another issue, and should be researched separately before such a notion can be incorporated into an action classification system that indicates susceptibility to injury risk.

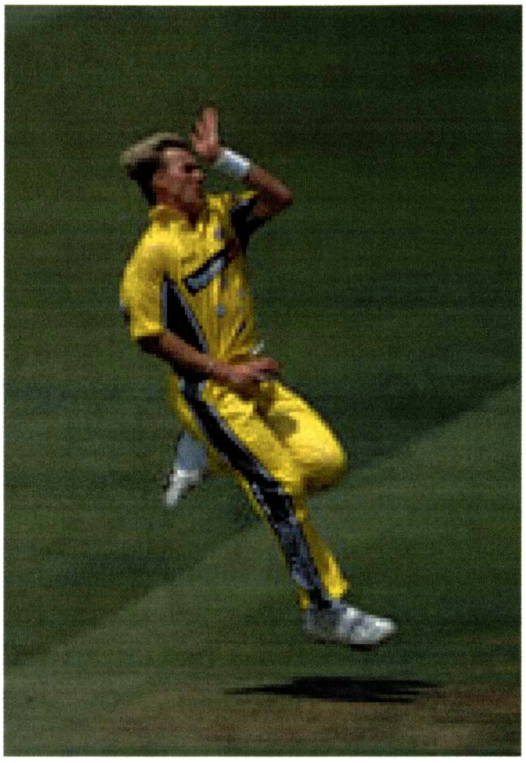

Figure 4-9: Brett Lee (Australia) one of the fastest bowlers in the world suffered stress fractures of the lower back, probably due to a side-on mixed action. Just prior to BFC the shoulders are closed and the hips are open.

Using the modified classification system, the percentage of mixed action bowlers was 61.8%, the majority of which (58.8%) were front-on mixed (Table 4-2). As the sample is large for bowling and representative of bowlers from a range of competition levels, these results suggest that fast bowlers in New Zealand have largely moved away from the traditional side-on action. Even considering the alternative classifications of action type, the percentage of side-on bowlers in the sample was still very low. Instead, there is evidence that the mixed action is now the predominant bowling technique in New Zealand. This signals a disturbing trend, as there is good evidence that susceptibility to lower lumbar injury is increased with the implementation of the mixed action technique (Elliott, 2000). Further, it is worth noting that Elliott (2000) suggests that although there is a continuum of counter-rotation for all bowlers, it is recommended that a standard

of 20° of counter-rotation be used to assist in classifying the mixed bowling technique. Therefore, the choice of 30° counter-rotation is not too stringent a measure to define the mixed action technique.

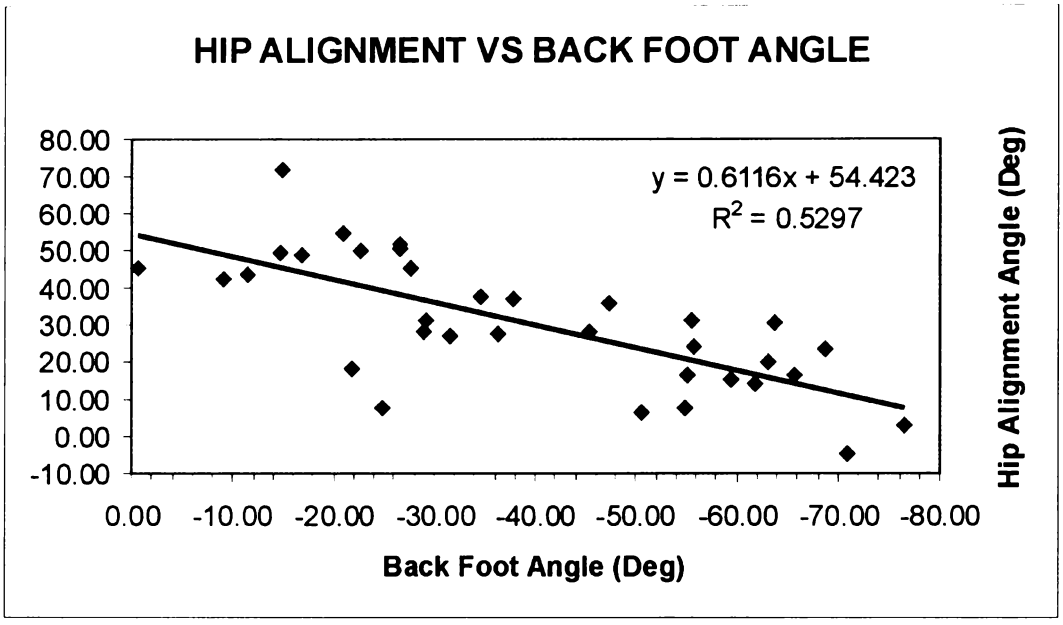

Figure 4-10: Hip alignment versus back foot angle. As the back foot points more towards the batter, the hips become more open (R = 0.73).

It is important to separate the mixed actions into their respective types because any suggested remediation measures to reduce the amount of counter-rotation would depend on the type of mixed action. Also, the modified classification system did not produce any unclassified bowlers, but there was one closed mixed bowler. Closed mixed bowlers, who do not also meet the criteria of a side-on mixed action, should be regarded as having an extreme high-risk action in terms of the extra stresses placed on the lower lumbar region due to the highly strained configuration that the technique imposes on the lower lumbar region.

The mean kinematic alignment characteristics show that even the side-on action was not performed in the classical manner with the shoulders in line with the stumps, and the head looking inside the front arm (Marylebone Cricket Club, 1976). Instead, the shoulders were still open, and some previous classification systems (i.e. shoulder alignment less than 20° at BFC) would have even defined many of these bowlers as front-on. However, for this bowling sample it does seem productive to have classified these bowlers as side-on because (i) there was

a large difference between the mean shoulder angles of the side-on and front-on groups, and (ii) the shoulder counter-rotation values of the side-on bowlers were the smallest of all the action types (Table 4-3). Therefore, the bowlers classified as side-on with a shoulder alignment less than 25° at BFC did possess markedly different alignment characteristics, which is one indication that the criteria for division were appropriate. Also, it could be argued that the side-on bowler of today is more appropriately defined as having a semi-front-on or semi-open action.

Table 4-3: Mean (± standard error) kinematic alignment characteristics for side-on, front-on and mixed action techniques.

ACTION TYPE	Shoulder Angle BFC(°)	Shoulder/Hip Separation BFC (°)	Shoulder Counter Rotation (°)
Side-on	21.7 ± 1.8	10.2 ± 3.3	11.0 ± 5.4
Front-on	41.6 ± 3.4	9.07± 3.1	21.5 ± 2.4
Mixed (front-on)	61.1 ± 2.7	28.4 ± 2.8	36.6 ± 2.3

The mean shoulder angle for the front-on bowlers was greater than 40° (Table 4-3). This was well in excess of the minimum shoulder angle criterion that defines a front-on action. In general, fast bowlers find it more difficult to maintain a more 'open' technique throughout the delivery stride (Portus et al., 2000). The data support this view as the mean shoulder counter rotation for the front-on bowlers was still greater than 20°, which satisfied some previous definitions of a mixed action technique. Therefore, even the actions of the front-on bowlers exhibited moderate levels of counter rotation. Bowlers should develop the semi-open front-on technique rather than the more open front-on technique wherever possible to prevent the possibility of degenerating to a mixed action technique, which becomes more likely under fatigue (Portus et al., 2000).

The mean shoulder angles of the mixed action bowlers were even higher than that of the front-on bowlers, i.e. the mixed action bowlers were about 20° more open that the front-on bowlers, which further supports the claim that the more open front-on technique is difficult to execute safely. The mean shoulder-hip separation

angle was almost 30°, and the mean shoulder counter-rotation slightly greater than the mean shoulder counter-rotation of 35.4° reported in the study of 24 young fast bowlers by Elliott and Khangure (2002). High mean values such as these usually reflect that there are some bowlers recording extreme counter-rotation values. For example, four bowlers had counter-rotation angles in excess of 40°, and three in excess of 50°. These latter three bowlers also adopted the most open front-on actions with shoulder alignments of 84.4°, 73.4°, and 85.4°. Therefore, such open front-on actions may be predictors of highly mixed actions. If these more open shoulder alignments generate the highest counter-rotation angles, then it is probable that they also register the highest counter-rotation rates. This would cause the shoulders and hips to rotate in opposite directions with high angular velocities while the trunk is laterally bending. The hypothesised stresses incurred on the lower lumbar region in the presence of such motion are suggested to cause progressive lumbar vertebra degeneration, pars interarticularis, and spondylolysthesis (Bartlett et al., 1996). Therefore, the higher the mean counter-rotation angle for a sample, the higher the susceptibility to serious lower lumbar injury.

Though the mixed action bowlers tended to use more open shoulder alignments, it must still be noted that it is still technically possible to use a shoulder alignment of greater than 40° and bowl successfully. *Malcolm Marshall* (West Indies) was able to maintain such an open shoulder alignment throughout delivery at high speeds without sustaining any significant lower lumbar injury (Figure 4-11). Therefore, it is not advisable to immediately close the shoulder alignment of a 'open' front-on bowler unless shoulder counter-rotation is also present. Similarly, the fact that *Malcolm Marshall* and other bowlers can use such open actions safely means that there should be alternative technical solutions to making such bowling actions safer rather than only considering the reduction of shoulder alignment angle at BFC.

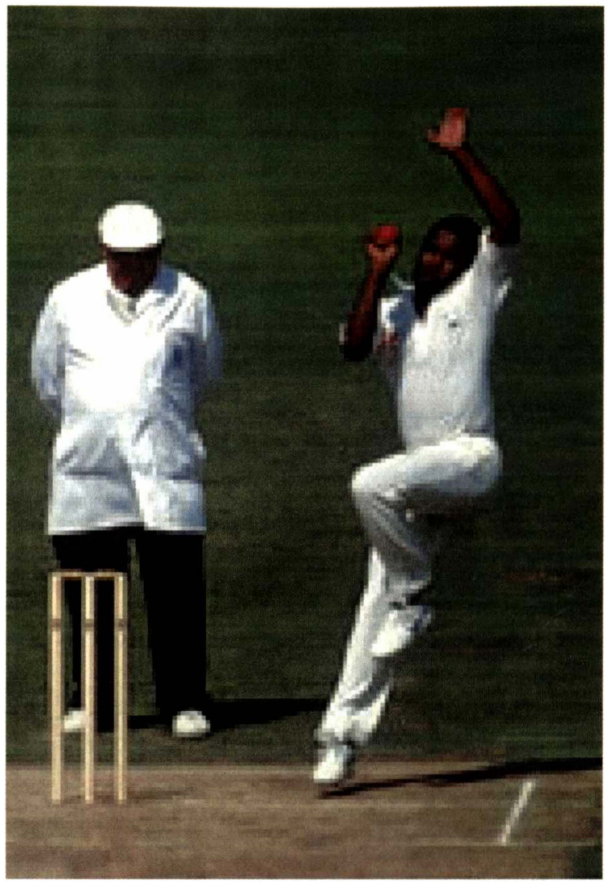

Figure 4-11: Malcolm Marshall (West Indies) had a very open shoulder alignment, but he maintained this throughout the delivery stride, while releasing the ball at high speeds. However, he did manage to keep the front foot slightly closed during FFC.

It has been well established that mixed action techniques increase the likelihood of lower lumbar injury. Apart from measuring shoulder-hip separation angle, and shoulder counter-rotation, it is important to ascertain what other factors could be indicators or characteristics of mixed action bowlers. An examination of mean foot and stride angles shows that as the shoulder alignment became more open, the foot and stride angle also opened up (Table 4-4). The large standard errors in front foot angle suggest that this characteristic is more a probabilistic indicator of action type. Therefore, to express the data in this form, front foot angle was discretely defined as open for an alignment angle of greater than 0°, and closed for an alignment of less than 0°. The frequency distribution of front foot angle-type occurrence with action-type shows that over 60% of the mixed action bowlers used an open front foot alignment (Figure 4-12). The side-on and front-on bowlers were over 70% more likely to use a closed front foot alignment.

Table 4-4: Front angle and stride angle versus action type.

ACTION TYPE	Front Foot Angle (°)	Stride Angle (°)
Side-on	-7.7 ± 4.9	-5.4 ± 0.8
Front-on	-3.8 ± 5.2	-1.2 ± 1.7
Mixed (front-on)	3.7 ± 3.1	1.5 ± 0.9
Mixed (closed)	20.5	3.6

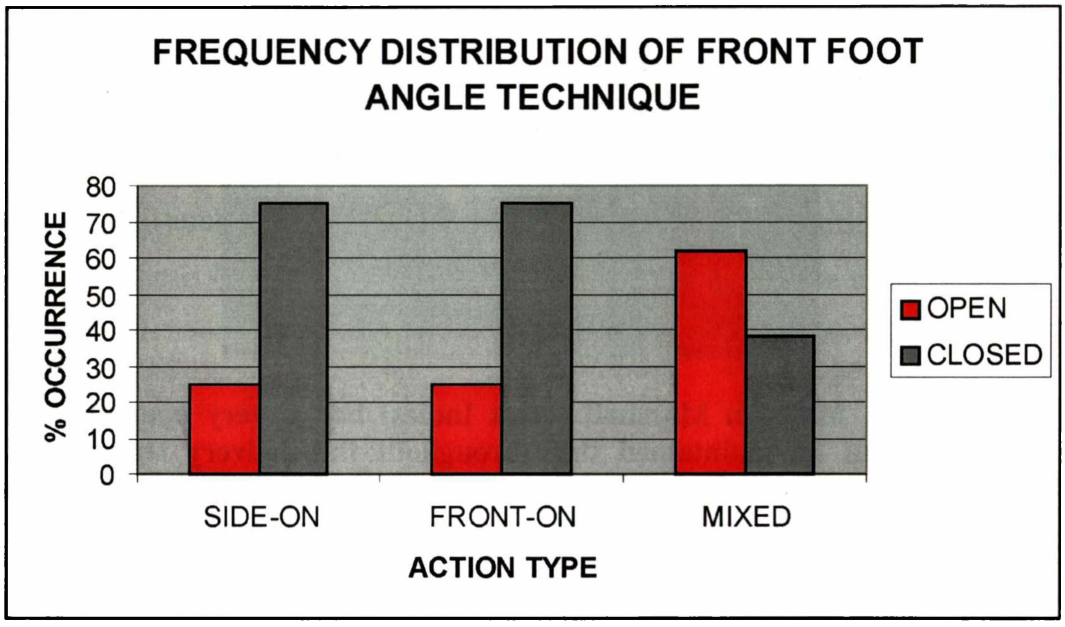

Figure 4-12: Frequency distribution of front foot alignement.

The occurrence of lower lumbar injury in fast bowlers, particularly young fast bowlers, has promoted much research in this area. To date it remains the most scientifically researched aspect of bowling technique. However, from the sample of bowlers tested, there appears to be a significantly high proportion of mixed action bowlers in New Zealand. With all the coaching schemes that are in place, and the emphasis on biomechanics in cricket, it is difficult to imagine how this situation could have arisen. Without data, it is not possible to ascertain whether this is the case in other countries which have similar coaching schemes, or whether New Zealand is unique in this respect. The calibre of research correlating mixed action type to lower lumbar injury, and to even reduced bowling accuracy (Portus et al., 2000) is generally high. Therefore, the prevalence of the mixed

action type in New Zealand should be an issue of utmost importance for cricket coaching councils to address throughout the country.

4.4 SEGMENTAL VELOCITY SEQUENCING

Biomechanists have always sought a general principle to explain the many different striking and throwing movements involving the coordination of multiple body segments. Research has suggested that many such movements exhibit characteristics of proximal-to-distal sequencing: the larger and heavier proximal segments initiating the motion which proceeds outwards to the smaller and lighter distal segments as the total energy increases. In its most ideal form, the principle is succinctly explained as the 'summation of speed principle'. The motion of each succeeding distal segment begins at the onset of maximum speed of its immediate proximal one, proceeding throughout the kinematic chain of linked segments, so that with each succeeding segment a larger end-point speed is generated than the proximal segment (Marshall & Elliott, 2000). Such sequencing patterns have been studied by examining a variety of kinematic and kinetic variables: linear segmental end-point velocities, segmental angular velocities, kinetic energy, joint moments, and so on. However, traditional proximal-to-distal sequencing concepts are inadequate to describe the complexity of the tennis serve or squash forehand (Marshall & Elliott, 2000; Elliott et al., 1995). The cricket bowling action is also a complex motion, so the sequencing information gathered from a study of joint velocities and segment angular velocities has to be interpreted with caution. The main purpose of such an analysis here is to obtain the general order of sequencing in bowling, but not to perform a comprehensive sequencing analysis, which would include such components as relating segment angular velocities to planes of motion, and calculating segment velocity contributions. Such an analysis is beyond the scope of this thesis.

4.4.1 Lower Trunk to Upper Trunk

Segmental angular velocity data of all subjects was collated and studied for patterns in segmental sequencing. Of primary concern were the upper trunk, lower trunk and arm segments, which all play a major role in the development of

ball release speed. The sequencing of these segments was examined from FFC to REL, which is the power phase of bowling as large external forces reaching approximately 4-7 times body weight (BW) are applied via the front foot to the system, and the bowling arm rotates vigorously forward (Bartlett et al., 1996; Elliott et al., 1990). Ensemble averages were taken for each of the four fast bowling groups.

By examining the absolute value of the trunk angular velocities, it was possible to determine the general sequencing order for the motion of the upper and lower trunk. For the fast group, the upper trunk long axis rotation angular became greater than long axis rotation of the lower trunk after 18% PC (Figure 4-13). The upper trunk flexion angular velocity became greater than the lower trunk flexion angular velocity after 61% PC. These *sequence transition points* (i.e. STPs at

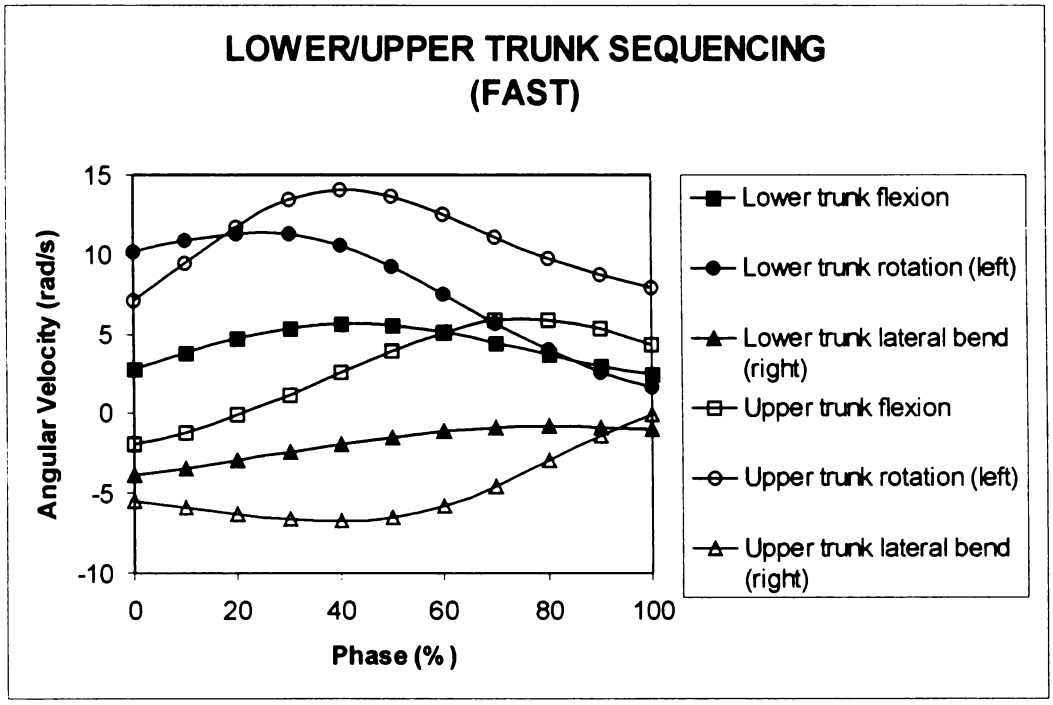

Figure 4-13: Lower and upper trunk 3-D angular velocities from FFC to REL about local reference coordinate systems. Positive is defined for flexion, rotation left, and lateral bend right (Variance ratios (VR): ■ 0.22 □ 0.30 ● 0.16 ○ 0.22 ▲ 0.52 Δ 0.28)

18%PC and 61%PC) occurred when their respective lower trunk angular velocities had reached their maximum angular velocities, as would be the case *if* the summation of speed principle applied. However, for the lateral bend angular

velocity, proximal to distal sequencing was not evident. Instead, from 0-94% PC the upper trunk lateral bend angular velocity (absolute value) was higher than that of the lower trunk. Only after STP at 94% PC did the lower trunk lateral bend angular velocity surpass that of the upper trunk.

The results show that the flexion and long axis rotations of the trunk acted sequentially from proximal to distal. Also, the fact that the upper trunk angular velocities for these motions surpassed those of the lower trunk at approximately the time of maximum angular velocity point to the summation of velocity principle. However, without examining the relative angles between the planes of motion between the lower and upper trunk, and calculating the segment velocity contributions for each of the rotation and flexion motions, it is not possible to establish whether this principle was operational.

The ensemble-averaged curves for the other bowling groups exhibited similar sequencing properties to the fast group in that in terms of absolute angular velocity magnitude, trunk long axis rotation and flexion was proximal to distal, and lateral bending distal to proximal (Appendix K). Also, the STPs for lateral bending occurred late in the power phase. However, there were some differences in the STPs between groups (Table 4-5). The fast group had delayed STPs for upper trunk flexion and long axis rotation compared to the other groups. As the fast group released the ball with higher speed, and the bowling arm is coupled with that of the trunk, if there is also a proximal to distal sequencing relationship between the upper trunk and bowling arm, then a delay in upper trunk STP could indicate that the average upper trunk angular velocity and/or angular acceleration was higher over this period than the other groups. In section 4.4.2, it is shown that there was a proximal to distal sequencing between the upper trunk and bowling arm, giving support to this argument. However, it is also important to realise that though there were some differences between the STPs of the fast group and the other groups, overall there was still much similarity between the groups in terms of phase-variation of the curves and occurrence of the STPs. This tends to indicate that the ball release speed was not just dependent on trunk sequencing characteristics, but also due to differences in segment angular velocity.

Table 4-5: Sequence transition points (STP) for upper trunk motion with respect to the lower trunk from FFC to ball release.

GROUP	Upper Trunk Flexion STP (PC)	Upper Trunk Rotation STP (PC)	Upper Trunk Lateral Bend STP (PC)
Fast	61%	18%	94%
Med-fast	54%	14%	99%
Medium	52%	7%	94%
Slow	53%	15%	92%

The fast group had the highest average upper trunk long axis rotational angular velocity of 14.2 ± 1.0 rad s^{-1}, followed by the medium group 11.6 ± 0.7 rad s^{-1}, then the med-fast group 9.7 ± 0.8 rad s^{-1}, and finally the slow group 6.9 ± 1.1 rad s^{-1}. A one-way ANOVA test found a significant difference between these groups ($p<0.0005$, $F=9.24$). Then a multiple comparison Boneferroni procedure was used to establish which of the groups were significantly different from each other. For a confidence interval of 95% (i.e. $\alpha=0.05$), there were significant differences in upper trunk rotational angular velocity between the fast and med-fast groups, fast and slow groups, and medium and slow groups (Appendix J, Figure J-1). This shows that although there were similarities in the general segmental sequencing for the trunk among the groups, there were significant differences in the magnitude of angular velocities, which could account for the differences in ball release speed. The slightly relatively delayed sequencing of the fast group for trunk long axis rotation and flexion was possible because of the higher angular velocities of these motions. However, it could also be hypothesised that this delay in sequencing influenced the generation of this higher angular velocity.

4.4.2 Upper Trunk to Upper Bowling Arm

Following the order of proximal to distal sequencing, the next coupling occurs between the upper trunk and upper arm of the bowling arm (upper bowling arm). The motion of the bowling arm is often referred to as circumduction, and involves

a complex combination of adduction, flexion and long axis rotation. These movements were defined about the local body-fixed coordinate system of the upper arm: positive rotation about the *X*-axis was horizontal adduction or flexion, positive rotation about the *Y*-axis was external rotation, and positive rotation about the *Z*-axis was vertical adduction (Figure 4-14).

Figure 4-14: Defining the motion of the upper arm as (i) positive rotation about the *X*-axis as horizontal adduction or flexion, (ii) positive rotation about *Y*-axis as external rotation, and (iii) positive rotation about the *Z*-axis as vertical adduction. Note that the *Z*-axis runs from the posterior to anterior direction and points out of the page.

For the fast bowling group, the horizontal adduction of the upper arm and the long axis rotation of the upper trunk were the primary movements, and generally had the highest angular velocities throughout the phase. The angular velocity of the upper arm horizontal adduction was almost equal to that of the upper trunk long axis rotation until approximately 40% PC. Then the upper arm horizontal adduction angular velocity became increasingly greater than that of the upper trunk long axis rotation (Fig. 4-15). The other trunk motions, lateral bending and flexion, had relatively low angular velocities. Also, the horizontal adduction angular velocity of the bowling arm was much higher than the other motions of the bowling arm for most of the phase. Therefore, from purely a kinematic

perspective, the two most important motions are upper trunk long axis rotation and upper arm horizontal adduction.

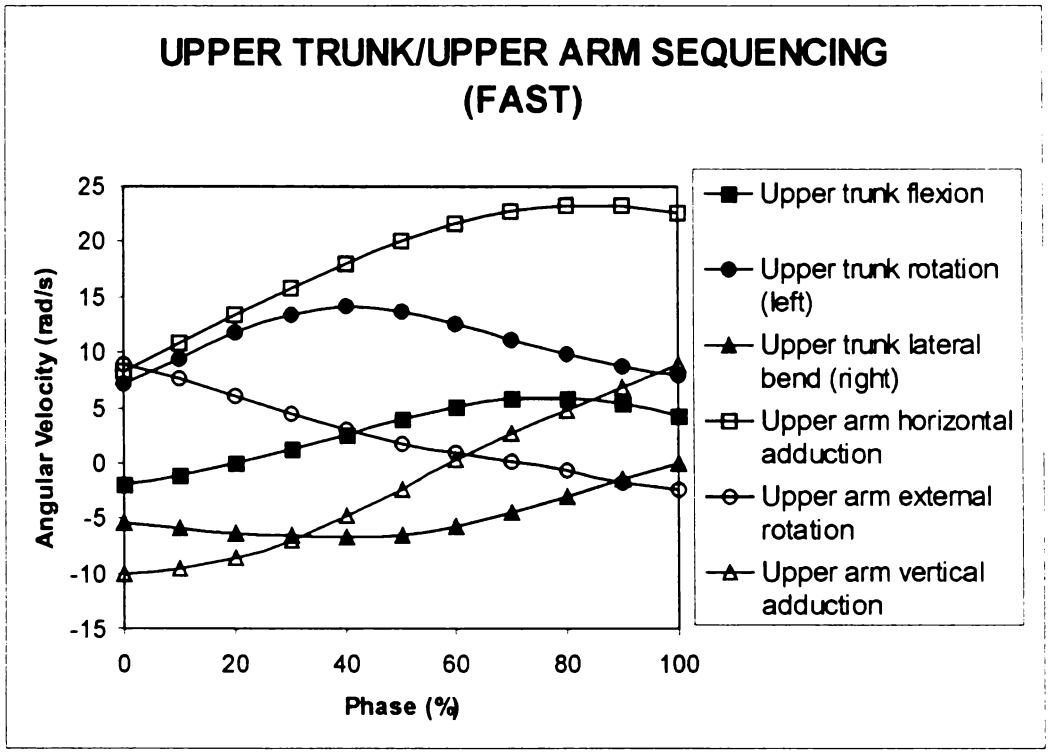

Figure 4-15: Upper arm and upper trunk angular velocities (ensemble averages) from FFC to REL for the fast group show segmental sequencing between upper trunk rotation and horizontal adduction of the upper bowling arm for the fast group. Positive is defined for flexion, rotation left, lateral bend right, horizontal adduction, vertical adduction, and external rotation. (VR: ■ 0.30 ● 0.22 ▲ 0.28 □ 0.20 ○ 0.89 Δ 0.82)

Though it is not possible to calculate the velocity contribution of upper trunk long axis rotation to upper arm horizontal adduction without considering the relative orientation of their respective local angular velocity vectors, the fact that their respective angular velocities are much higher than the other motions, and are almost exactly equal over the early power phase suggests that these two motions are coupled. Examination of the ensemble average angular velocity curves for the slower bowling groups shows that there was a larger average difference between the angular velocity of upper trunk long axis rotation and that of upper arm horizontal adduction over the first 20% PC (Figure 4-16). For instance, this angular velocity difference for the fast group was only 1.4 rad s^{-1}. However, for the other groups there were much larger differences: (med-fast, 4.0 rad s^{-1}; medium, 5.8 rad s^{-1}; slow, 4.5 rad s^{-1}). These data suggest that the two fastest

bowling groups, but in particular the fast group, kinematically coupled the upper trunk long axis rotation with the bowling upper arm horizontal adduction during the early power phase. For this to be an effective contributor of speed via proximal to distal sequencing, the planes of these two motions would have to be reasonably coincident.

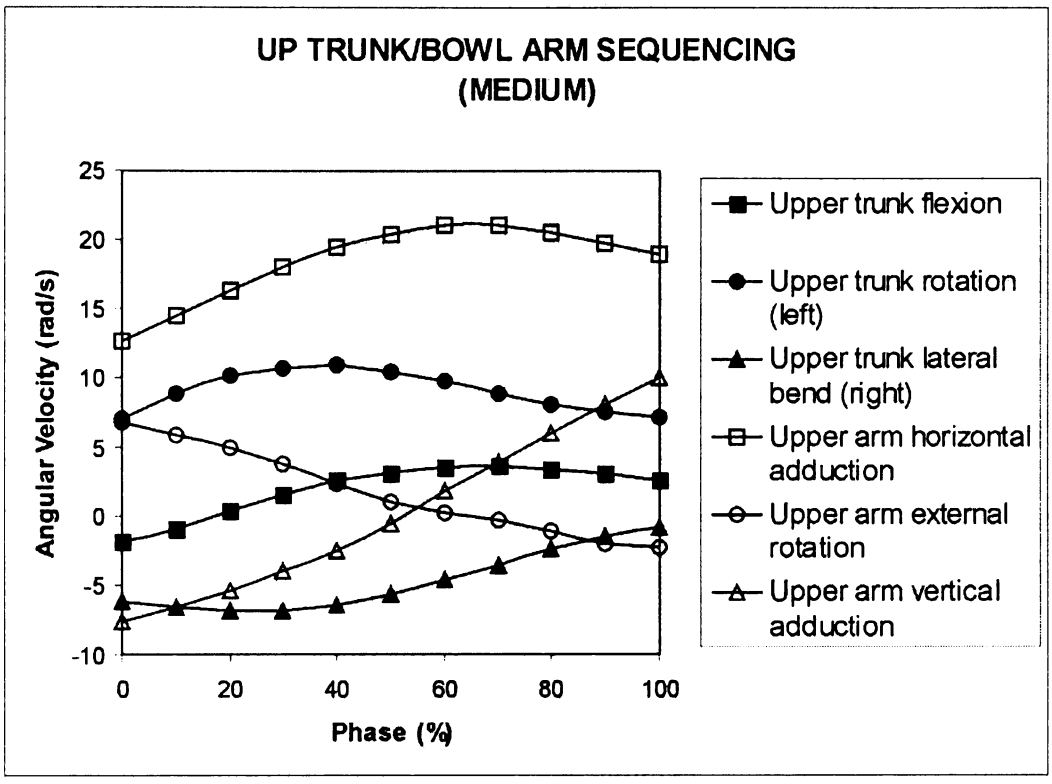

Figure 4-16: Upper arm and upper trunk angular velocities (ensemble averages) from FFC to REL show segmental sequencing between upper trunk rotation and horizontal adduction of the upper bowling arm for the medium group. Positive is defined for flexion, rotation left, lateral bend right, horizontal adduction, vertical adduction, and external rotation. (VR: ■ 0.30 ● 0.22 ▲ 0.28 □ 0.20 ○ 0.89 Δ 0.82)

In summary, the ensemble average curves of upper trunk and upper bowling arm angular velocities reveal differences between the bowling groups. It is reasonable to suggest that there is some coupling of motion between the upper trunk and bowling arm, otherwise a bowler should still be able to safely obtain high ball release speeds by merely rotating the bowling arm about the glenohumeral joint without any motion of the upper trunk. Long axis rotation of the upper trunk and bowling upper arm horizontal adduction had the highest angular velocities, and differences between them were lowest for the fast group, and much higher for the

slower groups. Contrary to the notion that the head stays still and upright during delivery, some of the most successful side-on fast bowlers, such as *Dennis Lillee*, dropped their heads horizontally to the left to allow the horizontal adduction of the bowling arm with respect to the plane of motion of the upper trunk (Figure 4-17). Further studies looking at the relative planes of these motions could further establish how these motions are coupled to produce speed, and whether there is a correlation of ball speed with the relative orientation of these planes.

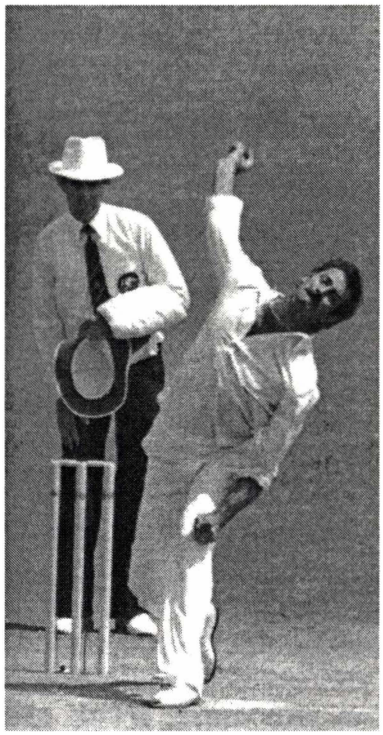

Figure 4-17: Even the great Dennis Lillee obliquely tilts the upper trunk to the left so that the head is almost horizontal, giving room for the horizontal adduction of the bowling arm during the power phase. [From Lewis, T. 1994. *MCC Masterclass. The New MCC Coaching Book.* Weidenfeld and Nicholson, London]

4.4.3 Upper Bowling Arm to Forearm

The next coupling has traditionally been of little interest to cricket researchers, as the bowling upper arm and forearm have been assumed to act as a single rigid lever. To test this assertion, the forearm segment angular velocities were compared to those of the upper arm. The motion of the forearm was defined in terms of the local body-fixed coordinate system at the distal end of the humerus so that (i) a positive rotation of the forearm segment about the X-axis, which

corresponded to the flexion axis, was called a *flexion axis rotation*, (ii) a positive rotation about the *Y*-axis corresponded to external rotation, and (iii) a positive rotation about the *Z*-axis was called a *adduction axis rotation* (Figure 4-18). This means that the forearm angular velocity about the forearm flexion axis equals the component of upper arm angular velocity about the forearm flexion axis, plus the elbow flexion angular velocity. A similar case holds true for the forearm segment angular velocity about the *Z*-axis, but that now the elbow angular velocity is either due to adduction or abduction, which is negligible except in clinically abnormal situations. The forearm segment angular velocity about the *Y*-axis equals the component of upper arm angular velocity about this axis, plus the forearm long axis rotation angular velocity. In general, if there is a difference between the forearm segment angular velocity and the component of upper arm angular velocity about a particular forearm axis of rotation, then there is independent forearm rotation. Otherwise, there is no relative motion between the upper arm and forearm.

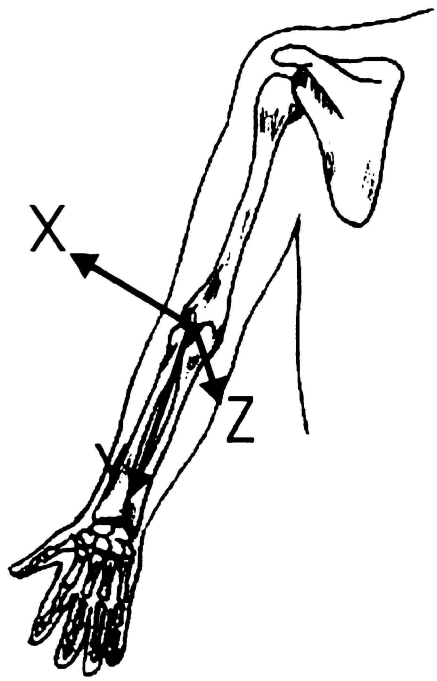

Figure 4-18: The motion of the forearm segment was defined as (i) positive rotation about the *X*-axis or flexion axis (flexion axis rotation), (ii) positive rotation about *Y*-axis (external rotation), and (iii) positive rotation about the *Z*-axis (adduction axis rotation). Note that the *Z*-axis runs from the posterior to anterior direction and points out of the page.

The highest angular velocities of the bowling arm were generated by upper arm horizontal adduction, and forearm flexion axis rotation. For the fast bowling group, the forearm flexion axis rotation angular velocity only equalled that of the upper arm horizontal adduction at 87% PC when the upper arm was horizontally adducting at its maximum angular velocity (Figure 4-19). After this STP, the forearm flexion axis rotation surpassed the horizontal adduction angular velocity, and reached a maximum value at ball release. There were differences in the sequential segmental timing between bowling groups. For the medium-fast and medium groups, the STPs of forearm flexion axis rotation occurred at 78% PC and 79% PC, respectively. The slow group achieved the STP at 70% PC. In general, the faster bowlers tended to increase the delay in forearm flexion axis rotation.

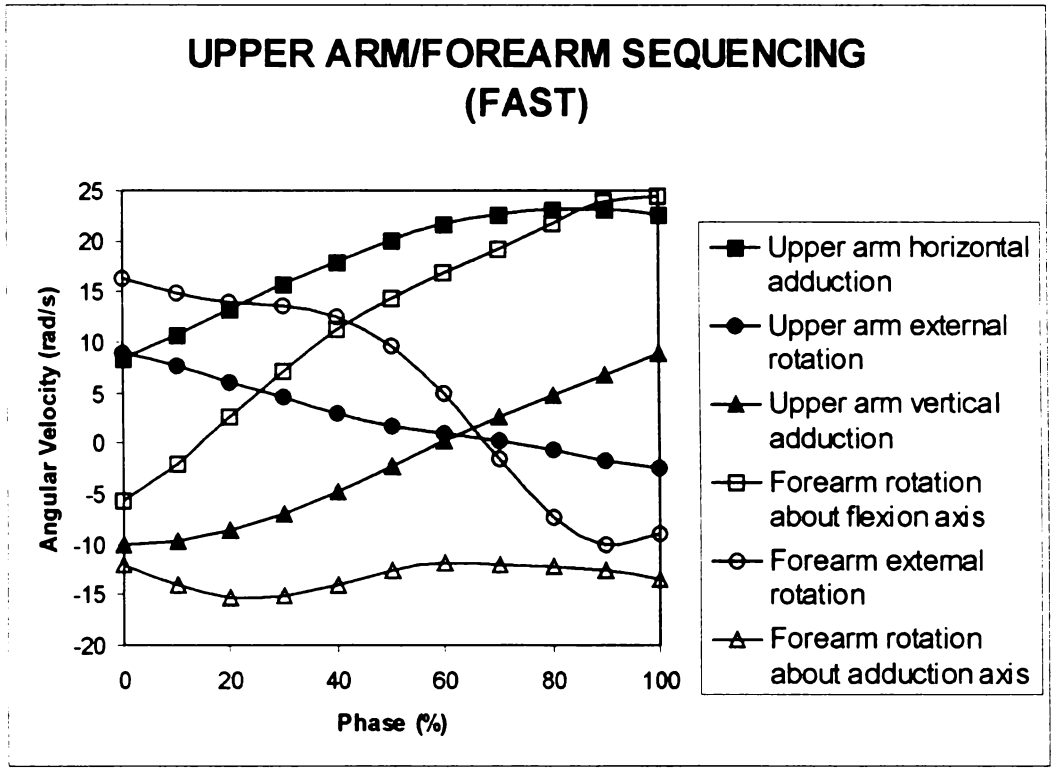

Figure 4-19: Angular velocity sequencing of upper arm to forearm (bowling arm) from FFC to REL. Positive is defined for horizontal adduction, vertical adduction, external rotation, forearm flexion rotation, and forearm adduction rotation. (VR: ■ 0.20 ● 0.89 ▲ 0.82 □ 0.42 ○ 0.56 Δ 0.45)

There were also differences in the timing of the STPs and upper arm horizontal adduction angular velocity. The STP for forearm flexion axis rotation for the fast group occurred exactly when the upper arm horizontal adduction angular velocity

had reached its maximum angular velocity (23.2 rad s^{-1}). However, the other groups achieved this only after the upper arm horizontal adduction angular velocity had passed its maximum value. For instance, the medium-fast group's STP for forearm flexion axis rotation occurred at 8% PC after upper arm adduction angular velocity had reached its maximum value of 22.0 rad s^{-1}. Similarly, the corresponding STPs for the medium and slow groups occurred 13% PC and 11% PC, respectively after maximum upper arm adduction angular velocity had been reached (medium, 21.2 rad s^{-1}; slow, 20.0 rad s^{-1}). The forearm increasingly internally rotates as the bowling arm moves towards release making the axis of upper arm horizontal adduction and the axis of forearm flexion axis rotation increasingly parallel. In such a case, it is plausible that the summation of velocity principle could apply in this instance, and was one factor utilised by the fast group to generate a higher ball release speed. Also, note that maximum upper arm horizontal angular velocity increased with bowling group speed.

Maximum forearm internal rotation also increased with the speed of bowling group. For the fast group, the maximum internal forearm rotation was 10.2 rad s^{-1}, which occurred at 92% PC. This was very much smaller for the medium-fast group generating 4.1 rad s^{-1} at 93% PC, which was followed by the medium group registering a value of 3.9 rad s^{-1} at 88% PC. Finally, the slow group had by far the smallest forearm internal angular velocity of 1.6 rad s^{-1} at 85% PC. Also, the two fastest bowling groups had a delayed occurrence of maximum angular velocity compared to the two slower groups.

Marshall and Ferdinands (2002) suggested that bowlers, who have a flexed elbow during the latter stages of delivery, carry the ball in the hand at some distance from the upper arm internal rotation axis, providing the opportunity to take advantage of this segmental rotation to contribute to ball speed (Figure 4-20). In bowling with a straight arm, the velocity at the wrist results from the angular velocity of arm (ω_A) times the shoulder distance (r_A). For a flexed arm, there is an additional contribution to wrist velocity from upper arm internal angular velocity (ω_{IR}) times the internal rotation axis-wrist distance (d). Their calculations

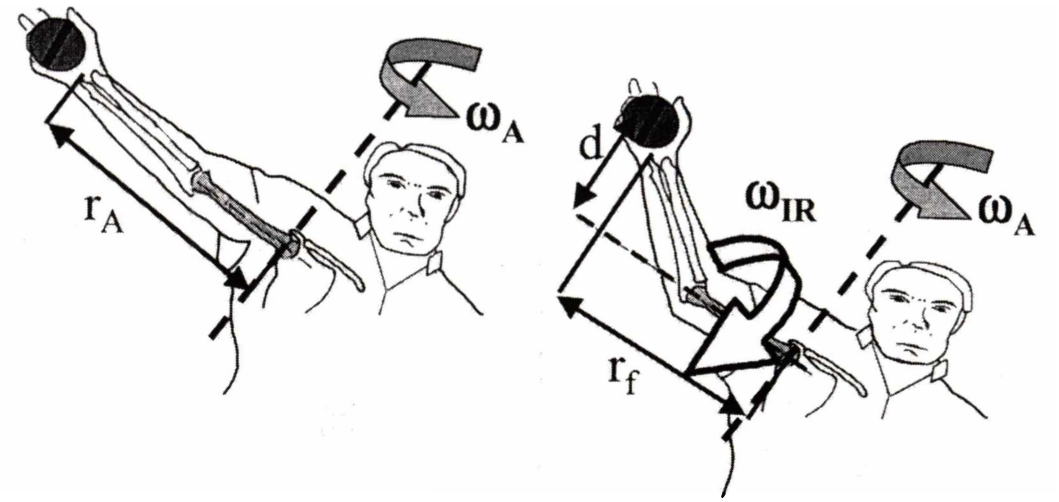

Figure 4-20: (Left) In bowling with a straight arm, the velocity at the wrist results from the angular velocity of arm (ω_A) times the shoulder distance (r_A). (Right) For a flexed arm, there is an additional contribution to wrist velocity from upper arm internal angular velocity (ω_{IR}) times the internal rotation axis-wrist distance (d). [From Marshall & Ferdinands, 2002]

also indicate that the generations of wrist speed via upper arm internal rotation significantly outweighs any loss of wrist speed due to a reduction in effective bowling arm length (i.e. $\mathbf{r}_F < \mathbf{r}_A$). This means that bowlers such as *Shoaib Akhtar* through his elbow deformity may gain considerable mechanical advantage in the generation of ball speed (Figure 4-21).

The differences between the bowling groups in forearm flexion axis rotation and forearm internal rotation show that the treatment of the upper arm and forearm as a single rigid body is only an approximation. The relative motion between the forearm and upper arm can be important, and this suggests that the faster bowlers may utilise small variations in elbow joint angle during the power phase to their best advantage in the development of ball speed.

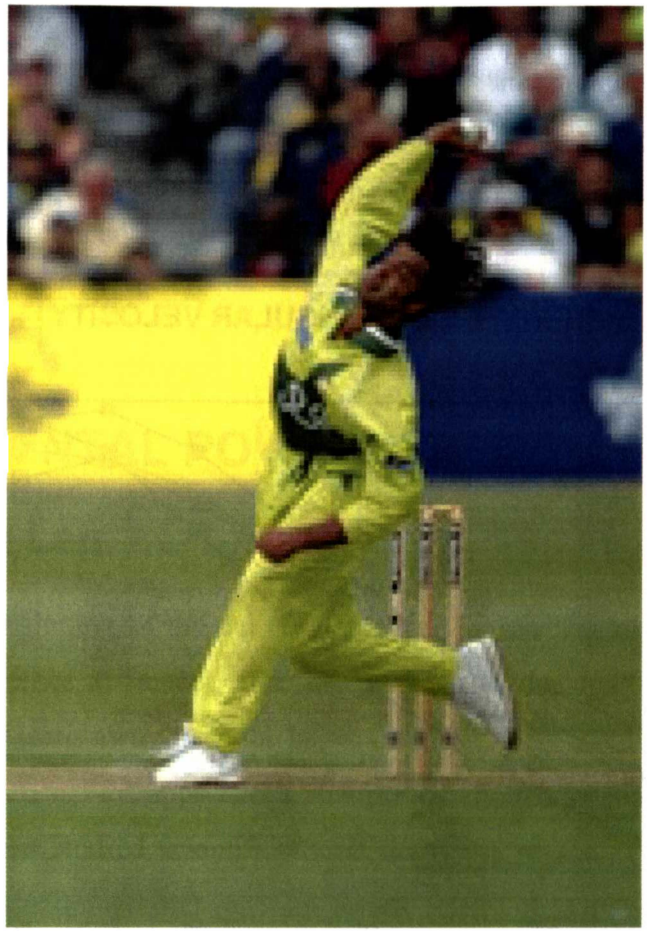

Figure 4-21: Shoaib Akhtar of Pakistan is the fastest recorded bowler in the history of the game. He has an abnormal elbow that initially hyperextends with a carry angle, and then flexes before delivery enabling him from a mechanical perspective to use internal rotation to generate high ball speed.

4.4.4 Bowling Forearm to Hand

The most significant motion of the hand in fast bowling is flexion (Figure 4-22). During the power phase, hand flexion angular velocity was lower than forearm flexion axis rotation initially, but then, surpassing it at a STP, further increased in value before again becoming lower than forearm flexion axis rotation just before ball release. The STP for hand flexion angular velocity of the fast group was 58% PC. The hand flexion angular velocity then decreased 19% below that of forearm flexion axis rotation at REL. For the medium-fast group, the hand flexion angular velocity reached the STP at 44% PC, and then decreased 38.7% below that of forearm flexion axis rotation at REL. The medium group was similar to the med-fast group with corresponding values of 47% and 41.5%. However, the corresponding values for the slow group were 46% and 110%, the latter value

representing a very large percentage drop in hand flexion angular velocity below that of forearm flexion axis rotation at ball release. The magnitude of maximum hand flexion angular velocity was also lowest for the two slowest groups: (fast, 28.7 rad s^{-1}; med-fast, 29.1 rad s^{-1}; medium, 25.6 rad s^{-1}; slow, 24.9 rad s^{-1}).

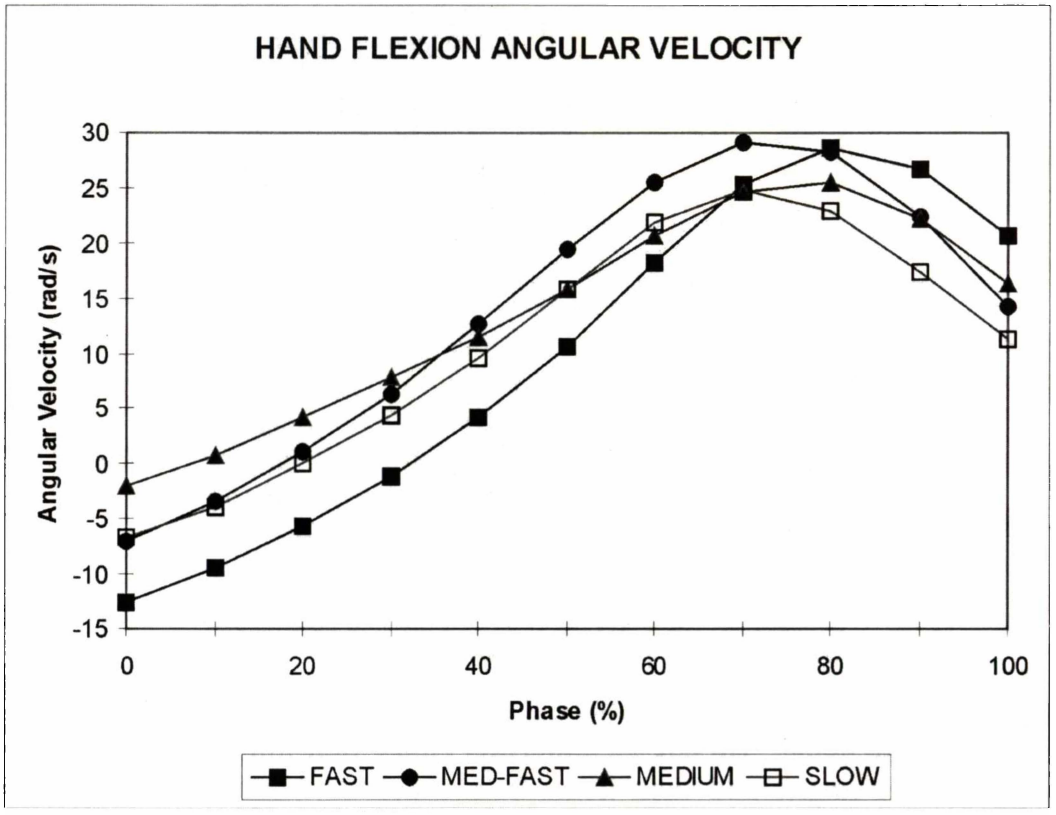

Figure 4-22: Ensemble average of hand flexion angular velocity curves from FFC to REL for all bowling groups (VR: fast, 0.31; med-fast, 0.33; medium, 0.42; slow, 0.31)

There were marked differences between the groups in forearm to hand sequencing, and in the reduction of hand flexion angular velocity at ball release. Also, the medium and slow groups had the slowest maximum hand flexion angular velocities of the bowling groups. The fast group delayed the hand flexion longer than the other groups, which may have contributed to this group having the smallest decrease in hand flexion angular velocity at ball release. This finding tends to support the study of Blanksby et al. (1976a), which found that the faster bowlers tended to delay the flexing at the wrist until the last moment in order to effectively summate the previously developed forces. The other bowling groups had hand flexion angular velocity STPs 11-14% earlier than the fast group, and had a greater reduction in hand flexion angular velocity at ball release. However,

with regards to this reduction in angular velocity, there could be some inaccuracy in the calculated values as ball release was approached, because the hand segment was defined from the wrist joint centre to the centre of the cricket ball itself. However, it could still be significant that the greatest difference occurred for the slow group, which reduced its hand flexion angular velocity more than twice that of the other groups at REL.

4.5 SEGMENTAL POWERS (BFC TO FFC)

4.5.1 Rear Leg

BFC marks the beginning of the delivery stride. The rear leg has to absorb the ground reaction forces at impact, and then respond to the dual motions of the trunk as it initially leans away from the batsman during early BFC, and then bends towards the batsman as FFC approaches. Unfortunately, the mechanics of rear leg action has not been studied scientifically. Perhaps the reason is that back foot contact involves smaller ground reaction forces (GRF) than those at front foot contact, and therefore its role is considered to be of less importance (Bartlett et al., 1996).

Shortly after landing, the rear thigh exerted a strong flexion torque that peaked near the time of maximum back foot GRF (Fig. 4-23). This flexion torque was maintained throughout the phase, but diminished progressively as FFC was approached, and the pressure of the rear foot on the ground was lessened. The VRs for the data within each group were high making it difficult to establish differences between the groups. However, it is worth noting that during the first 60% PC, when the rear foot was still in good contact with the ground, the slow group had much a lower thigh flexion torque than the other groups. The corresponding thigh power for all groups was negative, which indicated that the flexion torque acted to control the rate of thigh extension. The mean thigh flexion-extension power increased negatively with the speed of bowling group: fast, -203 W; med-fast, -176 W; medium, -138 W; slow, -102 W.

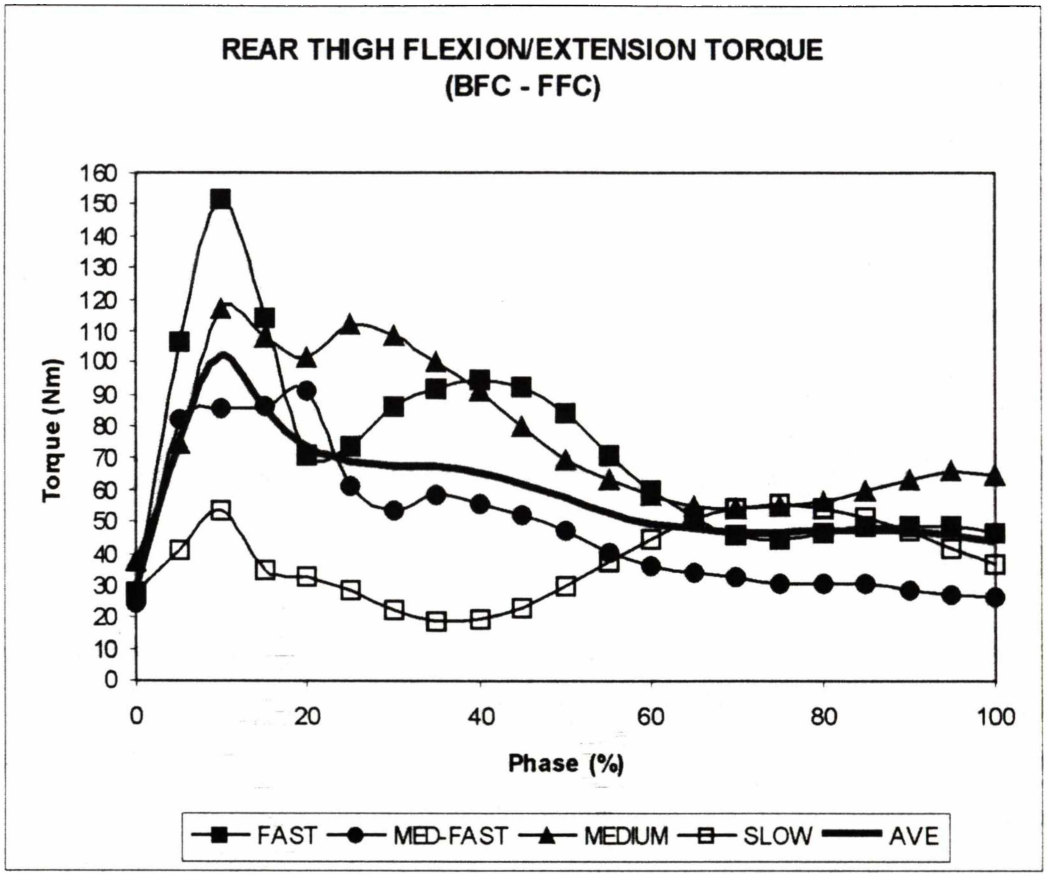

Figure 4-23: Ensemble averages of rear thigh flexion-extension from for all bowling groups. Solid line is the mean of all the ensemble average curves, which is equivalent to mean of the total sample. Positive is defined for flexion.

While the rear thigh was in controlled extension, it was also exerting strong abduction torques, which exhibited a similar phase variation to that of the flexion torques, peaking early in the phase when ground reaction forces were high, and remaining positive, and then gradually diminishing as FFC approached. Expressed as a percentage increase, the mean abduction torques were higher than the mean flexion torques: 72% (fast), 48 % (med-fast), 77 % (medium), 38 % (slow). The rear thigh abduction torque controlled the rate of rear thigh adduction, as the front leg and upper body moved forward during the delivery stride. Evidence of this is shown in the corresponding ensemble average curves of the rear thigh power, which was negative throughout almost the full phase for all groups (Fig. 4-24). There was a good separation between the groups. The medium group had the highest negative power, but otherwise the negative power

increased with the speed of the bowling group. As in the case for thigh flexion power, the slow group registered the lowest negative power.

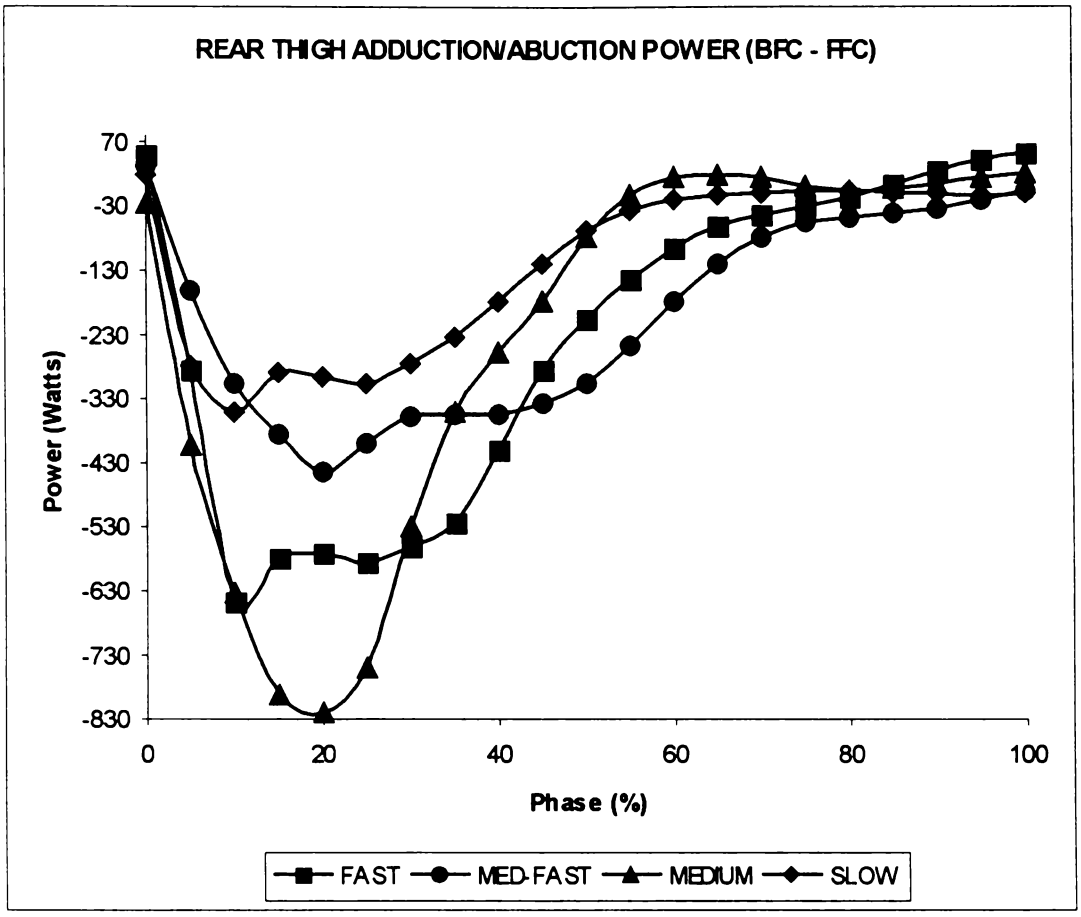

Figure 4-24: Ensemble averages of rear thigh adduction-abduction power for all bowling groups. There was good separation between the bowling groups. VR: 0.58 (fast), 0.65 (med-fast), 0.25 (medium), 0.62 (slow).

Of the thigh movements, abduction was more prominent that extension. There was significantly more variance in the thigh extension curves than those of abduction. It may be that the amount of thigh extension or adduction depends to some extent on the action type and rear foot orientation of the bowler. A bowler who plants the foot more or less parallel to the bowling crease may produce more rear thigh abduction than a front-on bowler, who places the feet more in the direction of the target. The opposite could hold true for thigh extension. It must be noted that the rear thigh generated negative extension and adduction powers during BFC, because the whole body is moving forwards due to the initial momentum of the run-up while the back foot remains in contact with the ground. Therefore, it would make good sense for fast bowlers to progressively increase the

capacity of the rear hip to eccentrically extend and adduct, to not only improve performance, but to also reduce the likelihood of groin injuries (Figure 4-26).

In response to BFC, the rear shank had a flexion torque about the knee, which produced a positive power, reaching a peak near 20% PC when ground reaction forces were high, and then reduced progressively as FFC approached (Fig. 4-25). Though in the last 30-40% PC prior to FFC, the power became slightly negative, shank flexion was essentially an active motion. Flexion of the shank was expected to play the role of shock absorption, in particular to reduce the dynamic load on the knee joint. It was expected that in response to the rear knee bending upon ground contact, a shank extension torque would control this rate of flexion. However, it appears that a shank flexion torque in combination with a strong thigh flexion torque served to modulate the response of the rear leg to the braking back foot ground reaction forces.

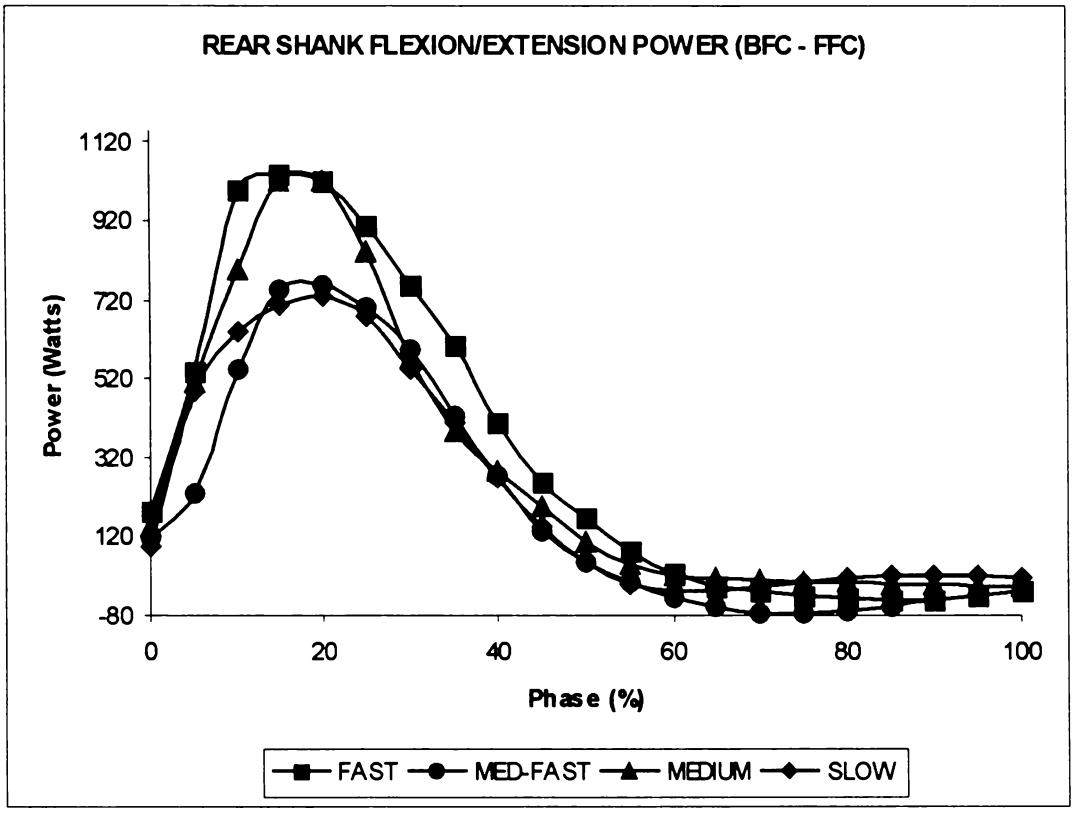

Figure 4-25: Ensemble averages of rear shank flexion-extension power for all bowling groups. VR: 0.54 (fast), 0.78 (med-fast), 0.35 (medium), 0.53 (slow).

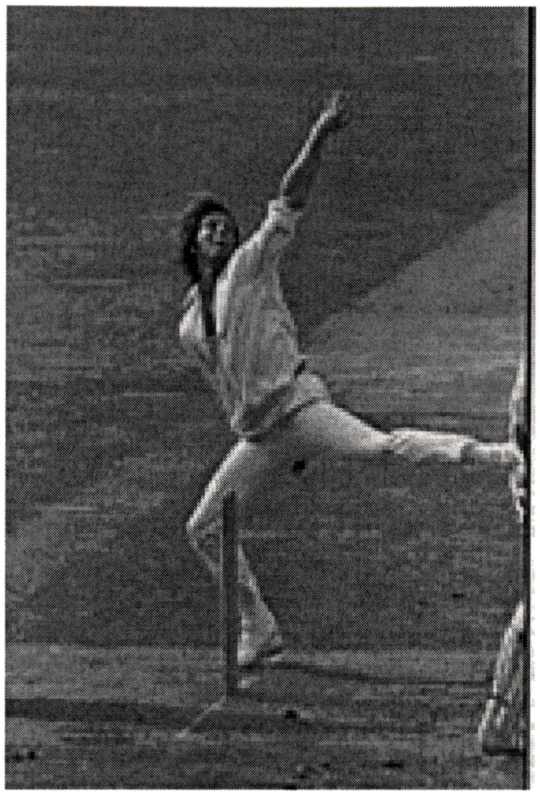

Figure 4-26: Australia's Jeff Thomson, probably the fastest bowler in the history of the game, showing eccentric extension and adduction of the rear hip during BFC.

In the future, rear leg mechanics should be given more prominence than in the past. The fact that ground reaction forces on the back foot are much lower than those on the front foot is not a good reason to relegate the importance of the rear leg in bowling. The action of the rear leg is what connects the run-up to the delivery phase, and the differences in the mechanics of rear leg action between bowling groups may cause different effects on the mechanics on the upper body.

4.5.2 Lower Trunk

Ensemble averages were taken of the joint force power flowing through the proximal end of the lower trunk, which is approximately midway between the hip joint centres. The joint force power was calculated in the direction of the local *x*-axis, which runs from right hip to left hip. This direction was of interest because the movement of the hip line describes the true horizontal linear motion of the lower trunk, even during rotation.

A comparison of the ensemble averages of the bowling groups shows that there were some common features in joint force power flow in the direction of the hips during delivery stride (Fig. 4-27). Initially, at BFC the power was negative that within 5% PC became positive, and generally stayed positive until approximately 60% PC before it once again became negative, remaining so until FFC. This negative power during the latter part of the cycle coincided with the time that the bowler's lower body was preparing for FFC, when flexion, long axis rotation, and lateral bending angular velocity of the lower trunk starts to increase. Though there was considerable variability among the med-fast, medium and slow groups, it could be still important that the fast group, which had the lowest VR of 0.104, had the most negative power after 60% PC. The linear velocity of the

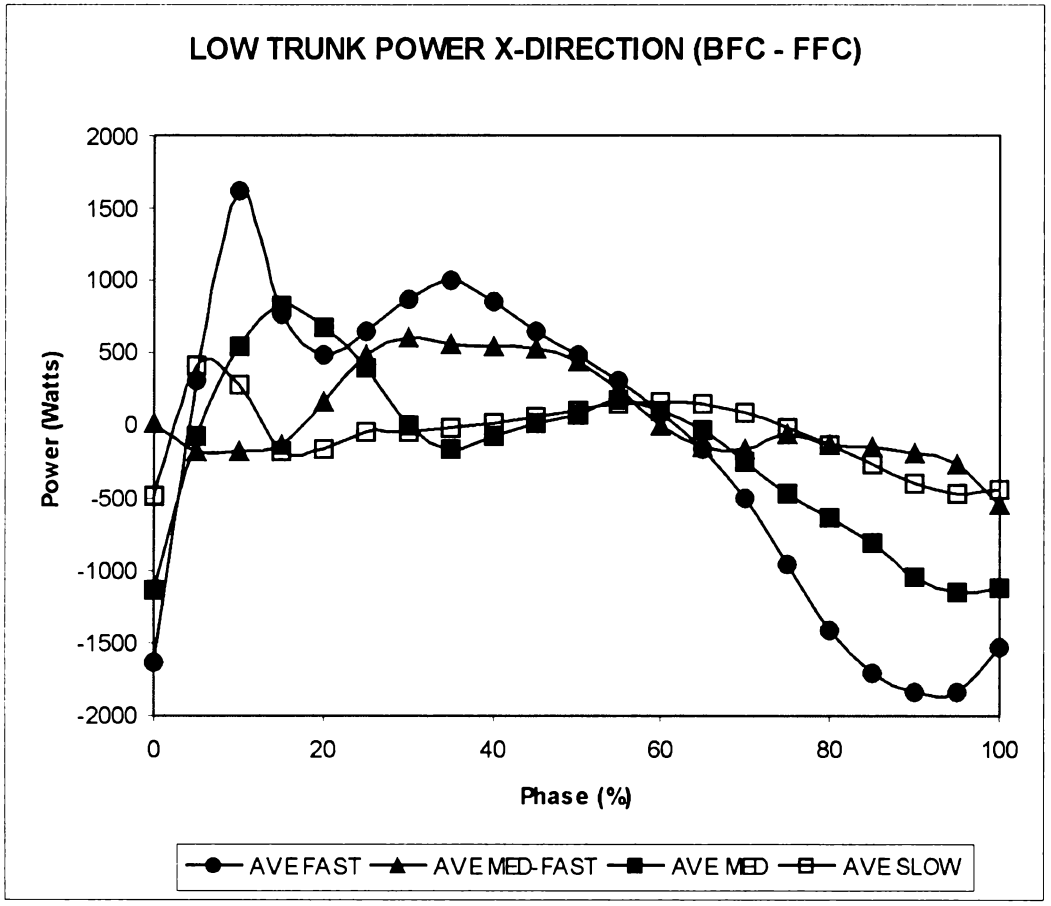

Figure 4-27: Ensemble average curves of lower trunk power in local x-direction. (VR: fast, 0.104; med-fast, 1.00; med, 0.611; slow, 1.00)

distal end of the lower trunk was positive throughout the phase, which meant that the force acting on the distal end became increasingly negative as FFC was

approached. This "pulling back" force would tend to increase the flexion and lateral bend angular velocity to the left of the lower trunk, which is an important component of fast bowling (Bartlett et al., 1996).

The general notion is that at BFC the trunk leans away from the direction of motion, and as the action proceeds towards FFC the non-bowling arm extends, aiding the trunk to 'bend forward' (Mason et al., 1989). However, the segment powers and torques indicate that the actuation of these movements was more complex (Figure 4-28). For the fast group, the data show that the lower trunk flexion torque was negative from 0 - 65% PC with an average value over the full phase of -37.1 ± 12.6 Nm. The corresponding power was positive from 16-95% PC with a maximum value of 141 W at 49% PC. A positive power and a negative torque indicate that there was a negative angular velocity (angular velocity = power/torque). Therefore, the lower trunk had a small extension angular velocity (mean, -0.31 ± 0.61 rad s^{-1}) from 16-65% PC. From 65-95% PC, both the torque and power became slightly positive, generating a small active flexion angular velocity. Then from 95-100% PC, just prior to FFC, both the torque and power became negative, generating a controlled flexion angular velocity. Therefore, lower trunk motion of the fast group consisted of three phases. There was an active extension phase, followed by an active flexion phase and then a controlled flexion phase, as shown by the multiple changes in power. Similar changes in power about the lower trunk flexion axis were observed for the other bowling groups. However, the slow group had slightly lower values of lower trunk extension from 25-75% PC, and a higher flexion angular velocity from 75-100% PC than the other groups, yielding an overall positive average angular velocity (0.15 ± 0.84 rad s^{-1}). This was probably related to differences in flexion torque. The slow group had the smallest mean negative torque (-15.7 ± 6.4 Nm), which was significantly smaller than the other groups ($p < 0.02$).

The other important bending motion performed by bowlers is lateral bending. For the fast group the lateral bending power was positive for the first 80% PC (max, 203 W), and then negative for the remainding phase (min, -507 W). Correspondingly, during these periods, the lateral bending torque was first negative and then positive. Therefore, the angular velocity was negative for the

entire period from BFC to FFC (mean, –2.2 ± 0.5 rad s^{-1}; min, -4.4 rad s^{-1}). These changes in power preserved the lateral bending motion to the left, and were also observed in the other bowling groups.

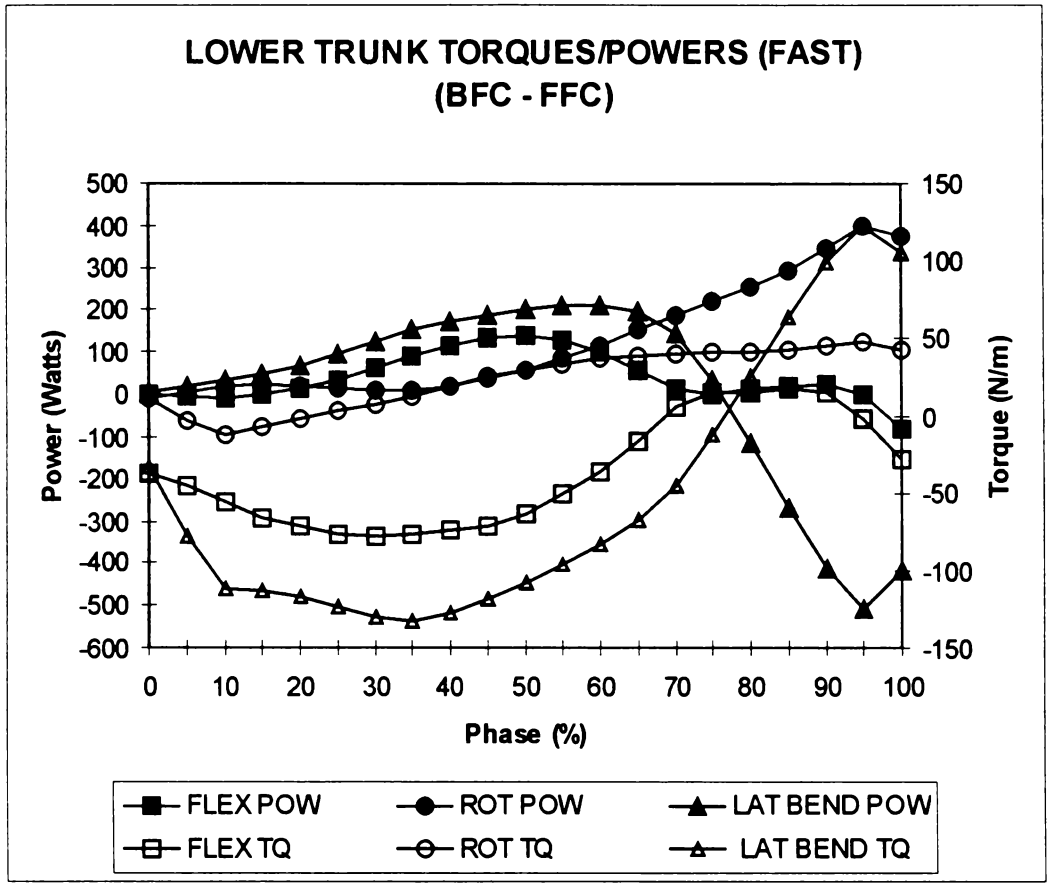

Figure 4-28: Ensemble averages of lower trunk powers and torques due to rotation. Positive torque is defined for flexion (VR = 0.78), rotation to the left (VR = 0.63), and lateral bend to the right (VR =0.14). Variance ratios for flexion, rotation and lateral bending powers were 0.86, 0.34 and 0.25, respectively.

Differences in the groups were apparent in the amount of lateral bending power to the left over the last 20% PC: fast (max, - 506 W; ave, -344 ± 55 W); med-fast (max, -452 W; ave, -305 ± 55 W); medium (max, -340; ave, -219 ± 42 W); slow (-205; ave, -102 ± 33 W). The average lateral bending power increased with each subsequently faster bowling group over this period. An ANOVA single factor test shows that there was almost significance between the groups ($p = 0.055$, $F = 3.138$, $F_{crit} = 3.238$). Also, there was a significant difference between the slow group and the two fastest groups ($p < 0.050$). This data showed that the faster

bowlers tended to more strongly laterally bend the lower trunk to the left than the slower ones as FFC was approached.

Apart from the bending-type motions in bowling, there is also lower trunk long axis rotation. Generally, apart from the short period from 20-45% PC, the torques and powers were both positive throughout the phase. In fact, this was the most active of the three trunk motions. The lower trunk generated large positive rotation powers that increased throughout the phase: fast, (mean, 126 ± 49 W; max, 401 W); med-fast, (mean, 64 ± 51 W; max, 302 W); medium, (mean, 73 ± 33 W; max, 276 W); slow, (mean, 46 ± 31 W; max, 208 W). There was also significant difference in the mean powers between the fast and slow groups ($p = 0.0313$, $F = 4.981$, $F_{crit} = 4.085$). The fast group also achieved the highest maximum rotation angular velocity of 9.0 rad s^{-1} at FFC. These results indicate that the faster bowlers were likely to rotate more powerfully to the left (away from the batter) than the slower ones.

4.5.3 Upper Trunk

In previous studies of bowling, the trunk was modelled as a single rigid structure (Mason et al., 1989; Ferdinands, 1999). However, in certain phases, the mechanical action of the upper trunk was considerably different from that of the lower trunk. The most striking difference occurred during long axis rotation (Figure 4-29). For the fast group, upper trunk long axis rotation power was small for the first half of the phase, then negative for a short period before it increased positively at a rapid rate from 75% PC onwards, generating a maximum value of 740 W at FFC. In contrast, the long axis rotation power of the lower trunk, gradually increased positively throughout the phase, and had a value of only 377 W at FFC.

The upper trunk long axis rotation torque for the fast group was negative from 0-45% PC, and then positive for the next 30% PC, whereas for the same periods the corresponding power was positive and negative, respectively. Therefore, from 0-75% PC the upper trunk had a negative angular velocity (mean, -2.4 ± 0.4 rad s^{-1}), i.e., the upper trunk was counter-rotating as in a mixed action. The

change in power directions indicate that initially the upper trunk long axis rotation torque was actively producing counter-rotation, before taking approximately 30% PC to reverse it. After this period of counter-rotation, the upper trunk rotated rapidly to the left reaching a maximum angular velocity of 7.4 rad s^{-1} at FFC.

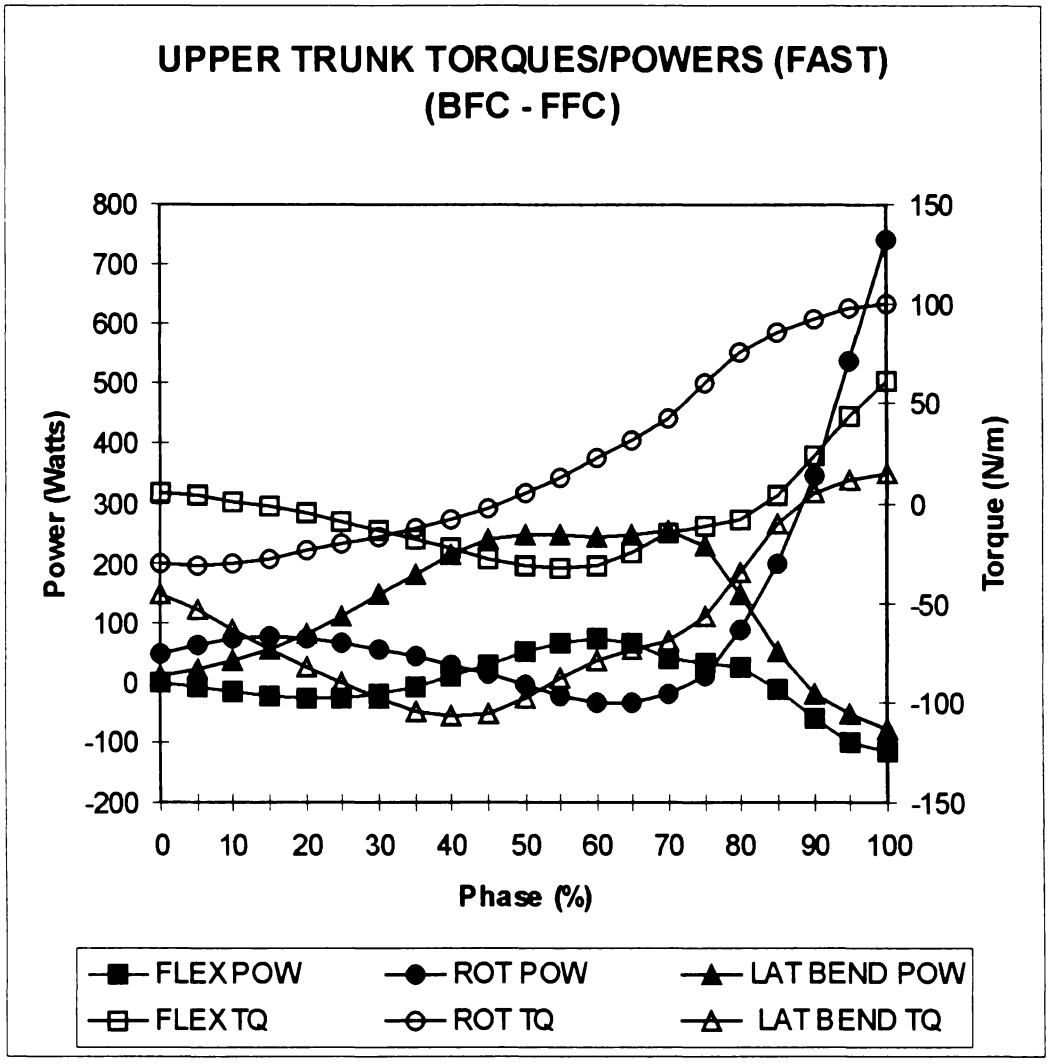

Figure 4-29: Ensemble averages of upper trunk powers (fast group) and torques due to long axis rotation. Positive torque is defined for flexion (VR = 0.73), rotation to the left (VR = 0.13), and lateral bend to the right (VR =0.36). VRs for flexion, rotation and lateral bending powers were 0.62, 0.37 and 0.44, respectively.

The long axis rotation powers and torques for the other groups followed much the same pattern (Fig. 4-30). There was a period of counter-rotation followed by rapid rotation. All the groups completed their counter-rotation at approximately 75% PC, after which the rate of long axis rotation power increased with the speed of bowling group: (fast, 29.1 W/%PC; med-fast, 23.0 W/%PC; medium, 17.5

W/%PC; slow, 13.6 W/%PC). This rate of change as the bowler approached FFC was the most pronounced differentiating feature of the power curves, and caused large differences in the maximum powers per group at FFC: (fast, 740 W; med-fast, 583 W; medium, 442 W; slow, 352 W). The faster bowlers actively produced more upper trunk long axis rotation from BFC to FFC. Also, the clear differentiation between rotation curves for the different speed groups suggests that rotation of the upper trunk is an important variable in the mechanics of ball speed generation.

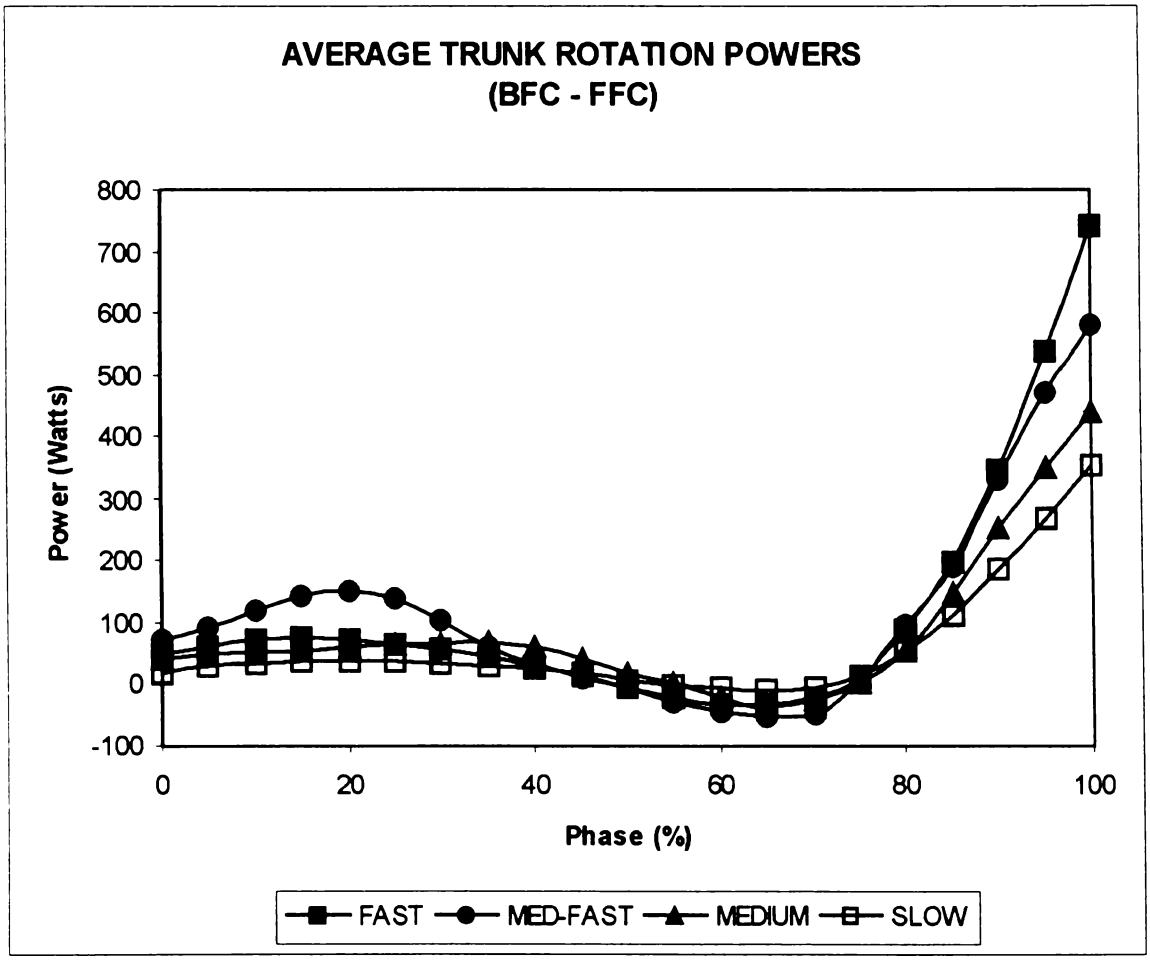

Figure 4-30: Comparison of upper trunk rotation power curves for each of the bowling groups. The faster the bowling group the greater the increase in power after 80% PC. VRs for the fast, med-fast, med and slow groups were 0.36, 0.40, 0.56 and 0.50, respectively.

The average upper trunk angular flexion and extension angular velocities were generally small during this period. However, at approximately 85% PC, the upper trunk began to extend, which coincided with the development of an

increasing flexion torque, which continued to increase until FFC. For instance, in this short period for the fast group, the upper trunk flexion torque increased from 0 - 61 Nm. There were correspondingly similar increases in upper trunk flexion torques for the med-fast and medium groups, 60.1 Nm and 62.2 Nm, respectively. The slow group had the smallest flexion torque increase of 30.0 Nm. The flexion torques were acting to reduce the extension angular velocity of the trunk, and perhaps were promoting the trunk into flexion after FFC. However, it is important to note that the power and torque generated by upper trunk flexion were much lower than those generated by upper trunk long axis rotation.

The upper trunk lateral bending power for the fast group was positive for the first 85% PC, while the corresponding torque was negative. During this time the torque was actively increasing the lateral bend angular velocity to the left (mean, -2.22 ± 0.49 rad s^{-1}). However, as FFC approached, the power changed to negative and the torque to positive. Therefore, the angular velocity was still negative (in the direction of a lateral bend to the left), but the torque was opposing or controlling this motion. The other bowling groups exhibited similar dual power flow characteristics. The lateral bending powers were relatively small when compared to long axis rotation, and therefore the range of motion may not be very significant. However, the upper trunk still had an extended period of lateral bending torque midway through the phase in the range of –50 Nm to -100 Nm, and therefore such a torque may play an important stabilisation role rather than as an actuator of movement.

4.5.4 Front Arm

The motion of the front arm is considered an important component of fast bowling. Initially the front arm is generally thrown high in the air with the eyes on the target from a position outside the arm for side-on bowler, or inside the arm for a front-on bowler (Lillee, 1977). From this position, the current teaching is that the front arm should be thrust down vigorously in the direction of the target to assist in the flexion and rotation of the trunk, and rotation of the bowling arm (Bartlett et al., 1996; Elliott & Foster, 1989; Tyson, 1976). The acceleration of

the elbow into the side is believed to facilitate this process (Marylebone Cricket Club, 1976).

An examination of the front upper arm torques tends to support the current notion that there is an some active motion of the front arm (Figure 4-31). The torques were negative throughout the phase and generated positive power curves, indicating that the upper front arm was actively vertically adducted with respect to the orientation of the trunk from BFC to FFC. The large variance ratios indicate that

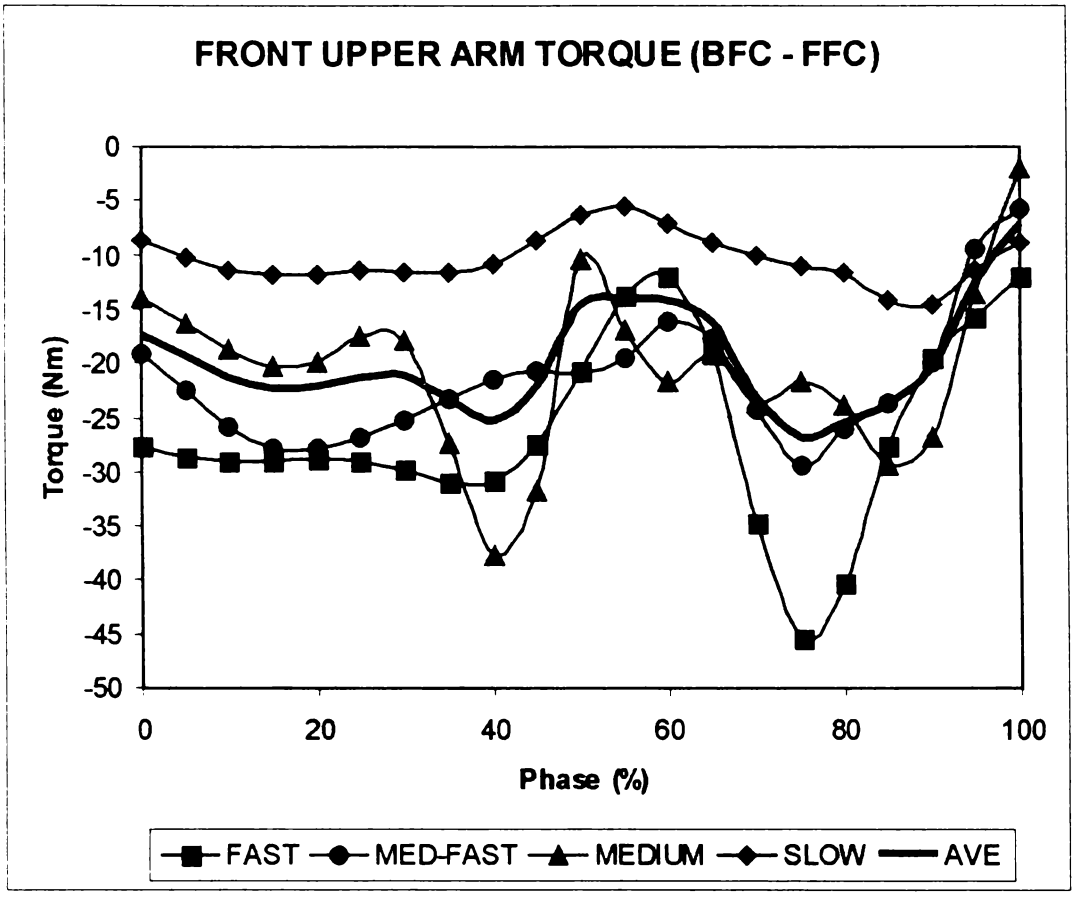

Figure 4-31: Ensemble averages of front upper arm torque about the local z-axis, which represents vertical adduction/abduction torques. Solid line is the mean of all the ensemble average curves, which was equivalent to the mean of the total sample. Negative is defined for vertical adduction. VRs for the fast, med-fast, med and slow groups were 0.83, 0.88, 0.99 and 1.00, respectively.

there was a large variation within the range of acceptable front upper arm torques, and this made it difficult to make comparisons between groups. However, it is worth noting that the slow group had by far the lowest vertical adduction torque

throughout most of the phase. Also, almost all of the variation in these torques among the individual subjects occurred in the negative range. Therefore, vertical adduction of the upper arm during BFC to FFC was a common property among the bowlers despite differences in ability and ball release speed. The other common factor was that the front upper arm vertical adduction torque decreased rapidly as FFC approached.

Front arm action also involves the rotation of the forearm about its flexion-extension axis. There has been little scientific treatment of this motion, but it is generally accepted that the front forearm is actively flexed to bring the elbow into the side as fast as possible. Ensemble averages of front forearm torque and power were compared, and there were little differences between the groups, so the mean of the full sample was calculated (Figure 4-32). From 0-50% PC, the front forearm exerted a small extension torque, which generated a period of positive power. The bowlers were therefore actively extending the elbow during this time. A comparison of the upper arm and forearm angular velocities confirmed this.

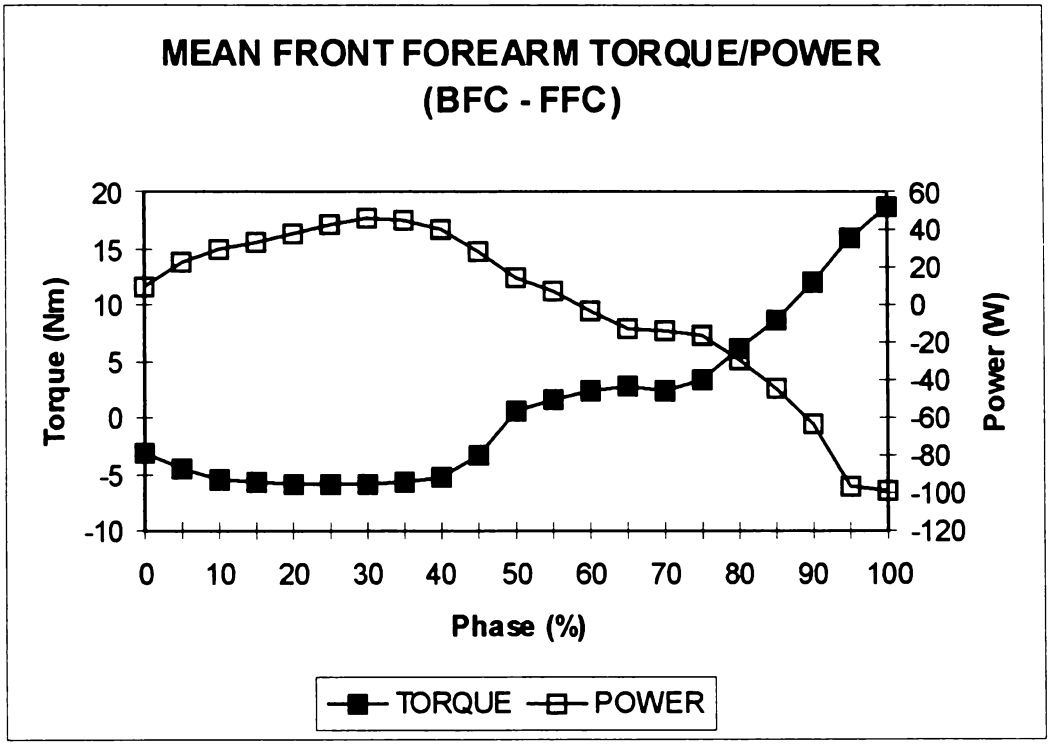

Figure 4-32: Grand mean of all front forearm torques and powers about the local z-axis, which is the forearm flexion/extension axis. Positive is defined for flexion. VR (torque): 0.47 (fast), 0.52 (med-fast), 0.70 (medium), 0.63 (slow). VR (power): 0.49 (fast), 0.75 (med-fast), 0.64 (medium), 0.85 (slow).

The mean front forearm extension angular velocity exceeded that of the front upper arm from 0-50% PC for all bowling groups (fast, 5.0 rad s^{-1} (upper arm), 7.2 rad s^{-1} (forearm); med-fast, 3.3 rad s^{-1} (upper arm), 7.9 rad s^{-1} (forearm); medium, 3.5 rad s^{-1} (upper arm), 5.7 rad s^{-1} (forearm); slow, 1.5 rad s^{-1} (upper arm), 3.8 rad s^{-1} (forearm)). Also, the mean extension angular velocities of the front upper arm and front forearm increased with the speed of bowling group. Therefore, during the first half of the period from BFC to FFC, there was no flexing of the elbow in an attempt to bring it quickly into the side. The main consideration at this point was to vertically adduct the front upper arm while extending the elbow.

From 50-100% PC, the front forearm torque became positive, and acted in the direction of flexion. However, the corresponding power during this time also became negative, which meant that the front forearm angular velocity was negative. Therefore, the elbow was still extending, but now the forearm torque was acting to control the rate of extension. On first appearance, this would suggest that the front elbow angle was increasing. However, while the front forearm was in controlled extension, the front upper arm torque was still promoting vertical adduction, which would act in a similar plane of motion as forearm extension. The upper front arm vertical adduction angular velocity now exceeded the front forearm extension angular velocity, the net effect of which caused the elbow to bend.

In summary, the motion of the front arm, commonly referred to as the non-bowling arm, is more complex than previously described. The technique of using the front arm effectively must consider the motions of both the upper arm and forearm, and at what stage they are in the BFC-FFC phase. During the first half of the phase, the upper arm was actively vertically adducting at a slower rate than the front elbow was being actively extended (Figure 4-33). Hence, the elbow angle was increasing. During the second half of the phase, the power flows reversed, as a result of the forearm torque opposing the direction of forearm extension, and the rate of upper arm vertical adduction now exceeded that of forearm extension. The net effect of this caused the front elbow to bend as FFC

was approached. The motion of the front arm therefore involved changes in power flows to achieve a slightly bent-arm configuration in front of the body at FFC.

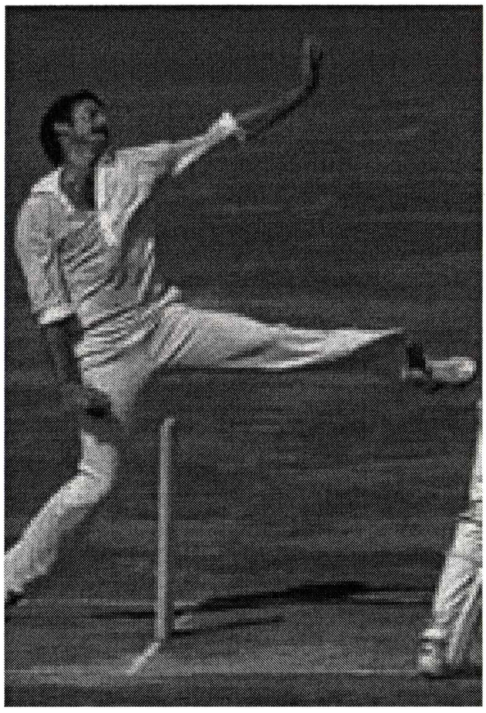

Figure 4-33: From approximately 0-50% PC, Dennis Lillee vertically adducted the front upper arm and extended the forearm.

4.5.5 Upper Bowling Arm

The powers and torques on the upper bowling arm during the entire BFC to FFC phase were relatively low (Figure 4-34). The most positive aspect of this motion was the torque about the local *X*-axis from 80% PC to FFC. For the fast group, this horizontal adduction torque increased during this period from 16.7 Nm to 35.3 Nm. Also, the corresponding power increased from 15.0 W to 252.1 W. The other bowling groups shared a similar increase in power. The torques were similar in magnitude for the three fastest groups, but slightly lower for the slow group. During this latter period (i.e., 80% PC to FFC) the bowling arm was moving into a horizontal position, and a rotation about the *X*-axis closely corresponded to a motion in the plane of horizontal adduction with respect to the upper trunk, which was obliquely tilted to the left. This suggests the bowlers were generating adduction torques of the upper bowling arm to bring the position of the

bowling arm at FFC into the classical horizontal position behind the back (Figure 4-35).

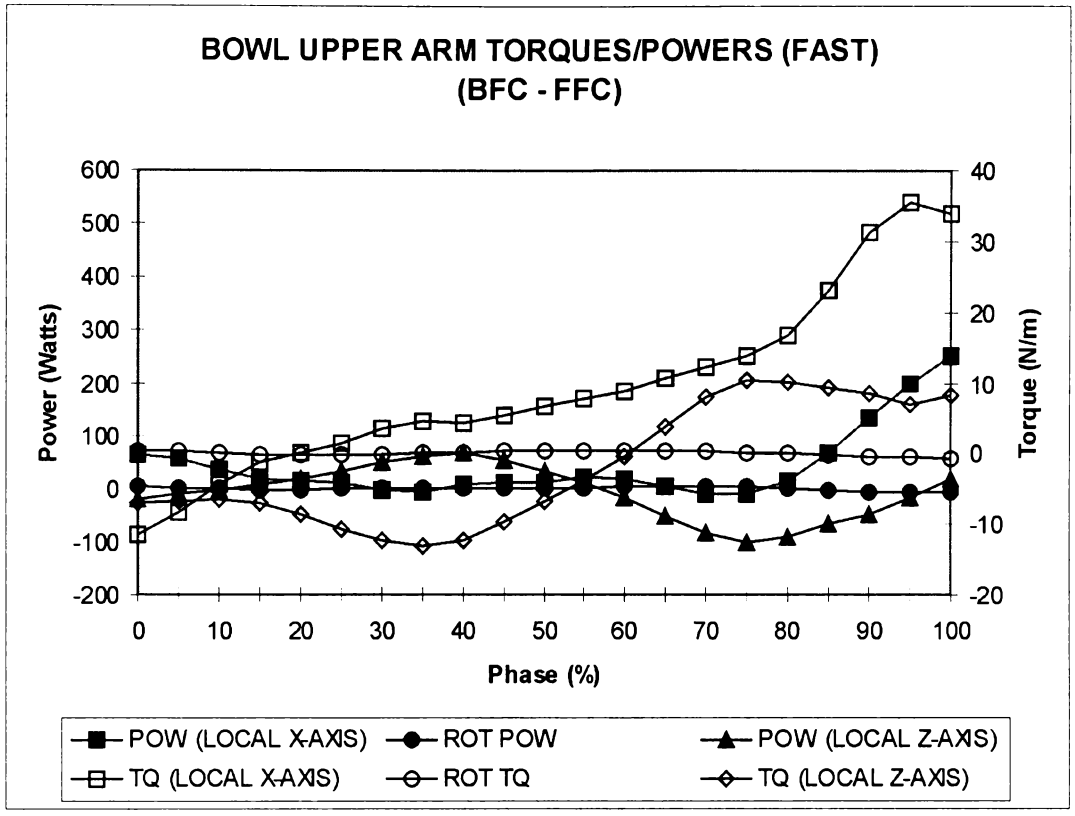

Figure 4-34: Ensemble averages of the bowling upper arm of the fast group of bowlers. The local *Z*-axis was defined as running from the posterior to anterior deltoid. The local *Y*-axis represents the direction of the longitudinal axis of rotation, and runs from proximal to distal. The local *X*-axis was found by taking the cross product of the local *Y*-axis vector with the local *Z*-axis vector. Therefore, the *X*-axis was generally orthogonal to the lateral surface of the proximal end of the upper arm. Positive torque and angular velocity about an axis is defined by the right-hand screw rule. VRs: power *X*-axis (0.87), power rotation longitudinal (*Y*-axis) (0.75), power *Z*-axis (1.00), torque *X*-axis (0.65), torque longitudinal rotation (*Y*-axis) (0.82), torque *Z*-axis (0.98).

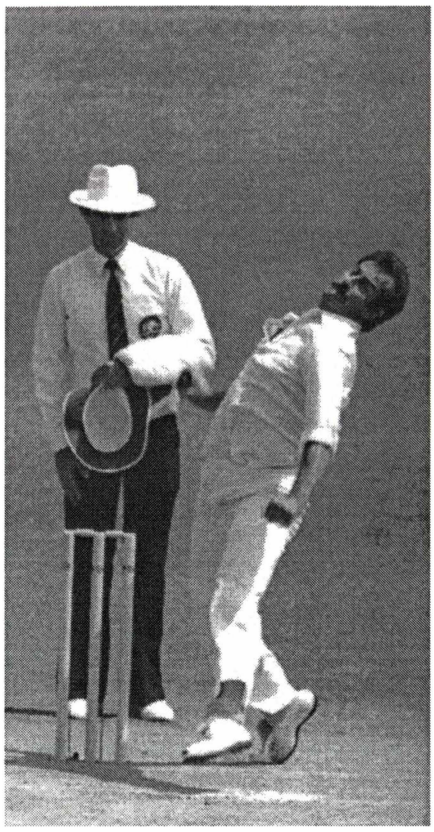

Figure 4-35: Just before BFC, Dennis Lillee brings the bowling arm into a horizontal abducted position behind the trunk.

4.6 SEGMENT POWERS (FFC TO REL)

4.6.1 Lower Trunk

As the fast bowler makes FFC, the main focus is to accelerate the bowling arm from a position of low angular velocity at or just below the level of shoulder behind the body to a position of high angular velocity at REL. Traditionally, it has been emphasised that in preparation for FFC the non-bowling arm and front leg are thrust down to bring about the flexion and rotation of the trunk, and subsequently the rotation of the bowling arm (Bartlett et al., 1996; Elliott & Foster, 1989a; Tyson, 1976). Studies have also shown that trunk flexion contributes significantly to ball release speed (Burden & Bartlett, 1990b; Davis & Blanksby, 1976b). This has influenced the coaching literature to recommend the flexion of the trunk to generate higher ball speed (Tyson, 1976).

The kinematic data in this study tend to confirm these findings. The average flexion angular velocities of the lower trunk were highest for the fast and med-fast bowling groups: (fast, 4.3 ± 0.4 rad s^{-1}; med-fast, 3.0 ± 0.2 rad s^{-1}; medium, 2.8 ± 1.3 rad s^{-1}; slow, 3.0 ± 1.0 rad s^{-1}). However, an analysis of the power curves indicates that this flexion was not actively performed (Figure 4-36). All the bowling groups displayed a strong extension torque throughout the phase. In fact, despite having the the highest average angular velocities, the fastest two groups had much larger average extension torques than the medium and slow groups (Table 4-6). Therefore, the muscles of the lower trunk were acting to resist or

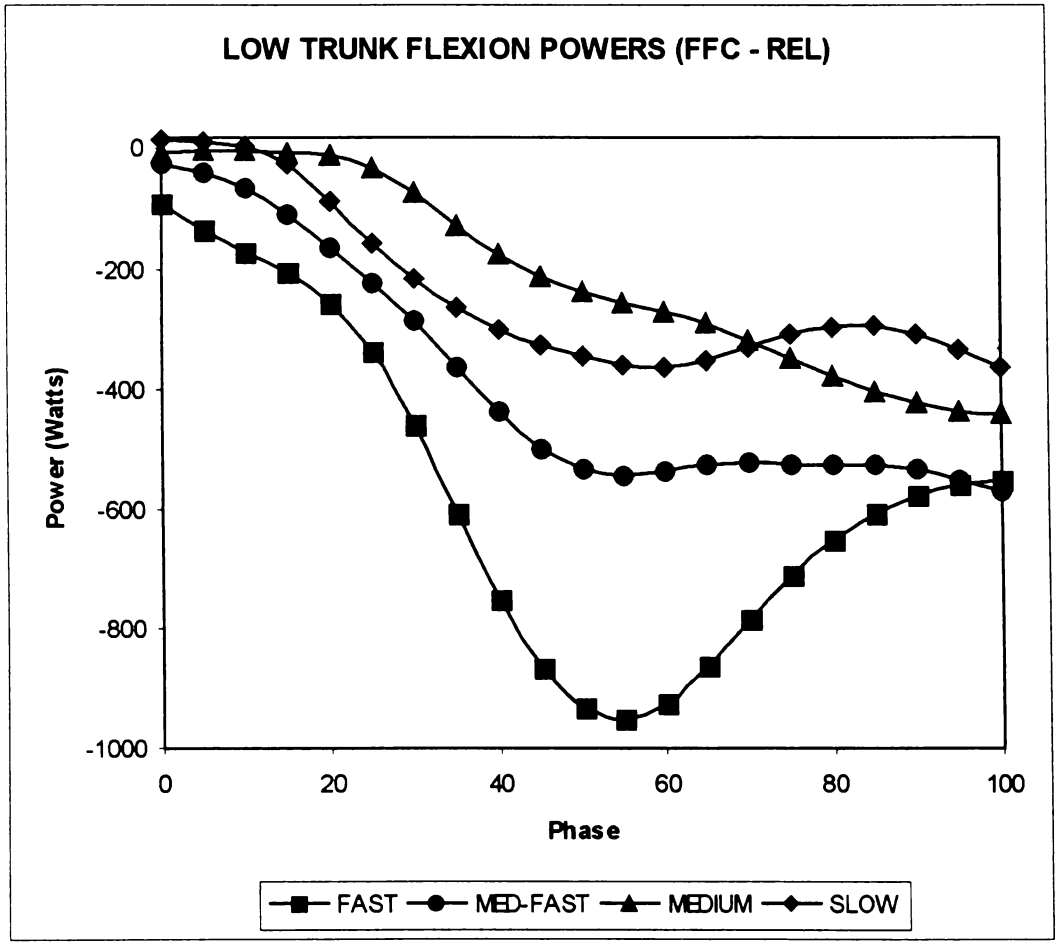

Figure 4-36: Ensemble averages of lower trunk flexion power curves from FFC to REL for all bowling groups. All groups have negative powers throughout the phase. The fast group clearly has the greatest negative power followed by the med-fast group. The medium and slow groups have the lowest negative powers. (VR: fast, 0.55; med-fast, 0.24; medium, 0.42; slow, 0.36).

control this movement. Therefore, lower trunk flexion was a controlled motion, and consequently the power of this motion was negative. A comparison of the flexion power curves shows how the negative power differed across the groups over the phase. Each of the power curves is discretely separate from each other, in particular the power curve of the fast group.

Table 4-6: Mean lower trunk flexion powers and torques for all bowling groups. Positive is defined for flexion.

BOWLING GROUP	Flexion Power	Flexion/Extension Torque
Fast	-597 ± 51 W (VR = 0.55)	-146.5 ± 16.7 Nm (VR = 0.54)
Med-fast	-391 ± 49 W (VR = 0.72)	-130.3 ± 14.1 Nm (VR = 0.53)
Medium	-241 ± 40 W (VR = 0.90)	-84.6 ± 13.5 Nm (VR = 0.77)
Slow	-241 ± 36 W (VR = 0.72)	-93.0 ± 12.6 Nm (VR = 0.40)

These results indicate that an analysis of segment motion based on kinematics alone can provide misleading information concerning the actuation status (i.e. active or controlled motion) of a segment. For instance, if the angular velocity of a particular segment has been correlated with high ball speed, then the attempt by the bowler to actively move this segment (in the belief that this would produce more ball speed), when a study of powers indicates that this motion should be controlled, could lead to excessive strain placed on the segment concerned. This could make its effects felt throughout the kinematic chain, either leading to impaired performance or an increased susceptibility to injury or both. A prevalent idea on the generation of ball speed is the implied necessity for the active flexion of the lower trunk during delivery. The results do not support this hypothesis. In fact, the fastest bowlers tended to resist lower trunk flexion most strongly. Therefore, in terms of coaching instruction it may be counterproductive to advise bowlers to flex the lower back strongly during the power phase (Figure 4-37).

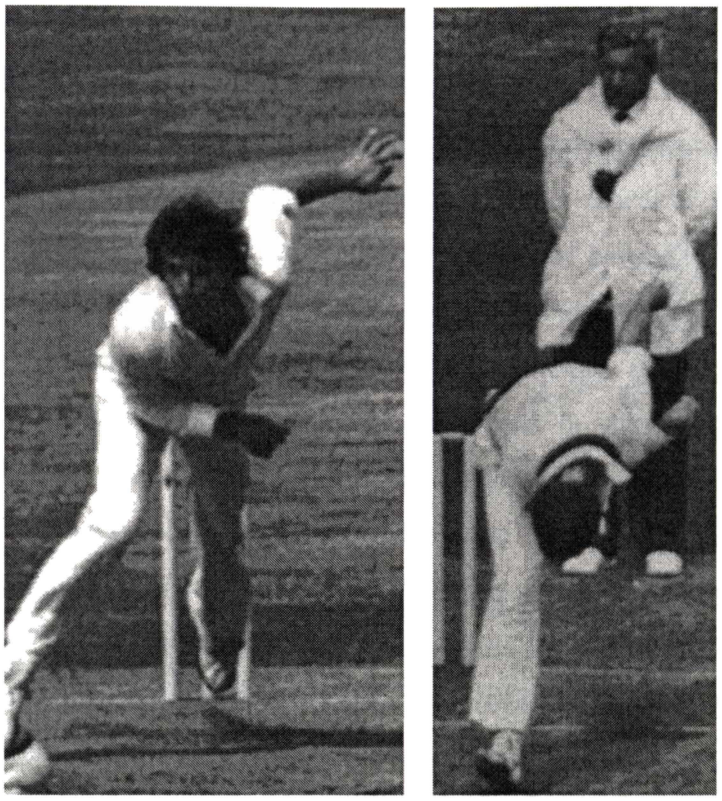

Figure 4-37: (Left) Imran Khan (Pakistan) maintained the lower trunk flexion angle above the horizontal. (Right) Geoff Lawson (Australia), who allowed his head to drop down during the follow through, allowed the lower trunk to flex to the horizontal. It is questionable whether such a degree of lower trunk flexion would aid in the production of high ball release speeds. [From B. Willis. 1984. *Fast Bowling with Bob Willis*. Willow Books, London]

Similarly, lower trunk long axis rotation was largely a controlled motion (Figure 4-38). For the fast group, there was a large negative power generated (mean, -1117 ± 110 W). The corresponding torque curve was negative and closely resembled the variance of the power curve. This was particularly the case in the first 50% of the phase, and indicated t a relatively constant positive angular velocity during this time. However, the important point is that as in the case for lower trunk flexion, the torque was acting to inhibit the rate of rotation for almost the entire phase. This action successfully helped reduce the angular velocity from a maximum value of 11.6 rad s^{-1} at 15% PC to just 1.7 rad s^{-1} at FFC.

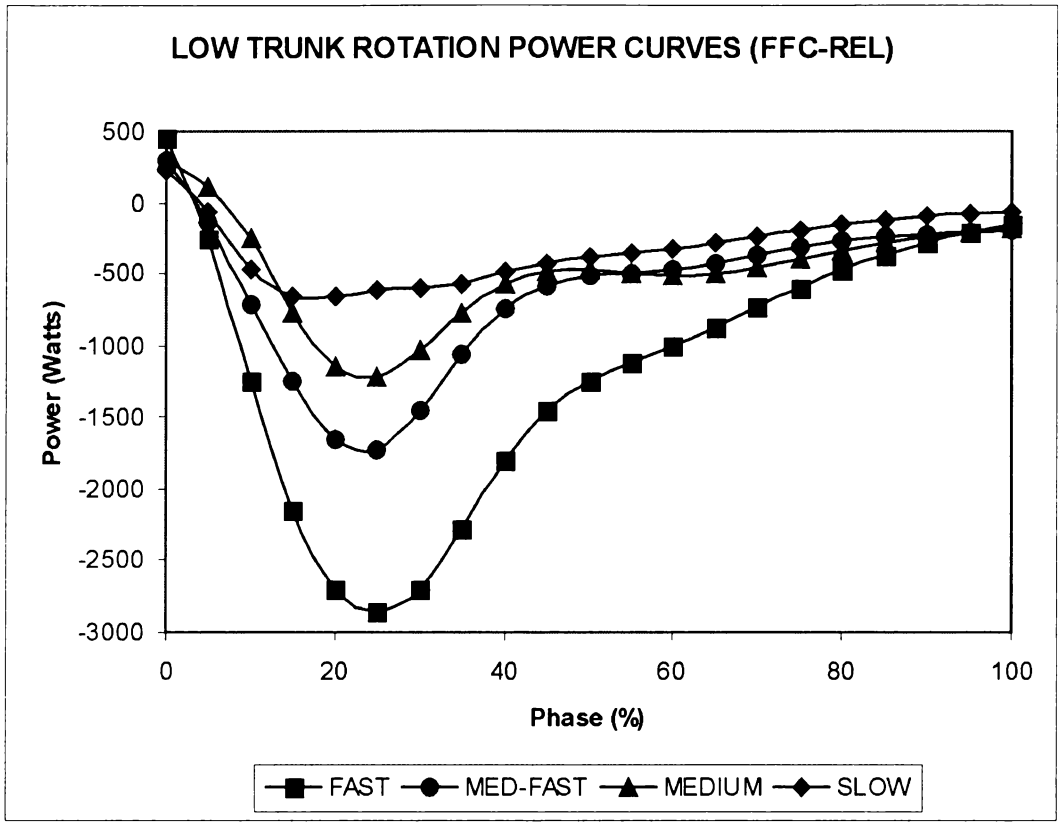

Figure 4-38: Ensemble averages of lower trunk rotation power curves from FFC to REL for all bowling groups. All groups have negative powers throughout the phase. The fast group clearly has the greatest negative power. Bowling groups are discretely separated from fast to slow with respect to their power curves. (VR: fast, 0.25; med-fast, 0.58; medium, 0.62; slow, 0.80)

The faster the bowling group, the more the lower trunk torque inhibited the lower trunk long axis rotation. For instance, though the average lower trunk angular velocity was higher for the faster groups (fast, 8.0 ± 1.3 rad s^{-1}; med-fast, 6.9 ± 1.1 rad s^{-1}; medium, 6.6 ± 1.9 rad s^{-1}; slow, 5.2 ± 0.9 rad s^{-1}), the corresponding average lower trunk torque was also higher (fast, -128.5 ± 11.6 Nm; med-fast, -88.1 ± 12.2 Nm; medium,-73.6 ± 8.0 Nm; slow, -61.3 ± 11.2 Nm). This generated high negative powers, which differentiated between the bowling groups: the faster the bowling group the more negative the power curve. The long axis rotation power was about three times the magnitude of the flexion power, and indicated that the lower trunk exerted a strong torque to counter the relatively fast rotations to the left.

As the local body-fixed coordinate system for lower trunk segment was defined at the point between the hip joint centres, lower trunk long axis rotation corresponds to what is commonly described as hip rotation in the cricket literature. There has been little formal scientific research performed on this aspect of bowling. Basic kinematic studies confirm that hip rotation is initiated before front foot contact (Bartlett et al., 1996). Davis and Blanksby (1976b) investigated the segmental component contribution to ball speed by systematically applying restraints to inhibit the development of muscular force in one or more segments. They concluded that leg action and hip rotation contribute approximately 23% to ball speed. Unfortunately, these were only kinematic studies and therefore did not specify how this was related to active or controlled muscle action. Coaches commonly talk about 'pivoting around the left side' (Andrew, 1986). Instructing the bowler to thrust the right hip forwards is believed to facilitate this. However, the data indicate that the faster bowlers produced higher lower trunk flexion and rotation angular velocities with higher inhibiting torques. This suggests that much of the hip action in fast bowling is controlled in response to the sequencing of other body segments.

Lateral bending of the lower trunk during this phase was to the left with a small angular velocity (e.g fast group: mean, -1.45 ± 0.46 rad s^{-1}). Interestingly, the torques that promoted such movements were relatively large (fast, -111.1 ± 27.6 Nm; med-fast, -87.4 ± 19.6 Nm; medium, -70.2 ± 27.0 Nm; slow, -81.4 ± 13.4 Nm). These torques were much larger than what would be expected to produce such small angular velocities. Of all the lower trunk motions, only lateral bending produced positive power for a significant portion of the phase. This power was small, but this does not necessarily diminish the importance of this motion. A segment that generates only a small amount of power in a particular plane of motion is still capable of bearing a significant dynamic load. The fast bowling group had a higher mean lateral bending torque to the left (i.e. negative torques) from 20% to 65% PC than the other groups, but this did not produce a corresponding increase in the power. In fact, the power actually reduced in this period. Such segment motions could be appropriately considered as providing reactive support or stabilisation. In a training programme, it could be very

important to strengthen the lower lumbar structure to produce lateral bending torques withstand externally imposed loads.

4.6.2 Upper Trunk

Proceeding to the upper trunk, the flexion power for the fast group was negative from 0-20% PC, then positive for the next 60%PC reaching a maximum value of 326 W, before becoming negative for the remaining 20% of the phase (Figure 4-39). The corresponding torque was positive from 0-80% PC before then

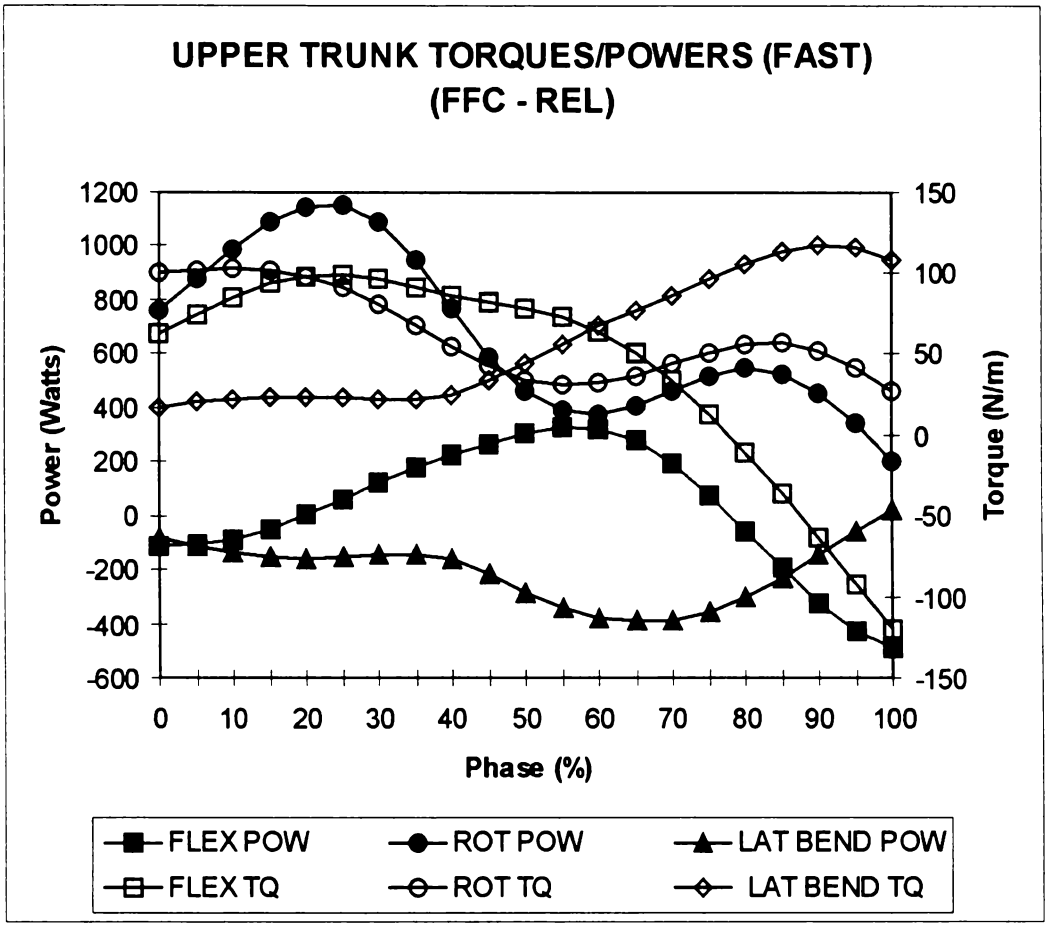

Figure 4-39: Ensemble averages of upper trunk powers and torques about local reference axes from FFC to REL. Positive torque is defined for flexion (VR = 0.26), rotation to the left (VR = 0.57), and lateral bend to the right (VR =0.60). VR for flexion, rotation and lateral bending powers are 0.82, 0.94 and 0.94, respectively.

becoming negative. Therefore, the actuation of upper trunk flexion involved three phases of motion. From 0-20% PC, upper trunk extension was controlled. Then from 20-80% PC upper trunk flexion was active, and for the remainder of the

phase (80-100%PC) upper trunk flexion became controlled. This variation in flexion power and torque was similar across the bowling groups. However, during the period of active flexion the mean upper trunk angular velocity was highest for the fast group (fast, 2.86 ± 0.94 rad s^{-1}; med-fast, 0.89 ± 1.37 rad s^{-1}; medium, 0.99 ± 1.18 rad s^{-1}; slow, 1.31 ± 0.57 rad s^{-1}).

Long-axis rotation was the fastest of the three upper trunk motions. The mean long-axis rotation angular velocities for the upper trunk increased with the speed of bowling group: (fast: mean, 11.0 ± 0.8 rad s^{-1}; max, 14.0 rad s^{-1}; med-fast: mean, 8.9 ± 0.5 rad s^{-1}; max, 11.4 rad s^{-1}; medium: mean, 8.1 ± 2.0 rad s^{-1}; max, 10.0 rad s^{-1}; slow: mean, 7.8 ± 0.7 rad s^{-1}; max, 10.9 rad s^{-1}). The long-axis rotation power and torque were both positive throughout the phase, showing similar variation over the phase, indicating that upper trunk long-axis rotation was a strong actively performed motion in fast bowling (Figure. 4-40).

A comparison of upper trunk long-axis rotation power over all the bowling groups shows that the fast group generated the higher power. The mean differences between the fast group and each other group were large: (fast/med-fast diff, 297 W; fast/medium diff, 267 W; fast/slow diff, 406 W). It was alluded to previously that the power and torque curves had similar variation over the phase. This often occurs when the torque makes a significant contribution to the power. To determine approximately the extent of the torque contribution to a power difference between any two bowling groups, the percentage difference in torque between groups is divided by the corresponding percentage difference in power. This ratio is defined as the *torque contribution difference factor* (TCDF). The TCDF was used to quantify the torque contribution to the power differences that existed between the fast group and the other groups (Figure 4-41). For example, for a particular segment motion, if the power generated by the slow group is 400 W, the power of the fast group 800 W, and the respective torques are 40 Nm and 80 Nm. Then the TCDF is 1, and the increase in power is due entirely to the increase in torque values, i.e. the doubling of power is due to the doubling of torque.

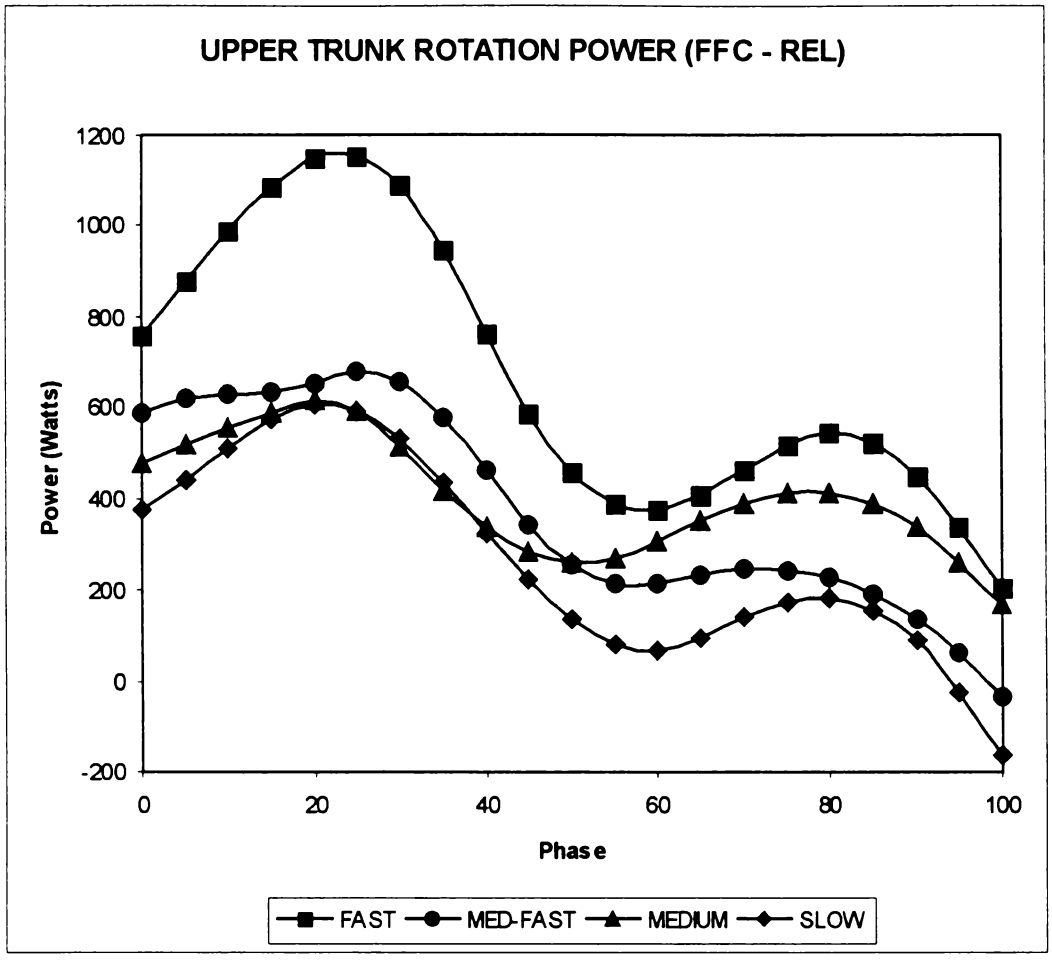

Figure 4-40: Ensemble averages of upper trunk rotation power curves from FFC to REL for all bowling groups. All groups had positive powers throughout the phase. The fast group clearly had the greatest positive power, particularly during the first 40% of the phase.

TCDFs for upper trunk long-axis rotation between the fast group and the other groups were similar. For instance, at 25% PC when the difference between the fast group power curves and the other groups was highest, the TCDF values were: fast/med-fast group, 0.62; fast/medium, 0.54; fast/slow, 0.55. Therefore, the upper trunk long-axis rotation torque accounted for more than 50% of the increased power of the fast group. However, it is worth noting that the contribution of the long-axis rotation torque to long-axis power increase was dependent on the phase position. For instance, at 60% PC, the contribution of the torque to the increased power of the fast group was no higher than 25%. At FFC, the contribution was almost 100%.

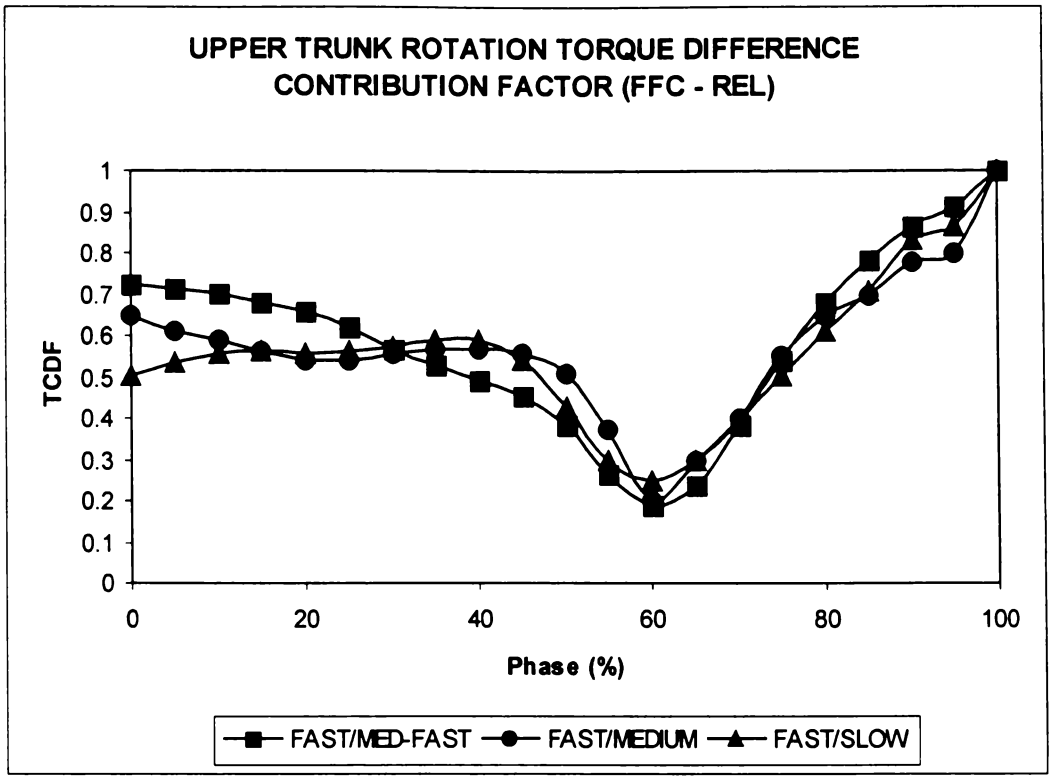

Figure 4-41: The torque contribution difference factor (TCDF) was used to quantify the difference between power curves for the fast group and the power curves of each other group.

Upper trunk long axis rotation has received little attention either in the coaching or scientific literature. It has not generally been considered that the upper trunk rotates on an oblique plane, and therefore may have the ability to pull the bowling arm around with it on a plane suitable for ball release. This may be the reason that the bowler needs to perform this motion actively throughout the phase, thereby generating a large active power and angular velocity. It was also shown that the fast group achieved a considerable advantage in this area by generating a higher long axis rotation power. The average TCDFs over the full phase were 0.59 (fast/med-fast), 0.57 (fast/medium), and 0.56 (fast/slow). The fast group, therefore, relied considerably on generating higher long axis rotation torques. However, it is just as important to note that over 40% of this power increase was not accountable by torque contribution. Therefore, significant power was also generated through the interaction of other body segments, i.e. through segmental sequencing.

The bowling action also requires the upper trunk to laterally bend to the left. The upper trunk lateral bending angular velocity to the left was similar across groups: (fast: mean, -4.8 ± 0.8 rad s^{-1}; med-fast: mean, -4.7 ± 0.4 rad s^{-1}; medium: mean, -4.3 ± 1.1 rad s^{-1}; slow: mean, -4.3 ± 0.7 rad s^{-1}). This supported the orthodox coaching literature, which emphasises pulling the non-bowling arm down into the hips to vigorously bend the trunk (i.e. by flexing and lateral bending) (Tyson, 1976). However, the lateral bending torque was steadily increasing to the right, and therefore resisted the lateral bend to the left (Figure 4-42). It would therefore be counterproductive for a bowler *to attempt* to actively laterally bend the trunk to the left. Like other motions of the trunk segments, the lateral bending of the trunk was largely a controlled action in response to the motion of the interacting segments. The lateral bending torques were similar for the groups, but it may be significant that the slow group exhibited the lowest lateral bending torque during the last 40% of the phase.

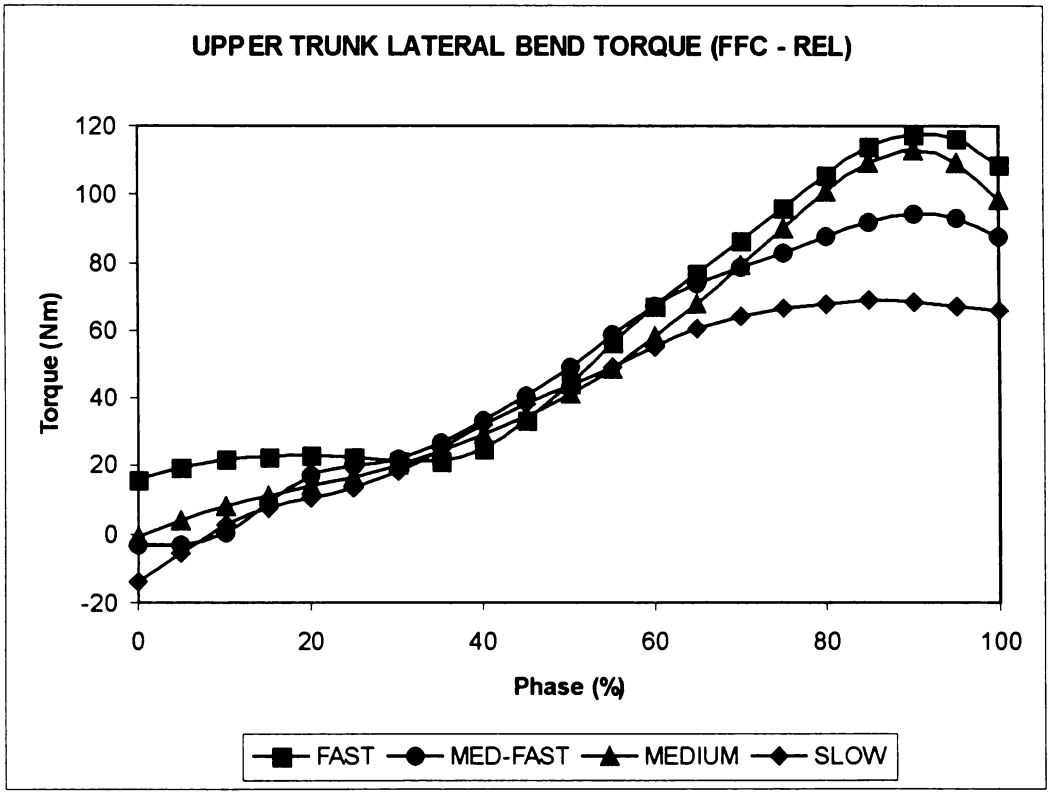

Figure 4-42: Ensemble averages of upper trunk lateral bend torques from FFC to REL for all bowling groups. All groups had positive torques through almost the entire phase. Positive is defined as lateral bend to the right. The slow group had the lowest lateral bending torques during the last 40% PC.

4.6.3 Bowling Upper Arm

Generally, it is considered that at FFC, the bowling arm is extended almost horizontally behind the back, from where it is circumducted about the glenohumeral joint so that the ball is released when the arm is approximately vertical. However, there is also a translation movement of the glenohumeral joint due to the net effect of the trunk and lower body motion. The local *Z*-axis at the distal end of the bowling upper arm was virtually tangential to the arc transcribed by the glenohumeral joint as the bowling arm moved. Calculating the forces and linear powers of the upper bowling arm in this direction would best account for the translation movement of the glenohumeral joint during the bowling action.

For approximately the first half of the phase, the force and linear power were positive, indicating that the glenohumeral joint was being thrust forwards (Figure 4-43 & 4-44). This was expected, as the bowler needs to transfer the glenohumeral joint from a position horizontally behind the back to a position approximately in line with the head at ball release. However, there was a transition point after which this force became negative, and then further increased negatively up until ball release. This transition point varied slightly with bowling group: fast (61%), med-fast (54%), medium (47%), slow (51%). After this transition, the power became increasingly positive, and the force increasingly negative, and therefore the velocity of the glenohumeral joint became negative.

These results suggest that the glenohumeral joint of the bowling arm was initially pulled forwards before being subject to an increasing negative force. The effect of this negative force was to pull backwards on the distal end of the upper arm, which could act to increase the positive angular velocity of the upper arm. There was little to distinguish between the groups, but the fast group had a higher negative increase in force from 83%PC to REL, which suggests that the fastest bowlers were more adept at retarding the linear motion of the glenohumeral joint as ball release was approached. Such an action would involve an appropriate scheme of segmental sequencing. This would probably start with the retardation of upper trunk rotation by the hips, which are constrained by the orientation of the front foot, closed slightly or pointed straight down the wicket. The retardation of

the lower trunk rotation would then inhibit the rotation of the upper trunk as it rotates to the left (i.e. chest opens towards the target). Rotation of the upper trunk carries the glenohumeral joint with it, so that when upper trunk rotation is retarded, most of the glenohumeral joint translation is as well.

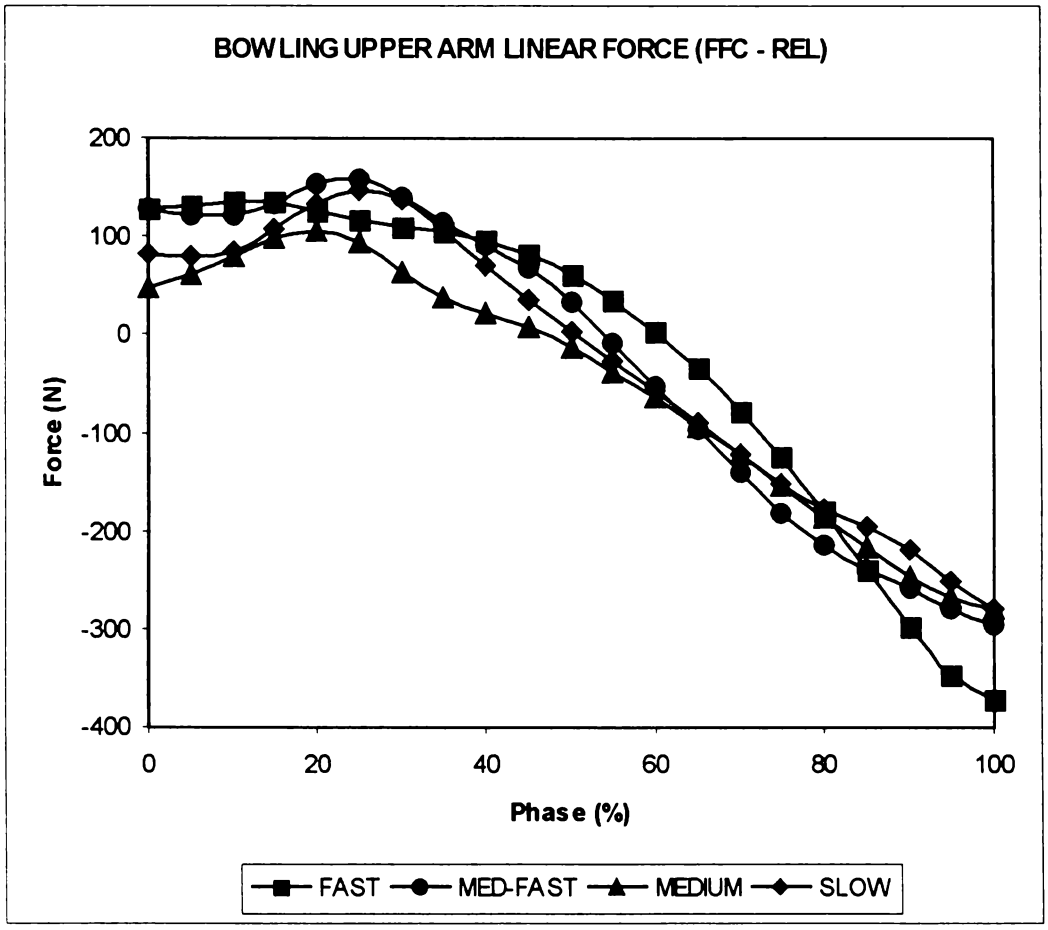

Figure 4-43: Ensemble average of joint force (all groups) at the glenohumeral joint of the bowing arm in the direction of the local z-axis. VR: 0.27 (fast), 0.25 (med-fast), 0.55 (medium), 0.22 (slow).

The most significant rotation power generated by the upper bowling arm was about the local *X*-axis. During this phase, the upper trunk was tilted obliquely to the left, and rotation of the upper bowling arm about its local *X*-axis was approximately a horizontal adduction with respect to the tilted upper trunk. However, as in the case for the upper arm linear power, the adduction power was positive for only a portion of the phase (Figure 4-45). The mean value of the ensemble average curve during the positive period was higher for the two faster groups compared to the two slower ones (fast, 442 W; med-fast, 442 W; medium,

190 W; slow, 324 W). In terms of the transition point at which the horizontal adduction power became negative, the two faster groups became negative later, in particular the fast group, compared to the two slower groups (fast, 64%; med-fast, 56%; medium, 41%; slow, 53%). Also, the two faster groups negatively increased their adduction power at a much higher rate than the two lower groups (fast, -3130 W/%PC; med-fast, -2403 W/%PC; medium, -1322 W/%PC; slow –1544 W/%PC). Therefore, despite the fast and medium-fast groups having the higher positive powers, and a later transition point, they still generated the highest mean negative power (fast, -1096 W; med-fast, -1055 W; medium, -1006 W phase; slow, -832 W). Beyond the transition point, the horizontal adduction-type motion of the bowling arm was strongly controlled.

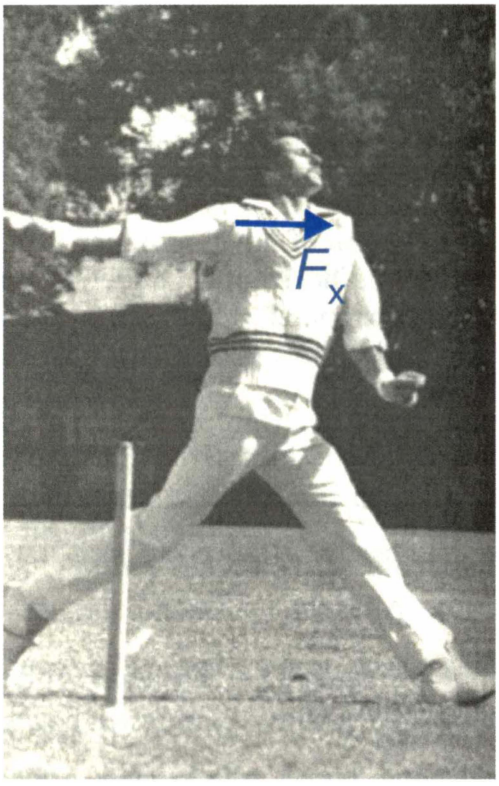

Figure 4-44: Richard Hadlee (New Zealand) during early FFC when the force on the glenohumeral head (F_x) acts in the direction of the motion.

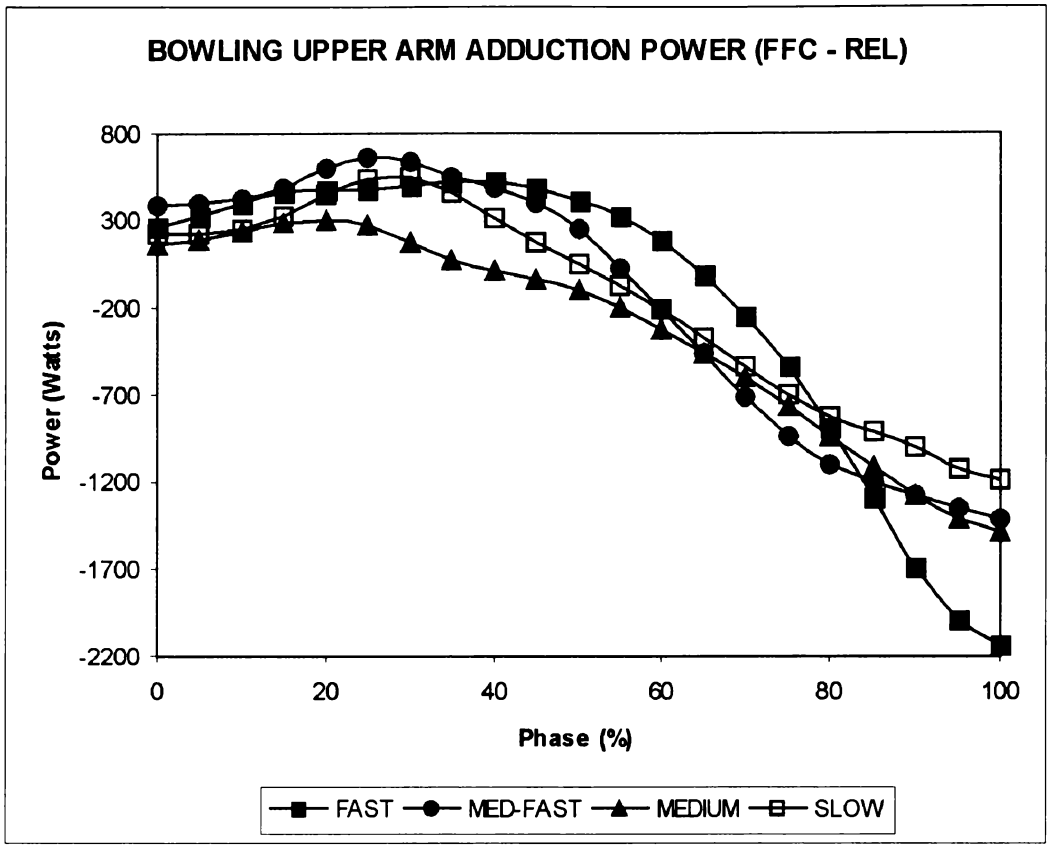

Figure 4-45: Ensemble averages of bowling upper arm power about local x-axis, which closely represents horizontal adduction power. All groups had positive power for approximately half the phase before becoming increasingly negative to REL. VR: 0.24 (fast), 0.25 (med-fast), 0.48 (med), 0.22 (slow).

The horizontal adduction torque similarly had a transition point when the torque changed from positive to negative (fast, 64%; med-fast, 56%; medium, 50%; slow, 52%) (Figure 4-46). After the transition point, the mean torque increased negatively with bowling speed group (fast, -51.3 Nm; med-fast, -46.9 Nm; medium, -37.1 Nm; slow, -37.1 Nm). The faster bowlers employed a higher negative horizontal adduction torque, which acted in the opposite sense to the angular velocity of the bowling upper arm. Therefore, though there was an initial period when the mean torque was positive (fast, 27.8 Nm; med-fast, 24.9 Nm; medium, 17.1 Nm; slow, 21.8 Nm), the fast and med-fast groups initially having higher positive torques than the slower two groups, after the transition point the torques increased negatively, and the motion was very much a controlled one. The most important result is that after the transition point, the fast and med-fast

groups resisted the horizontal adduction motion of the upper arm more vigorously than the slower groups.

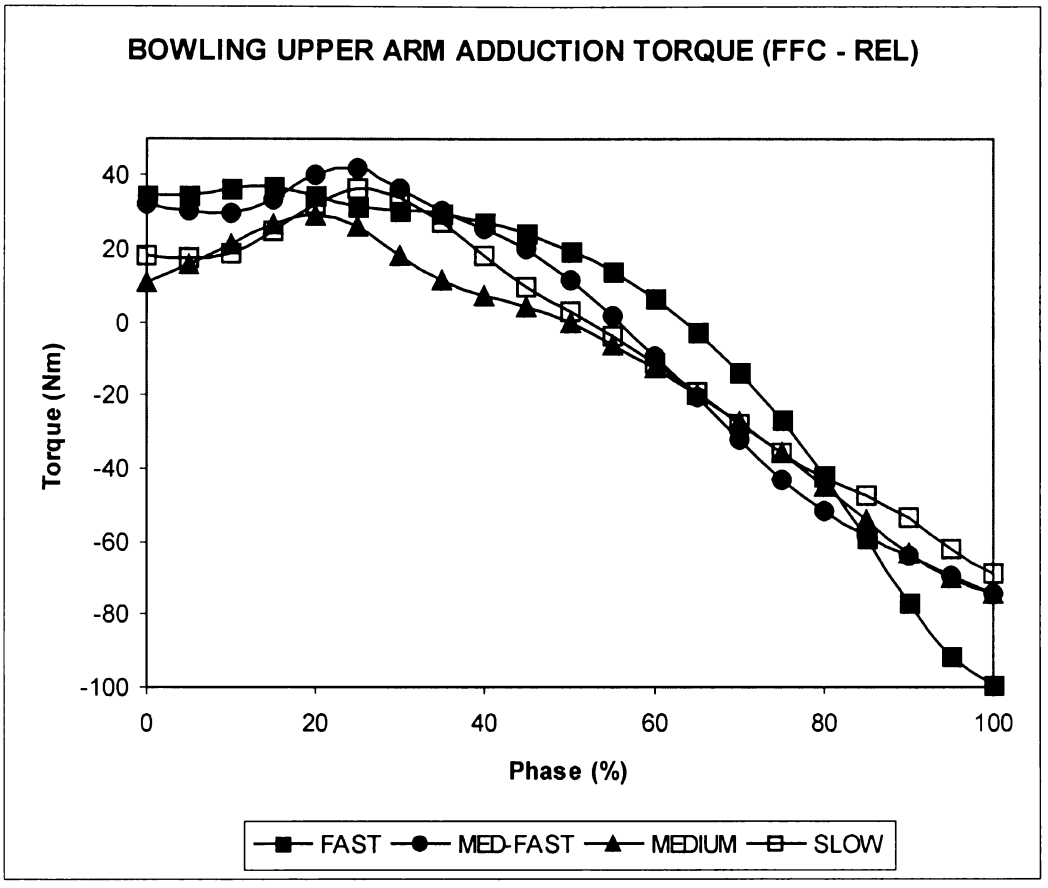

Figure 4-46: Ensemble averages of bowling upper arm torque about local x-axis, which closely represents horizontal adduction torque. All groups had positive torque for approximately half the phase after which the torque became increasingly negative until REL. VR: 0.24 (fast), 0.30 (med-fast), 0.55 (med), 0.22 (slow). Positive is defined for adduction.

Despite the rise of negative horizontal adduction torque after the transition point, the bowling upper arm steadily increased its angular velocity. In fact, maximum horizontal adduction angular velocity was achieved only a little before ball release (about 90% PC), and increased slightly with bowling group (fast, 21.9 rad s^{-1}; med-fast, 21.2 rad s^{-1}; medium, 20.3 rad s^{-1}; slow, 18.7 rad s^{-1}). This implies that there was another source of power behind bowling arm rotation. One candidate was the linear force in the direction of the local *Z*-axis. This force became negative at approximately the same time when the horizontal adduction torque became negative. Also, the horizontal adduction torque and linear force curves show similar variation over the phase. For instance, the curves for the fast group

in both cases have a relatively late transition point, and a similar rate of negative increase (after the transition point). These results suggest that the negative linear force plays a part in propelling the upper bowling arm after the transition point, while the horizontal adduction torque is given the task of resisting or controlling the horizontal adduction angular velocity (Figure 4-47).

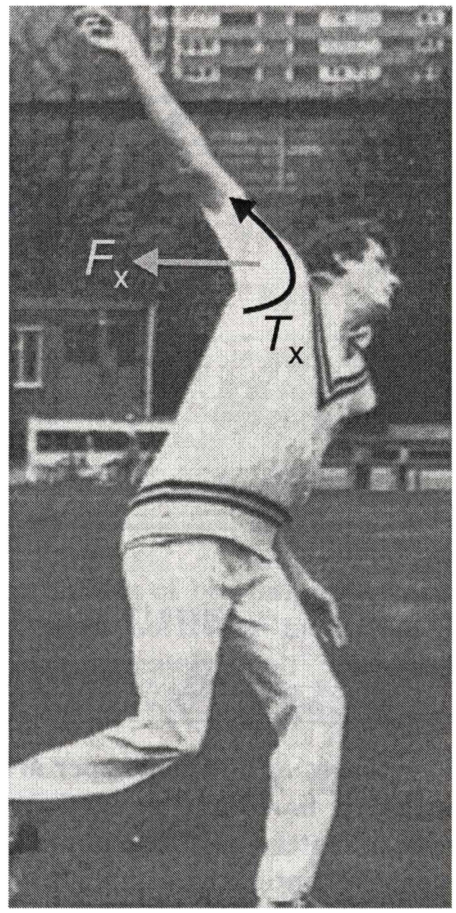

Figure 4-47: Bob Willis (England) at the stage of bowing corresponding to approximately 60% PC of the power phase. As the abduction torque (T_x) increases, the force on the glenohumeral head (F_x) increases in the negative direction. [From B. Willis. 1984. *Fast Bowling with Bob Willis*. Willow Books, London]

There was also upper arm power generated as vertical adduction (i.e. rotation about the local *Z*-axis). This power was small initially, and in all cases, except for the fast group, negative (though even this became negative at 42% PC). Then, at a certain point the vertical adduction power became positive (fast, 66%; med-fast, 51%; medium, 65%; slow, 49%). The vertical adduction torques were positive throughout the phase, so during approximately the last half of the phase, the

bowling upper arm was undergoing an active vertical adduction. However, it was difficult to find any relation with bowling group. For instance, after becoming positive, the medium-fast and slow groups had the highest mean powers, and the fast and medium groups the slowest mean powers (fast, 249 W; med-fast, 491 W; medium, 367 W; slow, 478 W). Also, the maximum vertical adduction angular velocity, which occurred at ball release, was highest for the medium and slow bowling groups, and lowest for the fast bowling group (fast, 4.3 rad s^{-1}; med-fast, 9.7 rad s^{-1}; medium, 7.7 rad s^{-1}; slow, 13.4 rad s^{-1}). Part of the uncertainty was due to the high VRs for the fast, med-fast, and medium groups (1.00, 0.78 and 0.80, respectively). Only the slow group had a low VR of 0.32. However, in the fast group, there was an equal amount of subjects who had positive and negative power curves during the last half of the phase. This suggests that bowlers could produce either active or controlled vertical adduction as ball release nears, and this could be dependent on the motion of interacting segments.

There was less variability in the vertical adduction torques (Figure 4-48). The mean torque shows a large difference between the fast and slow groups (fast, 71.7 Nm; med-fast, 58.7 Nm; medium, 67.0 Nm; slow, 48.4 Nm). However, it is worth noting that although the fast group had the highest vertical adduction torque it also displayed the lowest corresponding power. This situation was reversed for the slow group. Overall, the issue of the role of vertical adduction bowling upper arm is difficult to clearly resolve. From the magnitude of the powers, it is an important motion, and may be dependent on the relative angle between the plane of motion of the bowling arm and that of the upper trunk (Figure 4-49). However, it is difficult to make any definite relationships with bowling group speed.

Predictably, the longitudinal rotation of the upper arm generated only small power due to the very small moment of inertia of the upper arm about its longitudinal axis. Unfortunately, the corresponding angular velocity data could not be measured to a high degree of accuracy, and this may have caused the production of large VRs in the power data. In general terms, there is some evidence that there was a small external rotation during the first half of the phase, which was then followed by an internal rotation until ball release. Interestingly, except for about the last 5% PC, the upper arm torque always acted in the direction to

produce internal rotation (Fig. 4-50). There was little to separate between the groups. Traditionally, the bowling arm is supposed to be relatively straight during this phase, so the amount of internal upper arm rotation had not previously been considered important.

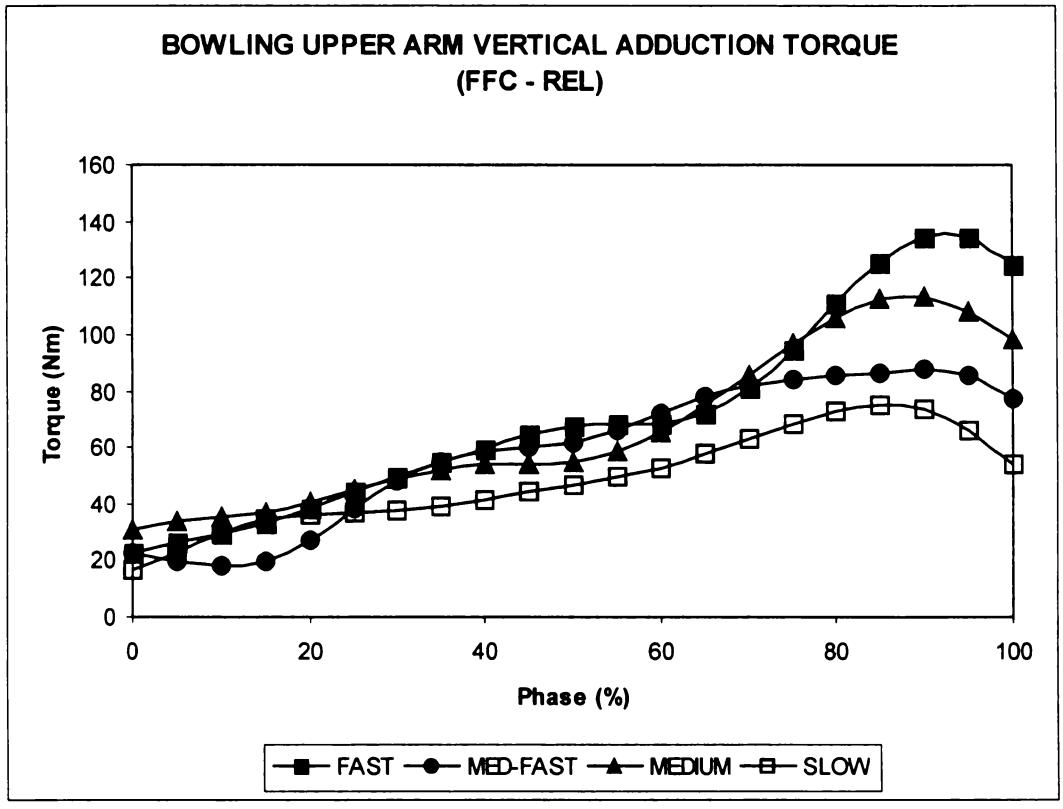

Figure 4-48: Ensemble averages of bowling upper arm torque about local z-axis, represents the vertical adduction torque. All groups had positive torques for the entire phase. VR: 0.24 (fast), 0.67 (med-fast), 0.47 (med), 0.59 (slow). Positive is defined for vertical adduction.

Davis and Blanksby (1976b) estimated that the bowling arm makes a 41% contribution to ball speed. Therefore, the motion of the bowling arm is very important in terms of ball speed generation. Yet, even the action of a rotating arm about a joint reveals complex dynamic characteristics. The angular velocities of the major adduction motions increased steadily over the phase. However, the torques show that the actuation strategies for horizontal adduction and vertical adduction were different. The former had a torque reversal during the latter half of the phase, whereas the latter had a torque that steadily increased over the phase. Also, the time of reversal of the linear force at the glenohumeral joint almost exactly coincided with the time of reversal of the horizontal adduction torque,

indicating that the interaction of these dynamic quantities may play a prominent role in rotating the bowling arm during the latter half of the phase. The presence of negative horizontal torque may occur when the bowling arm motion changes from horizontal adduction to vertical adduction with respect to the plane of upper trunk long axis rotation. The generation of negative linear force at the glenohumeral joint may depend on the restriction of upper trunk long axis rotation at ball release. This in turn depends in part on the range of rotation of the lower trunk, which is constrained by the placement and orientation of the front foot, effectively retarding the motion of the hips as they open up towards the front. This could have implications for the bowler who intends to increase bowling arm angular velocity. There is a complex interaction with the larger segments of the body, depending on their position in the phase and their planes of motion.

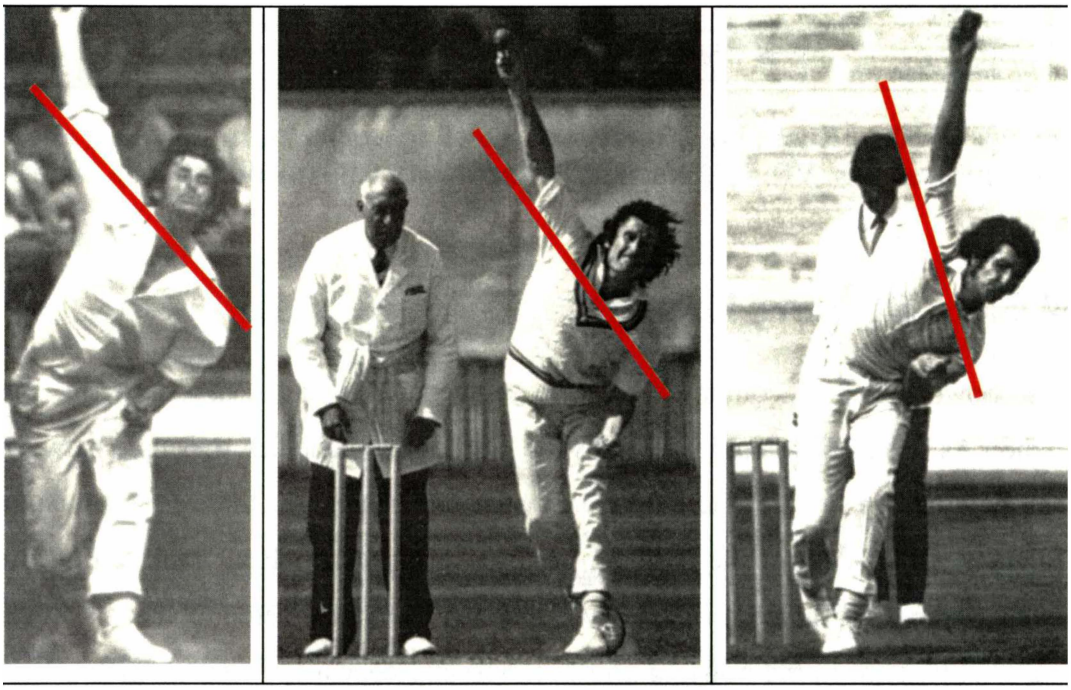

Figure 4-49: From left to right, three world-class fast bowlers – Richard Hadlee (New Zealand), John Snow (England), and Bob Willis (England) – show that as ball release nears the bowling arm plane of motion (red) separates from the plane of upper trunk long axis rotation, and this coincides with the development of upper arm vertical adduction torques. Note how the plane of upper trunk long axis rotation varies with head position and action type, which may also have an effect on the magnitude of upper arm vertical adduction power. [From B. Willis. 1984. *Fast Bowling with Bob Willis*. Willow Books, London]

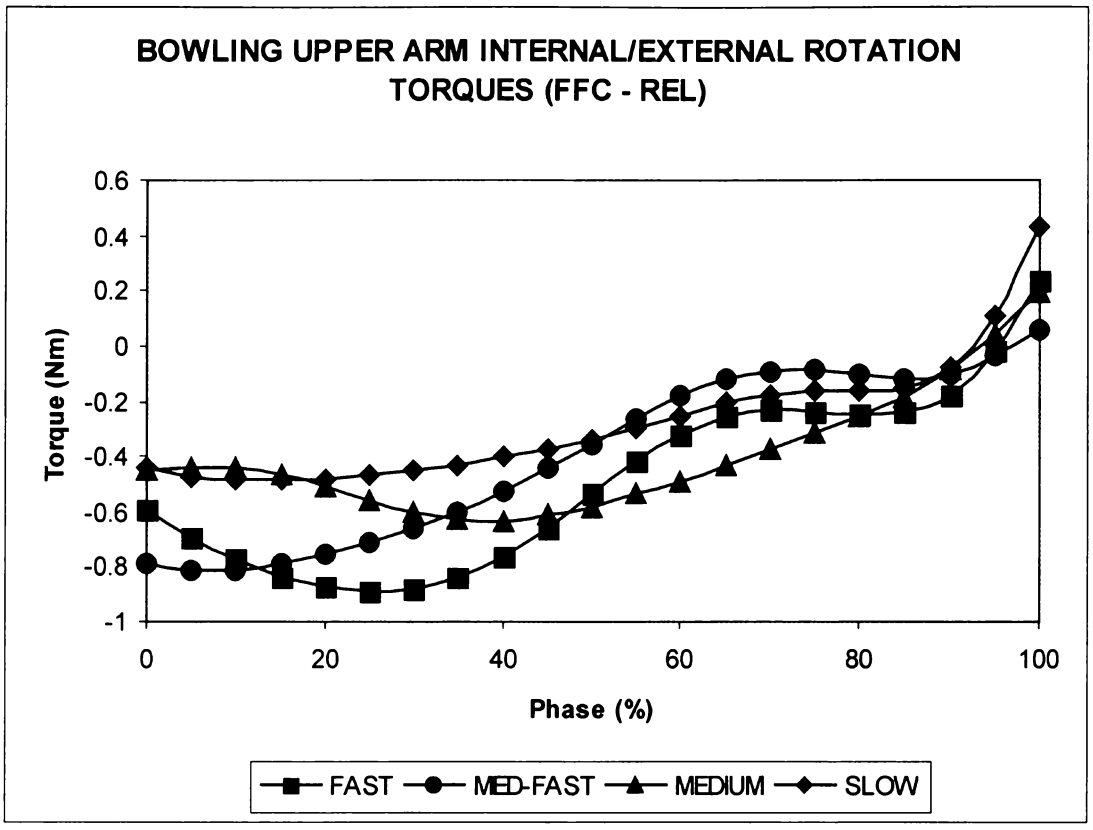

Figure 4-50: Ensemble average of bowling upper arm torques about longitudinal axis. VR: 0.72 (fast), 0.79 (med-fast), 0.88 (medium), 0.83 (slow).

4.6.4 Bowling Forearm

The bowling arm is composed of three segments: the upper arm, forearm, and hand. As it is a constraint imposed by the laws of the game that the angle between the bowling upper arm and forearm must not increase (i.e. there is a *minimum angle constraint*) after the bowling arm has reached shoulder level behind the back, the upper arm and forearm have generally been considered to act as a single rigid unit. Though the bowling arm does visually appear to move as such a unit, the powers and torques of the upper arm and forearm show that the motion of the upper arm and forearm used different actuation strategies.

To illustrate the difference between the dynamics of the upper arm and forearm, the powers are presented for the fast group (Figure 4-51). For both segments, the power about the local *Z*-axes, the vertical adduction axes, was similar until approximately 74% PC when the upper arm power surpassed that of the forearm, the difference between them continuing to increase up to ball release. However,

the main difference was between the bowling upper arm power about the local *X*-axis, the horizontal adduction axis, and the forearm power about the local *X*-axis, the forearm flexion axis. The horizontal adduction power of the upper arm was initially higher than the forearm flexion axis rotation power, but from 48% PC to FFC, the upper arm power became increasingly more negative than the forearm power, which remained positive and relatively constant. Therefore, during this time, the upper arm horizontal adduction was controlled, while forearm flexion axis rotation was active.

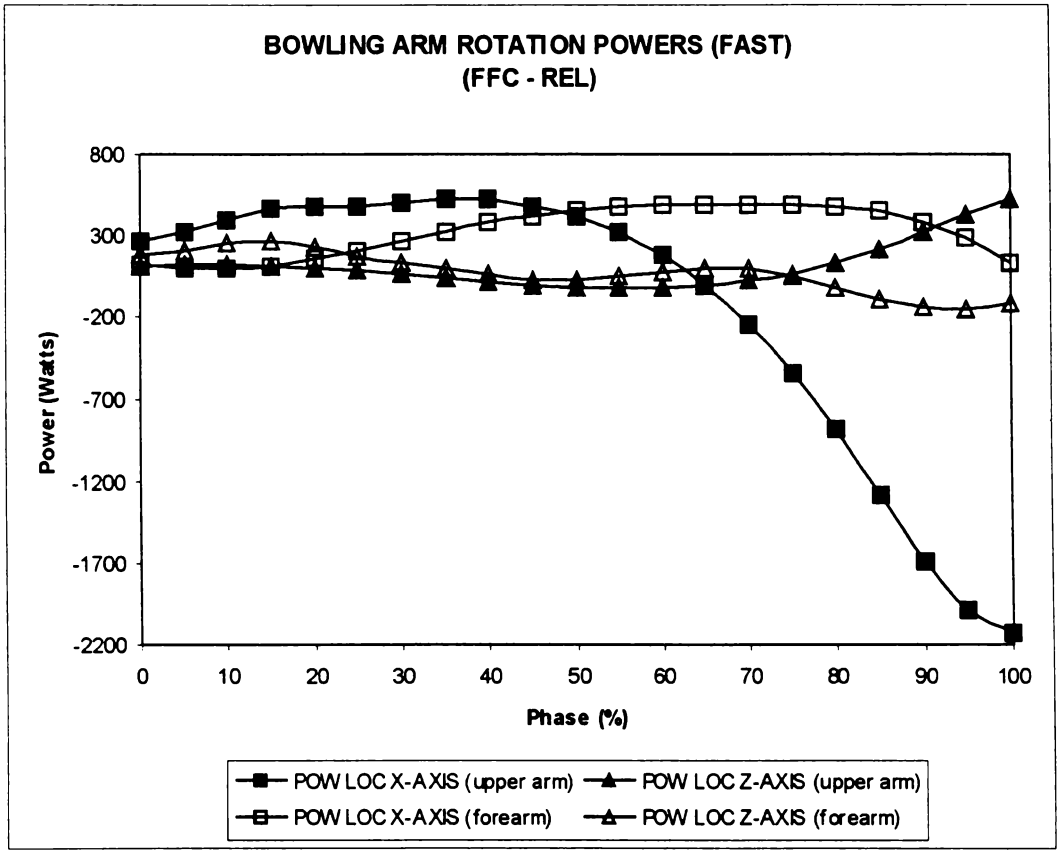

Figure 4-51: Upper arm and forearm powers of the bowling arm (fast group) show that there was a large difference in power about the respective local *X*-axes of the upper arm and forearm (VR: ■ 0.24 □ 0.90 ▲0.89 Δ 0.89)

The bowling upper arm and the forearm must work together to increase the angular velocity of the bowling arm. The controlled adduction motion of the bowling upper arm indicates that there were other mechanisms contributing to the generation of adduction angular velocity. The case for the negative horizontal force at the distal end of the humerus was presented before. However, the main role of the forearm, as it is currently accepted, is to maintain the minimum angle

constraint of the bowling arm. An examination of the forearm flexion torque (i.e. it was positive throughout the phase) shows that this was satisfied by the active production of forearm flexion power (Figure 4-52).

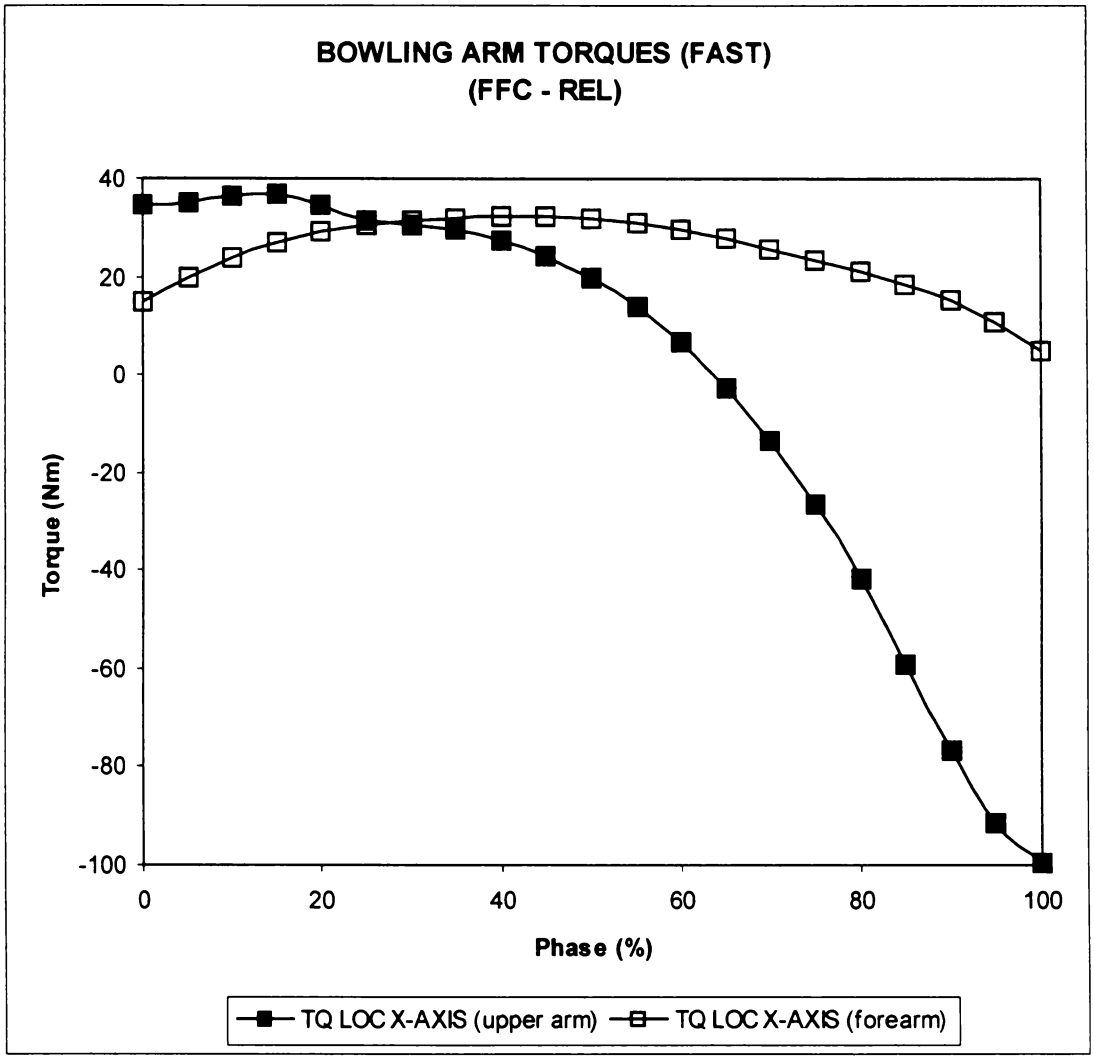

Figure 4-52: Upper arm and forearm torques of the bowling arm (fast group) show that the bowling upper arm adduction torque was negative for the most of the phase, while the forearm torque was always positive (VR:■ 0.32 □ 0.88). Forearm flexion torque is defined as positive.

The forearm power and torque about the local *Y*-axis, which was the forearm longitudinal axis, were small due to the small moment of inertia. Traditionally, the effects of internal and external rotation have been assumed to be small because the bowling arm is not considered to flex and straighten during the power phase. The forearm internal and external angular velocities were difficult to calculate very accurately. However, in general terms, the forearm externally rotated for

approximately the first 60% PC, and then internally rotated until ball release. Interestingly, during most of the phase, the corresponding torques of the upper arm and forearm, though small and variable, were acting in the direction to produce internal rotation or pronation. Also, the faster the bowling group the higher was the mean pronation torque (fast, -0.40 ± 0.05 Nm; med-fast, -0.34 ± 0.05 Nm; med, -0.25 ± 0.02 Nm; slow, -0.16 ± 0.05 Nm). A one-way ANOVA variance test shows that the difference between these groups was significant ($p = 0.0087$, $F = 4.825$). Performing multiple comparisons between the groups based on a 95% confidence level yielded a significant difference between the fast and slow groups, and a difference between the med-fast and slow group that was almost significant. Therefore, it is possible that forearm pronation torque does play a role in ball speed generation. This argument would be strengthened by accurate measurements of forearm pronation angular velocity, and an investigation into the angle between the upper arm and forearm (Figure 4-53). However, it is not clear by what mechanism forearm long axis rotation could directly influence ball release speed. It may be simply the by-product of humerus internal rotation.

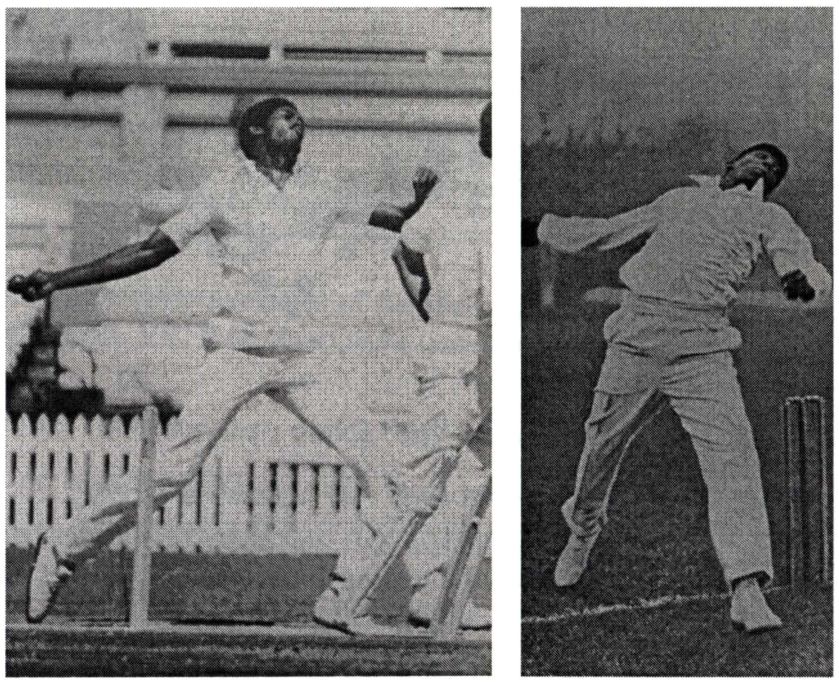

Figure 4-53: There could be small periods of elbow flexion during the power phase. There is a suggestion that two great West Indian fast bowlers of the past, Michael Holding (left) and Sir Learie Constantine (right), amongst many others used a slightly flexed elbow during the power phase.

4.6.5 Bowling Hand

The only significant motion of the bowling hand is flexion. Rotation of the hand cannot occur independently of forearm rotation, and the range of adduction and abduction is limited and not capable of imparting much power. The hand flexion power (from ensemble averaged data) only became important during the latter half of the phase, when it changed rapidly from negative to positive (Figure 4-54). An examination of the corresponding ensemble averaged torques shows that the torques were also undergoing a similar change from negative (extension) to positive (flexion) (Figure 4-55). In general, hand flexion underwent a short period of controlled flexion followed by a period of rapid active flexion until ball release.

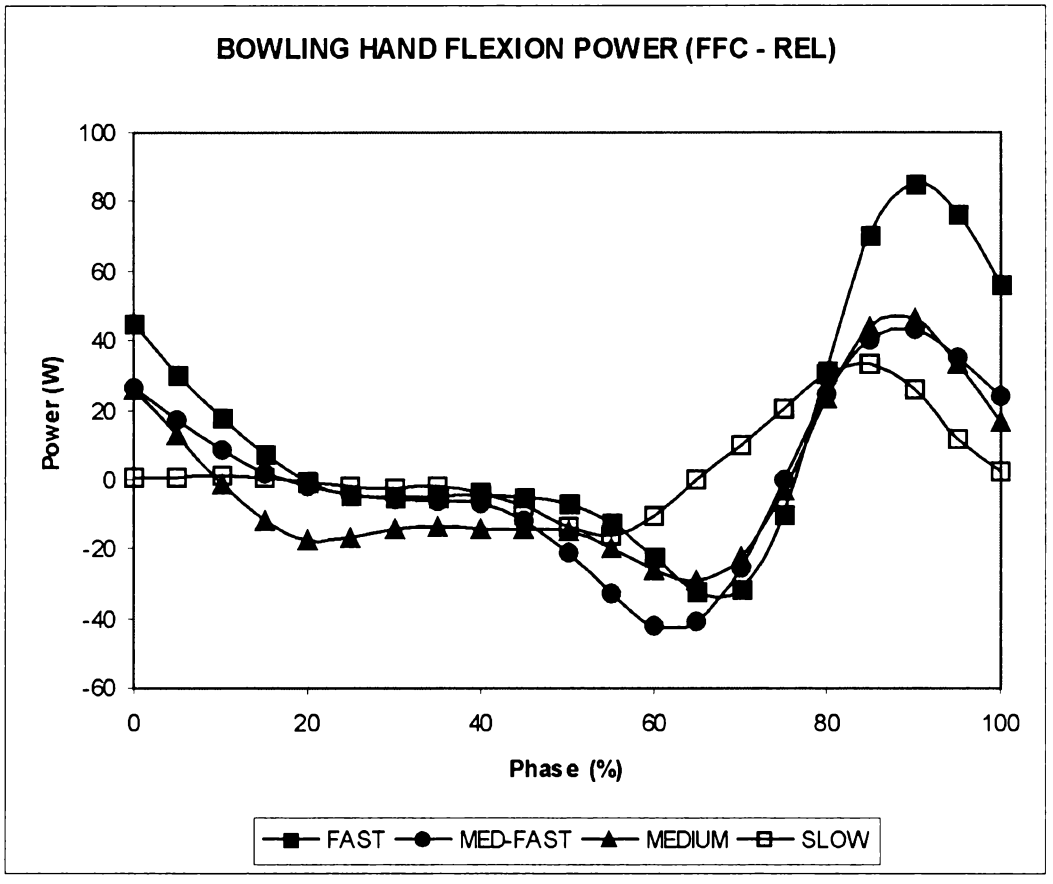

Figure 4-54: Ensemble averages of bowling hand flexion power. VR: 0.55 (fast), 0.81 (med-fast), 0.59 (medium), 0.92 (slow).

The period of hand extension torque varied with the bowling group: fast, 50-75% PC; med-fast, 40-65% PC; medium, 30-75% PC; slow, 15-60% PC (Figure 4-55). The mean extension torques during this period were highest for the fast and med-

fast groups followed by the medium group, and then the slow group: fast, -0.86 Nm; med-fast, -0.96 Nm; medium, -0.67 Nm; slow, -0.43 Nm. During these periods of negative torque the corresponding power was also negative. The mean power during this time was least negative for the slowest group: fast, -19.0 W; med-fast, -25.9 W; medium, -17.3 W; slow, -5.9 W. A negative torque and a

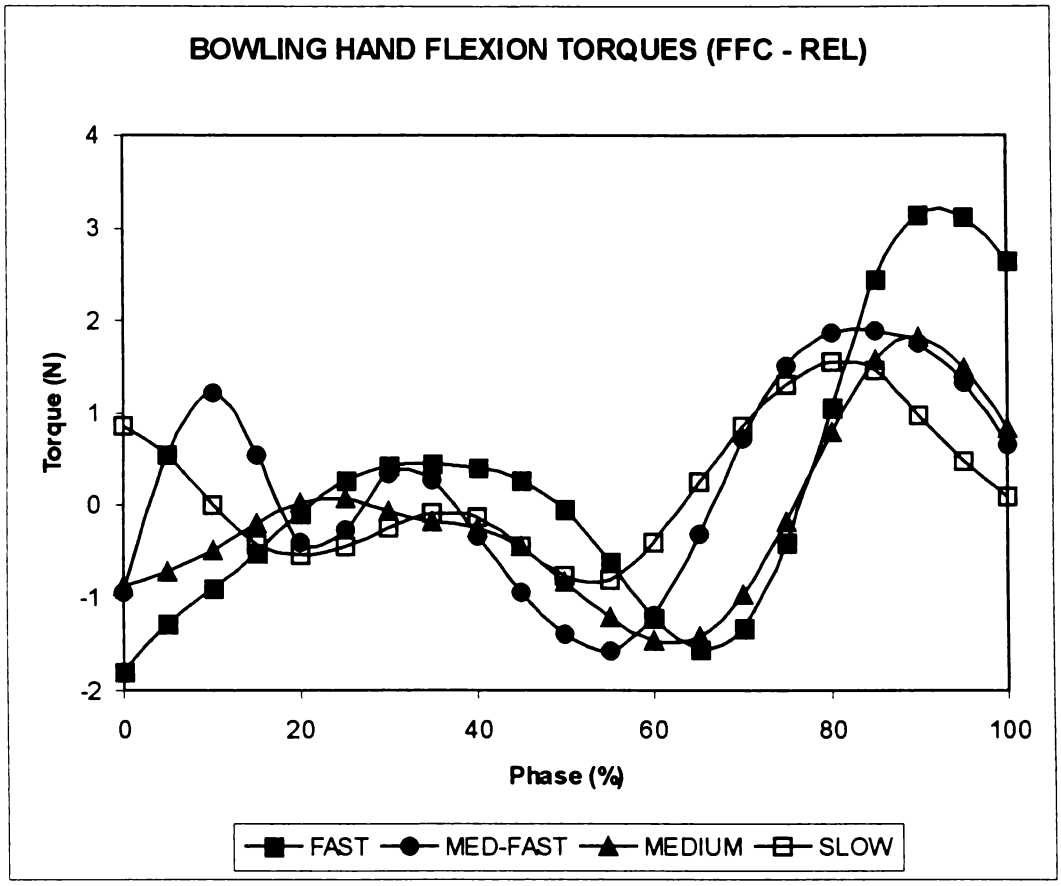

Figure 4-55: Ensemble averages of bowling hand flexion torque. Positive is defined for flexion. VR: 0.60 (fast), 0.93 (med-fast), 0.63 (med), 0.93 (slow).

negative power indicate that during this period the extension torque was controlling or resisting hand flexion, most strongly so by the faster bowling groups. This controlled flexion was followed by a period of positively increasing torque and power, which only decreased shortly prior to ball release. Both torque and power curves changed at similar rates, indicating that at least some of the increase in flexion power was caused by the increase in flexion torque. The mean active flexion power was highest for the fast group, followed by the med-fast and medium group, and then lastly the slow group: fast, 63.9 W; med-fast, 27.8 W; medium, 32.6 W; slow, 19.2 W. The corresponding flexion torques also increased

with speed of bowling group: fast, 2.48 Nm; med-fast, 1.39 Nm; medium, 1.30 Nm; slow, 0.87 Nm.

The importance of hand flexion in bowling technique has been the subject of much conjecture. In the past, scientific evaluation was limited to velocity contribution to ball speed. Davis and Blanksby (1976b) and Elliott et al. (1986) reported a percentage velocity contribution of the hand to ball speed of only 5%. However, Bartlett et al. (1996) stated that this might still make up the difference between bowling speed groups. By studying the powers and torques of hand flexion, it is apparent that the faster bowlers in general tended to control the flexion of their hand from approximately half-way during the phase for a short period of about 25% PC. This was followed by a period of relatively strong active flexion until ball release. The slower bowlers tended to start controlling the flexion of their hand earlier, maintained this for a longer period of time than the faster bowlers (approximately 45% PC), and then followed this up with a lower degree of active flexion. However, it was difficult to measure kinematic data very accurately due to the close proximity of the markers, the approximation of the hand segment definition, and perhaps some marker movement, which may have contributed to the relatively high VRs, making it difficult to establish significance between the groups. Still, it is worth noting that the hand flexion angular velocity contribution to ball speed was roughly approximated as 5% across all bowling groups, but the production of even this small hand velocity contribution appeared to elicit a different mechanical response from the bowling speed groups.

4.6.6 Non-bowling (front) arm

During the power period, the front arm is rapidly adducted (i.e, vertically adducted) and extended (Burden & Bartlett, 1990a). The motion of the front arm is considered to be an important aspect of bowling technique. It has been traditionally recommended that the front arm be initially used as an aiming device, and then accelerated into the side to assist in the rotation of the bowling arm (Marylebone Cricket Club, 1976). The emphasis is clearly on actively pulling down the front arm into the side as quickly as possible.

The front upper arm torques were quite variable, and it was therefore difficult to establish any significant differences between bowling groups (Figure 4-56). The lowest variability among the curves was for the fast group (VR = 0.63). In this group, the front upper arm torque was negative from 0-10% PC, indicating a vertical adduction torque, before becoming positive and remaining so until 50% PC. After this the torque became negative again, and continued to increase negatively until 78% PC, before then decreasing negatively as ball release approached. The medium-fast and slow groups were similar in phase variation, but had lower magnitudes. The medium group differed from the other groups in that the front upper arm exerted a vertical abduction torque from 0-64% PC before applying a vertical adduction torque.

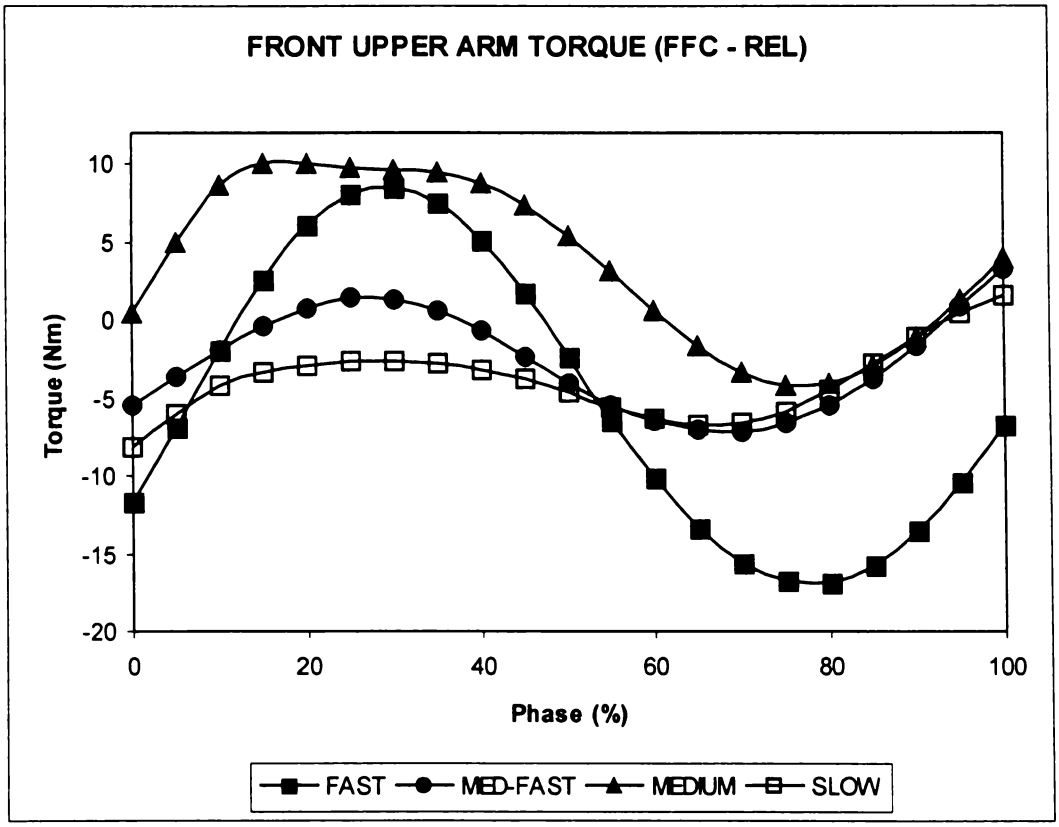

Figure 4-56: Ensemble averages of front arm upper arm torques about the local *Z*-axis, which represents a vertical abduction/adduction motion. Positive is defined for abduction. VR: 0.63 (fast), 1.00 (med-fast), 0.88 (medium), 1.00 (slow).

Probably the most important difference between the groups occurred during the last 20% of the phase. The torque curves for the medium-fast, medium, and slow groups converged at ball release so that the front upper arm torque approached

zero. This is what would be expected if the upper arm was becoming braced into the side, so that it could theoretically act as a block (as in various throwing events) to retard the motion of the trunk, and subsequently induce an angular acceleration of the bowling arm. However, this principle did not seem to apply to the same extent for the fast group, which retained the highest level of front upper arm vertical adduction torque at ball release.

The front upper arm torques show that there was a pulling down action of the front upper arm during *certain* phases. Despite the high VRs of all but the fast group, there was a notable presence of vertical adduction torque early in the phase that acted to accelerate the front arm downwards. However, a study of the corresponding power curves confirmed that a portion of the front upper arm motion was also controlled (i.e. below the solid line) (Figure 4-57). This was particularly true of the fast and medium groups, which controlled their front upper arm motion from 12–45% PC and 3–59% PC, respectively. The med-fast group motion also had a period of controlled motion, though not so markedly, from 20 – 39% PC. Only the slow group used an active front upper arm motion throughout the phase. However, there was high variability within the power curves of this group, and so the ensemble average masked the fact that within the slow group three of the seven bowlers also had a controlled period of the front upper arm motion. Therefore, the traditional teaching is partially correct if it deals with the motion of the front *upper arm.* There is evidence that in periods the vertical adduction of the front upper arm was performed actively, most powerfully during the beginning and latter half of the phase.

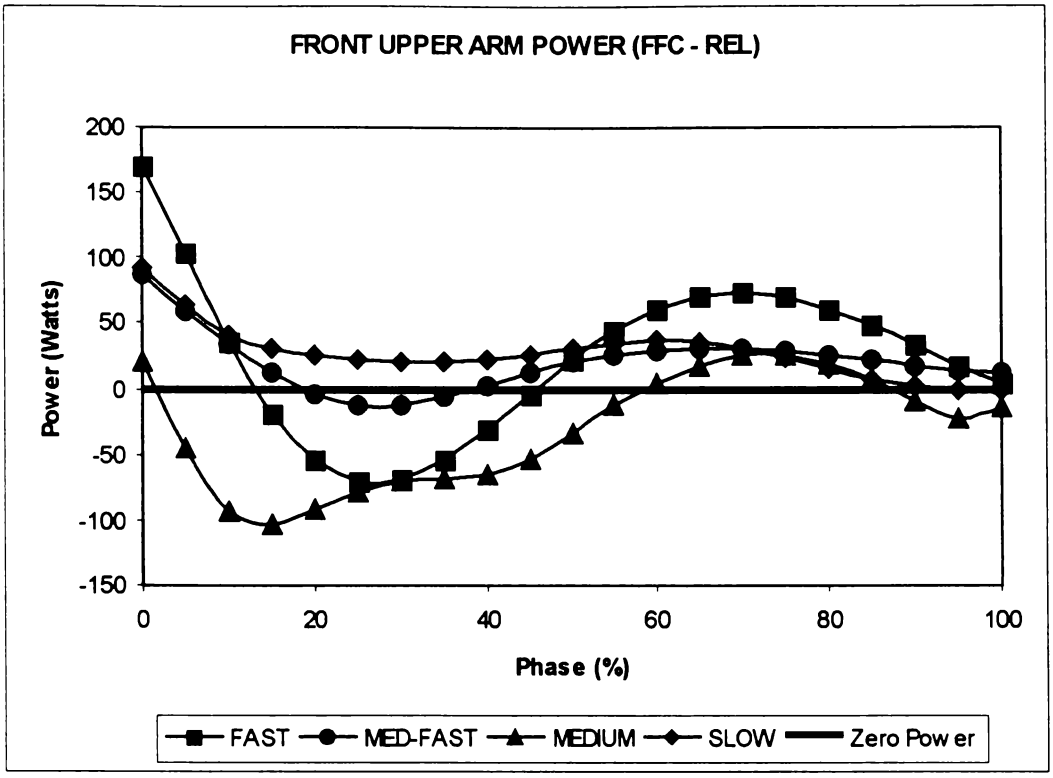

Figure 4-57: Ensemble averages of front arm upper arm power about the local *Z*-axis, which represents a vertical abduction/adduction motion. VR: 0.82 (fast), 0.57 (med-fast), 0.99 (medium), 1.00 (slow). The zero power line is shown to differentiate between active and controlled motion.

Front arm motion also involves the use of the forearm. Front forearm torques were always positive, therefore acting in the direction of extension, and reached a maximum value between 10-25% PC, before then decreasing almost linearly to a low value at ball release (Figure 4-58). There was some separation between the forearm torque curves of the bowling speed groups. The mean front forearm extension torque was highest for the fast group, and lowest for the slow group: fast, 16.2 ± 0.4 Nm; med-fast, 14.2 ± 1.8 Nm; medium, 14.3 ± 1.9 Nm; slow, 9.9 ± 1.92 Nm.

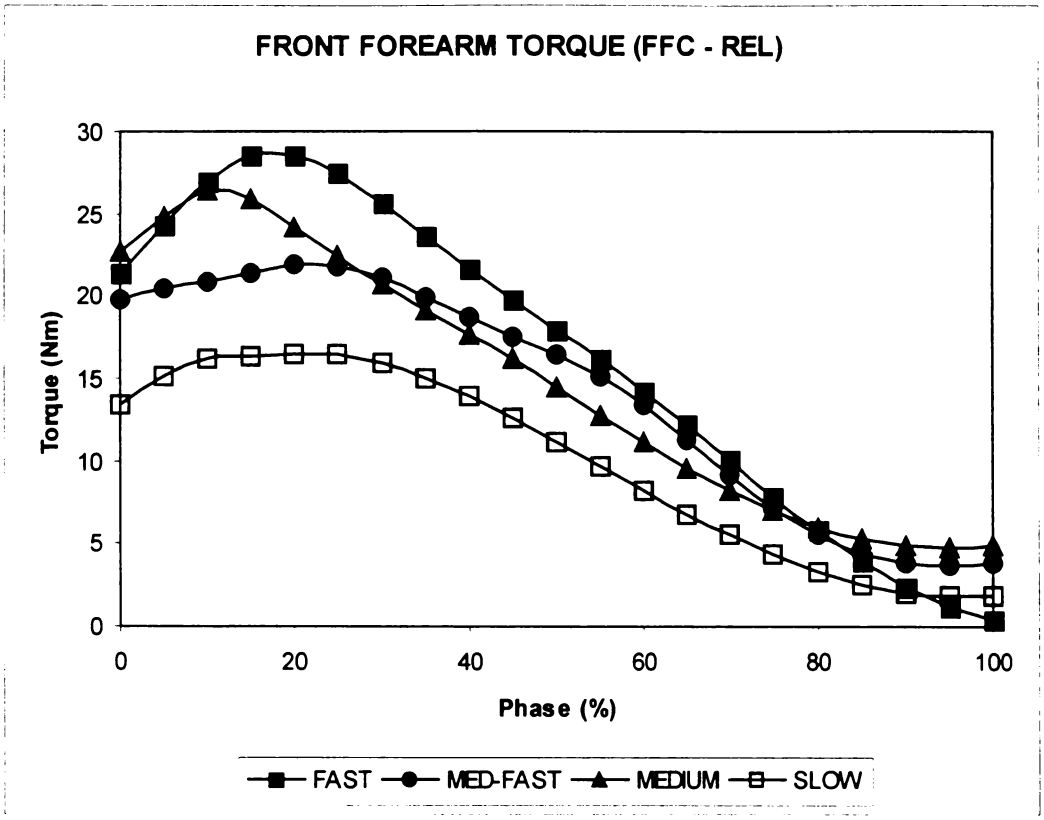

Figure 4-58: Ensemble averages of front arm forearm extension torques about the local *Z*-axis. Positive is defined for extension. VR: 0.39 (fast), 0.79 (med-fast), 0.63 (medium), 0.66 (slow).

A study of the corresponding front forearm powers show, with the exception of the medium group, that for the majority of the phase the power was negative (Figure 4-59). This means that much of the front forearm motion was controlled. The front forearm extension torque acted to reduce the rate of flexion angular velocity. The medium-fast and medium groups controlled forearm flexion throughout the entire phase. The fast group did the same for the first 47% of the phase, followed by only a small active flexion for the remainder of the phase. The only real exception was the medium group, which controlled the motion for only the first 13% of the phase, before then producing an active flexion until ball release. Further study of the medium group shows that 50% of the sample produced significant active power for a majority of the phase. Also, two of these bowlers reported that they had been coached to pull the front arm as fast as possible into the side. Interestingly, these were the two that registered the highest active forearm flexion powers.

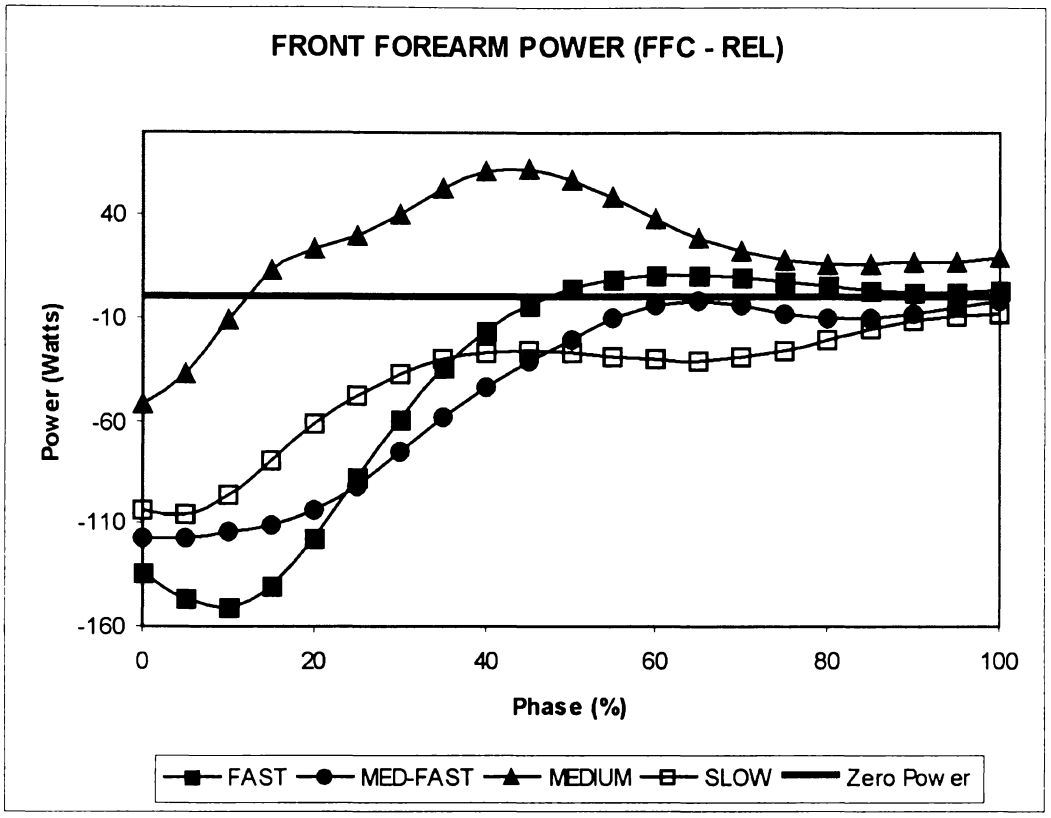

Figure 4-59: Ensemble averages of front arm forearm power about the local z-axis or flexion/extension axis. The zero power line is shown to differentiate between active and controlled motion. VR: 0.36 (fast), 0.60 (med-fast), 0.85 (medium), 0.91 (slow).

In summary, the advice to accelerate the front elbow into the side to assist bowling arm speed should be re-assessed. This theory was formulated based on visual observations and some kinematic analyses of bowlers. The dynamics and kinetics treatment that was presented here shows that front arm motion of the bowlers in this study was not a simple pulling action, and that the upper arm and forearm had different actuation strategies. The front upper arm was actively brought down initially, but then underwent a controlled period before once again being actively pulled until ball release. Therefore, a conscious effort to pull the front upper arm downwards as fast as possible could disrupt this sequencing pattern, which was most representative of the fast group in this study. Also, the front forearm produced an extension torque that controlled the rate of elbow flexion (Figure 4-60). As measured for the two bowlers in the medium group, who were attempting to accelerate the elbow down into the side as fast as possible, a premature and active bending of the elbow may have caused both the front upper arm and front forearm torques and powers to differ considerably from

those of the faster bowlers. At the present time, sound advice would be to keep the front arm as high as comfortably possible, perhaps pulling down slightly with the upper arm at the moment of front foot contact, while retaining a good angle at the elbow, and then letting the front arm (i.e. upper arm and forearm) respond naturally to the movements of the interacting segments.

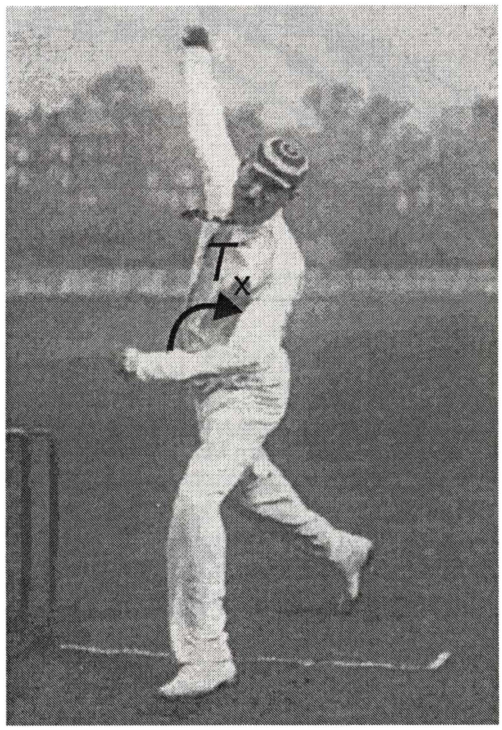

Figure 4-60: Fred Spofforth (Australia) at a position corresponding typically to that of 65-75% PC of the power phase would have probably exerted forearm extension torques (T_x) to retard the rate of forearm flexion.

4.6.7 Rear Leg

An active thrust of the rear leg forwards bent at knee is believed to generate power that can be utilised to produce high ball release speed. Coaches often talk about bringing the right thigh or hip forwards with a bent knee to bring the trunk around prior to the release of the ball (Gover, 1980). The only studies of this motion to date have been kinematic, which have examined the temporal sequencing and linear velocity contribution of the rear hip joint (Stockhill & Bartlett, 1994; Elliott et al., 1986; Davis & Blanksby, 1976a). These studies show that there is a correlation of the rear hip joint velocity with ball release speed; therefore, in part, reinforcing the coaching perspective. However, there has been no analysis of the thigh and shank movement that occurs in conjunction with the linear motion of

the hip joint. Also, segment dynamics or kinetics have not been performed to test how this motion occurs or whether it is an active or controlled motion.

The most powerful motions of the rear thigh were about the flexion/extension axis. The ensemble averages of the thigh flexion torques for each of the bowling groups were positive (Figure 4-61). Though there were high VRs, making it difficult to establish differences between the groups, the groups were separated, not sequentially from slow to fast, but with the fast group having the lowest flexion torques throughout the phase. In fact, despite the variability among the subjects, almost all of it was in the positive region: only four cases out of the thirty four samples collected had significant periods of negative thigh flexion torque. Also, the general trend for all groups was for the torque to decrease over the phase.

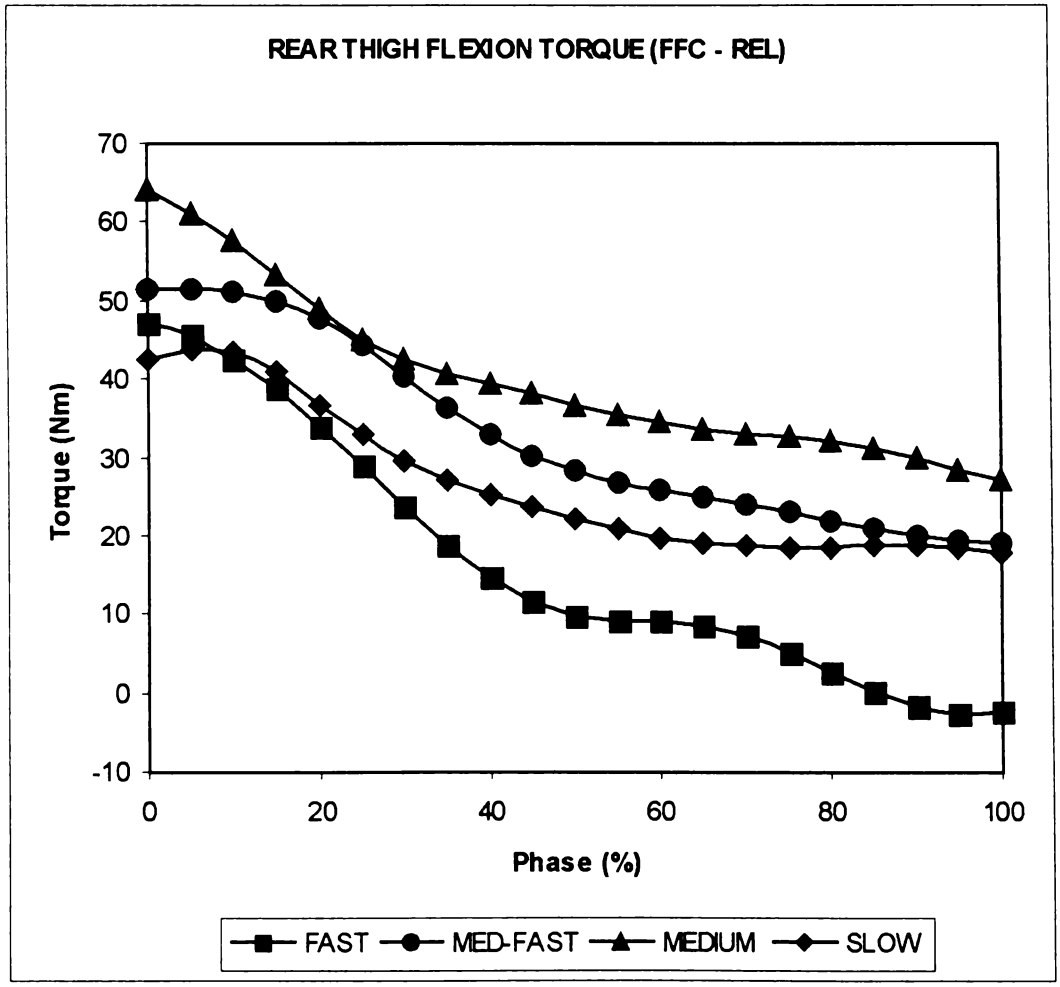

Figure 4-61: Ensemble averages of rear thigh flexion torque. Positive is defined for flexion. VR: 0.99 (fast), 0.93 (med-fast), 1.00 (medium), 1.00 (slow).

The large variability in these torque curves among the bowling groups indicates that there was some scope for variation in the application of thigh flexion torque. Some bowlers used a small thigh flexion torque initially, but then maintained this value more or less throughout the phase. A less common strategy was to start with a thigh extension torque, and then reduce it during the phase. However, it is plausible that there is an optimal phase-variant strategy of applying thigh flexion/extension torque. Nineteen of the thirty-four bowlers initially had relatively high thigh flexion torques, which decreased progressively through the phase. This was the most common strategy, and interestingly the percentage of bowlers that used this increased with speed of bowling group: slow, 25%; medium, 50%; med-fast, 70%; fast, 75%.

The average thigh flexion/extension powers for all groups were positive: fast, 27.7 ± 9.8 W; med-fast, 84.4 ± 26.7 W; medium, 86.7 ± 30.7 W; slow, 53.8 ± 20.3 W. The average power for the fast group was lower than the other groups because two of the bowlers in the sample, after having positive powers for the first 40-50% of the phase, became increasingly negative until ball release. In general, thigh flexion power was positive from about 15-85% PC. However, from approximately 0-15% PC, there was a strong negative power, because the thigh flexion torque was acting to reduce the high rate of hip extension. Therefore, the theory of thrusting the rear hip forwards is not consistent with this data. The extension of the rear hip occurred because during early FFC, the back foot was in contact with the ground, while the body was moving over the front leg (Figure 4-62). The fact that the negative powers were high suggests that it was important to control this motion.

Thigh adduction torques and powers were also positive for most of the phase, and followed a similar phase variation to that of hip flexion: positive initially and then decreasing as REL was approached. Expressing the mean thigh adduction torques and powers as a percentage of the corresponding thigh flexion values shows that the thigh adduction was not as large as thigh flexion: (fast: power (77%), torque (72%); med-fast: power (30%), torque (43%); medium: power (19%), torque (40%); slow: power (12%), torque (30%)). The relatively high percentage for the fast group was due to two bowlers in the sample having high negative thigh

adduction powers and torques during the latter part of the phase, which therefore significantly reduced the average value. In general, there was a steady active adduction of the rear thigh by all the bowlers. Also, the mean adduction power was slightly less for the medium and slow groups, so it could be that slower bowlers produced less active adduction of the rear thigh than the faster bowlers.

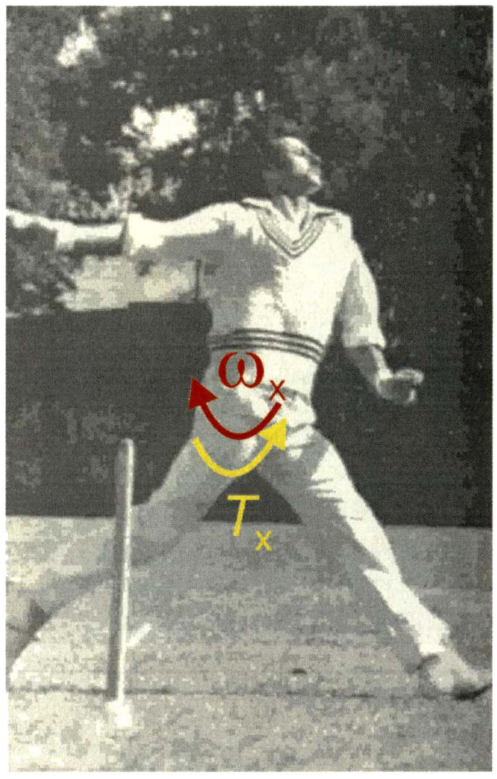

Figure 4-62: Richard Hadlee (New Zealand) during early contact before the front foot has been planted. During this early stage the thigh extension angular velocity (ω_x) is controlled by a strong thigh flexion torque (T_x). [From B. Willis. 1984. *Fast Bowling with Bob Willis*. Willow Books, London]

The ensemble averages of the rear shank torque about the local *X*-axis show that after a short initial period, the torques became increasingly negative (extension torques) (Fig. 4-63). In fact, the mean shank extension torque increased with bowling group speed: fast, -13.6 ± 5.7 Nm; med-fast, -11.0 ± 4.1 Nm; medium, -7.5 ± 3.7 Nm; slow, -6.0 ± 2.7 Nm. Also, there was some difference in the phase variation of shank torque between the fast group and the other groups, in particular between the fast and slow group. The fast group had an extension torque for the first 20% PC (mean, -4.5 Nm), whereas for this same period the med-fast and medium groups registered small flexion torques with means of 1.4

Nm and 2.3 Nm, respectively. During this period, the slow group had an even higher mean flexion torque of 15.5 Nm. Finally, in the last 40% of the phase, the shank extension torque of the fast group increased at a markedly higher rate than the other groups. In general, the shank exerted extension torques about the knee joint for the majority of the phase.

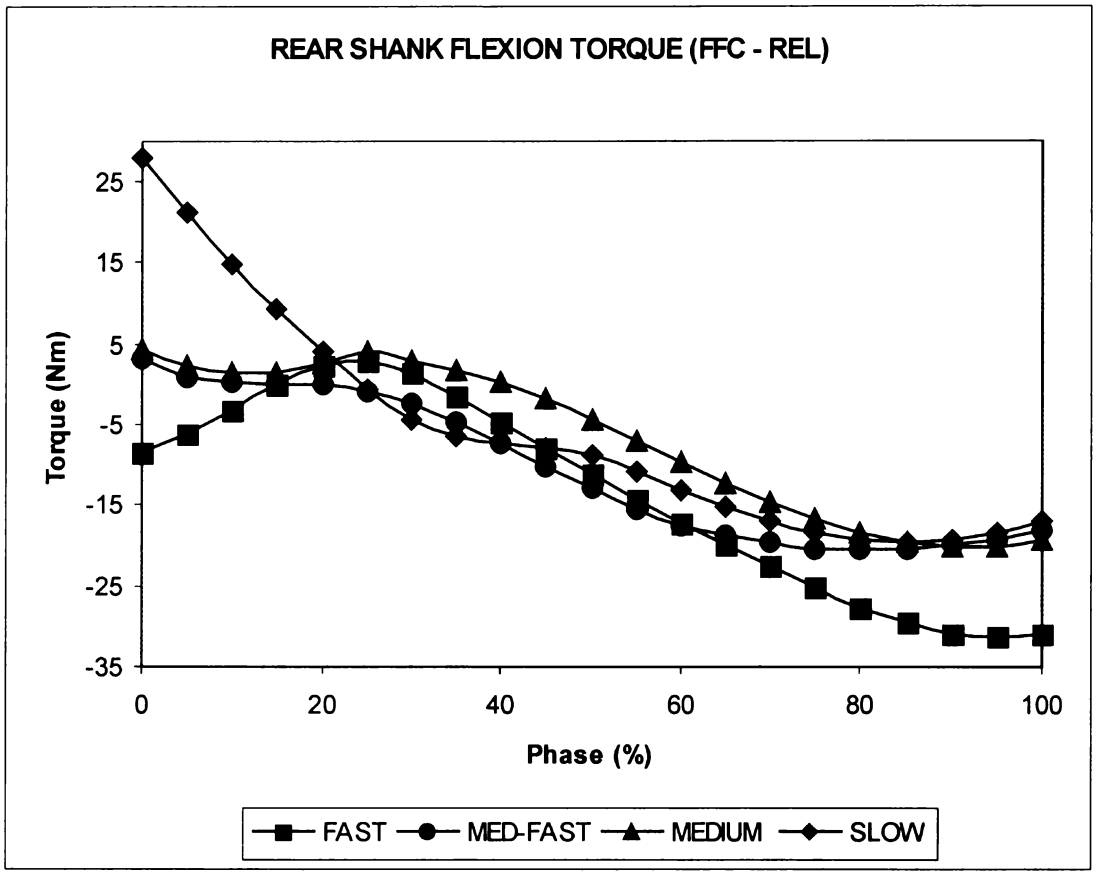

Figure 4-63: Ensemble averages of rear shank flexion torque. Positive is defined for flexion. VR: 0.82 (fast), 0.84 (med-fast), 0.75 (medium), 0.60 (slow).

To test a traditional theory that the rear knee needs to actively flex as the thigh is flexed and adducted, the shank powers were calculated. By comparing the powers with the torques, the type of motion throughout the phase was determined (Figure 4-64). Rear shank flexion did occur during the delivery stride as the thigh was flexed and adducted. However, the magnitude of the flexion angular velocity was small, and most of it was not active. Two cases are worth mentioning specifically. The fast group did not actively flex the rear shank at all. Instead, flexion was controlled from 0-65% PC, after which there was a controlled

extension of the shank. All the other bowling groups had periods of active flexion and active extension. Therefore, the rear knee did flex during delivery stride, but the fast group showed that there was no need to actively do so, and that for the other groups, the relatively short period of shank flexion was followed by a period of active extension.

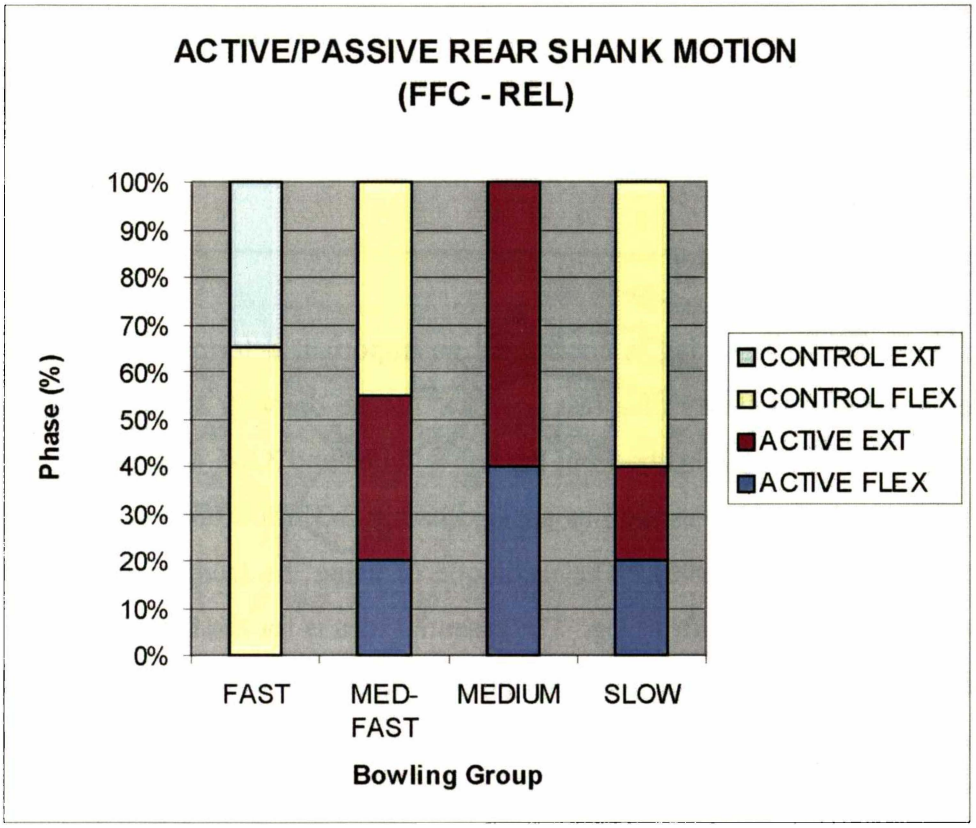

Figure 4-64: Active and controlled motion cycles for rear shank during FFC to REL. Only a small portion of the phase involved active shank flexion.

Rear leg action is considered important in bowling technique. Coaching literature has emphasised the importance of thrusting the rear leg forward with a bending of the knee. These results only partially confirm this view. The rear hip was actively flexing and adducting, most strongly at the beginning of the phase. However, this is quite different to "thrusting forward" in the direction of the target or batter. Flexion of the hip while the rear foot is grounded and the rear leg under load would initiate hip or lower trunk rotation to the left. Perhaps this rotation is promoted in the same way as the trailing leg in discus (Hay, 1993); however, with a much shorter radius, and therefore with much less effect. It could be that as the knee bends and is brought closer to the body, mostly as a result of a controlled

movement, the moment of inertia of the body is reduced about its longitudinal axis, and by means of the conservation of angular momentum, cause the trunk to rotate faster. Also, the fast group did not support the case for an active flexion of the knee, and the slower groups actively flexed the knee for only a short initial period. Rear leg motion is complex. It involves a combination of movements that are active or controlled depending on the position in the phase cycle, and this varies with bowlers. To prescribe a thrust forwards of the rear thigh while bending the knee is an over simplification and may consequently diminish the performance of a bowler.

4.6.8 Front Leg

The action of the front leg is considered an important determining factor in the speed and overall quality of a fast bowler. As the delivery stride proceeds and front foot contact is made, the front leg has to withstand 3.8-6.4 times bodyweight in the vertical direction as well as approximately 2-3 times body weight braking force (Bartlett et al., 1996). The technique of using the front leg effectively is known as "bracing" the front leg. The essential idea is for the front leg to act as a lever over which the upper body can propels itself. Traditionally, bowlers have been instructed to keep the front leg stiffly braced throughout the delivery stride (N.W.S.C.A., 1966). However, early biomechanical studies relaxed this criterion when it was observed that the front leg is used in a variety of ways to attenuate the ground reaction forces (Elliott et al., 1986). Some bowlers slightly flex the front knee upon ground contact, yet others keep the knee fully extended. Though there may be a slight mechanical advantage in keeping the front leg fully extended during front foot contact, the lack of any flexion to absorb the impact forces could place excessive strain on the knee joint (Mason et al, 1989). Whatever the case, it is generally acknowledged that efficient use of the front leg, which essentially consists of the flexion and extension of the thigh and shank segments, is an important part of bowling technique. However, there has been no published account of the mechanics required to achieve this.

The means of the ensemble average curves of front thigh flexion torque show that the thigh had an extension torque: fast, -119.0 ± 21.3 Nm; med-fast, -327.9 ± 43.9

Nm; medium, -186.7 ± 30.5 Nm; slow, -235.5 ± 42.6 Nm. It is difficult to find any pattern in the ensemble average curves with respect to bowling group speed, apart from the fast group having the lowest hip or thigh extension torques throughout most of the phase (Figure 4-65). The mean of the whole sample (solid curve) shows that in general the trend for thigh extension torque was to increase rapidly during early front foot contact, then decrease for a short period before remaining relatively constant.

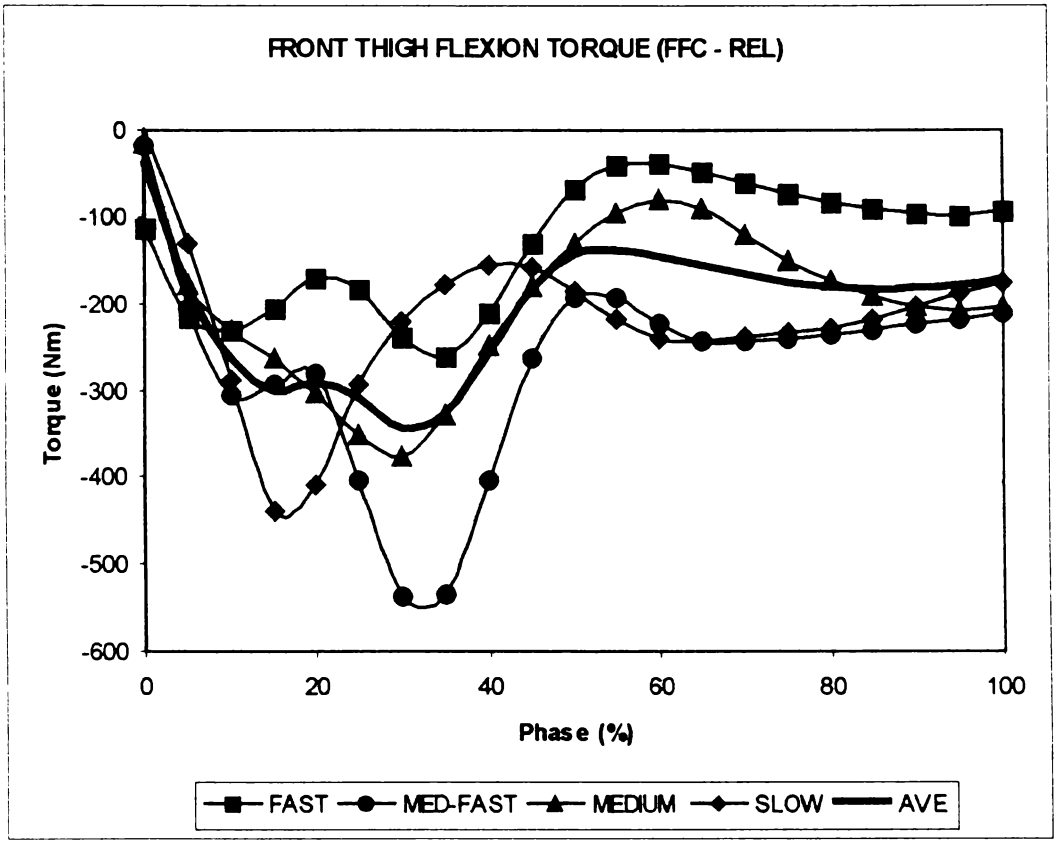

Figure 4-65: Ensemble averages of front thigh flexion torque. The mean of the total sample is represented with the solid black line. Positive is defined for flexion. VR: 0.77 (fast), 0.64 (med-fast), 0.25 (medium), 0.58 (slow).

The thigh flexion/extension power curves had relatively large VRs, and the differences between the curves were difficult to relate to bowling group speed. Therefore, the mean of the whole sample (solid curve) was used to generalise the process of thigh motion (Figure 4-66). This shows that the thigh power was generally positive throughout the phase with an initial sharp increase in power during early FFC from about 0-10% PC, a gradual decrease from about 10-55%PC, before a final increase to reach a maximum value at ball release. The

positive power in conjunction with the negative torque indicates the front thigh was actively extending throughout the phase. It may be significant that the mean thigh power of the fast group was highest for the fast group over the first 30% PC: fast, 463 W; med-fast, 152 W; medium, 322 W; slow, 144 W.

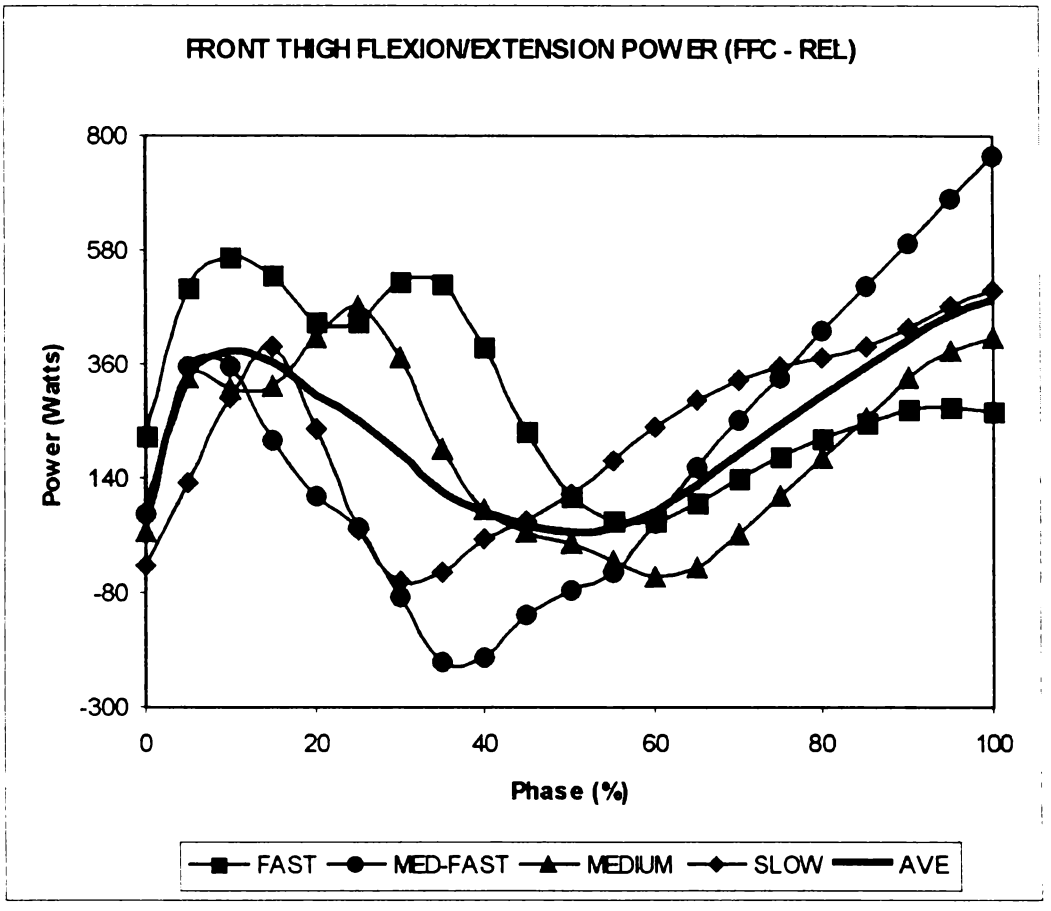

Figure 4-66: Ensemble averages of front thigh flexion/extension power. Mean of total sample (solid curve). VR: 0.86 (fast), 0.78 (med-fast), 0.52 (medium), 0.83 (slow).

In general, while the front thigh was extending, the front shank, apart from a short initial period from FFC to about 5% PC, had an extension torque, reaching a maximum value approximately at 20% PC (Figure 4-67). Towards the end of the phase (70-100 % PC) the fast group produced a small shank flexion torque. The medium group similarly produced a shank flexion torque, but it occurred later in the cycle from 90% PC to REL, and was of a smaller value. The other two groups had shank only extension torques throughout the phase.

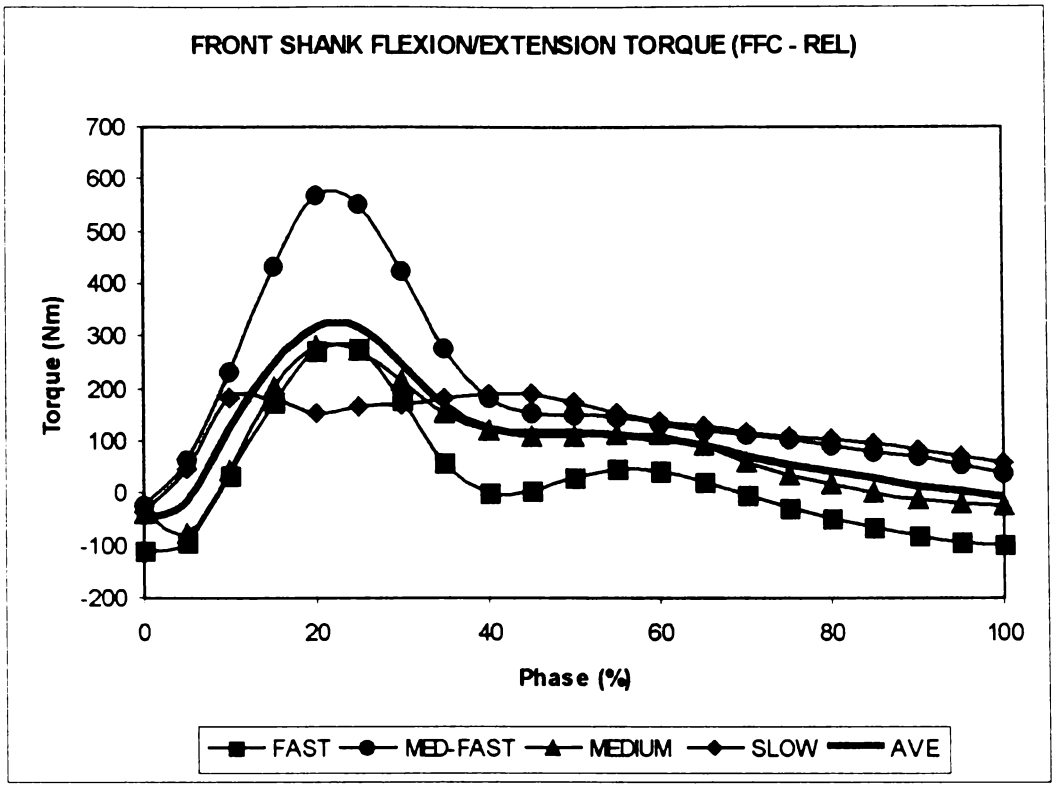

Figure 4-67: Ensemble averages of front shank flexion/extension torque curves. Positive is defined for flexion. VR: 0.57 (fast), 0.77 (med-fast), 0.58 (medium), 0.98 (slow).

The corresponding shank power curves reveal that the front shank was flexing throughout the phase, but only during 0-5% PC was this motion active (Figure 4-68). Otherwise shank flexion was a controlled motion: the phase period of extension torque (which was positive) corresponding with the period of negative power, therefore yielding a negative shank angular velocity, which was defined as flexion. The only exception was the fast group, which changed from a controlled shank flexion to an active flexion during the period 70% PC to REL. The fast group also differed from the other groups in that it had the lowest mean shank power: fast, -67 W; med-fast, -390 W; medium, -313 W; slow, -384 W. The shank, therefore, generally had an extension torque that acted to reduce the rate of shank flexion during delivery.

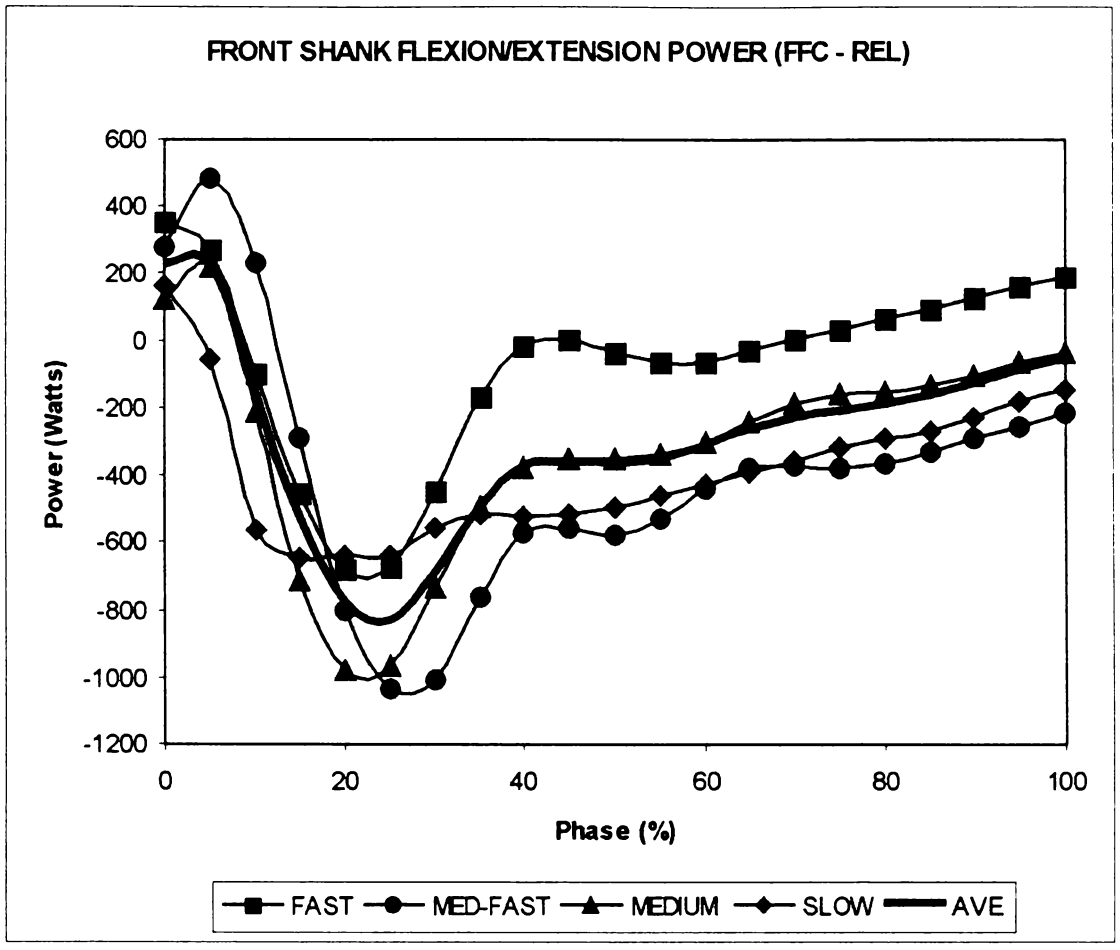

Figure 4-68: Ensemble averages of front shank flexion/extension power curves. VR: 0.68 (fast), 0.65 (med-fast), 0.75 (medium), 0.91 (slow).

In summary, these results identified certain key mechanical aspects of front leg action during the FFC - REL phase. Thigh extension was an important active motion, particularly during the early stages of FFC (Figure 4-69). The development of strong gluteal muscles is probably advisable based on the powerful 'pulling-back' action needed to extend the thigh while large ground reaction forces are transmitted through the front leg. However, brute strength and power are not alone sufficient to guarantee an effective front leg action. Analysis of the fast group shows that though these bowlers developed the highest thigh extension power, they also generated the lowest thigh extension torques. This suggests that a proportion of the thigh extension angular velocity was generated through the sequential motion of interacting segments, and therefore a sense of timing is important. The front shank was generally flexing throughout the phase, but a shank extension torque controlled the rate of this motion. Therefore, despite different actuation strategies, the combination of thigh extension and shank

flexion angular velocities generally acted keep the front leg relatively straight and firm during FFC. By comparing the ratio of mean thigh extension angular velocity over mean shank flexion angular velocity, it was found that the fast group had a much lower value than the other groups: fast, 1.10; med-fast, 0.39; medium, 0.26; slow, 0.48. This suggests that the front leg action of the fast group differed considerably from that of the other groups in that the front leg was overall straighter and firmer during delivery stride. However, it still could not concluded that the bowler should keep the front leg rigidly straight throughout delivery stride, because the fast group had an active shank flexion during the last 30% PC.

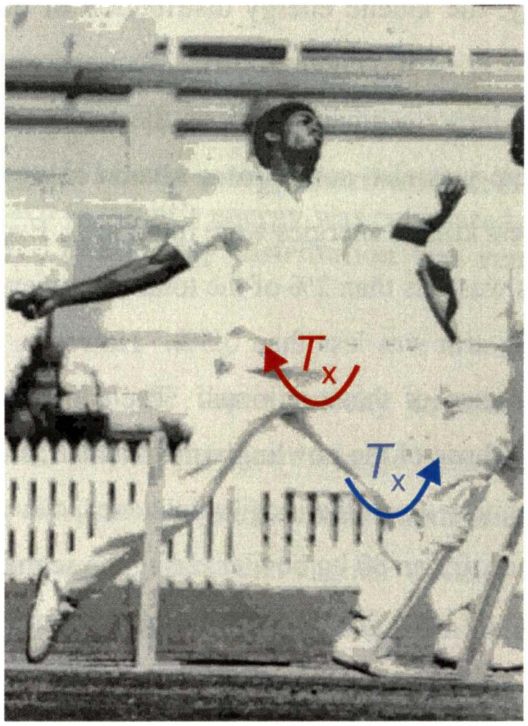

Figure 4-69: Michael Holding (West Indies) during front foot contact when a combination of a strong hip extension torque (red) and shank extension torque (blue) maintains a firm front leg. [From Mallett, A. 1982. *100 Cricket Tips*. Rigby Publishers, Adelaide]

4.7 SEGMENTAL KINETIC ENERGY

The sequencing of movements in bowling has not been widely reported (Bartlett et al., 1996). Though there have been studies that have examined the percentage contribution of joint velocities to ball release speeds (Davis & Blanksby 1976b; Stockhill & Bartlett, 1994), the temporal relationships between segments has not

been treated in detail. The use of segment kinetic energies to investigate the possible sequencing schemes used by bowlers has not been done previously.

4.7.1 Segmental Sequencing of Bowling Action

Most of the kinetic energy produced by the bowling action was linear. The mean rotation kinetic energy for the upper arm, forearm, upper trunk, and lower trunk was a small percentage of their corresponding linear values (fast group): 3.9%, 1.7%, 15.4%, and 8.7%, respectively. Similar percentages were found for the other bowling groups. By expressing segmental kinetic energy as a percentage of the total body energy, the kinetic energy distribution of the linear and rotation energies could be clearly seen (Figure 4-70). Most energy was expended in the linear motions of the larger segments such as the lower trunk, upper trunk and thigh segments. There was also some linear kinetic energy of the bowling arm segments. The smallest kinetic energies were rotational. Even the rotation energy of the trunk segments was less than 2% of the total energy expended. The rotation energy of the bowling arm was less than 0.5%. However, these percentages do not reflect the importance of these motions. The moments of inertia of these segments, particularly those of the bowling arm are small, and even small rotation kinetic energies, especially about the longitudinal axes, can produce large angular velocities. For instance, for an 80 kg bowler, using the segment inertia parameters of the upper arm from de Leva (1996), only 5 J of rotational kinetic energy about the transverse axis (e.g. horizontal adduction axis) is able to produce 23.14 rad s^{-1}. Such a value is comparable with the upper arm angular velocities measured in this study. A similar argument could explain the relatively small trunk rotation energies, despite the importance of trunk rotation in the bowling action. On the other hand, the segmental kinetic energy distribution does show that bowling requires the production of large amounts of linear kinetic energy, establishing the importance of generating a sufficient linear momentum by means of the run-up, and maintaining as much of this during the delivery stride.

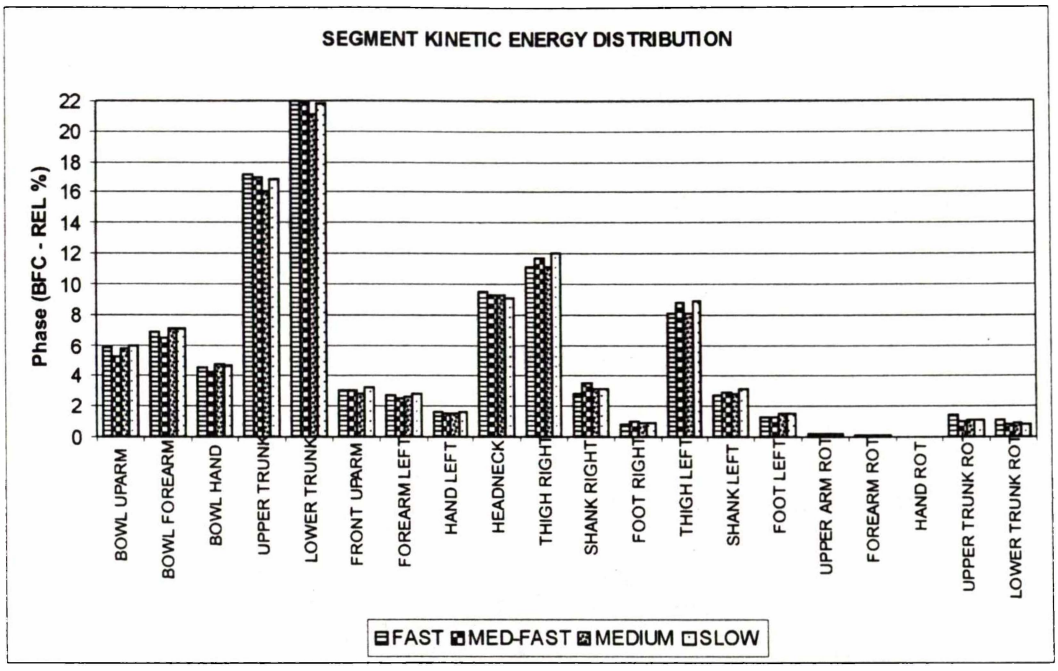

Figure 4-70: The segmental kinetic energy distribution from BFC to REL for all bowling groups. Each segment's energy was calculated as a percentage of the total body energy. The energy distribution was remarkably uniform across bowling groups.

Another important fact is that the linear velocity contribution to ball speed requires much more energy than to produce the same contribution from rotation. For instance, if the same 80 kg bowler with an arm length of 0.7 m delivers a ball at 35 m s^{-1}, and there is an equal linear and angular velocity contribution of the upper bowling arm to ball speed, then 82.3 J of linear kinetic energy is produced by the upper arm as opposed to just 2.9 J of rotation kinetic energy. Bowlers, therefore, produce much more linear kinetic energy than rotation kinetic energy because (i) there is a linear velocity contribution to ball speed and (ii) it takes only a relatively small amount of rotation kinetic energy to produce substantial angular velocities.

Having ascertained that both linear and kinetic energy are important in the delivery of a ball, the real purpose of these calculations was to determine the overall scheme of segmental sequencing. The sequencing pattern does not change significantly with the speed of bowling group. To quantify this pattern, the time of maximum energy from the segment kinetic energy curves was used as a marker to determine sequencing order for the fast group (Figure 4-71). The upper and

lower trunk started off with high linear kinetic energies by means of the initial momentum generated by the run-up. These energies slowly reduced while the front upper arm was increasing slightly to reach a maximum value of 70.6 J at 25% PC. As front foot contact approached (i.e. at 50% PC), the linear kinetic energy of the lower trunk reached a peak at 39% PC, which was closely followed

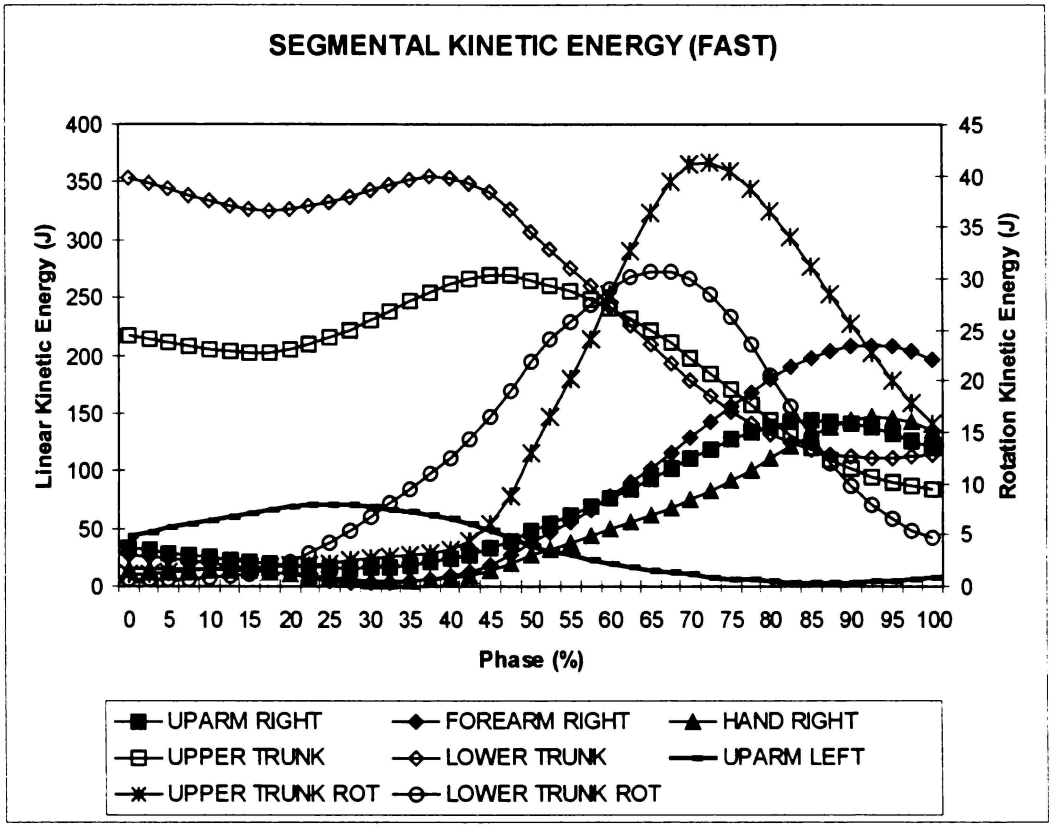

Figure 4-71: Kinetic energy of major segments in bowling action from BFC to REL. The curves are not calculated to time scale: 0% to 50% PC represents BFC to FFC, and 50% PC to 100% PC represents FFC to REL, even though these periods were not generally of the same duration. Linear kinetic energy was calculated for bowling upper arm, bowling forearm, bowling hand, upper trunk and lower trunk. Rotation kinetic energy was also calculated for the upper and lower trunk. Rotation kinetic energy for the other segments was small. Note that rotation energy refers to the total rotation energy of a segment, i.e. the sum of the rotation kinetic energy of a segment about each of its local body-fixed axes.

by the upper trunk, reaching a peak linear kinetic energy at 46% PC. Meanwhile, as FFC was approached, the front upper arm was reducing its energy, and the lower trunk rotation kinetic energy was increasing rapidly. Therefore, in summary, from BFC to FFC (i.e. 0-50% PC), the front upper arm kinetic energy, lower trunk linear kinetic energy, and upper trunk linear kinetic energy had

already reached their maximum values, while the lower and upper trunk rotation kinetic energies were rapidly increasing.

After FFC, as the linear trunk energies continued to decrease, the lower trunk rotation energy reached a peak value (30.8 J) at 66% PC, which was closely followed by the peak value of upper trunk rotation kinetic energy at 72% PC (41.4 J). The bowling arm linear kinetic energies (i.e upper arm, forearm, and hand) had started increasing just prior to FFC, but only reached their peak values after the trunk rotation energies had dropped considerably. The bowling upper arm, forearm and hand reached their peak energies at 86 % PC, 92% PC and 93% PC, respectively. Not shown in Figure 4-71 are the corresponding bowling arm rotation energies, which continued to increase slowly reaching their maximum values at approximately 100% PC or ball release.

With some initial help from the front arm, the general sequencing order for the bowling action was generally proximal to distal, starting from the lower trunk and working upwards, finally culminating at the bowling hand. The proximal segment generally started off with the higher energy, but was then surpassed by its immediate distal segment about the time when the proximal segment had reached its peak kinetic energy. The peak rotation kinetic energy of a segment generally occurred after its corresponding peak linear kinetic energy, and the rotation kinetic sequencing order was also from proximal to distal. For instance, the peak rotation energy of the lower trunk occurred 27.5% PC later than its linear kinetic energy. Then the peak rotation energy of the upper trunk occurred 6% PC later than the peak rotation energy of the lower trunk, which was 26% PC later than the peak linear energy of the upper trunk. This process was repeated for the bowling arm, which also had the rotation peak energies occurring after the peak linear energies.

The bowling hand motion was interesting, as its linear kinetic energy was only slightly above that of the upper arm, but well below that of the forearm. The flexion/extension motion of the hand almost exactly transcribes the plane of motion as the upper arm and forearm. Therefore, it appeared that there little linear energy transfer between the forearm and hand. To examine this more closely the

segment energies were normalised over the mean, and plotted on the same scale (Fig. 4-72). This is a simple method of visually comparing the variance of the curves over the same scale. For the case in hand, it is evident that the linear forearm and linear hand energy had very similar mean normalised energy curves, though the hand energy finally overcame the forearm energy at 85% PC, and then maintained a slightly higher level until REL. This indicates that relative to their respective means, the forearm and hand energy were increasing at a similar rate, and, as should be expected, there was an energy coupling of the forearm and hand.

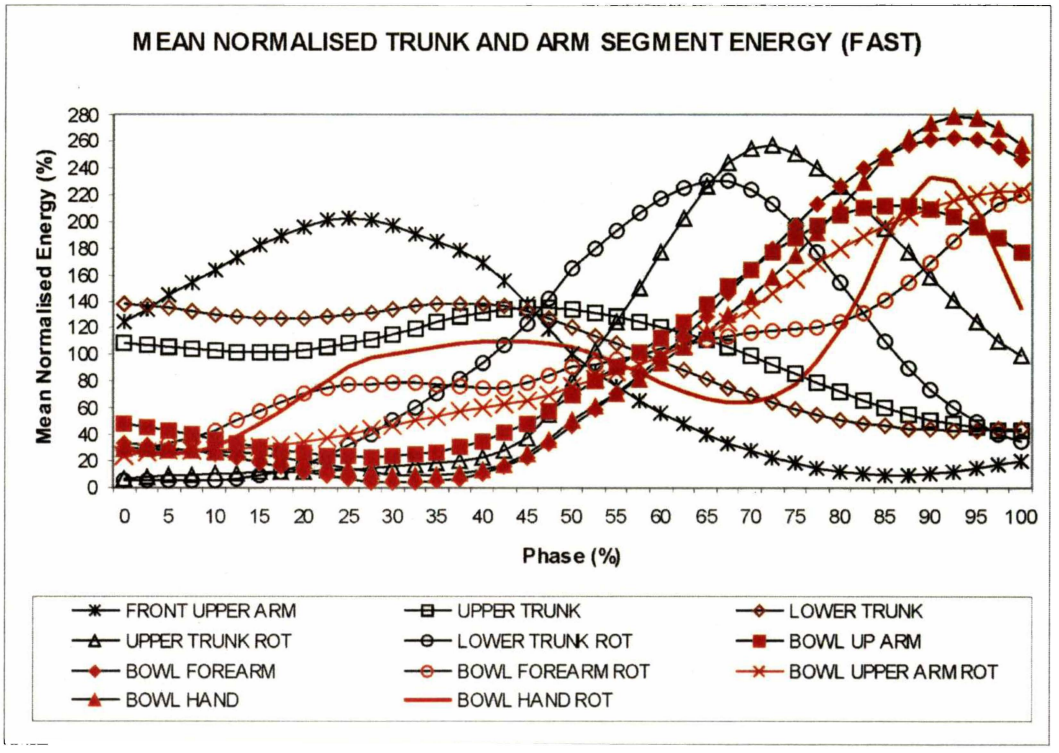

Figure 4-72: Mean normalised segment energies for fast group from BFC to FFC. Curves not drawn to time scale: BFC to FFC is represented from 0% PC to 50% PC, and FFC to REL from 50% PC to 100% PC. The bowling arm segments are drawn in red for clarity.

The mean normalised arm rotation energies continued to increase during the latter part of the phase. Initially the forearm rotation energy was increasing at a lower rate than that of the upper arm, but had made up the difference at REL. The hand rotation mean normalised energy in turn was below that of the forearm, but then increased rapidly from 70% PC to surpass that of the forearm at 88% PC, until it decreased below it again at 96% PC. The mean normalised energy curves also indicate that there was a proximal to distal sequencing of the bowling arm. Also,

due to the small inertial values of the arm segments, only small amounts of energy were required to produce substantial angular velocities. Observing the segment energy values alone could lead one to conclude that arm rotation energies were not significantly important. This highlighted the importance of normalising over the mean, or any other statistical process that could achieve the same end.

Continuing this analysis to the other segments, the upper left arm had its highest energy halfway during the BFC-FFC phase, and then was mostly inactive after FFC. The linear lower trunk and upper trunk mean normalised energies gradually increased before FFC with the lower trunk having a slightly higher value. This situation was reversed after FFC with the upper trunk maintaining a slightly higher value throughout most of this period. However, these differences were relatively small. The mean normalised linear energy of lower trunk and upper trunk did not vary much over the phase.

This was in contrast to the rotation energies of the trunk. The mean normalised values of the lower and upper trunk were both very small during the first 20% PC. Then there was a separation of values, as the lower trunk started increasing, and the upper trunk remained 'quiet'. The upper trunk began to increase only after 45% PC, gradually bridging the gap between itself and the lower trunk. The upper trunk only equalled the lower trunk, when the latter had reached a peak normalised energy at 66% PC, after which the upper trunk surpassed the lower trunk, and reached a peak normalised energy at 73 % PC. Both curves then decreased while the energy differential between upper trunk and lower trunk slightly increased up to REL. At the time of REL, the lower trunk rotation had a mean normalised energy of only 35%, whereas the upper trunk rotation still retained a value of 99%. In summary, the lower trunk started the phase with a much higher rotation kinetic energy, but as the phase progressed, the upper trunk rotation energy increased, eventually surpassing that of the lower trunk. At the time of ball release, both trunk rotation energies had reduced, but the lower trunk much more so.

Segmental kinetic energies, both standard and mean normalised, can be used to assist in determining the segmental sequencing. For the bowlers in the fast group,

there was a definite progression in kinetic energy from proximal to distal segments. This has been alluded to by previous kinematic studies such as Stockhill & Bartlett (1994). Also, it was important to differentiate between the sequencing of linear and rotation motion, particularly for the trunk and bowling arm segments. Though in both cases a general scheme of proximal to distal sequencing was observed, rotation occurred later in the phase, and showed more marked changes in energy.

One of the main purposes of studying segmental sequencing in fast bowling is to determine whether there are sequences that give rise to higher ball release speed. A way of quantifying sequential order is to observe the phase point (PC_{KEmax}) of maximum kinetic energy. Kinetic energy data was generally single-peaked, so that the passage of a peak in the data indicates that the values would decrease from that point onwards. The PC_{KEmax} was calculated for the main segments, and presented as a column graph contrasting the sequencing order between bowling groups (Fig. 4-73). The segments on the abscissa were sorted from left to right to match the sequential order of the fast group. Of importance was the striking similarity in sequencing between the bowling groups. Generally, the front side, such as the front leg and arm, reached their maximum kinetic energies first. Then the sequencing proceeded from proximal to distal, beginning with the trunk segments, and proceeding to the bowling arm, the rotation movements occurring later than the corresponding linear motions. Differences in sequencing between bowling groups were usually too small to establish significance, but perhaps could be established with the testing of much larger sample sizes.

Even if sequencing order could not be significantly correlated with ball release speed, there were still some important general sequencing characteristics that distinguished the fast group from the other groups. The percentage difference in the occurrence maximum energy was calculated for all the trunk and bowling arm segmental motions over FFC to REL. With the exception of the forearm rotation energy, the fast group had a delayed occurrence of maximum kinetic energy than the other groups (Table 4-7). Though the magnitude of these percentage differences appear to be small, the fact that this difference occurred almost uniformly across the entire range of trunk and bowling arm segmental motion

suggests that a delayed sequencing of these motions was a property of the fast group's bowling technique.

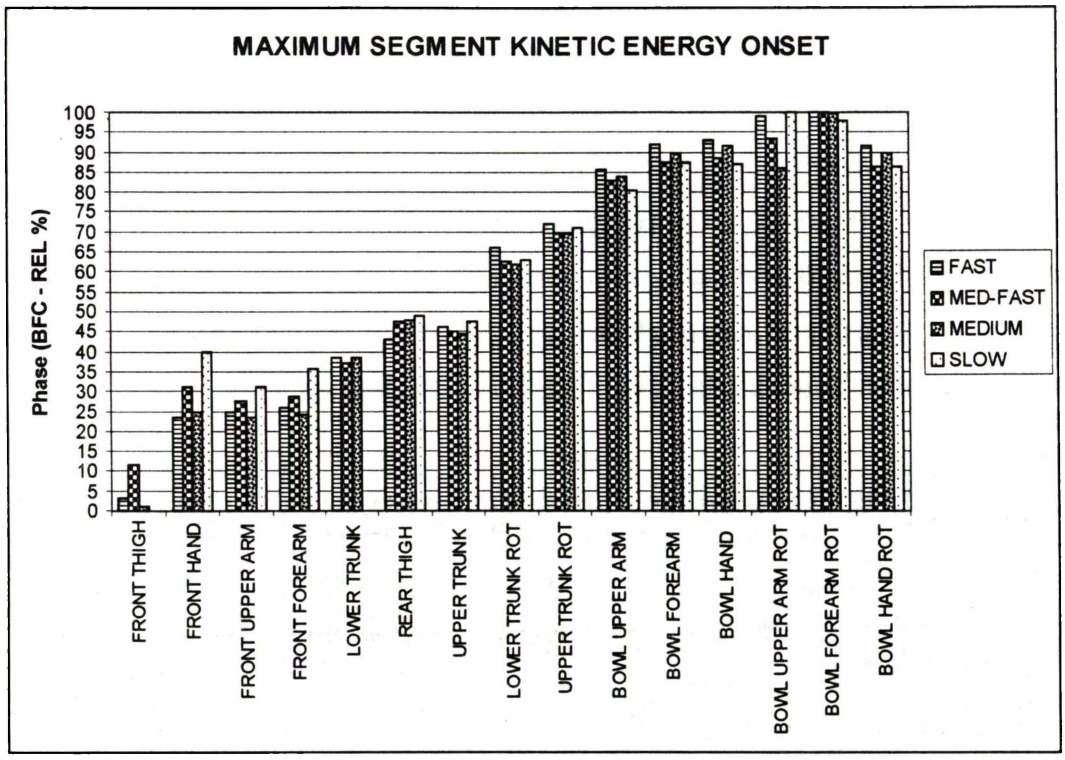

Figure 4-73: Occurrence of maximum segmental kinetic energy for selected segments and motions from BFC to REL. The segments were sorted in ascending order of the fast group's onset phase point. The general segmental sequencing was from proximal to distal, and similar across the bowling groups.

Of all the segment motions, the bowling upper arm rotation of the fast group incurred a large sequencing lag with medium-fast group (11%), and the largest sequencing lag with the medium group (26%). However, there was no such lag between the fast and slow group. This highlights the problem in assuming linear relationships between sequencing and ball speed. Also, sequencing properties of segments cannot generally be considered in isolation from the movement of the whole system.

The slow group had some sequencing characteristics that were different from the other groups. The largest difference was in linear lower trunk motion. The other bowling groups achieved a maximum linear kinetic energy of the lower trunk within a range of 37-39% PC, whereas for the slow group this occurred at 0% PC

(i.e. at BFC). Also, the front arm action of the slow group was delayed with respect to the other groups. For instance, taken over the period from BFC to FFC, when front arm motion was most active, the occurrence of maximum front upper arm energy of the slow group was 12% PC, 7%PC and 15% PC later than that of the fast, med-fast, and medium groups, respectively. Similarly, there was a 19% PC, 15% PC and 22% PC delay in the occurrence of the slow group's maximum front forearm energy over these respective groups. It is conceivable that within the speed range of the slow group different sequencing orders could be used. Therefore, the relatively late action of the bowling arm alone may not be an absolute indicator of bowling speed, but must be looked at within the context of the timings of other segments, such as the lower trunk and front arm.

Table 4-7: Percentage sequence delay of fast group segments compared to slower bowling groups over the period from FFC to REL.

SEGMENT MOTION	Med-fast	Medium	Slow
Lower Trunk Rot	7%	8%	6%
Upper Trunk Rot	5%	5%	2%
Bowl Upper Arm	5%	3%	10%
Bowl Forearm	9%	4%	9%
Bowl Hand	9%	3%	12%
Bowl Upper Arm Rot	11%	26%	0%
Bowl Forearm Rot	0%	0%	-2%
Bowl Hand Rot	10%	3%	1%

Ultimately, to produce a faster ball release speed, it is the energy of the bowling arm that matters. Therefore, for each succeeding bowling group in terms of ball speed, the mean bowling arm energy had to increase: fast, 204 J; med-fast, 203 J; medium, 183 J; slow, 148 J. However, this data by itself is of little value, because to produce this energy the bowling arm must depend heavily on the energy generation and sequencing of the larger segments. Therefore, it was important to assess where the differences in segmental energy increases existed between bowling speed groups.

The percentage increase in mean segmental kinetic energy over each succeeding slower group shows prominent differences (Fig. 4-74). Surprisingly, the med-fast group expended 7.1% more energy than the fast group. The extra energy was expended mostly in the lower limbs, and not in those segments most directly concerned with ball speed generation. Therefore, bowling upper arm rotation, bowling forearm rotation, bowling hand rotation, lower trunk rotation, and upper trunk rotation: all had higher kinetic energies for the fast group. The lower and upper trunk rotations of the fast group had the most marked increase in

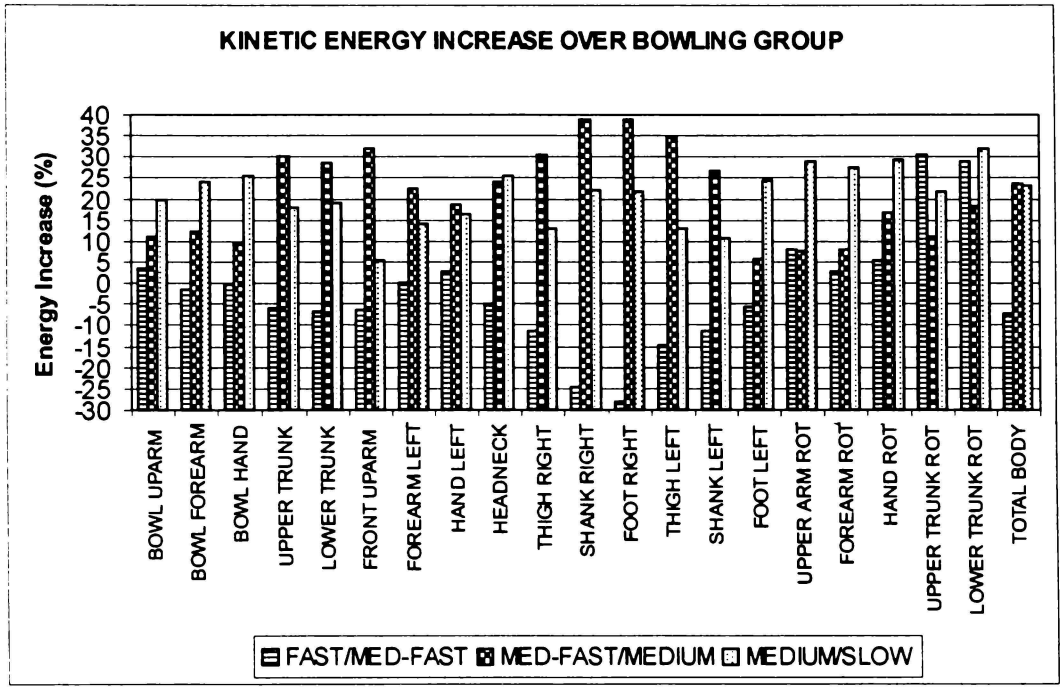

Figure 4-74: Percentage increases of mean segmental kinetic energy over sequential bowling groups from BFC to REL, i.e. fast/med-fast, med-fast/medium and medium/slow.

kinetic energy over the med-fast group: 32.0% and 21.6%, respectively. Though, the medium-fast group expended 16.0% more energy in the lower limbs than the fast group, the fast group ended up producing 4.69% more kinetic energy from the motion of the entire upper body. This indicates that the energy of med-fast group was either (i) not being transferred as efficiently up through the kinetic link chain as for the fast group, or (ii) was wasted on superfluous motion that did not contribute significantly to ball release speed. Perhaps it could be concluded that the fast group was more efficient than the medium-fast group, if ball release speed to mean kinetic energy output was considered the measure of efficiency.

The mean total energy increase of the med-fast group over the medium group was almost identical to that of the medium group over the slow group (approximately 23%). An examination of the mean segmental energy increases shows, however, that the med-fast group achieved much of this increased magnitude over the medium group through more activity of the lower limbs, and faster linear motion of the lower and upper trunk; whereas much of the increased energy of the medium group over the slow group was due to the power producing movements of trunk rotation and bowling arm motion (linear and rotation).

Chapter 5
CONCLUSIONS AND SUGGESTIONS FOR FURTHER RESEARCH

The purpose of the thesis was to resolve certain key hypotheses about fast bowling that would have important implications on improving bowling performance. To study the effects of the run-up, the centre of mass kinematics was calculated not only before back foot contact, but also during delivery stride until ball release. The segmental sequencing was examined for the trunk and arm segments. Also, the actuation of the body segments during the bowling action was determined by the calculation of active and controlled powers. It was hypothesised that these mechanical elements would not only provide a basis for providing a scientific understanding of bowling technique, but also show differences between bowling groups classified by range of ball release speed. Further, in recent times the issue of lower lumbar injury in fast bowlers has taken on an extra significance with the reporting of a high incidence of such injuries. Therefore, with the sample being relatively large and diverse in terms of competition level, it was expected that this would yield some information concerning the general 'safeness' of fast bowling actions in New Zealand.

The run-up is an extremely important part of fast bowling. However, the contribution that it makes to ball release speed is still not exactly known. It has been suggested in previous studies that there is a correlation between ball release speed and run-up velocity (Davis & Blanksby, 1976a, Elliott et al., 1986). The results of this study supported this view ($R^2 = 0.330$) with the largest difference between the fast and slow groups. To investigate what happened to this linear velocity during the bowling action, the centre of mass acceleration was calculated, and it was found that the average negative acceleration of the centre of mass increased with ball release speed. This shows that a fast bowler should not only

develop a fast run-up velocity suitable for the action, but also develop a technique that can withstand the ground reaction forces as the body negatively accelerates, and convert linear motion into rotation.

A study of the alignment angles to calculate shoulder-separation angle at BFC, and shoulder counter-rotation shows that depending on the classification system, between 60-85% of bowlers in the sample had mixed actions. The increased susceptibility of lower lumbar injury with mixed action techniques has been well established (Elliott, 2002; Burnett et al., 1995). The sample was large and comprised bowlers of the four major competition levels in New Zealand, so it is likely that the predominant bowling technique in New Zealand is the mixed action. If this is the case, then this is an area of concern, which should be taken up by the cricketing authorities of that country. If this is part of a world trend, then it is possible that similar results may also be found in other countries.

If the sequence of segment activation is defined as the time when the angular velocity surpasses that of its neighbouring segment, then the segmental sequencing of the fast bowling action is in general from proximal to distal. For instance, considering the results of lower to upper trunk sequencing from FFC to REL, first upper trunk rotation occurs after lower trunk rotation, and then upper trunk flexion occurs after lower trunk flexion. However, the proximal to distal sequencing does not apply with respect to the lateral bending of the trunk: lower trunk lateral bending to the left occurs after upper trunk lateral bending to the left. Moving distally to the next linkage point at the glenohumeral joint, the sequencing between the upper trunk and upper arm was proximal to distal, particularly between upper trunk rotation, and bowling upper arm horizontal adduction. Further, the smallest difference in upper trunk and bowling upper arm horizontal adduction angular velocities during early FFC tended to occur for the fastest two groups. This suggests that these motions are coupled during this period, and have similar planes of motion. Also, the relatively high magnitudes of these angular velocities highlight the importance of these motions in bowling.

Sequencing analysis had never before been performed between the upper arm and forearm, because it was assumed that these segments could be considered as a

single rigid segment. However, the results show that a forearm flexion angular velocity occurred just prior to release, and that there were differences between speed groups in the sequential timing of this movement. The fastest group tended to delay forearm flexion compared to the slower groups. Another important feature was forearm internal rotation, which was highest and initiated later by the fastest groups. The evidence suggests that the appropriate use of the forearm may be considered an important part of fast bowling technique in the future. The results for hand flexion were similar to those of previous studies. Hand flexion angular velocity was higher and occurred later for the fast group.

Kinematics can only report what is happening to a segment. However, the calculation of power is the dot product of torque and angular velocity, and requires knowledge of both the magnitude and sense of each of these vectors. Joint power calculations at the proximal end were used to determine the actuation status of a segment, either active or controlled, which had not been done before in the analysis of bowling technique. Therefore, this approach leads to a deeper understanding of the roles of segments in the bowling action.

Joint powers were calculated from BFC to FFC for the major power producing segments. The rear thigh was in controlled extension and controlled abduction throughout this phase. There were also differences between the bowling speed groups. In general, the faster groups generated higher rear thigh powers than the slower ones. At the same time, the rear shank was in active flexion. Linear powers calculated at the proximal end of the lower trunk show that initially the lower trunk was being actively pulled forwards (positive power), and then retarded (negative power) as front foot contact approached. The fast group had the highest negative power of all the groups, and this could have been related to the negative acceleration of the centre of mass. In general, the action of the trunk to laterally bend and extend during delivery stride was not straightforward and required a combination of active and controlled movements. The most active of the trunk motions was rotation, and the fast groups in general had higher positive rotation powers than the slower groups. Accompanying the trunk motion was an active vertical adduction of the front upper arm, the powers of which were very much lower for the slow group, while the front forearm had equal periods of first

active extension and then controlled extension about the elbow. Front forearm extension power was lowest for the slow group. Also, during the last half of the phase, the front elbow bent because the front upper arm vertical adduction angular velocity exceeded the front forearm extension angular velocity. The bowling upper arm was actively horizontally adducted towards the end of the phase to place it almost horizontally behind the bowler leading into the power phase.

The most important results generated by the power calculations were during the power phase from FFC to REL. The magnitudes of powers during this phase were considerably higher during this period than the preceding phase from BFC to FFC. Also, more differences could be established between the bowling speed groups. This indicates that there were variations in the execution of the bowling action during this period that caused differences in ball release speed.

During the power phase, it has generally been taught that the fast bowler needs to bend or flex the back to generate high ball release speed. However, the muscle power calculation for the lower trunk shows that though the lower trunk flexion angular velocities were increasing during this period, the motion was controlled. Further the fastest bowlers resisted or controlled this flexion movement more strongly than the slower ones. This was similar for the case of lower trunk rotation, which was more controlled for the fast and med-fast groups. The lower trunk lateral bending motion played more of support role. These results are significant. There is substantial concern at the rate of lower lumbar injury to young fast bowlers. It is plausible that the instruction of bowling technique needs to be such that bowlers are taught to control lower trunk flexion and rotation rather than actively try to produce them. This may consequently not only reduce injury rates, but increase ball release speed as well.

Of the upper trunk motions, the rotation power was the largest, and much higher for the fast group. Also, upper trunk rotation was actively performed producing angular velocities that increased with the speed of bowling group. In analysing bowling technique, because of the relatively high active power associated with this movement, it is advisable to measure the angular velocity of upper trunk rotation, and perhaps also study its plane of motion with respect to that of the

bowling arm. The other two trunk motions were less significant: upper trunk flexion was active and positive throughout most of the phase, while the lateral bending motion of the upper trunk was a small controlled motion.

The circumduction of the bowling upper arm was a complex movement. Early in the power phase an active horizontal adduction motion was the primary movement. Then from about half-way through the period, this motion became controlled, most noticeably by the fast group. During this time, a negative linear power acted on the distal end of the humerus, effectively pulling it backwards, and therefore acting to increase the bowling upper arm adduction angular velocity. The average negative linear power was highest for the fast group. Towards the end of the phase, there was an increase in vertical adduction velocity. Therefore, to bowl a ball faster is much more than trying to rotate the bowling arm faster. There is a definite sequence of movements, and phases of active and controlled movement.

This was even more apparent for the bowling forearm and hand. There was active forearm flexion followed by an active hand flexion. Both these movements were more delayed for the fast group. There was also active forearm internal rotation from about 60% PC onwards, and the forearm internal rotation torque increased with bowling group speed. These results suggest that the bowling arm cannot be sufficiently treated as a single rigid segment. Forearm flexion and extension may be effectively utilised by the faster bowlers to increase ball speed

The front arm motion in cricket has generally been prescribed as a rapid pulling-down action so that the elbow tucks into the side of the body. However, this instruction only approximates the actual movements of the front arm during the power phase. The results show that vertical adduction of the front upper arm motion was performed actively, but for only about half the power phase. The rest of the time, it was a controlled motion. The highest vertical adduction active power was at the beginning of the phase - largest for the fast group, and smallest for the slow group. The front forearm was in controlled extension, and the elbow bent as the forearm extension angular velocity was reduced. Overall, the motion of the front arm requires the coordinated movement of both upper arm and

forearm, and the power calculations show that bowlers used a combination of active and controlled movements to achieve this.

Rear leg action is generally considered important in athletic motions that require the release of a projectile. In this respect, bowling should be no different, but there has been almost no scientific treatment of this motion. Generally, the bowlers used a short controlled thigh extension initially (0-15% PC), before generating an active flexion, which gradually diminished during the phase, and was of significant magnitude from 15 - 50% PC. The fast group registered the lowest average hip flexion power. There was also an active adduction of the rear thigh, which decreased in magnitude as REL was approached. That the rear knee bends during the power phase was established, but there were different combinations of active and controlled motions to achieve this end. It was interesting that the fast group was the only group that did not employ a period of active shank flexion. It is difficult to exactly specify the correct rear leg action in bowling. There was a large variability in the results. The case for thrusting the rear leg forwards with a bent knee was considered too simplistic a notion.

Front leg action is given much emphasis by bowling coaches because it must withstand high ground reaction forces, and act as lever over which the upper body can rotate. Generally, the front thigh was extended actively, while the shank was in controlled flexion. Coaches often talk about the front leg being braced throughout the delivery stride. However, there was large variability in the front shank power curves calculated at the proximal end. Also, the fast group had a small active shank flexion torque towards the end of the phase. Overall, the results suggest that firmness of front leg is necessary, but that there is some scope for variation in the degree and timing of front knee flexion.

The calculations of segment kinetic energy show that the general sequencing order for bowling is proximal to distal. Also, the sequencing order was remarkably uniform for each of the bowling groups. Defining the timing of activation based on the occurrence of peak kinetic energy, the fast group had a more delayed sequencing pattern than the other groups. This suggests that timing in fast bowling is as important as the generation of power. Fast bowlers may benefit

from training procedures that can improve the overall rhythm of a bowling performance.

In any multi-segment athletic motion, the coach tries to identify the optimal sequencing scheme and the main sources of power. With this knowledge the coach then formulates a qualitative model of optimal technique that could be used to diagnose and correct faults in technique in a bid to improve performance. The cricket fast bowling coach adopts a similar philosophy. However, most of the current published material on what constitutes correct fast bowling technique has been through the medium of coaching manuals. Almost all of these have been based on previous texts of a similar nature, observations of top players or anecdotal evidence (Bartlett et al., 1996). Hence, the qualitative biomechanical models themselves need to be brought into question. In this thesis, a 3-D full body rigid body model was developed to study the kinematics and dynamics of fast bowling to shed new light on its mechanical principles, particularly with respect to sequencing and power generation. This provides the coach with a sounder basis on which to develop qualitative models of fast bowling, and therefore address issues of bowling technique from a scientific perspective.

This thesis is the first step in providing an understanding of the biomechanics of bowling technique. It is clear that the technique of bowling is complex because it involves the integrated motion of several body segments through a variety of sequencing schemes, including a combination of active and controlled movements. The aim of this thesis was to understand bowling technique more comprehensively in terms of its mechanical components.

Further research should include performing a segment velocity contribution analysis to understand the importance of each segment's motion with respect to the production of final ball release speed. This analysis should then try to ascertain how these segment velocity contributions vary with ball release speed. This should help resolve questions concerning the velocity contribution of the run-up: how this contribution varies with action type, and whether this influences the kinematic characteristics of segments during delivery. It would also be beneficial to calculate the relative planes of motion between segments that are

coupled - for instance, upper trunk long axis rotation, and bowling upper arm horizontal adduction. To test this proposition, the relative angles between the planes of these two respective motions could be calculated to investigate to what extent these motions are coupled. It may be that the angle between these planes is smaller for faster bowlers at a particular phase in the bowling action. A similar analysis of planes of motion could be calculated for the entire bowling action.

The most important development would be the use of forward solution dynamics models to simulate bowling actions. This would enable the researcher to test various theories of technique, and observe their effects on performance. To do this successfully, an adequate model of the shoe-ground interface would have to be modelled to calculate ground reaction forces. However, even forward solution kinematic models have the potential to resolve serious technical issues, such as the correcting of mixed action techniques. The most common bowling action in the test sample was the front-on mixed action technique. Questions commonly arise on the appropriate methods to correct the technique of a bowler who shows this type of action. Should the coach try to close the shoulders to match the hip alignment or should the bowler be encouraged to resist the tendency to counter-rotate the shoulders during delivery stride? Is there a common solution to all such bowlers or does the remediation measure vary with the individual? At the moment, there is no way to scientifically address these questions. The only tool the coach has at his/her disposal is the method of trial and error. However, even a forward solution kinematic model could effectively deal with such problems through the conservation of angular momentum principle, because most of the alignment problems occur while the bowler is airborne during the pre-delivery jump.

The further development of 3-D rigid body models into musculoskeletal models would provide information on the type, number, and sequencing of muscles involved in bowling actions. The potential for this kind of research is immense. By knowing which muscles are working, when they are activated, and the different roles that they play, strength and power training programmes can be designed more effectively. However, it must also be noted that such models are difficult to create, and need much validation to tune the muscle models. Still,

ultimately this is the future of bowling biomechanics. However, even if these models were a long way off, the further development of inverse and forwards dynamics models would still provide valuable information of bowling mechanics. The purely subjective qualitative models of bowling technique of the past have served a useful purpose, but their limitations make them an inappropriate choice of analysis today and in the future.

Appendix A: Testing Consent and Information Forms

TITLE: ***THREE-DIMENSIONAL MOTION ANALYSIS OF BOWLING IN CRICKET***

RESEARCH TEAM: ***Rene Ferdinands (MSc), Joe Hunter (MSc), Bob Marshall (PhD)***

SUPERVISORS: ***Assoc. Prof. Bob Marshall (University of Auckland), Dr. Howell Round (University of Waikato), Assoc. Prof. Kevin Broughan (University of Waikato).***

I have been given and have understood an explanation of this research project. I have had an opportunity to ask questions and have them answered.

I understand that I may withdraw myself or any information traceable to me at any time up to 3 months after the date of testing without giving a reason.

- I agree to take part in this research.
- I allow research results to be identified with my name.

Name: _____

Signed: _____

Date: _____

Figure A. 1: Subject Consent Form

PARTICIPANT INFORMATION SHEET

Title: Three-dimensional Motion Analysis of Bowling in Cricket

Venue: Gait Lab, Tamaki Campus, Department of Sport and Exercise Science, University of Auckland.

To: Subject

My name is Rene Ferdinands. I am a student at the University of Waikato, and I am working in conjunction with the University of Auckland (Department of Sport and Exercise Science) to research the biomechanics of the bowling action in cricket for my PhD degree. The objective of this research is to identify the underlying mechanical basis of successful bowling technique, and then use this knowledge to improve the performance of bowlers, and/or identify potential injury-causing mechanisms.

You have been invited to participate in this research. To meet the requirements of your study you will be required to perform **two** trials. In each trial you will deliver **six** balls along the athletics track at a set of stumps, a pitch length away. The length of the delivery will be measured to the nearest 0.1 m. If the ball misses the track, or is of inadequate length, i.e. shorter than 13 m, or longer than 20 m, then the ball will be rebowled. The specific differences between the trials are shown below:

Trial	Focus	Purpose
3. Bowl **over** the wicket	**Front foot** to hit force platform	Full body kinematics and dynamics of bowling action.
4. Bowl **over** the wicket	**Back foot** to hit force platform	Full body kinematics and dynamics of bowling action.

All trials are filmed with a fast-motion three-dimensional camera system. The eight cameras identify 45 reflective markers placed strategically around the body, and are attached with double-sided tape to the skin or tight fitting clothing. ***It is important that you wear only a singlet or vest, but preferably you should bowl with no clothing on the upper body. Also, you should wear shorts, preferably bicycle shorts. Also, you need to wear normal running shoes (no spikes!) cut at the sides so that the ankle is exposed.*** This would allow all markers to be placed securely on the body, and in clear view of the cameras. Within the track is a specialised force plate, which measures ground reaction forces during front foot and back foot contact in delivery stride. Advanced computer high-motion analysis software will record both video and force data, which will be analysed at a later date.

Figure A. 2: Subject Information Sheet

The time involved for the testing is approximately two hours. Sometimes a little longer or shorter depending on whether there are any unforeseen complications. Also, you will be given sufficient time to warm-up. Once you have completed the testing you have a 1-month period within which you can withdraw any information collected from. If you choose, all information will be confidential.

I hope you enjoy the testing experience, and wish you the best.

Regards

Rene Ferdinands
PhD Student
The Department of Sport and Exercise Science
The University of Auckland

Or

Department of Physics & Electronic Engineering
University of Waikato
Private Bag 3105
Hamilton
Email: redf1@waikato.ac.nz

Figure A. 2: Subject Information Sheet continued.

Trial Database: 3D Cricket Bowling Analysis

1.Subject Number:	**2**		
Testing Date:	**5/4/2001**		
2.Read consent form:	**Yes**		
3.Read information sheet:	**Yes**		
4.Subject Name:	**Somparle Jackson**		
5. Age:	**21**		
6. Current level of cricket:	**District**		
7. Highest level of cricket:	**First-Class**		
8. Last seasons stats:	**21 wickets; ave 17.2**		
9. Best figures:	**7/22**		
10.Weight (with shoes):	**75 kg**		
11.Weight (no shoes):	**74.4 kg**		
12.Shoe weight:	**0.6 kg**		
13.Height:	**1.80 m**	Thumb	Palm
14.Thumb & palm position of bowling arm hand when horizontal at back:		Up	Right
15.Thumb & palm position of non-bowling arm hand when vertical and horizontal in front:		Up	Forward

Force Platform Gain: 2

Trial No.	Front Foot Trials Ball length (m)	Features	Back Foot Trials Ball length (m)	Features
1	13.2		15.9	Heel may be slightly outside platform
2	18.9		15	
3	16.9	Maybe fastest ball	12.3	
4	13.3		15.9	
5	13.2	Front foot close to front edge of platform	19	Subject reported that he lost rhythm
6	15.5	Fast ball	12.6	
7	14.4		16.2	
8				
9				
10				

General Comments: Subject seemed to maintain the heel-off during back foot contact.

Figure A. 3: Subject Data Sheet (personal details not presented here).

Appendix B: Bertec Force Platform

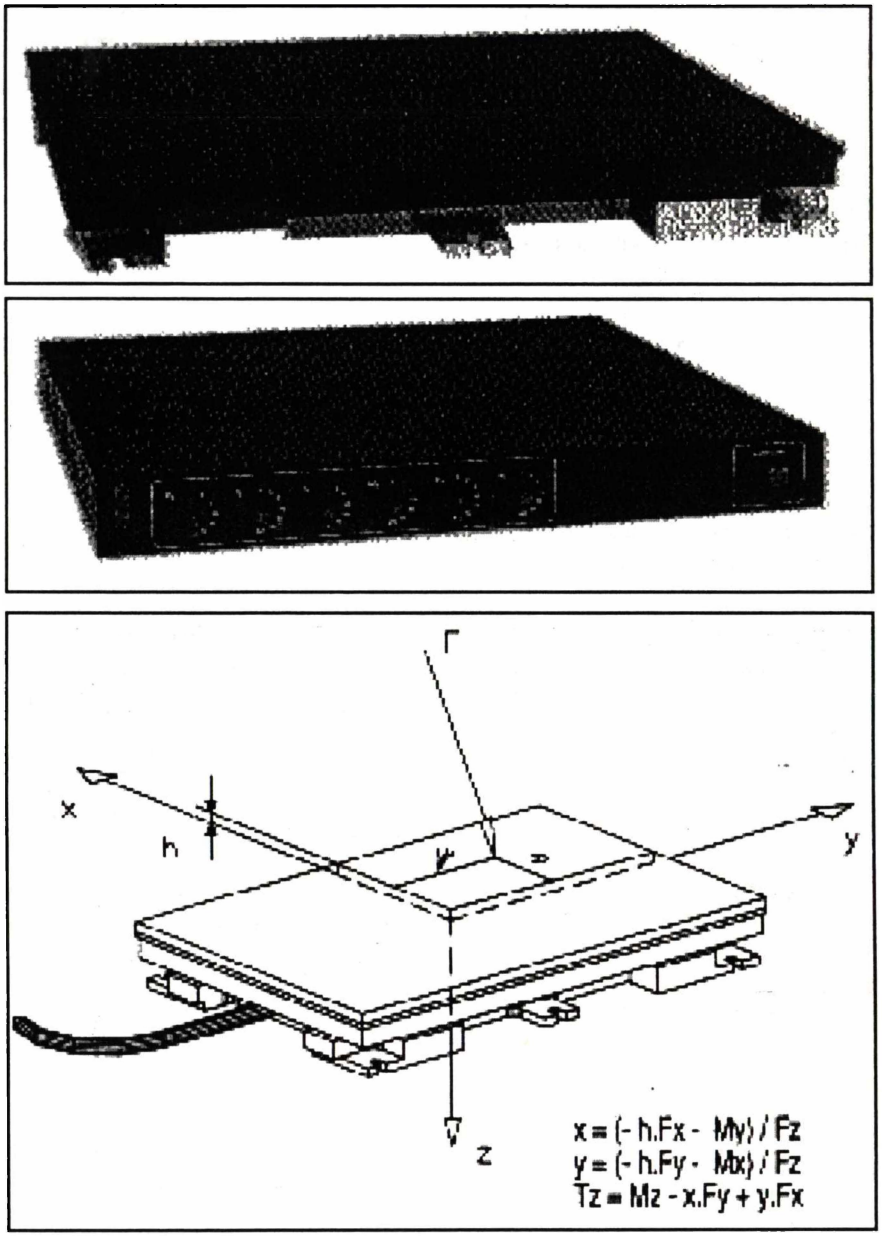

Figure B. 1: (Top) Bertec Force Platform; (Middle) Signal conditioning amplifier; (Bottom) Platform coordinate system and formulae for center of pressure and force platform couple calculations.

For Force Plate Number K70704, Type 60690-15, the calibration matrix is:

$$[C]=\begin{bmatrix} 1743.8 & -10.1 & -33.8 & -1.3 & 19.7 & 4.3 \\ 0.6 & 1750.1 & -44.1 & -22.7 & -6.2 & -6.7 \\ -3.2 & -7.7 & 3595.3 & -46.5 & -4.7 & 24.0 \\ 3.4 & -153.5 & -7.8 & 1906.0 & -4.4 & -5.2 \\ 138.7 & -3.0 & 1.4 & 2.1 & 1347.3 & 5.9 \\ 2.3 & -1.1 & -2.7 & 12.7 & 8.4 & 686.9 \end{bmatrix}$$

The force and moment components are calculated by multiplying the signals with the calibration matrix

$$\begin{bmatrix} F_X \\ F_Y \\ F_Z \\ M_X \\ M_Y \\ M_Z \end{bmatrix} = [C] \begin{bmatrix} S_1 \\ S_2 \\ S_3 \\ S_4 \\ S_5 \\ S_6 \end{bmatrix}$$

where F's and M's are the force and moment components in the force plate coordinate system (Figure B.1), and S's are the output signals corresponding to the channels indicated by their subscripts in volts, divided by the respective channel gains.

The center of pressure coordinates (i.e. x and y) and the torque acting on the force plate can be calculated from

$$\begin{aligned} x &= (-hF_X - M_Y)/F_Z \\ y &= (-hF_Y + M_X)/F_Z \\ T_Z &= M_Z - xF_Y + yF_X \end{aligned}$$

where h is the thickness of any material above the force plate.

APPENDIX C: Segment Joint Centre Calculations

Note that for linkage points on bilateral limbs, only the left side is described. Also, the linkage points are not presented in a proximal to distal order, as some the calculation of some linkage points depend on the prior definition of others.

Neck Linkage Point (i.e. Neck Joint Centre)

The neck linkage point was derived using:

- $VM2_{\%}$ with an offset of 50%.
- Origin marker: supra-sternal notch (permanent marker)
- *Y*-axis marker: 7th cervical vertebrae (permanent marker)

Vertex (of Head) Linkage Point

There was already a real marker placed on the crown of the head, however, the centroid of this marker was slightly above the surface of the head (a distance equivalent to the radius of the marker). Therefore, the position of the vertex linkage point was calculated at skin level:

- $VM2_{dist}$ with the offset distance equivalent to the radius of the marker.
- Origin marker: crown (permanent marker)
- *Y*-axis marker: neck linkage point (virtual marker)

Mid-Trunk Linkage Point

The chest linkage point was derived using:

- $VM2_{\%}$ with an offset of 50%
- Origin marker: xyphoid process (permanent marker)
- *Y*-axis marker: mid-back (permanent marker)

Wrist Linkage Point (i.e. Wrist Joint Centre)

The wrist linkage point was derived using:

- $VM2_{\%}$ with an offset of 50%
- Origin marker: medial wrist (permanent marker)
- *Y*-axis marker: lateral wrist (permanent marker)

3rd Knuckle Joint (of the Hand) Linkage Point

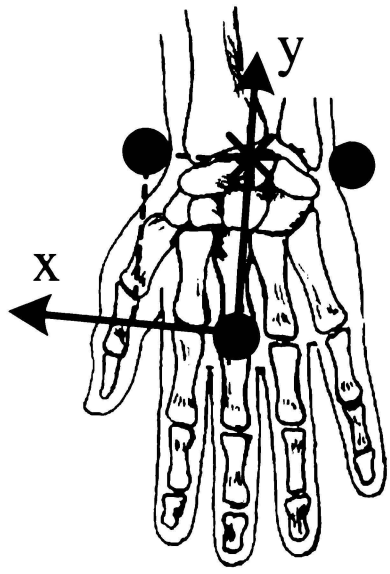

Figure C-1: Intermediate coordinate system used to calculate the 3rd knuckle linkage point of the left hand. The black spots represent the medial and lateral wrist markers and the hand marker. The asterix represents the wrist joint centre (a virtual marker). The *Z*–axis of the coordinate system (not shown in the diagram) projects downwards into the page.

The 3rd knuckle linkage point was derived using an intermediate coordinate system (Figure C-1):

- Origin marker: hand (permanent marker)
- *Y*-axis marker: wrist joint centre (virtual marker)
- *XY*–plane marker: lateral wrist (permanent marker)
- *Z*-axis: cross product of vectors describing XY-plane marker and Y-axis marker.
- $VM3_{dist}$ with an offset, along the *Z*–axis, equivalent to the radius of the marker plus half the thickness of the knuckle. *X*– and *Y*–axes offsets are zero.

- To avoid having to measure the thickness of the knuckle for each individual subject, a default offset value 1cm plus the radius of the marker' was used.

Elbow Linkage Point

(i.e. Elbow Joint Centre)

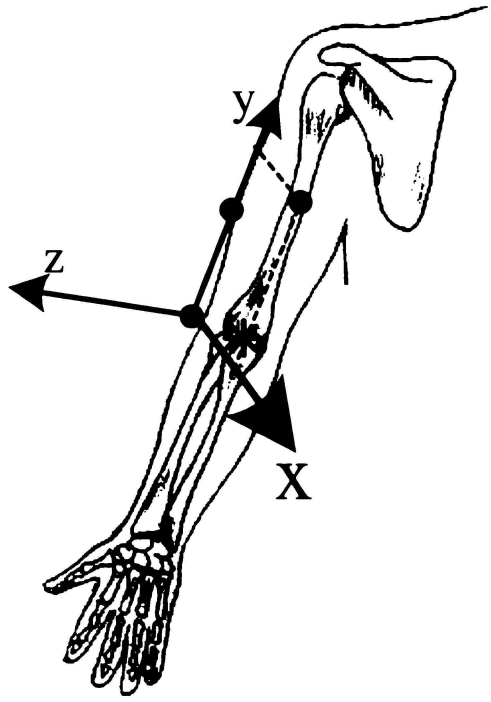

Figure C-2: The intermediate coordinate system used to calculate the left elbow joint centre. The diagram shows a rear view of the left arm and shoulder. The black dots represent the lateral elbow, lateral biceps, and high triceps markers. The elbow joint centre to be calculated is represented by the large asterix.

For the static trial, the elbow joint centre was derived by measuring the mid-point between the lateral and medial elbow markers. However, the medial elbow marker was removed after the static trial, and was therfore a virtual marker for the moving trials. The following steps were used to create the elbow joint centre:

Step 1 – from the static trial, create an intermediate virtual marker of the elbow joint center (i.e., the mid-point between the medial and lateral elbow markers):

- $VM2_{\%}$ with an offset of 50%
- Origin marker: medial elbow (temporary marker)

- *Y*-axis marker: lateral elbow (permanent marker)

Step 2 – Set up an appropriate intermediate coordinate system: For the left elbow, intermediate coordinate system is (Figure C-2):

- Origin marker: lateral elbow (permanent marker)
- *Y*-axis marker: lateral biceps (permanent marker)
- *XY*-plane marker: high triceps (permanent marker)

Step 3 – from the static trial, measure the relative position of the intermediate elbow joint centre (calculated in step 1) relative to the intermediate coordinate system: All *X*, *Y* and *Z* coordinates are required.

Step 4 – during the moving trials, create a virtual marker of the elbow joint centre: The medial elbow marker was not available during the moving trials; however, this was not required because the position of the elbow joint centre relative to the intermediate coordinate system was known. A $VM3_{dist}$ was used to create a virtual marker of the elbow joint centre.

Glenohumeral Linkage Point (i.e. Shoulder Joint Centre)

Calculation shown in Chapter 4.

Hip Linkage Point (i.e. Hip Joint Centre)

The hip linkage point (i.e. the hip joint centre) was derived using a hybrid method based on an experimental review of a number of previous methods. Bell (1990) proposed that this hybrid method is capable of locating the hip joint centre with a mean total error of 1.07 cm. This method requires the location of the left and right ASIS markers, mid-PSIS marker, and the greater trochanter markers, which were removed after the static trial. The following steps were used to calculate the left hip joint centre:

Step 1 – create ASIS skin level virtual markers: The real marker centroids were not at skin level, so intermediate virtual markers called 'skin level ASIS' were

created by offsetting by the marker radius in an intermediate coordinate system and using a $VM3_{dist}$:

- $VM3_{dist}$ set with *X* equivalent to the radius of the marker, $Y = 0$, and $Z = 0$
- Origin marker: left ASIS (permanent marker)
- *Y*-axis marker: right ASIS (permanent marker)
- *XY*-plane marker: mid-PSIS (permanent marker)

Although the actual offset was not shown Figure C-3, the offset was along the *X*-axis and equivalent to the radius of the marker, creating an ASIS virtual marker at skin level. A similar intermediate coordinate system and appropriate offset was used for the right ASIS marker.

Step 2 – set up an intermediate coordinate system using the skin level ASIS virtual markers: The second step was to set an intermediate coordinate system similar to that in Step 1, except for the use of skin level ASIS virtual markers (Figure C-3). For the left side of the body the intermediate coordinate system was:

- Origin marker: left skin-level ASIS (intermediate virtual marker)
- *Y*-axis marker: right skin-level ASIS (intermediate virtual marker)
- *XY*-plane marker: mid-PSIS marker (permanent marker)

Step 3 – from the static trial, use the intermediate coordinate system to measure the relative location of the greater trochanter marker (temporary marker). Only the *X* coordinate was required. The reason becomes apparent in Step 5.

Step 4 – measure the distance between the left and right ASIS markers. The distance between the ASIS markers was obtained from the static trial.

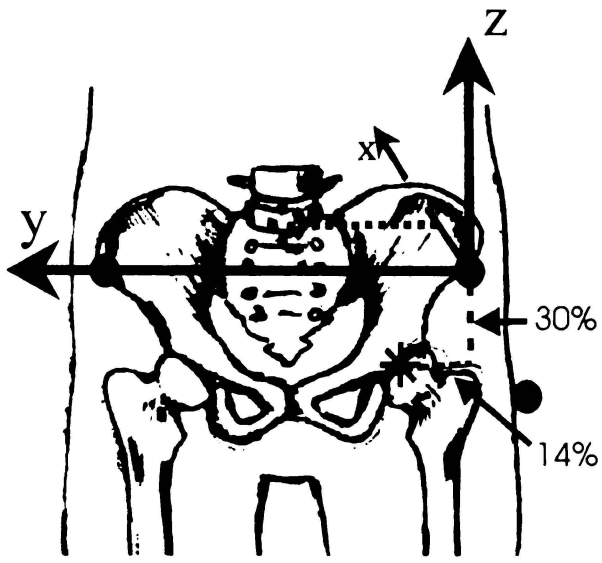

Figure C-3: Intermediate co-ordinate system used to calculate the left hip joint centre. The black dots represent the let and right skin-level ASIS virtual markers, and the left greater trochanter. The dashed circle indicates the mid-PSIS marker. The left hip joint centre to be calculated is represented by the large asterix. Note, that the greater trochanter marker was removed after the static trial.

Step 5 – during the moving trials, create the hip joint centre virtual marker. This used the *X*-distance obtained from the static trial, the inter-ASIS distance obtained from step 4, and the intermediate coordinate system set up in step 2, to create a virtual marker of the hip joint center based on the empirical calculations of Bell (1990). The $VM3_{\%}$ method was used:

- $VM3_{\%}$ with an *X* offset obtained by expressing the *X*-distance (from step 3), *Y* = 14% medial of the ASIS skin level marker as a percentage of inter-ASIS distance, and *Z* = 30% distal of the ASIS skin level marker as a percentage of inter-ASIS distance (Bell, 1990)
- The coordinate system was that specified in step 2.

Pelvis Linkage Point

The pelvis linkage point was mid-way between the two hip (joint centre) linkage points and calculated by using

- $VM2_{\%}$ with an offset of 50%
- Origin marker: left hip joint centre (virtual marker)

- *Y*-axis marker: right hip joint centre (virtual marker)

Knee Linkage Point (i.e. Knee Joint Centre)

The knee joint centre was derived by measuring the mid-point between the lateral and medial knee markers. However, the medial knee marker was removed after the static trial. The following steps were used to create the knee joint markers during the moving trials:

Step 1 – from the static trial, create an intermediate virtual marker of the knee joint center. The mid-point between the medial and lateral knee joint markers was calculated by setting

- $VM2_{\%}$ with an offset of 50%
- Origin marker: lateral knee marker (permanent marker)
- *Y*-axis marker: medial knee marker (temporary marker)

Step 2 – set up an appropriate intermediate coordinate system: For the left knee, the intermediate coordinate system was set up as

- Origin marker: lateral knee marker (permanent marker)
- *Y*-axis marker: lateral ankle marker (permanent marker)
- *XY*-plane marker: mid-shank (permanent marker)

Step 3 – from the static trial, measure the position of the intermediate knee joint centre (calculated in step 1) relative to the intermediate coordinate system: All *X*, *Y* and *Z* coordinates are required.

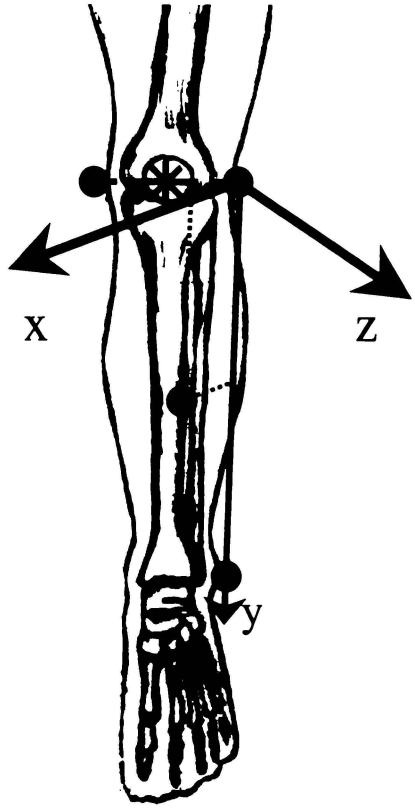

Figure C-4: Intermediate coordinate system used to calculate the left knee joint centre. The black dots represent the lateral and medial knee joint markers, mid-shank, and lateral ankle markers. The knee joint centre to be calculated is represented by the large asterix. The medial knee marker was removed after the static trial.

Step 4 – during the moving trials, create a virtual marker of the knee joint centre: The medial knee marker was not available during the moving trials. Therefore, the position of the knee joint center was calculated relative to the intermediate coordinate system (Figure C-4). A $VM3_{dist}$ was used to create a virtual marker of the knee joint centre.

Ankle Linkage Point (i.e. Ankle Joint Centre)

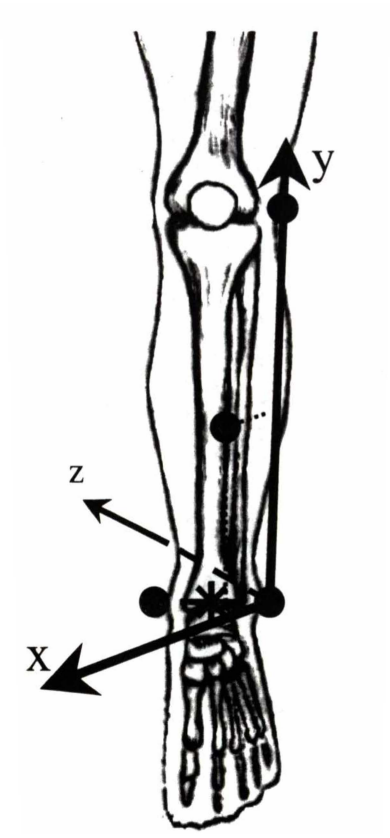

Figure C-5: Intermediate coordinate system used to calculate the left ankle joint centre. The black dots represent the lateral and medial ankle joint markers, mid-shank marker, and lateral knee marker. The ankle joint centre to be calculated is represented by the large asterix. The medial ankle marker was removed after the static trial.

The ankle joint centre was derived by measuring the mid-point between the lateral and medial ankle markers. However, the medial ankle marker was removed after the static trial. The following steps were used to create the knee joint markers during the moving trials:

Step 1 – from the static trial, create an intermediate virtual marker of the ankle joint center. The mid-point between the medial and lateral knee joint markers was calculated by specifying

- $VM2_{\%}$ with an offset of 50%
- Origin marker: lateral ankle marker (permanent marker)
- *Y*-axis marker: medial ankle marker (temporary marker)

Step 2 – Set up an appropriate intermediate coordinate system (Figure 3-13)*:*

- Origin marker: lateral ankle marker (permanent marker)
- *Y*-axis marker: lateral knee marker (permanent marker)
- *XY*-plane marker: mid-shank (permanent marker)

Step 3 – from the static trial, measure the relative position of the intermediate ankle joint centre (calculated in step 1) relative to the intermediate coordinate system. All X, Y and Z coordinates were required.

Step 4 – during the moving trials, create a virtual marker of the ankle joint centre: The medial ankle marker was not available during the moving trials. Therefore, the position of the ankle joint center was calculated relative to the intermediate coordinate system (Figure C-5). A $VM3_{dist}$ was used to create a virtual marker of the knee joint centre.

Toe Tip Linkage Point

The following steps were taken to specify the toe tip linkage point, which required offsetting the centroid of the front toe marker back to the level of the shoe, and removing the front toe marker during the moving trials:

Step 1 – for the static trial, create an intermediate virtual marker of the toe tip at shoe level:

- $VM2_{dist}$ with distance offset equivalent to the radius of the marker
- Origin marker: toe tip (temporary marker)
- *Y*-axis marker: heel marker (permanent marker)

Step 2 - calculate the position of the intermediate toe tip virtual marker (at shoe level) with respect to the following coordinate system (Figure C-6):

- Origin marker: heel marker (permanent marker)
- *Y*-axis marker: forefoot marker (permanent marker)
- *XY*-plane marker: ankle joint centre (virtual marker)

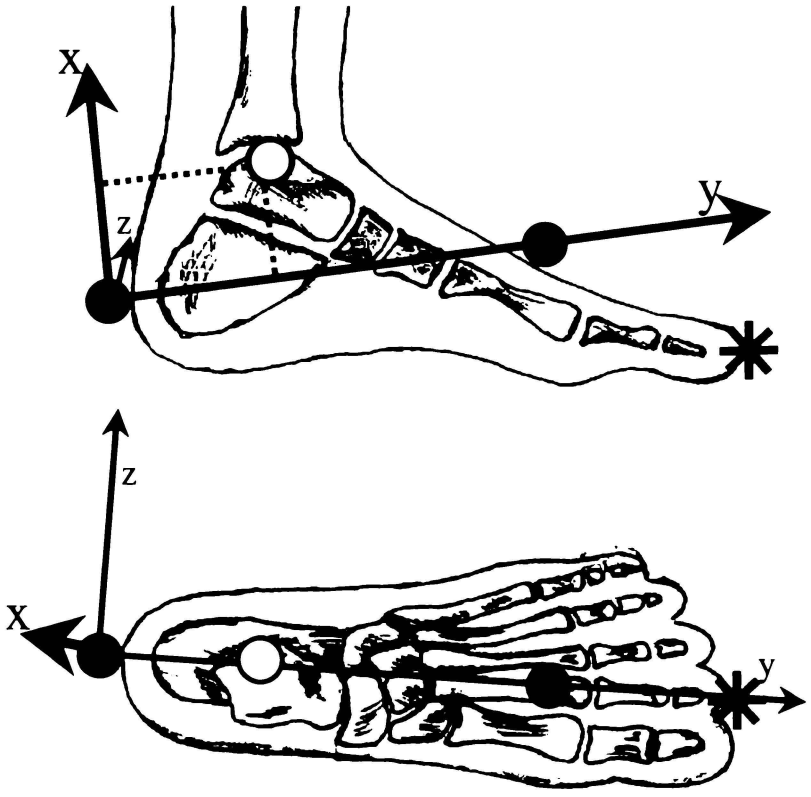

Figure C-6: Side and top views of the intermediate coordinate system used to calculate the position of the toe tip virtual marker. The black spots represent the heel and forefoot markers. The white spot represents the previously calculated ankle joint centre, which is used as the *XY*-plane marker. The position of the toe tip virtual marker, is represented by the large asterix .

Step 3 – during the moving trials, create a virtual maker of the toe tip (at shoe level): Use the $VM3_{dist}$ with offsets as measured in step 2.

Note:

- The toe tip linkage point (at shoe level) was required for the foot model. The foot is represented as a link from the posterior heel linkage point to the toe tip.

Heel Linkage Point

During the moving trials, the heel linkage point was created by offsetting the heel marker centroid to the level of the shoe (Figure C-7):

- $VM2_{dist}$ with distance offset equivalent to the radius of the marker
- Origin marker: heel marker (real marker)

- *Y*-axis marker: toe tip at shoe level (virtual marker)

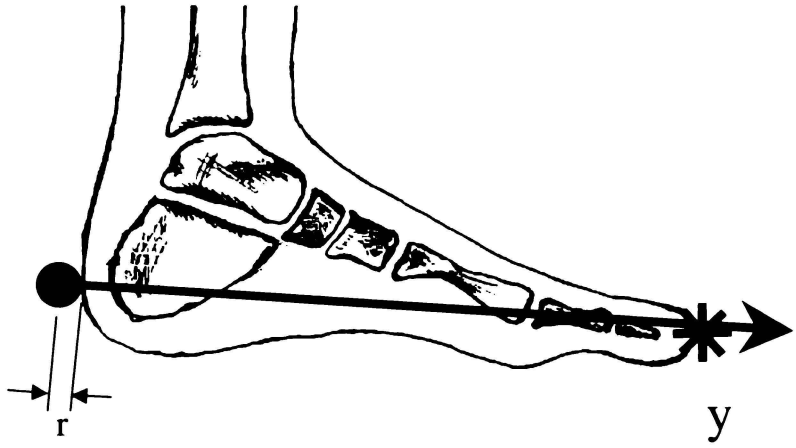

Figure C-7: The centroid of the heel marker was offset to shoe level. The *Y*-axis has the heel marker as the origin, and stops at the toe tip virtual marker (at shoe level). The offset (*r*) is equivalent to the radius of the marker.

APPENDIX D: Local Segment Coordinate System Calculations

Foot Right

Origin marker: HeelR $_{xyz}$
Y marker: Toe-ShoeR $_{xyz}$
XY plane marker: Lateral ankleR $_{xyz}$

Y_{fooRt} = Toe-ShoeR$_{xyz}$ – HeelR$_{xyz}$
XY_{footR} = Lateral ankleR$_{xyz}$ – HeelR$_{xyz}$
$Z_{footR} = XY_{footR}$ x Y_{footR}
$X_{footR} = Y_{footR}$ x Z_{footR}

Foot Linkage Coordinate System: (X_{footR} ,Y_{footR} , Z_{footR})

Foot Left

Origin marker: Heel $_{xyz}$
Y marker: Toe-Shoe $_{xyz}$
XY plane marker: Lateral ankle $_{xyz}$

Y_{footL} = Toe-ShoeL$_{xyz}$ – HeelL$_{xyz}$
XY_{footL} = Lateral ankleL$_{xyz}$ – HeelL$_{xyz}$
$Z_{footL} = Y_{footL}$ x XY_{footL}
$X_{footL} = Y_{footL}$ x Z_{footL}
Left Foot Linkage Coordinate System: (X_{footL} ,Y_{footL} , Z_{footL})

Shank Right

Origin marker: JC kneeR $_{xyz}$ (virtual)
Y marker: JC ankleR $_{xyz}$ (virtual)
XY plane marker: Lateral kneeR $_{xyz}$

Y_{shankR} = JC ankleR $_{xyz}$– JC kneeR $_{xyz}$
XY_{shankR} = Lateral kneeR$_{xyz}$ – JC kneeR $_{xyz}$
$Z_{shankR} = XY_{shankR}$ x Y_{shankR}
$X_{shankR} = Y_{shankR}$ x Z_{shankR}

Right Shank Linkage Coordinate System: (X_{shankR} ,Y_{shankR} , Z_{shankR})

Shank Left

Origin marker: JC kneeL $_{xyz}$ (virtual)
Y marker: JC ankleL $_{xyz}$ (virtual)
XY plane marker: Lateral kneeL $_{xyz}$

$\boldsymbol{Y_{shankL}}$ = JC ankleL $_{xyz}$– JC kneeL $_{xyz}$
$\boldsymbol{XY_{shankL}}$ = Lateral kneeL$_{xyz}$ – JC kneeL $_{xyz}$
$\boldsymbol{Z_{shankL}}$ = $\boldsymbol{Y_{shankL}}$ x $\boldsymbol{XY_{shankL}}$
$\boldsymbol{X_{shankL}}$ = $\boldsymbol{Y_{shankL}}$ x $\boldsymbol{Z_{shankL}}$

Shank Linkage Coordinate System: ($\boldsymbol{X_{shankL}}$,$\boldsymbol{Y_{shankL}}$, $\boldsymbol{Z_{shankL}}$)

Thigh Right

Origin marker: JC hipsR $_{xyz}$ (virtual)
Y marker: JC kneeR $_{xyz}$ (virtual)
XY plane marker: Lateral kneeR $_{xyz}$

$\boldsymbol{Y_{thighR}}$ = JC kneeR $_{xyz}$– JC hipsR $_{xyz}$
$\boldsymbol{XY_{thighR}}$ = Lateral kneeR$_{xyz}$ – JC hipsR $_{xyz}$
$\boldsymbol{Z_{thighR}}$ = $\boldsymbol{XY_{thighR}}$ x $\boldsymbol{Y_{thighR}}$
$\boldsymbol{X_{thighR}}$ = $\boldsymbol{Y_{thighR}}$ x $\boldsymbol{Z_{thighR}}$

Right Thigh Linkage Coordinate System: ($\boldsymbol{X_{thighR}}$,$\boldsymbol{Y_{thighR}}$, $\boldsymbol{Z_{thighR}}$)

Thigh Left

Origin marker: JC hipsL $_{xyz}$ (virtual)
Y marker: JC kneeL $_{xyz}$ (virtual)
XY plane marker: Lateral knee $_{xyz}$

$\boldsymbol{Y_{thighL}}$ = JC kneeL $_{xyz}$– JC hipsL $_{xyz}$
$\boldsymbol{XY_{thighL}}$ = Lateral kneeL$_{xyz}$ – JC hipsL $_{xyz}$
$\boldsymbol{Z_{thighL}}$ = $\boldsymbol{Y_{thighL}}$ x $\boldsymbol{XY_{thighL}}$ **(*interchanged XY and Y so that Z points forwards)**
$\boldsymbol{X_{thighL}}$ = $\boldsymbol{Y_{thighL}}$ x $\boldsymbol{Z_{thighL}}$

Left Thigh Linkage Coordinate System: ($\boldsymbol{X_{thighL}}$,$\boldsymbol{Y_{thighL}}$, $\boldsymbol{Z_{thighL}}$)

Lower Trunk

Origin marker: JC hips $_{xyz}$ (virtual)
Y marker: JC knee $_{xyz}$ (virtual)
XY plane marker: Lateral knee $_{xyz}$

$\boldsymbol{Y_{thigh}}$ = JC knee $_{xyz}$– JC hips $_{xyz}$
$\boldsymbol{XY_{thigh}}$ = Lateral knee$_{xyz}$ – JC hips $_{xyz}$
$\boldsymbol{Z_{thigh}} = \boldsymbol{XY_{thigh}}$ x $\boldsymbol{Y_{thigh}}$
$\boldsymbol{X_{thigh}} = \boldsymbol{Y_{thigh}}$ x $\boldsymbol{Z_{thigh}}$

Lower Trunk Linkage Coordinate System: ($\boldsymbol{X_{thigh}}$,$\boldsymbol{Y_{thigh}}$, $\boldsymbol{Z_{thigh}}$)

Upper Trunk

Origin marker: JC mid-back $_{xyz}$ (virtual)
Y marker: JC neck $_{xyz}$ (virtual)
XY plane marker: Xiphoid process $_{xyz}$

$\boldsymbol{Y_{uptrunk}}$ = JC neck $_{xyz}$ - JC mid-back $_{xyz}$
$\boldsymbol{XY_{uptrunk}}$ = Xiphoid process $_{xyz}$ – JC mid-back $_{xyz}$
$\boldsymbol{Z_{uptrunk}} = \boldsymbol{Y_{uptrunk}}$ x $\boldsymbol{XY_{uptrunk}}$ x $\boldsymbol{Y_{uptrunk}}$ **(*so that Z points forwards)**
$\boldsymbol{X_{uptrunk}} = \boldsymbol{Y_{uptrunk}}$ x $\boldsymbol{Z_{uptrunk}}$

Upper Trunk Linkage Coordinate System: ($\boldsymbol{X_{uptrunk}}$,$\boldsymbol{Y_{uptrunk}}$, $\boldsymbol{Z_{uptrunk}}$)

Head

Origin marker: JC neck $_{xyz}$ (virtual)
Y marker: crown $_{xyz}$
XY plane marker: forehead $_{xyz}$

$\boldsymbol{Y_{head}}$ = crown $_{xyz}$ - JC neck $_{xyz}$
$\boldsymbol{XY_{head}}$ = forehead $_{xyz}$ – JC neck $_{xyz}$
$\boldsymbol{Z_{head}} = \boldsymbol{Y_{head}}$ x $\boldsymbol{XY_{head}}$ x $\boldsymbol{Y_{head}}$ **(*so that Z points forwards)**
$\boldsymbol{X_{head}} = \boldsymbol{Y_{head}}$ x $\boldsymbol{Z_{head}}$

Head Linkage Coordinate System: ($\boldsymbol{X_{head}}$,$\boldsymbol{Y_{head}}$, $\boldsymbol{Z_{head}}$)

Upper-arm Right

Origin marker: JC shoulderR $_{xyz}$ (virtual)
Y marker: JC elbowR $_{xyz}$ (virtual)
XY plane marker: lateral bicepR $_{xyz}$

Y_{uparmR} = JC elbowR $_{xyz}$ - JC shoulderR $_{xyz}$
XY_{uparmR} = lateral bicepR $_{xyz}$ – JC shoulderR $_{xyz}$
Z_{uparmR} = XY_{uparmR} x Y_{uparmR}
X_{uparmR} = Y_{uparmR} x Z_{uparmR}

Right Upper Arm Linkage Coordinate System: (X_{uparmR},Y_{uparmR} , Z_{uparmR})

Upper-arm Left

Origin marker: JC shoulderL $_{xyz}$ (virtual)
Y marker: JC elbowL $_{xyz}$ (virtual)
XY plane marker: lateral bicepL $_{xyz}$

Y_{uparmL} = JC elbowL $_{xyz}$ - JC shoulderL $_{xyz}$
XY_{uparmL} = lateral bicepL $_{xyz}$ – JC shoulderL $_{xyz}$
Z_{uparmL} = Y_{uparmL} x XY_{uparmL}
X_{uparmL} = Y_{uparmL} x Z_{uparmL}

Left Upper Arm Linkage Coordinate System: (X_{uparmL},Y_{uparmL} , Z_{uparmL})

Forearm Right

Origin marker: JC elbowR $_{xyz}$ (virtual)
Y marker: JC handR $_{xyz}$ (virtual)
XY plane marker: medial wristR $_{xyz}$

$Y_{forearmR}$ = JC handR $_{xyz}$ - JC elbowR $_{xyz}$
$XY_{forearmR}$ = medial wristR $_{xyz}$
$Z_{forearmR}$ = $XY_{forearmR}$ x $Y_{forearmR}$
$X_{forearmR}$ = $Y_{forearmR}$ x $Z_{forearmR}$

Right Forearm Linkage Coordinate System: ($X_{forearmR}$,$Y_{forearmR}$, $Z_{forearmR}$)

Forearm Left

Origin marker: JC elbowL $_{xyz}$ (virtual)
Y marker: JC handL $_{xyz}$ (virtual)
XY plane marker: medial wristL $_{xyz}$

$Y_{forearmL}$ = JC handL $_{xyz}$ - JC elbowL $_{xyz}$
$XY_{forearmL}$ = medial wristL $_{xyz}$
$Z_{forearmL}$ = $Y_{forearmL}$ x $XY_{forearmL}$
$X_{forearmL}$ = $Y_{forearmL}$ x $Z_{forearmL}$

Left Forearm Linkage Coordinate System: ($X_{forearmL}$,$Y_{forearmL}$, $Z_{forearmL}$)

Hand Right

Origin marker: JC handR $_{xyz}$ (virtual)
Y marker: handR $_{xyz}$
XY plane marker: medial wristR $_{xyz}$

Y_{handR} = handR $_{xyz}$ - JC handR $_{xyz}$
XY_{handR} = medial wristR $_{xyz}$
Z_{handR} = XY_{handR} x Y_{handR}
X_{handR} = Y_{handR} x Z_{handR}

Right Hand Linkage Coordinate System: (X_{handR},Y_{handR} , Z_{handR})

Hand Left

Origin marker: JC handL $_{xyz}$ (virtual)
Y marker: handL $_{xyz}$
XY plane marker: medial wristL $_{xyz}$

Y_{handL} = handL $_{xyz}$ - JC handL $_{xyz}$
XY_{handL} = medial wristL $_{xyz}$
Z_{handL} = Y_{handL} x XY_{handL}
X_{handL} = Y_{handL} x Z_{handL}

Left Hand Linkage Coordinate System: (X_{handL},Y_{handL} , Z_{handL})

APPENDIX E: XYZ to Euler

EXAMPLE: *Z-Y-X* Euler angle sequence – numerical example for left shank. Calculation based on actual 3D motion analysis data.

Step 1: Find the three defining markers of the local coordinate system.

Origin marker: JC kneeL $_{xyz}$ (virtual) ={-2076.5979, 324.49524, 621.06537}

Y marker: JC ankleL $_{xyz}$ (virtual) = {-2337.76855, 272.61816, 262.56369}

XY plane marker: Lateral ankleL $_{xyz}$ = {-2336.84326, 335.0976, 245.5437}

Step 2: Express each axis of the local coordinate system as a vector

$\mathbf{Y}_{shankL}$ = JC ankleL $_{xyz}$– JC kneeL $_{xyz}$ = {-261.171, -51.8771, -358.502}

$\mathbf{XY}_{shankL}$ = Lateral ankleL$_{xyz}$ – JC kneeL $_{xyz}$ = {-260.245,10.6024, -375.522}

$\mathbf{Z}_{shankL}$ = $\mathbf{Y}_{shankL}$ x $\mathbf{XY}_{shankL}$ = {23281.9, -4776.84, -16269.8}

$\mathbf{X}_{shankL}$ = $\mathbf{Y}_{shankL}$ x $\mathbf{Z}_{shankL}$ = {-868476 ,-1.25958 x 10^{7} , 2.45537x 10^{6} }

Shank Local Vector Coordinate System in global coordinates:

($\mathbf{X}_{shankL}$, $\mathbf{Y}_{shankL}$, $\mathbf{Z}_{shankL}$) =

{{-868476 **i** -1.25958 x 10^{7} **j** + 2.45537 x 10^{6} **k**}

{-261.171 **i** - 51.8771 **j** -358.502 k},{23281.9 **i** - 4776.84 **j** - 16269.8 k }}

Step 3: Convert local coordinate vector system into Euler angles

Set the global coordinate system G: {*x* **i** *y* **j**, *z* **k**}

Rotation 1 → ψ about *Z*: L_{R1}: {*X*′ **I**′, *Y*′ **J**′, *Z*′**K**′}

Rotation 2 → θ about *Y*: L_{R2}: {*X*″ **I**″, *Y*″ **J**″, *Z*″**K**″}

Rotation 3 → ϕ about *Y*: L_{R2}: {*X* **I**, *Y* **J**, *Z* **K**}

The first Euler angle ψ is the projected angle of the local **X**-axis vector (i.e. $\mathbf{X}^{xy}_{shankL}$) on the global *xy*-plane, and is given by

$$\psi = \frac{\left(\mathbf{x} \times \mathbf{X}^{xy}_{shankL}\right) \cdot \mathbf{Z}_{shankL}}{\left|\left(\mathbf{x} \times \mathbf{X}^{xy}_{shankL}\right) \cdot \mathbf{Z}_{shankL}\right|} ArcCos\left[\frac{\mathbf{X}^{xy}_{shankL} \cdot \mathbf{x}}{\left|\mathbf{X}^{xy}_{shankL}\right|\left|\mathbf{x}\right|}\right] \qquad \text{(D.1)}$$

where $\mathbf{x} = \{1, 0, 0\}$ is the global **x**-axis vector.

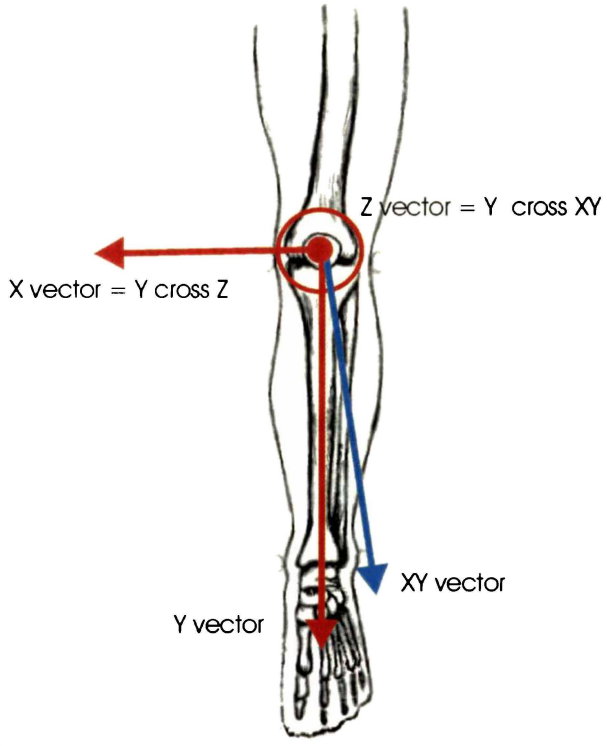

:

Figure E-1: Calculating Euler 3-2-1 sequence for left shank from the XYZ coordinates of markers from the *Eva 6.0 .trc* file. The coordinate system (red) is the body fixed axis system, with the *Z*-axis out of the page.

Each coordinate vector defines an axis of the body fixed shank coordinate system with respect to the global reference system. The projection of $\mathbf{X}_{shankL}$ on the global *xy*-plane is

$$\mathbf{X}^{xy}_{shankL} = \{-868476\ \mathbf{i} - 1.25958 \times 10^{7}\ \mathbf{j} + 0\ \mathbf{k}'\}$$

Therefore, the first Rotation ψ about z axis is found by substituting **x**, $\mathbf{Z}_{shankL}$ and $\mathbf{X}^{xy}_{shankL}$ into Equation D.1 yielding

$$\psi = -1.63964 \text{ radians or } -93.9443 \text{ degrees.}$$

The second Euler angle is θ. It is the included angle between the local X-axis and the X'-axis. It is first necessary to calculate the projection of the X'-axes and Y'-axes on the global xy-plane in terms of global vectors given by

$$\begin{aligned} \mathbf{X}' &= cos(\psi)\mathbf{i} + sin(\psi)\mathbf{j} \\ \mathbf{Y}' &= -sin(\psi)\mathbf{i} + cos(\psi)\mathbf{j} \end{aligned} \qquad \text{D.2}$$

Substituting the value of ψ found previously gives

$$\mathbf{X}' = 0.068782\,\mathbf{i} + 0.997632\,\mathbf{j}$$

$$\mathbf{Y}' = -0.997632\,\mathbf{i} + 0.068782\,\mathbf{j}$$

Then θ is found by using the following relation

$$\theta = \frac{(\mathbf{X}' \times \mathbf{X}_{shankL}) \cdot \mathbf{Y}'}{|(\mathbf{X}' \times \mathbf{X}_{shankL}) \cdot \mathbf{Y}'|} ArcCos\left[\frac{\mathbf{X}_{shankL} \cdot \mathbf{X}'}{|\mathbf{X}_{shankL}||\mathbf{X}'|}\right] \qquad \text{D.3}$$

which yields

θ = -0.192076 radians or -11.0052 degrees.

The final Euler angle is φ. It is the included angle between the local Y-axis and the Y''-axis. The first step is to express the Y''-axis as a vector $\mathbf{Y}''$ in terms of global coordinates by using rotation matrices

$$\begin{bmatrix} \mathbf{i} \\ \mathbf{j} \\ \mathbf{k} \end{bmatrix} = ([\mathbf{R}_2][\mathbf{R}_1])^T \begin{bmatrix} \mathbf{I}'' \\ \mathbf{J}'' \\ \mathbf{K}'' \end{bmatrix} \qquad \text{D.4}$$

so that vector $\mathbf{Y}''$ equals

$$\mathbf{Y}'' = -sin(\psi)\mathbf{i} + cos(\psi)\mathbf{j} \qquad \text{D.5}$$

Then $\mathbf{Y}''$ can be found by using equation D.5 giving

$$\mathbf{Y}'' = -0.997632\,\mathbf{i} + 0.068782\,\mathbf{j}$$

The final Euler angle ϕ is found by using the relation below

$$\phi = \frac{(\mathbf{Y}'' \times \mathbf{Y}_{shankL}) \cdot \mathbf{X}_{shankL}}{|(\mathbf{Y}'' \times \mathbf{Y}_{shankL}) \cdot \mathbf{X}_{shankL}|} ArcCos\left[\frac{\mathbf{Y}_{shankL} \cdot \mathbf{Y}''}{|\mathbf{Y}_{shankL}||\mathbf{Y}''|}\right] \qquad \text{D.6}$$

yielding

ϕ = -2.18396 radians or -125.132 degrees.

Therefore the orientation of the left shank as an Euler *ZYX* sequence at the measured instant in time is (-93.9°, -11.0°, -125.1°).

APPENDIX F: Derivation of Newton-Euler Equations of Motion

The derivation of the Newton-Euler equations for spatial dynamics is taken directly from Haug (1989).

With reference to Section 3-27, Newton's equation of motion for differential mass $dm(P)$ is

$$\ddot{\mathbf{r}}dm(P) - \mathbf{F}(P)dm(P) - \int_m f(P,R)dm(R)dm(P) = 0 \qquad \text{(F.1)}$$

where integration of the internal force $\mathbf{f}(P, R)$ is taken over the whole body.

Let $\delta\mathbf{r}^P$ denote a virtual displacement of P. Then premultiplying both sides of Equation F.1 by $\delta\mathbf{r}^{PT}$ and integrating over the total mass yields

$$\int_m \delta\mathbf{r}^{PT}\ddot{\mathbf{r}}^P dm(P) - \int_m \delta\mathbf{r}^{PT}\mathbf{F}(P)dm(P) - \int_m\int_m \delta\mathbf{r}^{PT} f(P,R)dm(R)dm(P) = 0 \qquad \text{(F.2)}$$

Manipulation of the double integral that appear in Equation F.2 shows that

$$\begin{aligned}
&\int_m\int_m \delta\mathbf{r}^{PT}\mathbf{f}(P,R)dm(R)dm(P) \\
&= \frac{1}{2}\int_m\int_m \delta\mathbf{r}^{PT}\mathbf{f}(P,R)dm(R)dm(P) \\
&\quad + \frac{1}{2}\int_m\int_m \delta\mathbf{r}^{RT}\mathbf{f}(R,P)dm(P)dm(R) \\
&= \frac{1}{2}\int_m\int_m (\delta\mathbf{r}^P - \delta\mathbf{r}^R)^T\mathbf{f}(P,R)dm(P)dm(R)
\end{aligned} \qquad \text{(F.3)}$$

where the first equality simply rewrites the expression and interchanges dummy variables P and R of integration in the second integral. The second equality follows from interchanging of the order of integration and uses Newton's third law of action and reaction; that is $\mathbf{f}(P,R)dm(P)dm(R) = -\mathbf{f}(R,P)dm(R)dm(P)$.

For a rigid body with distance constraints between all points

$$(\mathbf{r}^P - \mathbf{r}^R)^T(\mathbf{r}^P - \mathbf{r}^R) = C$$

Taking the differential of both sides yields

$$(\delta\mathbf{r}^P - \delta\mathbf{r}^R)^T(\mathbf{r}^P - \mathbf{r}^R) = 0 \tag{F.4}$$

Since the internal force $\mathbf{f}(P,R)$ in the present model of a rigid body acts between points P and R so that

$$\mathbf{f}(P,R) = k(\mathbf{r}^P - \mathbf{r}^R) \tag{F.5}$$

where k is constant from Equation F.4, and the right side of Equation F.3 is zero assuming the collinearity of $\mathbf{f}(P,R)$ and $\mathbf{f}(R,P)$. Note that the right side of Equation F3 represents the virtual work of the internal forces in a rigid body (which are workless).

Substituting Equation F.4 and Equation F.5 into Equation F.3

$$\int_m \int_m \delta\mathbf{r}^{PT} f(P,R)dm(P)dm(R) = 0 \tag{F.6}$$

Using this result, Equation F.2 simplifies to

$$\int_m \delta\mathbf{r}^{PT}\ddot{\mathbf{r}}^P dm(P) - \int_m \delta\mathbf{r}^{PT}\mathbf{F}(P)dm(P) = 0 \tag{F.7}$$

which must hold for all virtual displacements $\delta\mathbf{r}^P$ that are consistent with constraints on the body.

To take full advantage of Equation F.7, the virtual displacement of point P may be written in terms of a virtual displacement of the origin of the $x'y'z'$ frame and a virtual rotation of the body ($\delta\pi'$). A virtual displacement of point P is given by

$$\delta\mathbf{r}^P = \delta\mathbf{r} - \mathbf{R}\tilde{\mathbf{s}}'^P\delta\pi' \tag{F.8}$$

where $\mathbf{R}$ is the rotation matrix vector, and $\tilde{\mathbf{s}}'_P$ is the constant skew-symmetric matrix of the distance of point P with respect to the $x'y'z'$ frame.

The acceleration equation for point P is

$$\ddot{\mathbf{r}}^P = \ddot{\mathbf{r}} + \ddot{\mathbf{R}}\mathbf{s}'^P \tag{F.9}$$

Now a definition of $\mathbf{w}$ can be made in terms of the rotation transformation matrix $\mathbf{R}$ such that

$$\tilde{\mathbf{w}} = \dot{\mathbf{R}}\mathbf{R}^T \tag{F.10}$$

Multiplying both sides of Equation F.10 on the right by $\mathbf{R}$ yields the relationship

$$\dot{\mathbf{R}} = \tilde{\mathbf{w}}\mathbf{R} \tag{F.11}$$

Therefore, differentiating Equation F.11, and using the matrix algebraic property that $\tilde{\mathbf{w}}\mathbf{R} = \mathbf{R}\tilde{\mathbf{w}}'$ the relationships for the second time derivative of the transformation matrix $\mathbf{R}$ are obtained

$$\ddot{\mathbf{R}} = \mathbf{R}\tilde{\dot{\mathbf{w}}}' + \mathbf{R}\tilde{\mathbf{w}}'\tilde{\mathbf{w}}' \tag{F.12}$$

Substituting Equation F.12 for $\ddot{\mathbf{R}}$ of Equation F9 yields another form of the acceleration equation

$$\ddot{\mathbf{r}}^P = \ddot{\mathbf{r}} + \mathbf{R}\tilde{\dot{\mathbf{w}}}'\mathbf{s}'^P + \mathbf{R}\tilde{\mathbf{w}}'\tilde{\mathbf{w}}'\mathbf{s}'^P \tag{F.13}$$

Substituting Equation F.8 and Equation F.12 into the variational equation of F.7 yields

$$\begin{aligned}\int_m (\,\delta\mathbf{r}^T + \delta\boldsymbol{\pi}'^T\tilde{\mathbf{s}}'^P\mathbf{R}^T\,)(\,\ddot{\mathbf{r}} + \mathbf{R}\tilde{\dot{\mathbf{w}}}'\mathbf{s}'^P + \mathbf{R}\tilde{\mathbf{w}}'\tilde{\mathbf{w}}'\mathbf{s}'^P\,)dm(P) \\ - \int_m (\,\delta\mathbf{r}^T + \delta\boldsymbol{\pi}'^T\tilde{\mathbf{s}}'^P\mathbf{R}^T\,)\mathbf{F}(P)dm(P) = 0\end{aligned} \tag{F.14}$$

where all $\delta\mathbf{r}$ and $\delta\boldsymbol{\pi}'$ that are consistent with constraints that act on the body.

Expanding the integrals of Equation F.14 gives

$$\begin{aligned}&\delta\mathbf{r}^T\ddot{\mathbf{r}}\int_m dm(P) + \delta\mathbf{r}^T(\,\mathbf{R}\tilde{\dot{\mathbf{w}}}' + \mathbf{R}\tilde{\mathbf{w}}'\tilde{\mathbf{w}}'\,)\int_m \mathbf{s}'^P dm(P) \\ &\quad + \delta\boldsymbol{\pi}'^T\int_m \mathbf{s}'^P dm(P)\mathbf{R}^T\ddot{\mathbf{r}} + \delta\boldsymbol{\pi}'^T\int_m \tilde{\mathbf{s}}'^P\tilde{\dot{\mathbf{w}}}'\mathbf{s}'^P dm(P) \\ &\quad + \delta\boldsymbol{\pi}'^T\int_m \tilde{\mathbf{s}}'^P\tilde{\mathbf{w}}'\tilde{\mathbf{w}}'\mathbf{s}'^P dm(P) - \delta\mathbf{r}^T\int_m \mathbf{F}(P)dm(P) \\ &\quad - \delta\boldsymbol{\pi}'^T\int_m \tilde{\mathbf{s}}'^P\mathbf{F}'(P)dm(P) = 0\end{aligned} \tag{F.15}$$

where for all $\delta\mathbf{r}$ and $\delta\boldsymbol{\pi}'$ that are consistent with constraints.

To simplify the form of Equation F.15, a body-fixed $x'y'z'$ reference frame is selected with its origin at the center of mass of the body, i.e. centroidal body reference frame. The total mass is

$$m \equiv \int_m dm(P) \tag{F.16}$$

and, by definition of the centroid,

$$\int_m \mathbf{s}'^P dm(P) = 0 \tag{F.17}$$

The total external force acting on the body is simply

$$\mathbf{F} \equiv \int_m \mathbf{F}(P) dm(P) = 0 \tag{F.18}$$

and the moment of the external forces with respect to the origin of the $x'y'z'$ frame is

$$\mathbf{n}' \equiv \int_m \mathbf{s}'^P \mathbf{F}(P) dm(P) = 0 \tag{F.19}$$

The fourth integral integral in Equation F.15 can be written as

$$\begin{aligned} \int_m \mathbf{s}'^P \tilde{\dot{\mathbf{w}}}' \mathbf{s}'^P dm(P) &= -\left(\int_m \tilde{\mathbf{s}}'^P \tilde{\mathbf{s}}'^P dm(P) \right) \dot{\mathbf{w}}' \\ &\equiv \mathbf{J}' \dot{\mathbf{w}}' \end{aligned} \tag{F.20}$$

where the constant *inertia matrix* $\mathbf{J}'$ with respect to the $x'y'z'$ centroidal frame is defined as

$$\begin{aligned} \mathbf{J}' &\equiv -\int_m \tilde{\mathbf{s}}'^P \tilde{\mathbf{s}}'^P dm(P) \\ &= \int_m \begin{bmatrix} (y'^P)^2 + (z'^P)^2 & -x'^P y'^P & -x'^P z'^P \\ -x'^P y'^P & (x'^P)^2 + (z'^P)^2 & -y'^P z'^P \\ -x'^P z'^P & -y'^P z'^P & (x'^P)^2 + (y'^P)^2 \end{bmatrix} dm(P) \end{aligned} \tag{F.21}$$

where the diagonal elements in the matrix $\mathbf{J}'$ are called the *moments of inertia* and the off-diagonal terms are called the *products of intertia.*

By using the basic matrix algebraic relations $\tilde{\mathbf{a}}\mathbf{b} = -\tilde{\mathbf{b}}\mathbf{a}$ and $\widetilde{(\mathbf{a}+\mathbf{b})} = \tilde{\mathbf{a}} + \tilde{\mathbf{b}}$ then the integrand of the fifth integral in Equation F.15 can be expanded as

$$\begin{aligned} \tilde{\mathbf{s}}'^P \tilde{\mathbf{w}}' \tilde{\mathbf{w}}' \mathbf{s}'^P &= -\tilde{\mathbf{s}}'^P \tilde{\mathbf{w}}' \tilde{\mathbf{s}}'^P \mathbf{w}' \\ &= -\tilde{\mathbf{w}}' \tilde{\mathbf{s}}'^P \tilde{\mathbf{s}}'^P \mathbf{w}' - \mathbf{w}' \mathbf{s}'^{PT} \tilde{\mathbf{s}}'^P \mathbf{w}' - \mathbf{s}'^P \mathbf{w}'^T \tilde{\mathbf{w}}' \mathbf{s}'^P \\ &= -\tilde{\mathbf{w}}' \tilde{\mathbf{s}}'^P \tilde{\mathbf{s}}'^P \mathbf{w}' \end{aligned} \tag{F.22}$$

Integrating both sides over the mass of the body yields

$$\int_m \tilde{\mathbf{s}}'^P \tilde{\mathbf{w}}' \tilde{\mathbf{w}}' \mathbf{s}'^P dm(P) = \tilde{\mathbf{w}}' \left(-\int_m \tilde{\mathbf{s}}'^P \tilde{\mathbf{s}}'^P dm(P) \right) \mathbf{w}' = \tilde{\mathbf{w}}' \mathbf{J}' \mathbf{w}' \tag{F.23}$$

Substituting Equation F.16 to F.22 into Equation F.15 yields the *variational Newton-Euler equations of motion* for a rigid body with a centroidal body-fixed reference frame

$$\delta\mathbf{r}^T\left[m\ddot{\mathbf{r}} - \mathbf{F}\right] + \delta\boldsymbol{\pi}'^T\left[\mathbf{J}'\dot{\mathbf{w}}' + \tilde{\mathbf{w}}'\mathbf{J}'\mathbf{w}' - \mathbf{n}'\right] = 0 \qquad \text{(F.24)}$$

which must hold for all virtual displacements $\delta\mathbf{r}$ and virtual rotations $\delta\boldsymbol{\pi}'$ of the centroidal $x'y'z'$ frame that are consistent with constraints that act on the body.

APPENDIX G: Special Cases

Shoulders and Hips in Local Coordinate System

Once a point has been defined as a *Mechanical Systems Pack Body* function object it is specified in the local coordinate system of that segment. This is a convenient way of expressing points that are a fixed distance from each other at each instant in time. For instance, the two points delimiting the elbow and wrist joint of the upper arm segment are a fixed distance apart. Only the global position of the center of mass, needed to be specified. Then the location and orientation of the upper arm segment would be directly determined by the definitions in the *Body* and *Constraint* functions. However, the location of the shoulders, and hips could not be accurately expressed as a fixed distance apart from another point. Therefore, these segment endpoints had to be converted from their global XYZ coordinates (*.trc* file) into the local coordinate system of their respective bodies.

The shoulder joint centers had to be defined with respect to the upper trunk. As the upper trunk is not a rigid body segment, the shoulder joint center could not be defined as a fixed distance from a point on the upper trunk. Also, shoulder joint center itself is not fixed with respect to the upper trunk: the shoulder being able to elevate, depress, protract, and retract. Therefore, the most accurate way to account for this was to specify the location of shoulder joint center from a point on the upper trunk at each instant in time. The general procedure was to subtract the global XYZ coordinates of the proximal end of upper trunk from that of the shoulder joint, and then convert these coordinates into the local coordinate system of the upper trunk by multiplying with the Euler 321 rotation matrix. An example for the general procedure for the right shoulder joint is shown below:

$$(\boldsymbol{UpperArmRIGHTXYZ}[T] - \boldsymbol{UpperTrunkXYZ}[T]) * \boldsymbol{R}_{321} - \{0, \boldsymbol{UpperTrunkCoM}, 0\}$$

where, *SegmentNameXYZ[T]* is the global XYZ coordinates of the proximal end of the segment expressed as function of time, and R_{ZYX} is the Euler ZYX rotation

matrix. Subtracting {0, SegmentNameCoM, 0} set the origin of the local coordinate system at the center of mass (CoM). In this case, the proximal end of the right upper arm was the right shoulder joint center, and the proximal end of the upper trunk the mid-trunk 'joint centre' or end point. The process was repeated for the left shoulder joint center.

For the hip joint center, the same process was followed with the global XYZ coordinates of the lower trunk proximal end subtracted from that of the hip joint center, and then converted into the local coordinate coordinate system of the lower trunk. For the right hip joint center

$$(\boldsymbol{ThighRIGHTXYZ}[T] - \boldsymbol{LowerTrunkXYZ}[T]) * \boldsymbol{R}_{321} - \{0, \boldsymbol{LowerTrunkCoM}, 0\}$$

where the proximal end of the right thigh segment is the right hip joint center, and the proximal end of lower trunk the mid-hips 'joint center' or endpoint. The same process was carried out for the left hip joint center.

Shank to Foot connection

The connection of the shank to foot does not occur at ankle joint center, because the foot model was based on that of de Leva (1996), who established an empirical relationship between the inertia properties of the foot and the longitudinal length from the heel to the end of the second toe. Therefore, in the *Mech3D* rigid body model there could not be any direct linkage between the distal end of the shank and the foot. The foot and shank in real life articulates at the ankle joint, which is not part of the foot model. Instead, the *RelativeX1*, *RelativeY1*, and *RelativeZ1* constraint function was used to specify the X, Y, and Z coordinates of the heel to be a certain distance greater than the X, Y, and Z coordinates of distal end of the shank, respectively. The distance between the heel and distal end of the shank during motion is not a fixed distance, and so was expressed as a function of time based on the output *Eva 6.0 .trc* file.

APPENDIX H: Common Mech3D Output Functions

AccelerationTerms[*cnum*] returns the part of the right-hand term of the current acceleration constraint expressions associated with constraint *cnum*.

Alpha[*bnum*] returns the angular acceleration of body *bnum*.

CompositeInertia[{*centroid1, mass1, inertia1*}, ...,{*centroidn, massn, inertian*}] returns the list {*centroid, mass, inertia*} of the inertia properties of a composite body *B* made up of the *n* specified subcomponents. In **Mech3D**, arguments to **CompositeInertia** can have the form {*centroidn, massn, inertian, rotationn*} to specify subcomponents that are rotated relative to the composite body *B*.

DDistanceDT[*point1, point2*] returns the time derivative of the absolute distance between the two points.

D2DistanceDT2[*point1, point2*] returns the second time derivative of the absolute distance between the two points.

Direction[*vector*] returns the direction vector of a *Mech* vector object in global coordinates.

Distance[*point1, point2*] returns the absolute distance between the two points.

EulerParameters[*bnum*] returns the Euler parameters associated with body *bnum* as {*eo, ei, ej, ek*}.

IncludedAngle[*vector1, vector2*] returns the positive angle between the global direction vectors of the two *Mech* vector objects.

Jacobian[*cnum, bnum*] returns the submatrix of the current Jacobian associated with constraint *cnum* and body *bnum*.

Omega[*bnum*] returns the angular velocity of body *bnum*.

Magnitude[*vector*] returns the length of *vector*.

MassMatrix[*bnum*] returns the submatrix of the current system mass matrix associated with body *bnum*.

PointToLocal[*bnum, point*] returns the local coordinates of *point*, in the coordinate system of body *bnum*.

ProjectedAngle[*vector1, vector2, vector3*] returns the counterclockwise angle measured from the direction of *vector2* to the direction of *vector1*, as projected on a plane that is orthogonal to *vector3*.

Reaction[*cnum, bnum, point*] returns the reaction loads applied by constraint *cnum* to body *bnum*, calculated about the specified *point*. Loads are returned in the format: {*force, moment*}. **Reaction** accepts the option **Coordinates**□**Local** to return the load vectors in local coordinates, relative to body *bnum*. **Reaction** is also a setting for the **Type** option for **Loads**.

RelativeVelocity[*bnum, point*] returns the velocity of *point*, relative to body *bnum*, in global coordinates.

Rotation[*bnum*] returns the angle of rotation associated with the orientation of 2D body *bnum*, or the list {*ang, axis*} specifying the angle and axis of rotation associated with 3D body *bnum*.

RotationMatrix[*bnum*] returns the 2D/3D rotation matrix associated with body *bnum*.

Unit[*vector*] returns a unit vector pointed in the direction of the *Mech* vector object.

VelocityTerms[*cnum***]** returns the part of the right-hand term of the current velocity constraint expressions associated with constraint *cnum*.

APPENDIX I: Ball Speed of Test Sample

Table I-1: Bowlers ranked in order of increasing maximum ball release speed.

Rank (speed)	ID	Max Speed (m/s)	Ave Speed (m/s)	Standard Deviation	Standard Classifcation	Speed Classification
1	MCK	36.51	35.81	0.4435	NATIONAL B	FAST
2	BUT	36.16	35.30	0.5397	INTERNATIONAL	FAST
3	BON	36.04	35.06	0.5243	INTERNATIONAL	FAST
4	SHE	35.92	35.49	0.3676	NATIONAL B	FAST
5	MART	35.19	34.49	0.4227	INTERNATIONAL	FAST
6	YOV	34.70	33.84	0.3895	NATIONAL A	FAST
7	COR	34.23	33.84	0.3447	NATIONAL A	FAST
8	GAR	34.17	33.77	0.4316	NATIONAL B	FAST
9	HEN	34.01	33.25	0.5729	NATIONAL B	FAST
10	LAN	33.32	32.65	0.4609	LOCAL	MED-FAST
11	HOO	33.28	32.39	0.7146	NATIONAL B	MED-FAST
12	KAL	33.17	32.69	0.3914	LOCAL	MED-FAST
~~13~~	~~ELI~~	~~33.04~~	~~32.08~~	0.5317	~~NATIONAL B~~	~~MED-FAST~~
14	ECK	32.91	32.43	0.2592	PROVINCIAL	MED-FAST
15	FRA	32.49	32.03	0.5918	INTERNATIONAL	MED-FAST
16	PAR	32.26	31.42	0.5710	PROVINCIAL	MED-FAST
17	JAM	32.19	31.74	0.3827	LOCAL	MED-FAST
18	BAT	32.09	31.47	0.3169	NATIONAL B	MED-FAST
19	JOS	32.07	31.46	0.4608	PROVINCIAL	MED-FAST
20	MAX	31.90	31.04	0.5435	LOCAL	MEDIUM
21	STY	31.54	30.91	0.3988	INTERNATIONAL	MEDIUM
22	SAN	31.53	30.83	0.6958	NATIONAL A	MEDIUM
23	RAS	31.49	30.98	0.3303	NATIONAL B	MEDIUM
24	SHA	31.13	30.33	0.5549	LOCAL	MEDIUM
25	COL	31.05	30.75	0.2837	NATIONAL A	MEDIUM
26	NAI	30.95	30.73	0.2851	LOCAL	MEDIUM
27	MEE	30.63	30.14	0.4720	PROVINCIAL	MEDIUM
28	SIM	30.42	29.67	0.4563	LOCAL	SLOW
29	TOD	28.58	28.07	0.4271	LOCAL	SLOW
30	WHI	27.95	27.08	0.8191	PROVINCIAL	SLOW
31	MAR	27.72	26.87	0.6320	LOCAL	SLOW
32	REN	27.53	26.07	0.8717	LOCAL	SLOW
33	RUW	27.51	27.12	0.4687	LOCAL	SLOW
34	RUS	26.70	26.29	0.5354	LOCAL	SLOW

Table I-2: Bowling subjects sorted according to highest competition level.

Rank (speed)	ID	Max Speed (m/s)	Ave Speed (m/s)	Standard Deviation	Standard Classifcation	Speed Classification
2	BUT	36.16	35.30	0.5397	INTERNATIONAL	FAST
3	BON	36.04	35.06	0.5243	INTERNATIONAL	FAST
5	MART	35.19	34.49	0.4227	INTERNATIONAL	FAST
15	FRA	32.49	32.03	0.5918	INTERNATIONAL	MED-FAST
21	STY	31.54	30.91	0.3988	INTERNATIONAL	MEDIUM
6	YOV	34.70	33.84	0.3895	NATIONAL A	FAST
7	COR	34.23	33.84	0.3447	NATIONAL A	FAST
22	SAN	31.53	30.83	0.6958	NATIONAL A	MEDIUM
25	COL	31.05	30.75	0.2837	NATIONAL A	MEDIUM
1	MCK	36.51	35.81	0.4435	NATIONAL B	FAST
4	SHE	35.92	35.49	0.3676	NATIONAL B	FAST
8	GAR	34.17	33.77	0.4316	NATIONAL B	FAST
9	HEN	34.01	33.25	0.5729	NATIONAL B	FAST
11	HOO	33.28	32.39	0.7146	NATIONAL B	MED-FAST
13	ELI	33.04	32.08	0.5317	NATIONAL B	MED-FAST
18	BAT	32.09	31.47	0.3169	NATIONAL B	MED-FAST
23	RAS	31.49	30.98	0.3303	NATIONAL B	MEDIUM
14	ECK	32.91	32.43	0.2592	PROVINCIAL	MED-FAST
16	PAR	32.26	31.42	0.5710	PROVINCIAL	MED-FAST
19	JOS	32.07	31.46	0.4608	PROVINCIAL	MED-FAST
27	MEE	30.63	30.14	0.4720	PROVINCIAL	MEDIUM
30	WHI	27.95	27.08	0.8191	PROVINCIAL	SLOW
10	LAN	33.32	32.65	0.4609	LOCAL	MED-FAST
12	KAL	33.17	32.69	0.3914	LOCAL	MED-FAST
17	JAM	32.19	31.74	0.3827	LOCAL	MED-FAST
20	MAX	31.90	31.04	0.5435	LOCAL	MEDIUM
24	SHA	31.13	30.33	0.5549	LOCAL	MEDIUM
26	NAI	30.95	30.73	0.2851	LOCAL	MEDIUM
28	SIM	30.42	29.67	0.4563	LOCAL	SLOW
29	TOD	28.58	28.07	0.4271	LOCAL	SLOW
31	MAR	27.72	26.87	0.6320	LOCAL	SLOW
32	REN	27.53	26.07	0.8717	LOCAL	SLOW
33	RUW	27.51	27.12	0.4687	LOCAL	SLOW
34	RUS	26.70	26.29	0.5354	LOCAL	SLOW

APPENDIX J: ANOVA & Bonefferoni procedure for trunk rotation angular velocity

```
Analysis of Variance
Source     DF        SS        MS        F        P
Factor      3    216.24     72.08     9.24    0.000
Error      29    226.18      7.80
Total      32    442.42

                                      Individual 95% CIs For Mean
                                      Based on Pooled StDev
Level       N      Mean     StDev  -------+---------+---------+---
------
C1          8    14.231     2.770                          (-----*--
--)
C2         10     9.707     3.245             (----*----)
C3          8    11.637     1.947                 (-----*-----)
C4          7     6.927     2.920    (-----*-----)
                                      -------+---------+---------+---
------
Pooled StDev =    2.793                   7.0       10.5       14.0
```

Figure J-1: Minitab statistical session output for one-way ANOVA test on trunk long axis rotation angular velocity. Calculation of confidence intervals based on a pooled standard deviation estimator is based on the Bonefferoni procedure for making multiple comparisons between groups: fast – C1, med-fast – C2, medium, C3, and slow – C4.

APPENDIX K: TRUNK SEQUENCING

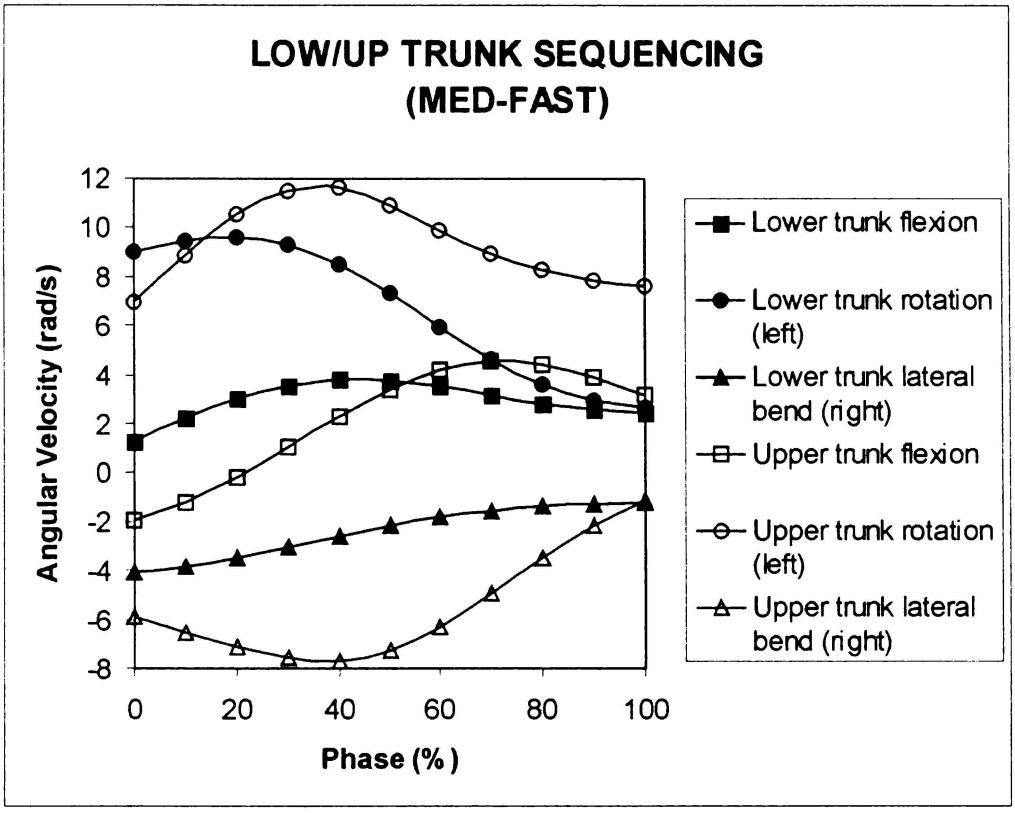

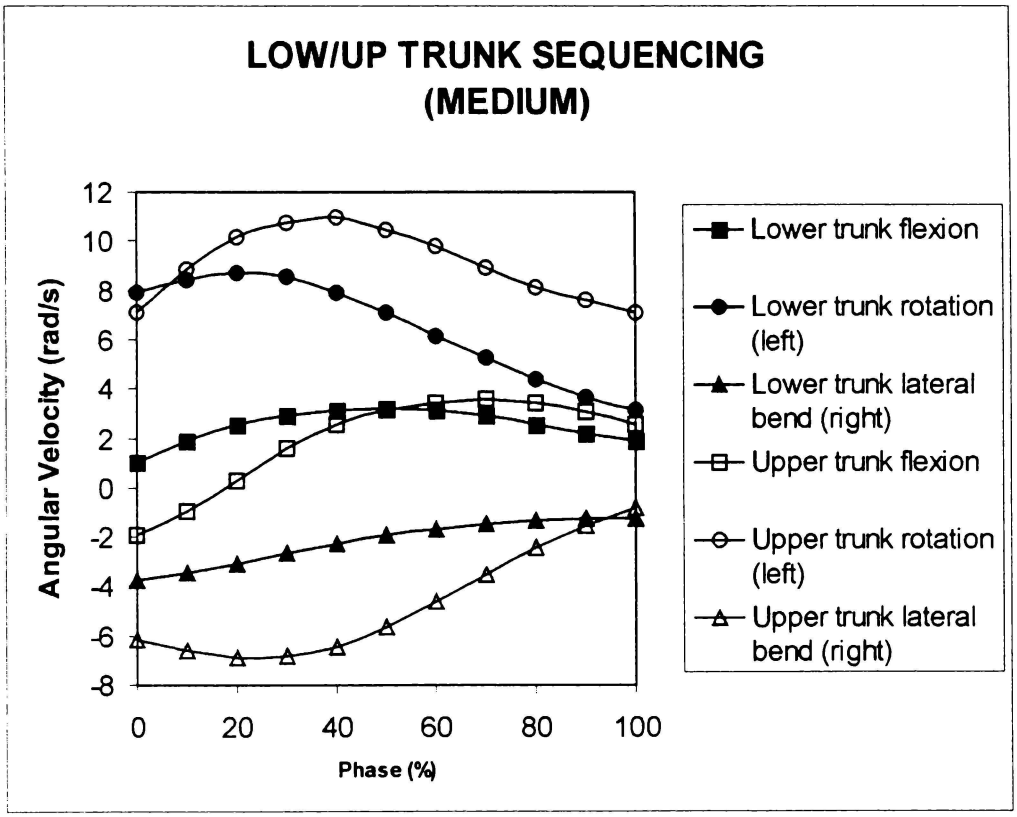

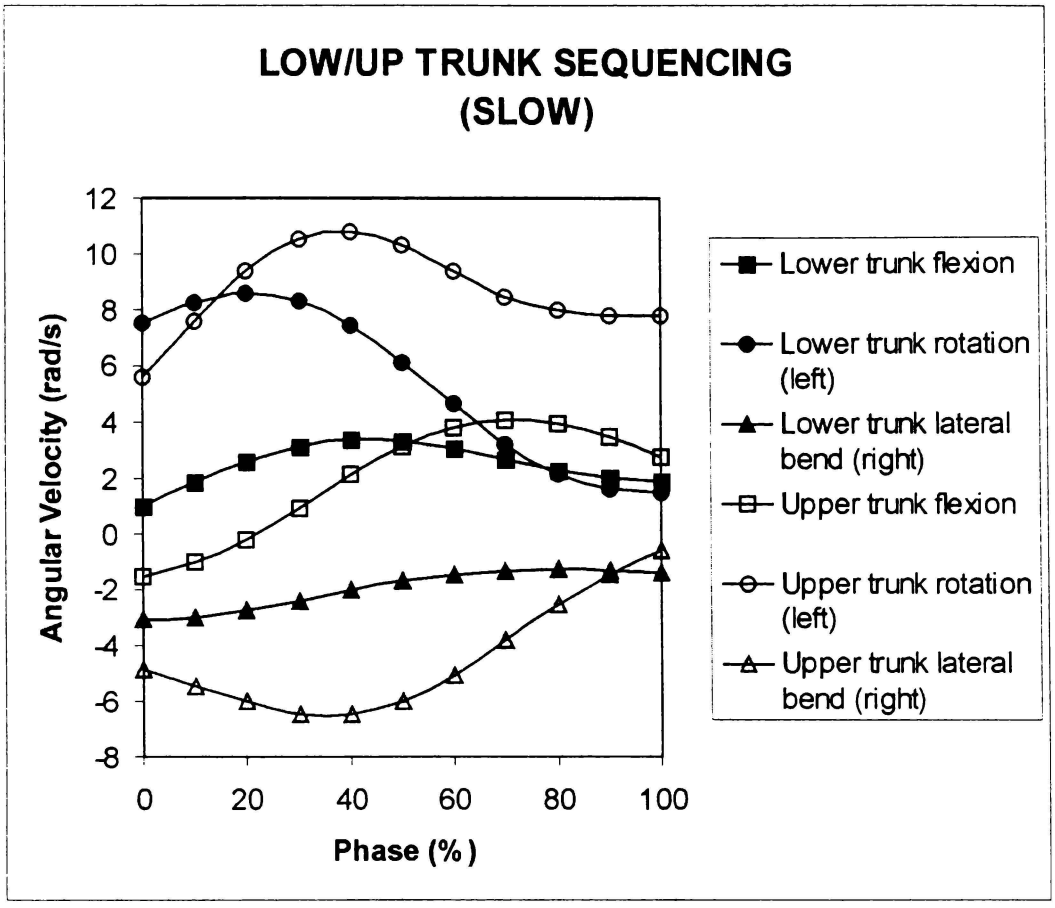
LOW/UP TRUNK SEQUENCING
(SLOW)
Angular Velocity (rad/s)
12
10
8
6
4
2
0
-2
-4
-6
-8
0
20
40
60
80
100
Phase (%)
Lower trunk flexion
Lower trunk rotation (left)
Lower trunk lateral bend (right)
Upper trunk flexion
Upper trunk rotation (left)
Upper trunk lateral bend (right)

APPENDIX L: FIELD PLACING

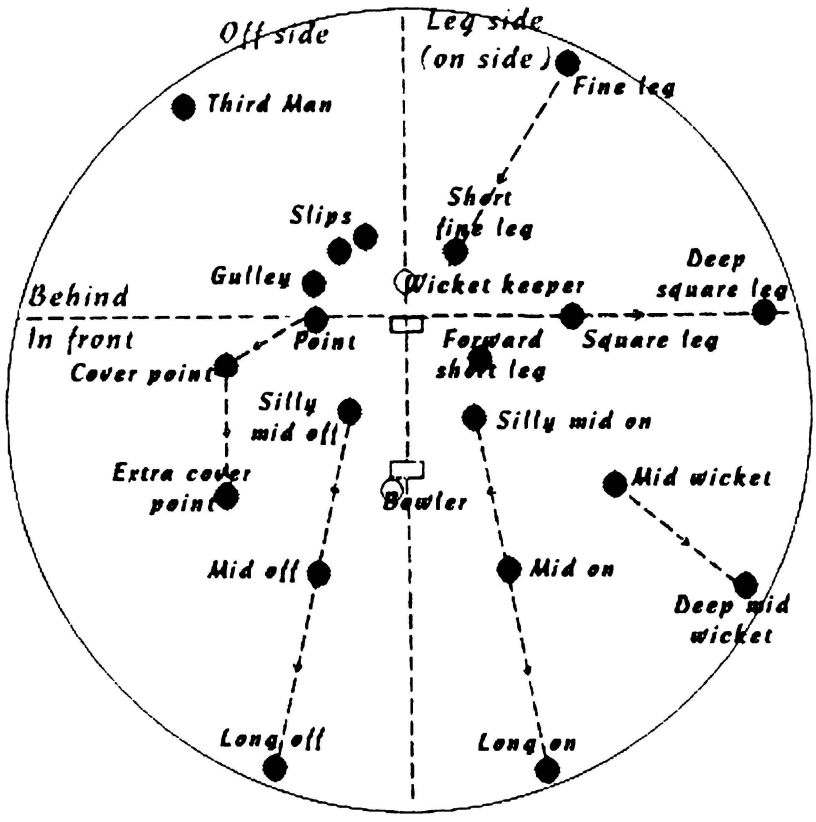

BIBLIOGRAPHY

Abernethy, B. 1981. Mechanics of skill in cricket batting. *Australian Journal of Sports Medicine*, 13, 3-10.

Atkinson, K.E. 1978. *An Introduction to Numerical Analysis*. Wiley, New York.

Andrews, J.G. 1995. Euler's and Lagranges equations for linked rigid-body models of three dimensional human motion. In P. Allard, I.A.F. Stokes & J.

Bartlett, R.M. 1996. The biomechanics of fast bowling in men's cricket: A Review. *Journal of Sports Sciences*, 14, 403-424.

Blanchi (eds), *Three-Dimensional Analysis of Human Movement*, Human Kinetics, Champaign, Illinois, pp. 145-175.

Baraff, D. 1996. Linear-time dynamics using Lagrange multipliers. *Computer Graphics Proceedings, Annual Conference Series*, pp. 137-146.

Baruh, H. (1999). *Analytical Dynamics.* McGraw-Hill, Singapore.

Bell, A. L., Pedersen, D. R., and Brand, R. A. (1990). A comparison of the accuracy of several hip center location prediction methods. *Journal of Biomechanics, 23*(6), 617-621.

Bell, P. A.1992. Spondylolysis in fast bowlers: principles of prevention and a survey of awareness among cricket coaches. *British Journal of Sports Medicine*, 26(4), 273 - 275.

Bradman, D. 1958. *The Art of Cricket.* Hodder and Stoughton, London.

Colby, J. & Fricker, P. 1984. Can we prevent back injuries to elite women gymnasts. *Sports Sci Med Q*, 1(1), 13-15.

Benaud, L.R. 1976. *The Young Cricketer.* Angus & Robertson Publishers, London.

Benaud, R.B. 1981. Teaching cricket. In J. Main (ed.), *How to Play Cricket Australian Style*, Lloyd O'Neil Pty. Ltd., Melbourne, pp. 92-113.

Brees, A.J. 1989. A cinematographical analysis of the effect of varying the run-up speed on ball release velocity, accuracy and body kinematics of fast bowling in cricket. Unpublished undergraduate dissertation, Crewe + Alsager College of Higher Education.

Burden, A.M. & Bartlett, R.M. 1989. A kinematic analysis of fast bowling in cricket. *Journal of Sports Sciences*, 7, 75.

Burden, A.M. & Bartlett, R.M. 1990a. An elctromyographical analysis of fast-medium bowling in cricket. In P.A. Anderson, D.J. Hobart and J.V. Danoff (eds), *Electromyographical Kinesiology: Proceedings of the VIIIth Congress of the International Society of Electrophysiological Kinesiology*, Excerpta Medica, Amsterdam, pp. 457-460,

Burden, A.M. & Bartlett, R.M. 1990b. A kinematic comparison between elite fast bowlers and college fast-medium bowlers. In *Proceedings of the Sports Biomechanics Section of the British Association of Sports Sciences*, No. 15, BASS, Leeds.

Burnett, A.F., Elliott, B.C. and Marshall, R.N. 1995. The effect of a 12-over spell on fast bowling technique in cricket. *Journal of Sports Sciences*, 13, 329-341.

Cheze, L. 2000. Comparison of different calculations of three-dimensional joint kinematics from video-based system data. *Journal of Biomechanics*, 33, 1695-1699.

Davis, K. & Blanksby, B. 1976a. A cinematographic analysis of fast bowling in cricket. *Australian Journal of Health, Physical Education, and Recreation*, 71, 9-15.

Davis, K. & Blanksby, B. 1976b. The segmental components of fast bowling in cricket. *The Australian Journal for Health, Physical Education and Recreation*, 71(March [Suppl]), 6-8.

de Leva, P. 1996. Adjustments to Zatsiorsky-Seluyanov's segment inertia parameters. *Journal of Biomechanics, 29*(9), 1223-1230.

Devore, J.L. 1987. *Probability and Statistics for Engineering and the Sciences.* Brooks/Cole Publishing Company, Monterey.

De Mestre, N. 1990. *The Mathematics of Projectiles in Sport.* Cambridge University Press, Cambridge.

Elliott, B.C. 2000. Back injuries and the fast bowler in cricket. *Journal of Sport Sciences*, 18, 983-991.

Elliot, B. C. & Foster, D. H. 1984. A biomechanical analysis of the front-on and side-on fast bowling techniques. *Journal of Human Movement Studies*, 10, 83-94.

Elliot, B. C. & Foster, D. 1989a. Fast bowling technique. In B.C. Elliott & D. Foster (eds), *Send the stumps flying: the science of fast bowling*, University of Western Australia Press, Nedlands, W.A., pp. 26-36.

Elliot, B. C. & Foster, D. 1989b. Factors that may predispose a fast bowler to injury. In B.C. Elliott & D. Foster (eds), *Send the stumps flying: the science of fast bowling*, University of Western Australia Press, Nedlands, W.A., pp. 54-59.

Elliott, B.C & Khangure, M.S. 2002. Disk degeneration and fast bowling in cricket: an intervention study. *Medicine and Science in Sports and Exercise*, 34 (11), 1714-1718.

Elliot, B. C., Foster, D. H. and Gray, S. 1986. Biomechanical and physical factors influencing fast bowling. *The Australian Journal of Science and Medicine in Sport,* 18(1), 16 - 21.

Elliott, B.C., Foster, D and John, D. 1990. The biomechanics of side-on and front-on fast bowling in cricket. In, Draper, J. (ed.), *Third report on the National Sports Research Program*, July 1988-June 1990, Australian Sports Commission, Belconnen, p. 9-12.

Elliott, B.C., Hardcastle, P.H., Burnett, A.F. and Foster, D.H. 1992. The influence of fast bowling and physical factors on radiological features in high performance young fast bowlers. *Sports Medicine, Training and Rehabilitation*, 3, 113-130.

Elliott, B.C., Davis, J.W., Khangure, M.S. and Hardcastle, P. 1993. Disc degeneration and the young fast bowler in cricket. *Clinical Biomechanics*, 8, 227-234.

Elliott, B.C., Marshall, R. and Noffal, G. Contributions of upper limb segment rotations during the power serve in tennis. *Journal of Applied Biomechanics*, 11, 433-442.

Ferdinands, R.E.D. 1999. Biomechanical analysis of the bowling action in cricket. Unpublished Master's thesis, University of Waikato.

Ferdinands, R.E.D., Broughan, K.A. and Round, H., 2000a. Cricket bowling: a two-segment Lagrangian model. In *Proceedings of the XVIII International Symposium on Biomechanics in Sports*, edited by Hong, Y. and Johns, D. (Hong Kong: CUHK Press), pp. 517-520.

Ferdinands, R.E.D., Broughan, K.A. and Round, H., 2000b. Cricket bowling: a two-segment Lagrangian model. In *Proceedings of the Fifth Australian Conference on Mathematics and Computers in Sport,* edited by Cohen, G. and Langtry, T. (Sydney: UTS Printing Services), p. 197.

Ferdinands, R.E.D., Broughan, K.A., Round, H. and Marshall, R.N., 2001a. A fifteen-segment 3-D rigid body model of bowling in cricket. In *Computer Simulation in Biomechanics*, edited by Casolo, F., Lorenzi, V. and Zappa, B. (Milan: Libreria CLUP), pp. 99-104.

Ferdinands, R.E.D., Broughan, K.A., Round, H. and Marshall, R.N., 2001b. A fifteen-segment 3-D rigid body model of bowling in cricket. In *XVIII Congress of the International Society of Biomechanics*, edited by Muller, R., Gerber, H., and Stacoff, A. (Zurich: ETH), p. 236.

Ferdinands, R.E.D., Broughan, K.A. and Round, H. 2002a. A time-variant forward solution model of the bowling arm in cricket. In *International Research in Sports Biomechanics,* edited by Hong, Y. (London: Routledge), pp. 56-65.

Ferdinands, R., Marshall, R.N., Round, H., and Broughan, K.A. 2002b. Bowling arm and trunk mechanics of fast bowlers in cricket. In *Proceedings of the Fourth Australasian Biomechanics Conference*, edited by T.M. Bach, D. Orr, R.Baker, W.A. Sparrow (Melbourne: La Trobe University), pp. 176-177.

Ferdinands, R.E.D., Marshall, R.N., Round, H. and Broughan, K.A. 2003a. Ball speed generation by fast bowlers in cricket. In *Proceedings of the XVIII Congress of the International Society of Biomechanics*, edited by Milburn,P., Wilson, B. and Yanai, T. (Dunedin: University of Otago), p. 103.

Ferdinands, R.E.D., Marshall, R.N., Round, H. and Broughan, K.A. 2003b. An inverse/forward solution model of bowling in cricket. In *Proceedings of the IX International Symposium on Computer Simulation in Biomechanics*, edited by Smith, R., Casolo F., Hubbard, M., Sinclair P., Glitsch, U. (Sydney: University of Sydney), p. 33.

Fitch,K. 1989. Common injuries to the fast bowler. In B.C. Elliott & D. Foster (eds), *Send the stumps flying: the science of fast bowling*, University of Western Australia Press, Nedlands, W.A., pp. 60-67.

Foster, D.H. & Elliot, B.C. 1985. Fast bowling: an impact sport. A profile of D.K. Lillee. *Sports Coach*, 9, 3-7.

Foster, D.H. & Elliott, B.C. 1989. The art of swing bowling. In B.C. Elliott & D. Foster (eds), *Send the stumps flying: the science of fast bowling*, University of Western Australia Press, Nedlands, W.A., pp. 37-42.

Foster, F., Elliot, B.C., Gray, S. and Herzberg, L. 1984. Guidelines for the fast bowler. *Sports Coach*, 7, 47-48.

Foster, D., John, D., Elliott, B., Akland, T. and Fitch, K. 1989. Back injuries to fast bowlers in cricket: A prospective study. *British Journal of Sports Medicine*, 23, 150-154.

Ginsberg, J. H. 1998. *Advanced Engineering Dynamics.* Cambridge University Press, Cambridge.

Gover, A. 1980. *Cricket Manual. A Pictorial Guide to Batting, Bowling, Wicket-keeping and Fielding.* Lutterworth Press, Surrey.

Greenwood, D. T. 1988. *Principles of Dynamics.* Prentice-Hall, Englewood Cliffs (New Jersey)

Haug, E.J. 1989. *Computer Aided Kinematics and Dynamics of Mechanical Systems Volume 1: Basic Methods.* Allyn & Bacon, Masachusetts.

Hay, J.G. 1993. *The Biomechanics of Sports Techniques.* Prentice-Hall, New Jersey

Hershler C. & Milner, M. 1978. An optimality criterion for processing electromyographic criterion for processing electromyographic (EMG) signal relating to human locomotion. *IEEE Transactions of Biomedical Engineering BME*, 25, 413-420.

Kadaba, M.P., Wootten, M.E., Gainey, J. and Cochran, G.V.B. 1985. Repeatability of phasic muscle activity: performance of surface and intramuscular wire electrodes in gait analysis. *Journal of Orthopaedic Research*, 3, 350-359.

Kane, T.R. & Levinson, T.R. 1985. *Dynamics: Theory and Applications*. McGraw Hill, New York.

Lanczos, C. *The Variational Principles of Mechanics* (4th Ed.). University of Toronto Press, Toronto.

Lillee, D. 1977. *The Art of Fast Bowling*. W. Collins Publishing pty Ltd., Sydney.

Lillee, D. 1994. Fast bowling. In T. Lewis (ed.), *MCC Masterclass. The New MCC Coaching Book.* Weidenfield & Nicholson, London.

Lindwall, R. 1957. *Flying Stumps*. The Anchor Press, Essex.

Luttgens, K., Deutsch, H., Hamilton, N. 1992. Kinesiology. Scientific Basis of Human Motion (8th Ed.). Brown & Benchmark, Dubuque, Iowa.

Marshall, R.N. & Elliott, B.C. 2000. Long-axis rotation: the missing link in proximal-to-distal sequencing. *Journal of Sports Sciences*, 18, 247-254.

Marshall, R and Ferdinands, R. 2002. The Effect of a Flexed Elbow on Bowling Speed in Cricket. *Sports Biomechanics*, 2 (1), 65-71.

Marylebone Cricket Club. 1962. *MCC Cricket Coaching Book.* William Heinemann Ltd., London.

Marylebone Cricket Club. 1964. *MCC Cricket Coaching Book.* William Heinemann Ltd., London.

Marylebone Cricket Club. 1976. *MCC Cricket Coaching Book.* William Heinemann Ltd., London.

Mason, B. R., Weissensteiner, J. R. and P. R. Spence. 1989. Development of a model for fast bowling in cricket. *Excel*, 6(1), 2-12.

Meuleman, K. 1983. Quickies are the workhorses. *In The Sunday Independent Newspaper*, March 6th, Perth.

Moon, F. C. 1998. *Applied Dynamics with Applications to Multibody and Mechatronic Systems.* John Wiley & Sons, Inc., Toronto.

Nikravesh, P. E. 1988. *Computer-Aided Analysis of Mechanical Systems.* Prentice Hall, New Jersey.

Onyshko, S. & Winter, D. A. 1980. A mathematical model for the dynamics of human locomotion. *Journal of Biomechanics*, 13, 361-368.

N.W.S.C.A. 1966. Calling All Cricketers. A Cricket Coaching Manual. Hogbin Poole Pty. Ltd., Sydney.

Penrose, T., Foster, D. and Blanksby, B. 1976. Release velocities of fast bowlers during a cricket test match. *The Australian Journal for Health, Physical Education and Recreation*, 71(March [Suppl]), 2-5.

Peterson, M. W. 1973. The Segmental Components in Skilled Baseball Throwing. Unpublished Master's Thesis, University of Illinois.

Philpott, P. 1973. *How to Play Cricket.* Pollard Pty. Ltd., Sydney.

Portus, M.R., Sinclair, P.J., Burke, S.T, Moore, D.J.A. and Farhart, P.J. 2000. Cricket fast bowling performance and technique and the influence of selected physical factors during an 8-over spell. *Journal of Sports Sciences*, 18, 999-1011.

Rau, G., Disshelhorst-Klug, C. and Schmidt, R. 2000. Movement biomechanics goes upwards: from the leg to the arm. *Journal of Biomechanics*, 33, 1207-1216.

Saunders, G.C. & Coleman, S.G.S. 1991. The ground reaction forces experienced by medium/fast bowlers in cricket. *Journal of Sports Sciences*, 9, 406.

Sly, C. 1951. *How to Bowl Them Out - A Handbook for Young Cricketers.* Thursons, London.

Smith, E. "International Bowling Speeds". 2002. Wisden Cricinfo Ltd. 10 January 2004. <http://www.cricket.org/link_to_database/STATS/FC/BOWLING/BOWLING_SPEEDS.html>

Sobers, S. & Smith, P. 1985. *Gary Sober's Way of Cricket.* The Five Mile Press, Victoria.

Spiegel, M. R. (1967). *Theory and problems of Theoretical Mechanics with an introduction to Lagrange's equations and Hamilton theory.*Schaum Publishing Co., New York.

Stockhill, N. P. & Bartlett, R. M. 1992. A three-dimensional cinematographical analysis of the techniques of international and english county cricket fast bowlers. In R. Rodano, G. Ferrigno and G. C. Santambrogio (eds), *Proceedings of the International Society of Biomechanics in Sports*, Edi Ermes, Milan, pp. 52-55.

Stockill, N. & Bartlett, R.M. 1994. An investigation into the important determinants of ball release speed in junior and senior international cricket bowlers. *Journal of Sports Sciences*, 12, 177-178.

Tyson, F. 1976. *Complete Cricket Coaching.* Thomas Nelson (aust.) Ltd., Melbourne.

Wilkins, B. 1991. *The Bowler's Art. Understanding Spin, Swing and Swerve.* A & C Black, London.

Winter, D.A. 1984. Kinematic and kinetic pateerns in human gait: variability and compensating effects. *Human Movement Science*, 3, 51-76.

Winter, D. A. 1987. *Biomechanics and Motor Control of Human Gait.* University of Waterloo Press, Waterloo.

Winter, D. A. 1990. *Biomechanics and Motor Control of Human Movement* (2nd ed), John Wiley & Sons, Inc., Toronto.

Winter, D.A., Sidwall, H.G. and Hobson, D.A. 1974. Measurement and reduction of noise in kinematics of locomotion. *Journal of Biomechanics*, 7, 157-159.

Zatsiorsky, V.M. 1998. *Kinematics of Human Motion.* Human Kinetics, Champaign, Illinois.

Zatsiorsky, V.M., Seluyanov, V.N. and Chugunova, L.G. (1990). Methods of determining mass-inertial characteristics of the human body. In G.G. Chernyi and S.S. Regirer (Eds), *Contemporary problems of Biomechanics*, pp. 272-291, CRC Press, Massachusetts.